H D M – 4

Highway Development & Management

Volume SIX

MODELLING ROAD DETERIORATION AND WORKS EFFECTS

Version 2

Greg Morosiuk
Mike J Riley
J B Odoki

6

THE HIGHWAY DEVELOPMENT AND MANAGEMENT SERIES

About This Manual

This manual provides details on modelling road deterioration and works effects in the HDM model. It is one of seven volumes comprising the suite of HDM-4 documentation (see Figure 1). It is intended to be used by specialists interested in technical issues or responsible for setting up the HDM model. It provides the full background to the development and theoretical basis for the models in HDM-4 used for road deterioration and road works effects.

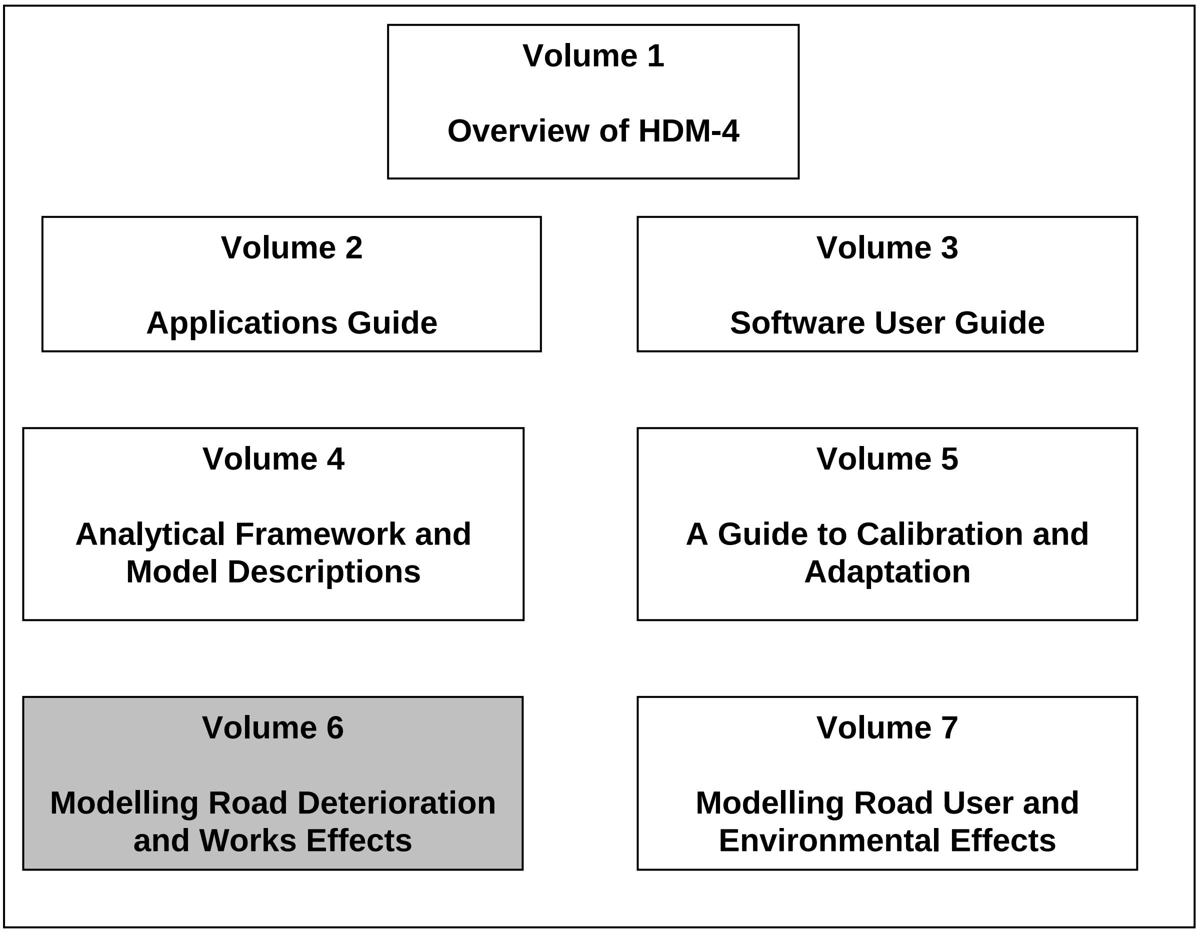

Figure 1
HDM-4 Documentation Suite

The suite of documents comprises:

- **Overview of HDM-4 (Volume 1)**
  A short executive summary describing the HDM-4 system. It is intended to be used by all readers new to HDM-4, particularly high level management within a road organisation

- **Applications Guide (Volume 2)**
  A task oriented guide describing typical examples of different types of analyses. It is to be used by users who wish to know how to perform a task or create a study.

- **Software User Guide (Volume 3)**

  Describes the HDM-4 software. It is a general purpose document which provides an understanding of the software user interface.

- **Analytical Framework and Model Descriptions (Volume 4)**

  Describes the analytical framework and the technical relationships used within the HDM-4 model. It contains comprehensive reference material describing the characteristics of the modelling and strategy incorporated in HDM-4. It is to be used by specialists or experts whose task is to carry out a detailed study for a road management organisation.

- **A Guide to Calibration and Adaptation (Volume 5)**

  Suggests methods for calibrating and adapting HDM-4 models to allow for local conditions existing in different countries.

- **Modelling Road Deterioration and Works Effects (Volume 6)**

  Describes the development and basis for the relationships in HDM-4 used for modelling road deterioration and works effects.

- **Modelling Road User and Environmental Effects (Volume 7)**

  Describes the development and basis for the relationships in HDM-4 used for modelling road user and environmental effects.

Structure of this Manual

The information in this document is structured into five sections as follows:

- **Part A – Concepts and Approach**

  This section gives the general concepts and approaches historically used in modelling road deterioration and works effects (RDWE) in HDM.

- **Part B – Bituminous Pavements**

  This section presents details of the RDWE models used in HDM for bituminous pavements.

- **Part C – Concrete Pavements**

  This section presents details of the RDWE models used in HDM for concrete pavements.

- **Part D – Block Pavements**

  This section presents details of the RDWE models proposed for use in HDM for block pavements. Currently the models for block pavements have not been incorporated in the HDM-4 software.

- **Part E – Unsealed Pavements**

  This section presents details of the RDWE models used in HDM for unsealed pavements.

ISOHDM Products

The products of the International Study of Highway Development and Management Tools (ISOHDM) consist of the HDM-4 suite of software, associated example case study databases, and the Highway Development and Management Series collection of guides and reference manuals. This Volume is a member of that document collection.

Customer Contact

Should you have any difficulties with the information provided in this suite of documentation please do not hesitate to report details of the problem you are experiencing. You may send an E-mail or an annotated copy of the manual page by fax to the number provided below.

The ISOHDM Technical Secretariat welcomes any comments or suggestions from users of HDM-4.

Comments on Volume 6 – Modelling Road Deterioration and Works Effects should be sent to the following address:

E-mail: isohdm@ham.ac.uk
Telephone: +44 – 121 – 414 5053/6717
Fax +44 – 121 – 414 3675/5051

Post ISOHDM Technical Secretariat
School of Civil Engineering
The University of Birmingham
Edgbaston
Birmingham B15 2TT
United Kingdom

The authors can be contacted at :

E-mail: gmorosiuk@trl.co.uk

Change Details

A draft edition (Version 1.0) of Volume 6 was produced in February 2001.

This is the second edition (Version 2.0) of Volume 6.

Related Documentation

HDM-4 documents

The Highway Development and Management Series Collection is ISBN: 2-84060-058-7, and comprises:

Volume 1 – Overview of HDM-4, ISBN: 2-84060-059-5
Volume 2 – Applications Guide, ISBN: 2-84060-060-9
Volume 3 – Software User Guide, ISBN: 2-84060-061-7
Volume 4 – Analytical Framework and Model Descriptions, ISBN: 2-84060-062-5
Volume 5 – A Guide to Calibration and Adaptation Manual, ISBN: 2-84060-063-3
Volume 6 – Modelling Road Deterioration and Works Effects, ISBN: 2-84060-102-8
Volume 7 – Modelling Road User and Environmental Effects, ISBN: 2-84060-103-6

Terminology handbooks

PIARC Lexicon of Road and Traffic Engineering - First edition. Permanent International Association of Road Congresses (PIARC), Paris 1991. ISBN: 2-84060-000-5

Technical Dictionary of Road Terms - Seventh edition, English - French. PIARC Commission on Terminology, Paris 1997. ISBN: 2-84060-053-6

General reference information

Further details on HDM-4 may be obtained from the following:

- ISOHDM Technical Secretariat
  School of Civil Engineering
  The University of Birmingham
  Edgbaston
  Birmingham
  B15 2TT
  United Kingdom
  Tel: +44 - 121 - 414 6717 (or 5049)
  Fax: +44 - 121 - 414 3675 (or 5060)
  E-mail: ISOHDM@bham.ac.uk
  Web: http://www.bham.ac.uk/isohdm

- The World Road Association (PIARC)
  La Grande Arche
  Paroi Nord, niveau 8
  92055 La Defénse Cedex
  France
  Tel: +33 1 47 96 81 21
  Fax: +33 1 49 00 02 02
  E-mail: piarc@wanadoo.fr
  Web: http://www.piarc.org

Acknowledgements

The authors would like to express their appreciation to all those who have contributed to developing this manual, in particular, but not limited to, the following people.

- William D O Paterson, World Bank
- Juan-Pablo Covarrubias, Inter-American Federation of Cement Producers (FICEM)
- John Rolt, TRL Limited, UK
- Henry Kerali, University of Birmingham, UK
- Neil Robertson, ISOHDM Project Coordinator, PIARC, France
- Tyrone Toole, Australian Road Research Board
- Louw Kannemeyer, Department of Transport, South Africa
- Pierre Joubert, LCPC, France
- Jon Roberts, Australian Road Research Board
- Peter Cenek, Opus International Consultants, New Zealand
- Gustav Rohde, Africon, South Africa
- Chris Parkman, Transit, New Zealand

Development of HDM-4

The World Road Association (PIARC) has managed the International Study of Highway Development and Management (ISOHDM) project since 1998, following the action supported by the World Bank when the research and development efforts of several years reached the point when HDM Technology products could be brought into practice. Under PIARC management, the first products, the Highway Develoment and Management Series publications, and the software suite HDM-4 Version 1, were released in early 2000, dissemination was organized in addition to training of users. In 2002, PIARC launched the development of a Version 2 of the software.

The initial part of the development of HDM-4 has been sponsored by several agencies, primarily:
Asian Development Bank (ADB)
Department for International Development (DFID) in the United Kingdom
Swedish National Road Administration (SNRA)
The World Bank
with significant contributions made by:
Finnish Road Administration (FinnRA)
Intra-American Federation of Cement Producers (FICEM)

The development of Versions 1 and 2 has been made by funding by the World Road Association with sponsorship received from the governments of the following countries:
Algeria, Australia, Canada-Québec, France, Italy, Japan, Latvia, Madagascar, Mongolia, New-Zealand, Norway, Portugal, Sweden, Switzerland, Tanzania, United-Kingdom, USA
and from
Asian Development Bank (ADB)
The World Bank.
Many organisations and individuals in a number of countries have also contributed in terms of providing information, or undertaking technical review of products being produced.

The development of the software was carried out by the ISOHDM Technical Secretariat at the University of Birmingham in the United Kingdom. A number of organisations participated in the development including

- **FinnRA**

  Specification of the strategic and programme analysis applications.

- **FICEM**

  Development of deterioration and maintenance relationships for Portland cement concrete roads.

- **The Highway Research Group**, School of Civil Engineering, The University of Birmingham, UK

  Responsible for system design and software development.

- **Laboratoire Central des Ponts et Chaussées (LCPC)** in France

  Responsible for overseeing the definition of the specifications for Version 2 and the sofware development.

- **Training and Research Institute (IKRAM)** in Malaysia supported by N D Lea International (NDLI)

  Responsible for providing updated relationships for road deterioration and road user costs.

- **TRL Limited** in the United Kingdom

  Responsible for review and update of bituminous pavement and unsealed road deterioration relationships.

- **SNRA**

  Responsible for developing deterioration relationships for cold climates, road safety, environmental effects, and supporting HRG with system design.

All research organisations received support from local and regional staff, visiting experts and external advisers, to ensure that a high standard of quality and international consensus was achieved. A number of other countries and individuals have supported this work through supplying expert advice and reviewing the products.

Copyright statement

The publication of this edition of Volume 6 of the HDM-4 documentation has been made possible through a grant from the **Asian Development Bank**.

CONTENTS

MODELLING ROAD DETERIORATION AND WORKS EFFECTS

This document is the sixth volume in the series of seven volumes of HDM-4 documentation. The road deterioration and works effects (RDWE) models currently in HDM-4 are given in Volume 4 (Odoki and Kerali, 2000). This volume gives a detailed description of the RDWE models currently in HDM-4 and provides some background to their development, particularly from HDM-III to HDM-4. Also included are possible enhancements to some of the models currently in HDM-4. In addition, other deterioration models are presented in this document for consideration in future versions of HDM-4.

The general concepts and approaches historically used in modelling road deterioration and works effects in HDM are discussed in Part A. The RDWE models for bituminous, concrete, block and unsealed pavements are then described in Parts B, C, D and E respectively.

Throughout this volume, extracts are regularly taken from, and references made to, three publications; Paterson (1987), Watanatada, et al (1987) and NDLI (1995). The first two are the main sources of information for the HDM-III model and the other source details the findings of the original International Study of Highway Development and Management (ISOHDM) into HDM-4.

PART A. CONCEPTS AND APPROACH

A1. BACKGROUND AND HISTORY

This chapter describes the background to the road deterioration and works effects (RDWE) models in HDM-4. The HDM-III model contains relationships for predicting road deterioration and works effects as a function of pavement characteristics, traffic and the environment (Watanatada, et al, 1987). The model was the outcome of two principal studies conducted in tropical countries.

The first such study was in Kenya during the period 1971-75 (Hodges, et al, 1975). The results of this study formed the basis of the relationships in an earlier version of the model, HDM-II. A second and larger study was carried out in Brazil between 1975-82 (GEIPOT, 1982). The results of the Brazil study formed the basis of the models in HDM-III (Paterson, 1987), but the relationships were validated using data from a number of other studies in various countries. Since its release, HDM-III has been used in projects covering a range of climates and conditions, and the basic structure and predictions of the relationships have been widely confirmed.

The limitations of HDM-III are primarily in its scope. For example, road safety issues are not included; the road deterioration and works effects models do not encompass all of the pavement types (e.g. rigid pavements); the range of climates is primarily tropical and temperate; vehicle emissions and similar environmental effects are not included; the economic analysis module is too restrictive. This list is not exhaustive. Recognising the need for a more comprehensive model, an international collaborative study was initiated in 1993 to extend the scope of the model and to update the relationships and the software.

This study, the International Study of Highway Development and Management (ISOHDM), was a multi-national collaborative study funded by four principal sponsors:

- the Asian Development Bank (ADB)
- the Department for International Development (DFID) of the United Kingdom
- the World Bank
- the Swedish National Roads Administration (SNRA) of Sweden

The study was carried out by a number of research teams based in several countries, supported by various organisations and individuals. The principal teams were:

- the Highway Development and Management Technical Relationships Study (HTRS), based in Malaysia investigating road user effects along with road deterioration and maintenance effects for flexible pavements
- the Software Development Team, based at the University of Birmingham in the United Kingdom
- the South American team based in Chile investigating rigid pavements under the sponsorship of the Inter-American Federation of Cement Producers (FICEM)
- the Swedish Team, primarily based at the Swedish Road and Transport Research Institute addressing elements of road user effects and pavement deterioration

The Steering Committee, chaired by the World Bank, was responsible for the overall direction and guidance of the various projects. The ISOHDM project Secretariat, established at the University of Birmingham, facilitated the co-ordination and communication between projects and with the international audience.

The time scale and funding of the ISOHDM meant that it was not practical to undertake basic new research. Instead, the study teams relied primarily on reviewing and/or adapting previous research, or re-analysing available databases.

The outputs from the ISOHDM were aimed at addressing the limitations listed above. As far as the RDWE models are concerned, HDM-4 now includes:

- A greater range of physical environments (climatic zones). This encompasses cold (freeze/thaw) climates, very high temperatures and a very wide range of temperature variations such as desert conditions, and very high moisture regimes.
- Rigid/concrete pavements and a wider range of flexible pavements.
- Deterioration and maintenance of side-drains and their effects on pavement strength.
- Texture depth and skid resistance models.
- Edge break, particularly on narrow roads.
- A broader range of routine maintenance operations and effects.
- A broader range of improvement/new construction works options.

A2. CONCEPTS OF DETERIORATION

A2.1 Classes and Types of Models

Condition projection methods can be grouped into two basic categories (Robinson, et al, 1998):

Probabilistic – where condition is predicted as a probability function of a range of possible conditions.

Deterministic – where condition is predicted as a precise value on the basis of mathematical functions of observed or measured deterioration.

In HDM, deterministic models are used. The two general classes of deterministic models used for road deterioration are mechanistic and empirical.

Mechanistic models are based on knowledge of the stresses and strains in the pavement calculated using fundamental theories of behaviour. They are usually very data intensive and rely on parameters which are difficult to quantify in the field.

Empirical models are usually based on statistical analyses of locally observed deterioration trends, and may not be applicable outside the specific conditions upon which they are based.

To overcome these problems, Paterson (1987*)* adopted a **structured empirical** approach for developing the road deterioration and maintenance effects component of the HDM-III model. This was based on identifying the functional form and primary variables affecting each form of deterioration from both mechanistic and empirical information and then using various statistical techniques to quantify their impacts. This had the advantage that the resulting models combined both the theoretical and experimental bases of mechanistic models with the behaviour observed in empirical studies. The RD and WE relationships included in HDM-4 are therefore mainly structured empirical models.

There are two types of models that can be used for predictive purposes, **absolute** models and **incremental** models. Absolute models predict the condition (or distress) at a particular point in time as a function of the independent variables. Incremental models give the change in condition from an initial state as a function of the independent variables. Absolute models have the disadvantage that they are usually confined to the specific conditions upon which they are based and thus cannot be readily applied under different conditions. Incremental models can, on the other hand, be applied to a variety of different initial conditions and offer much more flexibility than absolute models.

Because of their advantages, incremental models were adopted wherever possible as the basis for pavement deterioration in HDM. The models predict the change of distress over a period, which is based on either time or the passage of traffic.

The families of pavement performance models are based on the road surface classes:

- Bituminous – described in Part B
- Concrete – described in Part C
- Block – described in Part D
- Unsealed – described in Part E

The deterioration of block pavements is not modelled in the HDM-4 software (version 2.0). However, it is envisaged that this type of pavement will be included in future versions of the sofware.

A2.2 Pavement Deterioration

Pavement deterioration manifests itself in various kinds of distresses, each of which is modelled separately in HDM-4. Model forms that use combinations of distresses in the form of a single index of ‘condition’, or damage function, are too restrictive. The ideal maintenance treatment for a particular section of road will depend on the principal cause of distress and this can be concealed where index methods are used. Table A2-1 gives a summary of the individual pavement defects that are modelled in HDM-4.

Table A2-1
Pavement defects modelled in HDM-4

Bituminous	Concrete	Block *	Unsealed
Drainage	Cracking	Rutting	Gravel loss
Cracking	Joint Spalling	Roughness	Roughness
Ravelling	Joint Faulting	Surface Texture	
Potholing	Failures		
Edge Break	Roughness		
Rutting			
Roughness			
Texture Depth			
Skid Resistance			

* Not currently modelled in HDM-4

Parts B, C, D and E of this document describe separately the road deterioration and road works effects models for the four individual types of pavement listed in Table A2-1. This introduction describes those elements of the models that are common to all the pavement types.

Pavement deterioration is an inherently complex phenomenon because of the interactions between many of the deterioration mechanisms. For example, total road roughness consists of a number of components representing different distresses, all of which contribute in different ways to the overall roughness value. Thus cracks eventually spall and lead to potholes which increase roughness, but cracks allow the ingress of water which, in turn, weakens the road structure, the amount depending on the pavement materials and the condition of the drainage system amongst other things. This, then leads to deformation or rutting which also contributes to roughness. The magnitude of all these effects depends on traffic, environment, material qualities, maintenance policy, to mention just some of the variables.

In order to model road deterioration properly it is necessary to identify homogeneous road sections in terms of physical attributes and condition so that a particular set of road deterioration relationships can be applied. The basic unit of analysis is therefore the **homogeneous** road section, to which several investment options can be assigned for analysis.

A2.3 Pavement Classification

A versatile framework of pavement classification has been developed to cater for the expanded scope of RD and WE modelling. The system uses broad definitions of road surfacing and base types as described in the original ISOHDM report from Malaysia (NDLI, 1995). The definitions are described below:

Surface category
Divides all pavements into two groups:

- Paved
- Unpaved

These are mainly used for the reporting of network statistics.

Surface class
Sub-divides the paved category into bituminous, concrete and block surfaces. Together with the unsealed class there are thus four classes that are used to define the family of distress models used for performance modelling.

Surface type
Divides bituminous surfacings into two types:

- Asphaltic Mix (AM)
- Surface Treatment (ST)

Divides concrete surfacings into three types:

- Jointed Plain (JP)
- Jointed Reinforced (JR)
- Continuously Reinforced (CR)

Divides block surfacings into three types:

- Concrete Block (CB)
- Brick (BR)
- Set Stone (SS)

Divides unsealed roads into three types of surfacings:

- Gravel (GR)
- Earth (EA)
- Sand (SA)

A surface type is designated by a two-character code.

Base type
For bituminous pavements, there are four types of base:

- Granular Base (GB)
- Stabilised Base (SB)
- Asphalt Base (AB)
- Asphalt Pavement (AP)

The AP base type is used when a surfacing is laid on top of an existing asphalt pavement.

For concrete pavements, there are three types of base:

- Granular Base (GB)
- Stabilised Base (SB)
- Asphalt Base (AB)

For block pavements, there are two types of base:

- Granular Base (GB)
- Stabilised Base (SB)

Each base type is designated by a two-character code.

Pavement type

Integrates surface and base types. Each type is designated by a four-character code, combining the surface and base type codes listed above. For unsealed roads, the code used for the base type is UP, to conform with the four-character code used for the other types of pavements. The pavement classification is summarised in Table A2-2.

Table A2-2
Pavement classification system

Surface category	Surface class	Pavement type	Surface type	Base type
Paved	Bituminous	AMGB	AM	GB
Paved	Bituminous	AMAB	AM	AB
Paved	Bituminous	AMSB	AM	SB
Paved	Bituminous	AMAP	AM	AP
Paved	Bituminous	STGB	ST	GB
Paved	Bituminous	STAB	ST	AB
Paved	Bituminous	STSB	ST	SB
Paved	Bituminous	STAP	ST	AP
Paved	Concrete	JPGB	JP	GB
Paved	Concrete	JPAB	JP	AB
Paved	Concrete	JPSB	JP	SB
Paved	Concrete	JRGB	JR	GB
Paved	Concrete	JRAB	JR	AB
Paved	Concrete	JRSB	JR	SB
Paved	Concrete	CRGB	CR	GB
Paved	Concrete	CRAB	CR	AB
Paved	Concrete	CRSB	CR	SB
Paved	Block	CBGB	CB	GB
Paved	Block	CBSB	CB	SB
Paved	Block	BRGB	BR	GB
Paved	Block	BRSB	BR	SB
Paved	Block	SSGB	SS	GB
Paved	Block	SSSB	SS	SB
Unpaved	Unsealed	GRUP	GR	UP
Unpaved	Unsealed	EAUP	EA	UP
Unpaved	Unsealed	SAUP	SA	UP

A series of generic deterioration relationships have been developed for the main pavement types defined in Table A2-2. In most cases, the relationships for a particular distress are of the same form for all the pavement types, but the coefficients of the variables in the models may be different. It is envisaged that in the future, all the model coefficients in the deterioration relationships in HDM-4 will be either surface or base material specific, although at the moment this is not the case.

For pavement type STGB, for example, the rate of deterioration of a particular distress may be different if the ST is a single surface dressing or a slurry seal. Furthermore, this rate of deterioration may be influenced by whether the GB is a natural gravel or crushed stone.

The application of the classification system depends upon the type of analysis being undertaken. For example, network level analyses are generally based on coarse data. In these instances the minimum requirement for analysis would be the definition of surface class and pavement type. Default materials and distress model coefficients would then be applied in the modelling. Project level analyses require a much greater level of detail. Here, surface and/or base materials may be specified together with user defined distress model coefficients.

It should be noted that the surface class and pavement type may change during an analysis period, depending on the types of works applied to the pavement. For example, the initial pavement type for a section may be AMGB (asphaltic mix surface on granular base); if an asphalt overlay is applied, the pavement type will change to AMAP (asphaltic mix surface on asphalt pavement) and different model parameters will apply. If the same initial pavement is given a surface treatment it will change to STAP (surface treatment on asphalt pavement).

A2.4 Calibration Factors

It is important to note that as each mode of distress develops and progresses at different rates in different environments, the RD relationships should always be calibrated to local conditions before they are used in any form of analysis. To facilitate this, the models include a number of calibration factors denoted by the letter K together with identifying subscripts. These factors are multiplicative and are used to change the scale of a particular distress. The default value for all the "K" factors is 1.0.

For example, K_{cia} is the calibration factor for the initiation of all structural cracking in bituminous pavements. By increasing the value of K_{cia} to 2.0, for example, the time to the initiation of all structural cracking is doubled, implying that the pavement will last longer before cracks appear than that predicted by default by HDM-4. Similarly increasing the calibration factor for the progression of all structural cracking, K_{cpa}, to 2.0, implies that the pavement will deteriorate, in terms of the rate of crack progression, twice as fast as that predicted by default by HDM-4.

In addition to an increased number of calibration factors, another important addition to the models in HDM-4 is the use of adjustable model coefficient values, referred to as the a_i values and mentioned in Section A2.3. In HDM-4, the a_i values for the variables in each relationship will not be hard coded into the software. Instead a default value has been assigned to each of these model coefficients, which the user will be able to alter.

The calibration factors should be used to adjust the rates of deterioration for specific road sections or regions, for particular types of pavement. For example, a section of road in a hilly region may deteriorate at a different rate to a section of road in a flat area, even though the two sections are nominally homogeneous in all other respects. The model coefficients should be used to adjust the rates of deterioration for different types of material. For example, a porous asphalt AM pavement type may deteriorate at a different rate to a hot rolled asphalt AM pavement type.

Calibration is discussed in detail in Volume 5 of the HDM-4 series – A Guide to Calibration and Adaptation (Bennett and Paterson, 2000).

A2.5 Key Variables Affecting Deterioration

The variables used in the various deterioration relationships described in this document are defined in the appropriate sections. However, the key variables that are common to most of the deterioration models are described in detail below; i.e. traffic-associated and environment-associated variables and the age of the pavement.

A2.5.1 Traffic

The existing traffic volumes on the road being analysed are specified in terms of **vehicle type** or **class**, depending on the kind of analysis to be performed. The value entered for each vehicle type is expressed as the annual average daily traffic (AADT), where AADT is defined as follows:

$$AADT = \frac{\text{Total annual traffic in both directions}}{365} \qquad \text{. . . (A2.1)}$$

This constitutes the baseline flow for the analysis period. It is assumed that seasonal variations in traffic flows have already been accounted for when estimating the AADT from traffic counts carried out over shorter periods.

The following measures of traffic are also required to predict the impacts of vehicles on pavement deterioration and works effects:

- **Numbers of vehicle axles (YAX)**
  Defined as the total number of axles of all vehicles traversing a given link in a given year.
- **Number of equivalent standard axle loads (ESA)**
  This combines the damaging effects of the full spectrum of axle loading using a common damage-related unit. ESA is considered on each link, for each year of the analysis period.

A2.5.1.1 Vehicle Axles

For each vehicle type (k), the number of vehicle axles, YAX_k, traversing a given section in a particular year is calculated from the volume of traffic multiplied by the number of axles per vehicle of the type involved.

$$YAX_k = \frac{T_k\left(NAXLES_k\right)}{ELANES \times 10^6} \qquad \text{. . . (A2.2)}$$

The total number of all axles, YAX, in a given year is obtained by summing the YAX's for all vehicle types.

$$YAX = \sum_{k=1}^{K} YAX_k \qquad \text{. . . (A2.3)}$$

where

YAX	=	annual total number of axles of all vehicle types (millions per lane)
T_k	=	annual traffic volume of vehicle type k, (k = 1, 2, . . , K)
$NAXLES_k$	=	number of axles per vehicle type k
ELANES	=	effective number of lanes for the road section

The effective number of lanes (ELANES) is used to model the effect of traffic load distribution across the carriageway width.

A2.5.1.2 Equivalent Standard Axle Load Factors

The equivalent standard axle load factor is defined as the number of applications of a standard 80 kN dual-wheel single axle load that would cause the same amount of damage to a road as one application of the axle load being considered. The value of ESALF for each vehicle type may be specified by the user or calculated from axle load information.

For each vehicle type, ESA_k is computed using information on the different damaging effects of various axle configurations. For each type of axle group *j*, a standard load, $SAXL_j$, is used to determine the loading ratio. The expression for calculating ESALF is:

$$ESALF_k = \sum_{i=1}^{I_k} \frac{P_{ki}}{100} \sum_{j=1}^{J_k} \left(\frac{AXL_{kij}}{SAXL_j} \right)^{LE} \qquad \text{. . . (A2.4)}$$

where

$ESALF_k$ = equivalent standard axle load factor for vehicle type *k*, in equivalent standard axle loads

I_k = the number of subgroups *i* (defined in terms of load range) of vehicle type *k* (i = 1, 2, . . ., I_k)

P_{ki} = percentage of vehicles in subgroup *i* of vehicle type *k*

LE = axle load equivalency exponent (default = 4.0)

J_k = number of single axles per vehicle of type *k*

AXL_{kij} = average load on axle *j* of load range *i* in vehicle type *k* (tonnes)

$SAXL_j$ = standard single axle load of axle group type *j*; usually the value of 8.16 tonnes for dual-wheel single axles is used for all single axles

The factor $ESALF_k$ is therefore an average over all vehicles of type *k*, loaded and unloaded, in both directions on the given road section.

In HDM-4, the annual number of equivalent standard axle loads is denoted by YE4, as in HDM-III, the number "4" denoting that the fourth power was used in calculating ESALF (see equation A2.4).

$$YE4 = \sum_{k=1}^{K} \frac{T_k \left(ESALF_k \right)}{ELANES \times 10^6} \qquad \text{. . . (A2.5)}$$

where

YE4 = annual total number of equivalent standard axle loads, in millions/lane

all other variables are as previously defined

A2.5.1.3 Cumulative Traffic Loading

The cumulative traffic loading parameters are used for modelling road deterioration and as intervention criteria for some road works activities. These parameters are calculated from the accumulated traffic since the time of the last surfacing or construction works on the road section in question.

The cumulative number of equivalent standard axle loads (ESA) since the last rehabilitation or construction works (NE4) is given by:

$$NE4 = \sum_{y=1}^{AGE3} YE4_y \qquad \text{. . . (A2.6)}$$

where

NE4 = cumulative number of equivalent standard axle loads since last rehabilitation (overlay), in millions/lane
$YE4_y$ = number of equivalent standard axle loads in year *y*, in millions/lane
AGE3 = number of years since last rehabilitation, in years

A2.5.1.4 Light and Heavy Vehicles

The modelling of some pavement distress modes and the calculation of the deterioration of unsealed roads requires input of the amounts of **light** and **heavy** vehicles. Heavy vehicles are categorised as those with operating weight equal to or greater than 3.5 tonnes; other vehicles are categorised as light. The Average Daily Light vehicles (ADL) and the Average Daily Heavy vehicles (ADH) are specified in terms of vehicles per day for each year of the analysis period.

The modelling of the changes in pavement skid resistance requires the specification of the flow of heavy commercial vehicles per lane per day (QCV).

$$QCV = \frac{ADH}{ELANES} \qquad \text{. . . (A2.7)}$$

where
QCV = flow of heavy commercial vehicles per lane per day
ADH = average daily heavy vehicles ($\geq$ 3.5 tonnes), total in both directions
ELANES = effective number of lanes for the road section

The modelling of changes in pavement texture depth requires the specification of the annual number of equivalent light vehicle passes (ΔNELV) over the road section. This is calculated from the following expression:

$$\Delta NELV = 365\,[ADL + 10\,(ADH)] \qquad \text{. . . (A2.8)}$$

where
ΔNELV = number of equivalent light vehicle passes during an analysis year
ADL = average daily light vehicles (< 3.5 tonnes), total in both directions

The number of vehicles with studded tyres is required for modelling pavement rutting during freezing seasons. The number of vehicle passes with studded tyres (PASS) is calculated as follows:

$$PASS = \frac{365(ST)(AADT_y)\,x\,10^{-5}}{NTFD} \qquad \text{. . . (A2.9)}$$

where
PASS = annual number of vehicle passes with studded tyres in one direction, in thousands
$AADT_y$ = annual average daily traffic (AADT) in year *y*, in veh/day
ST = percentage of annual number of vehicle passes with studded tyres
NTFD = number of traffic flow directions

A2.5.2 Climate and Environment

The climate in which a road is situated has a significant impact on the rate at which it deteriorates. Important climatic factors are related to temperature, precipitation and winter conditions. This section describes the principal climatic data that are used in the road deterioration models for the different categories of roads.

In HDM-4, the environment is classified by five moisture and five temperature classifications. This is an increase on the classifications used in HDM-III. The moisture classifications are defined in Table A2-3 and the temperature classifications are defined in Table A2-4.

Table A2-3
Moisture classification

Moisture Classification	Description	Thornthwaite Moisture Index	Annual Precipitation (mm)
Arid	Very low rainfall, high evaporation	-100 to –61	< 300
Semi-arid	Low rainfall	-60 to –21	300 to 800
Sub-humid	Moderate rainfall, or strongly seasonal rainfall	-20 to +19	800 to 1600
Humid	Moderate warm seasonal rainfall	+20 to +100	1500 to 3000
Per-humid	High rainfall, or very many wet-surface days	> 100	> 2400

Table A2-4
Temperature classification

Temperature Classification	Description	Temperature Range (^{o}C)
Tropical	Warm temperatures in small range	20 to 35
Sub-tropical - hot	High day cool night temperatures, hot-cold seasons	-5 to 45
Sub-tropical - cool	Moderate day temperatures, cool winters	-10 to 30
Temperate - cool	Warm summer, shallow winter freeze	-20 to 25
Temperate - freeze	Cool summer, deep winter freeze	-40 to 20

Precipitation

The Mean Monthly Precipitation (MMP) is used in modelling road deterioration, and is expressed in mm/month. In HDM-III MMP was expressed in metres/month.

Freezing Index

The freezing index, FI, expresses the cumulative effect of the intensity and duration of sub-freezing (< 0^{o}C) air temperatures. FI is expressed in degree-days and represents the difference between the highest and lowest points on a curve of cumulative degree-days versus time for one freezing season. The degree-days for any one day equals the difference between the average daily air temperature and 0 ^{o}C, and are expressed as positive when the average daily temperature is below freezing.

The freezing index is calculated as:

$$FI = \sum_{i=1}^{ndays} abs\left[\min(TEMP, 0)\right] \quad \ldots (A2.10)$$

where

FI = freezing index
TEMP = temperature, in ^{o}C
ndays = number of days in one freezing season

FI is only required as input data for the two Temperate temperature zones, and is used in modelling the performance of concrete pavements.

Temperature Range

Temperature range (TRANGE) is defined as the mean monthly ambient temperature range. Its calculation is based on the temperature ranges for each of the 12 months of the year, hence the difference between the maximum and minimum temperature for each month. The 12 values obtained are then averaged to obtain the variable TRANGE, which is used for modelling concrete pavements.

Days With Temperatures Greater Than 90ºF

The number of days in a year when the ambient temperature exceeds 90ºF (32ºC) is denoted as DAYS90. This variable is required for modelling the performance of concrete pavements.

Drainage Coefficient

Drainage coefficients were introduced in the 1986 revisions to the AASHTO Design Guide and maintained in the more recent version of the Guide (AASHTO, 1993). The drainage coefficients are determined by considering the quality of drainage and the percentage of time that the pavement is exposed to moisture levels approaching saturation. Table A2-5 gives the guidelines on rating the quality of drainage (AASHTO, 1993).

The quality of drainage is in turn a function of the permeability of the subsurface materials, the crossfall and longitudinal slopes, the drainage distance (the length that subsurface moisture must travel in order to exit the pavement structure), and the type of drainage structures. The saturation of the pavement is affected by both the drainability of the pavement structure and the rainfall.

Table A2-5
Relationship between drainage time and quality of drainage

Quality of Drainage	Water Removed From Layer Within
Excellent	2 hours
Good	1 day
Fair	1 week
Poor	1 month
Very Poor	water will not drain

Source: AASHTO (1993)

The AASHTO (1993) recommended ranges of drainage coefficients for a variety of drainage qualities and saturation times have been reproduced in Table A2-6. The drainage coefficient C_d is used as a variable in modelling the deterioration of concrete pavements.

Table A2-6
Drainage coefficient values

Quality of Drainage	Per cent of Time Pavement Structure is Exposed to Moisture Levels Approaching Saturation			
	< 1%	1 to 5%	5 to 25%	> 25%
Excellent	1.40 – 1.35	1.35 - 1.30	1.30 - 1.20	1.20
Good	1.35 – 1.25	1.25 - 1.15	1.15 - 1.00	1.00
Fair	1.25 – 1.15	1.15 - 1.05	1.00 - 0.80	0.80
Poor	1.15 – 1.05	1.05 - 0.80	0.80 - 0.60	0.60
Very Poor	1.05 – 0.95	0.95 - 0.75	0.75 - 0.40	0.40

Source: AASHTO (1993)

A2.5.3 Age of Pavement

In HDM-III, three variables defining the age of the pavement were used in the models; AGE1, AGE2 and AGE3. Each of these variables is related to the age of the pavement surface since a particular type of roadworks has been carried out. A fourth age variable, AGE4, has been introduced in HDM-4, which is used in the modelling of the initial densification component of rutting of bituminous pavements (see Section B8.4.1). These four variables are defined below.

AGE1 is referred to as the preventive treatment age. It is defined as the time, in number of years, since the latest preventive treatment, reseal, overlay, pavement reconstruction or new construction activity.

AGE2 is referred to as the surfacing age. It is defined as the time, in number of years, since the latest reseal, overlay, pavement reconstruction or new construction activity.

AGE3 is referred to as the rehabilitation age. It is defined as the time, in number of years, since the latest overlay, pavement reconstruction or new construction activity.

AGE4 is referred to as the base construction age. It is defined as the time, in number of years, since the latest reconstruction or new construction activity that involves the construction of a new base layer.

A3. CONCEPTS OF WORKS EFFECTS

A3.1 General Concepts

When making a life-cycle cost analysis of a road it is normally necessary to simulate in the modelling the effects of various types of roadworks during the analysis period. The option of doing nothing for a road over a period of, typically 20 years, is rarely a sensible option. In this section the following are addressed:

- what is meant by roadworks in a modelling context?
- how are roadworks defined?
- how is a particular operation invoked at a particular point in time?
- what are the effects of roadworks and how are they evaluated?
- what are the costs and benefits of roadworks?

The term “roadworks” is used to embrace any change to the physical characteristics of a road and may embrace operations ranging from simple maintenance, such as cleaning detritus from the road surface, to the construction of a new road link. One of the purposes of economic analysis is to find the combination of roadworks, which over an analysis period, will deliver the optimum solution for a given funding level. For every dollar spent on roadworks there should be a corresponding benefit of a dollar or more, otherwise the works should not be carried out. Benefits of roadworks can be almost immediate or longer term and arise from reduced society costs (vehicle operation, environmental effects) and/or reduced cost to the road agency in future maintenance of the road. This is illustrated in Figure A3-1.

Figure A3-1
Immediate and long term effects of roadworks

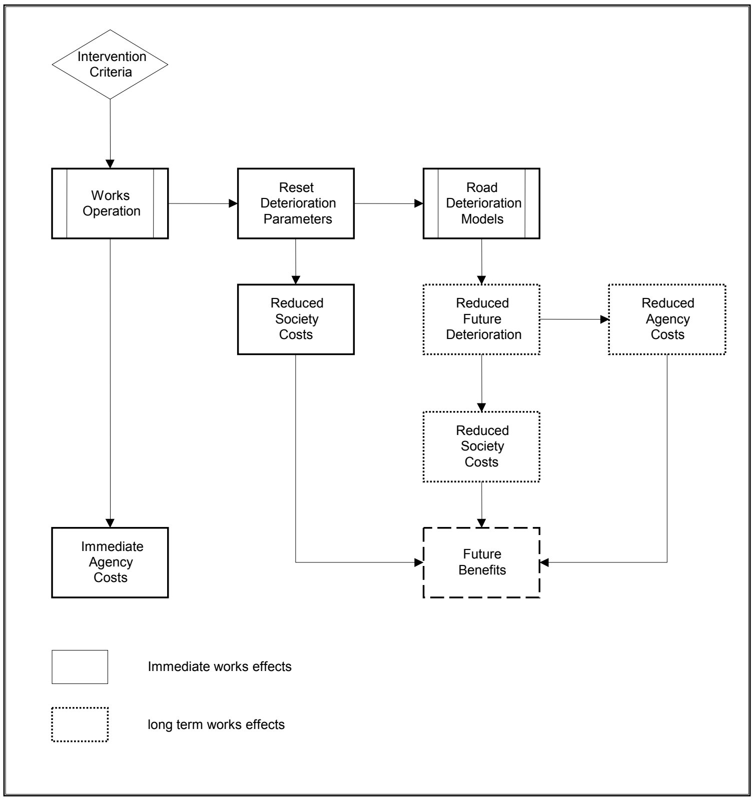

Some form of intervention criterion is used to decide when a particular operation should be applied. The operation results in a cost to the agency and a change to one or more of the parameters that are used in the model to describe the road. This change to the characteristics of the road may give an immediate benefit to road users (or other members of the public in reduced noise for example), or the benefit to society may only be of significance in the future due to reduced deterioration of the road. Reduced deterioration may also give reduced maintenance needs in the future and hence lower long term costs to the agency. All of these effects can be combined in some way to define the benefit of executing the roadworks operation. By comparing the initial cost and the immediate and long term benefits, the economic efficacy of the type and timing of the operation can be evaluated.

An important point sometimes overlooked in roadworks modelling is that, if two operations are tested that have identical effects on the modelling parameters, they will yield identical future benefits. Economic evaluation will then select the one with the lower initial cost.

A3.2 Roadworks Operations

A road can be considered as a number of complementary features or elements, each of which can be the subject of a variety of maintenance or improvement options. The principal features of a road are shown in Table A3-1.

Table A3-1
Road features

Road Feature	
Formation	I
Pavement	D
Shoulders, medians, verges	D
Footways, NMT lanes	D
Drainage system	D
Bridges	I
Other structures	I
Landscaping	N
Road furniture	I
Lighting	I
Utilities	N

Note: D – directly modelled in HDM-4
I – indirectly modelled in HDM-4
N – not modelled in HDM-4

A roadworks operation may concern only one road feature or several. If a new road is constructed it may involve all the features shown in Table A3-1. Although the cost of each operation should bring a corresponding benefit, it is not always possible to quantify some benefits or translate them into monetary terms, allowing comparison with the initial cost. For example, the benefits of street lighting in urban areas may appear obvious. But no robust models exist to evaluate the benefits, in terms of reduced accident costs or street crime, from providing street lighting. Only those road features and related operations for which the effects can be predicted and quantified are included in HDM-4.

Some features and associated roadworks are directly addressed in the HDM-4 models. This includes pavement, drainage, shoulders and NMT lanes. In these cases, operations are applied which specifically modify the characteristics used to define the features; for example, widening will change the width of the pavement.

Other features are modelled indirectly when major improvements are applied. For example, realignment may require earthworks, expressed in engineering terms as volumes of cut and fill, together with new structures and drainage systems. In the HDM-4 model, the change in alignment is expressed in terms of rise/fall and curvature.

Other features are not modelled at all in HDM-4, such as utilities. Although these may not be considered, strictly speaking, as a part of the road, by being underneath the road they often give rise to defects in the pavement that necessitate roadworks or affect road users.

Roadworks can be hierarchically classified as described in Volume 4 of the HDM-4 Series – Analytical Framework and Model Descriptions (Odoki and Kerali, 2000). However, in terms of modelling, what matters to the model is the effect of the works operation on the modelling parameters. If one considers the road pavement and the three major works classes, the groups of parameters directly affected are shown in the matrix in Table A3-2.

Table A3-2
Effect of works class on pavement parameters

Pavement Parameters	Works Class		
	Routine Maintenance	Periodic Maintenance	Improvement
Condition	D	D	D
Structure	I	D	D
Geometry			D

Note: D – Directly affected
I – Indirectly affected

As an example, crack sealing will reduce the cracked area but will not directly affect the pavement structure and will not change the geometry. But by reducing the ingress of water to the pavement it may indirectly increase the pavement strength.

To the model, the label and class of the operation are of no concern. The model only considers the change in model parameters; the label and class are only for reporting purposes. The definition of a works operation is therefore inseparable from the definition of the direct effects of the operation.

A3.3 Specifying Works Effects

As set out above, a works operation is merely a definition of one or more direct effects on the characteristics of the road being modelled. The change in characteristic (the immediate works effect) can be specified in several ways, summarised as:

1. The parameter is set to zero; e.g. after an asphaltic overlay, cracking becomes zero.
2. The parameter is reset to an absolute value which is defined as part of the operation; e.g. the roughness after an overlay is set to 2 m/km IRI.
3. The parameter is reset using a formula which may include other model parameters; e.g. the roughness after an overlay is reset as a function of the previous roughness and the thickness of the overlay.
4. The parameter is not reset; e.g. the width of the pavement is unchanged after an overlay.

Indirect effects of a works operation (e.g. increased pavement strength after crack sealing) are defined by the relevant deterioration models (in this case the model that relates strength to cracking and rainfall). Later parts of this volume describe the background and derivation of works effects models of type 3 above which are relevant to bituminous, concrete and unsealed pavements.

A3.4 Intervention Criteria

A3.4.1 Intervention Parameters

There are many parameters that a user may want to apply to restrict the use of different types of treatment. They can be grouped into a number of classes and the following sections discuss these.

Time

There is often a need to restrict treatments to specific analysis years. For example, if a 5-year rehabilitation programme is being developed, one might test alternative works operations in analysis years 1 - 5, applying a long term maintenance policy for the remainder of the analysis period. In another example, one might not want to test a major geometric improvement after a certain year because a parallel road will then be opened. Time in this sense (defined by analysis year) is distinct from time-scheduled periodic maintenance (e.g. seal every 5 years - discussed below under the heading of history).

Time may also be applied within a year. Examples are grading frequency for a gravel pavement or response time to pothole patching.

Traffic

This is frequently used in intervention criteria for both engineering and economic reasons. The most common parameter is AADT as the service level of a road is linked to the volume of traffic using it. Other traffic parameters are axle loading and measures of road capacity.

Axle loading may be used as an intervention criteria for pavement strengthening. The intervention may be expressed as the annual or cumulative loading. Although cumulative loading is commonly used in pavement design, it should be treated with caution in a life-cycle analysis of an existing road unless history data is reliable.

The method of handling capacity is less tractable, given the use of different flows with different hourly volumes. The intervention, expressed in hourly volume or volume/capacity ratio, might apply to the highest (peak) period or the daily average.

Geometry

The parameters in this group include width, horizontal alignment and vertical alignment, and would be used to trigger treatments from minor widening to major geometric improvements. The alignment parameters may also be applied in conjunction with skid resistance as interventions for resurfacing treatments or for the use of specific asphalt mixes (e.g. high stability AC on steep gradients).

Pavement Structure

Potential parameters include types of materials (surfacing and base), pavement type and adjusted structural number. Their application would be quite wide; pavement and materials types would restrict the use of incompatible materials, while strength, in combination with a traffic parameter, might define the use or otherwise of structural treatments.

Pavement Condition

Pavement condition is used for interventions in HDM-III, but limited to roughness and surface distress when applied to periodic and rehabilitation treatments. HDM-4 offers a wider range of distress parameters that might be used as intervention criteria, including cracking, ravelling, rutting, roughness and surface texture.

History
The different ages (e.g. age since construction or latest overlay or surface treatment) would, among other applications, govern scheduled treatments. For example, seal every 5 years would be expressed as seal when surface age reaches 5 years.

Environment
Where freeze/thaw conditions apply certain treatments may not be considered desirable, especially if seasonal modelling is applied. Rainfall may also govern the intervention levels for treatments aimed at improving skid resistance. It would be desirable to include these parameters if defining generalised intervention criteria for a network where climatic conditions vary significantly.

Adjacent Lanes and Road Features
When modelling by lane, the use of overlays is restricted as a drop-off between lanes is not usually acceptable. In urban areas with kerbs and sidewalks, the addition of more material by overlaying may not be permissible as it may reduce the kerb height below an unacceptable minimum. The edge step to the shoulder can also be a criteria; not only for the restoration of unsealed shoulders as a treatment, but also for allowable treatments to the carriageway if the shoulder is sealed.

If not modelled as a separate lane, generalised shoulder condition must be an intervention parameter for shoulder resurfacing or rehabilitation. Shoulder elevation (edge step) is also an important intervention criterion for replacement of shoulder material.

Road Function and Land Use
The inclusion of road use in HDM-4 is intended to govern the hourly distribution for congestion modelling. It may, however, be a factor in restricting the use of certain treatments. For example, chip seals may be undesirable on certain types of road due to the effects of loose chippings. It is intended to model noise in HDM-4, and this is a factor connected with land use, which again may influence the choice of surfacing types and materials.

Earthworks and Drainage
While drainage condition would obviously be a trigger for a treatment limited to drain improvement, it may also act in conjunction with other parameters to limit the use of certain treatments which are known to perform badly with poor drainage conditions. As drainage is often connected with the earthworks (poor if in cutting), this parameter may also be a desirable option in defining intervention sets.

A3.4.2 Defining Intervention Ranges

Each numeric parameter selected for use as an intervention criterion must be assigned a value or range at which a works operation should or should not be applied. Where a parameter is a code (e.g. pavement type) then the intervention will be equality rather than a range.

A consistent logic must be used with mathematical operators to ensure that all increments in a range are included when several intervention sets are defined, for example:

>= lower limit of intervention range
< upper limit of intervention range

Operands (and, or) may also be needed to combine ranges of different parameters. If different operands are used in the same intervention criterion, parentheses may be needed to ensure their correct interpretation. For example:

AADT >= 500 .AND. (ACRA >= 50 .OR. IRI >= 10)

is not the same as:

(AADT >= 500 .AND. ACRA >= 50) .OR. IRI >= 10

This can be overcome by only allowing the AND operand. If OR is needed, it can be provided as another intervention set. For the first example above, two sets would be made:

AADT >= 500 .AND. ACRA >= 50

AADT >= 500 .AND. IRI >= 10

Many parameters may also be used to exclude the use of a certain operation. As mentioned earlier, the presence of kerbs and gutters on an urban road might preclude the use of a thick overlay and the intervention criterion for an overlay may be of the form:

IRI >= 5 AND KERB = False

where KERB is a model parameter of Boolean type.

A3.4.3 Priorities

If two different interventions are found to apply to a particular works operation during analysis no problem is encountered - the operation is applied. If, however, two different operations meet their intervention criteria in the same year then the model must select only one if they are mutually exclusive. For this to happen all operations must be given a priority ranking. Normally more comprehensive operations will take higher priority, for example pavement reconstruction would take priority over overlay.

PART B. BITUMINOUS PAVEMENTS

This part of the document describes the modelling of the performance of bituminous pavements. The first section describes the modelling philosophy in HDM-4 for bituminous pavements, followed by a section detailing the pavement characteristics used as descriptors of bituminous pavements in the deterioration models. The following sections describe the deterioration models for the various distresses; cracking, ravelling, potholing, edge break, permanent deformation, roughness and finally pavement texture (texture depth and skid resistance). This is followed by a description of the works effects models.

B1. MODELLING PHILOSOPHY

B1.1 Model Forms and Independent Variables

The models used to predict the deterioration of bituminous pavements in HDM-4 have several common characteristics:

- individual types of deterioration are modelled rather than a composite index
- the deterioration models are of the structured empirical form described in Section A2.1
- deterioration models for a particular type of distress are interactive with other types of distress

The types of deterioration of a bituminous pavement can be categorised into cracking, surface disintegration, permanent deformation, longitudinal profile and friction. The development of these modes of deterioration may be dependent on a number of factors which can be broadly classed as pavement strength, materials properties, traffic loading and environment. Table B1-1 shows the distress types which are modelled and the independent variables which are used in the deterioration models.

Table B1-1
Types of distress and independent variables

Distress Mode	Distress Type	Pavement Strength	Materials Properties	Traffic Loading	Environment
Cracking	Structural	4	4	4	4
	Reflection	4		4	
	Transverse thermal		4		4
Disintegration	Ravelling		4	4	4
	Potholing	4	4	4	4
	Rutting – surface wear			4	4
	Edge break		4	4	4
Deformation	Rutting – structural	4	4	4	4
	Rutting – plastic flow		4	4	4
Profile	Roughness	4	4	4	4
Friction	Texture depth		4	4	
	Skid resistance		4	4	

Part A introduced the system of pavement classification used in HDM-4. The structure of a model used to predict the initiation or progression of a certain distress may be governed by surface type, base type or a combination of both (pavement type). In other cases the model structure is the same for all types of surfacing and base but the default model coefficients are dependent on surfacing or base type. In other cases the model structure and default coefficients are independent of both surfacing and base types. Table B1-2 summarises these relationships.

Table B1-2
Effect of pavement classification on deterioration models

Distress Mode	Distress Type	Surfacing Type	Base Type
Cracking	Structural	S	S
	Reflection	C	C
	Transverse thermal		C
Disintegration	Ravelling		C
	Potholing		
	Rutting – surface wear		
	Edge break	C	C
Deformation	Rutting – structural		C
	Rutting – plastic flow	C	
Profile	Roughness		
Friction	Texture depth	C	
	Skid resistance	C	

S – structure of model may change by pavement type
C – coefficients of model may change by pavement type

B1.2 Interaction Between Model Parameters

Pavement deterioration is a complex mechanism in which both external variables and distress modes interact. Pavement strength is influenced by the environment and the deterioration of the pavement itself, whilst the progression of deterioration is often dependent on the residual pavement strength.

The inclusion of all model interactions in one diagram presents a complicated and confusing picture; the dependence of particular distress types on other models is more clearly presented in the following flow diagrams.

As shown in Figure B1-1, structural cracking in particular has a recursive effect on pavement performance. Crack initiation and progression is a function of the structural strength of the pavement, while the pavement is weakened due to the presence of cracking and the consequent ingress of water to the unbound pavement layers.

Potholing is a secondary distress mechanism which derives from spalled cracks and ravelled areas. As shown in Figure B1-2, it is also dependent on traffic loading, pavement strength and environmental conditions.

Figure B1-3 shows how the structural component of rutting is dependent on other models including cracking.

The roughness model uses the output, directly or indirectly, from all other distress models as shown in Figure B1-4. Pavement roughness, combined with shoulder deterioration and edge break, provides the model for effective roughness on narrow pavements where road users are forced to use the shoulder to pass other vehicles (Figure B1-5).

Figure B1-1
Interaction between pavement strength and structural cracking

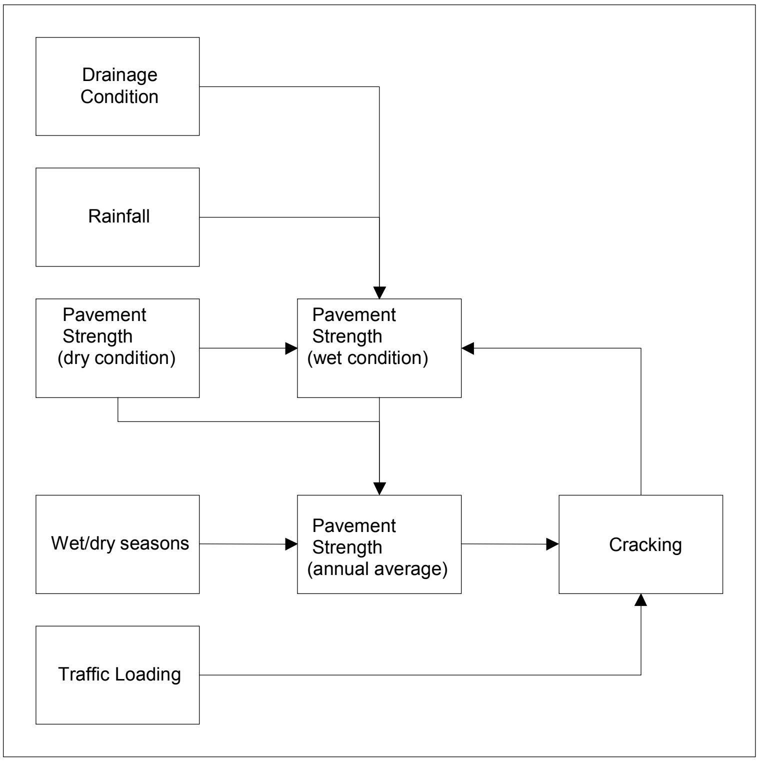

Figure B1-2
Dependence of potholing on other model parameters

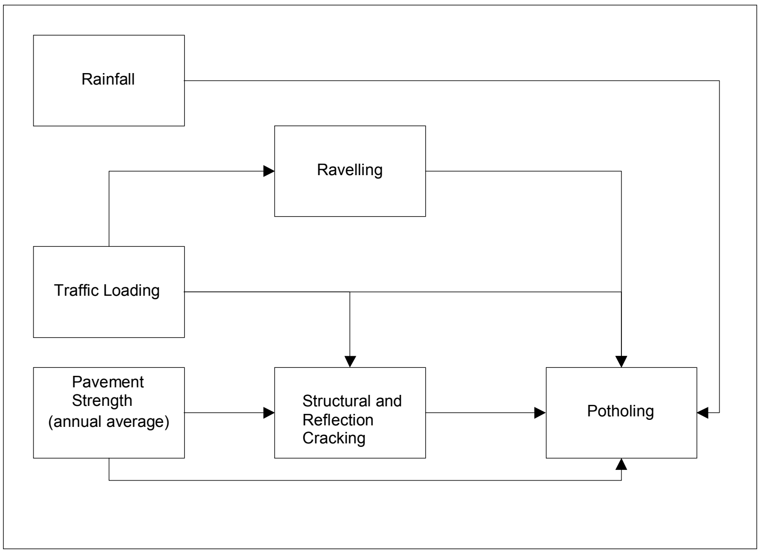

Figure B1-3
Dependence of structural rutting on other model parameters

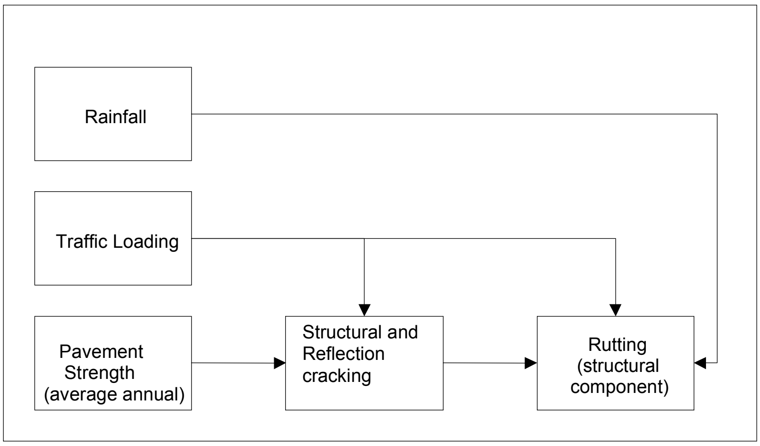

Figure B1-4
Dependence of roughness on other model parameters

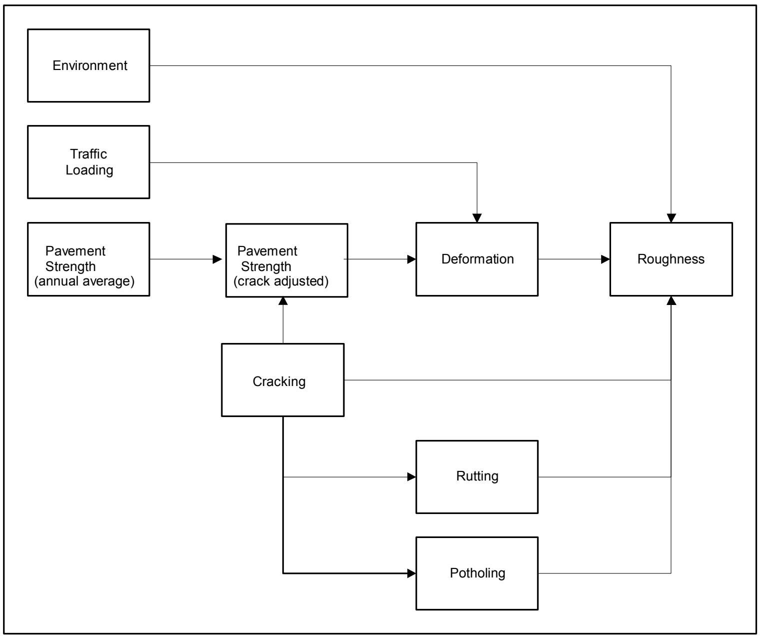

Figure B1-5
Shoulder deterioration, edge break and effective roughness

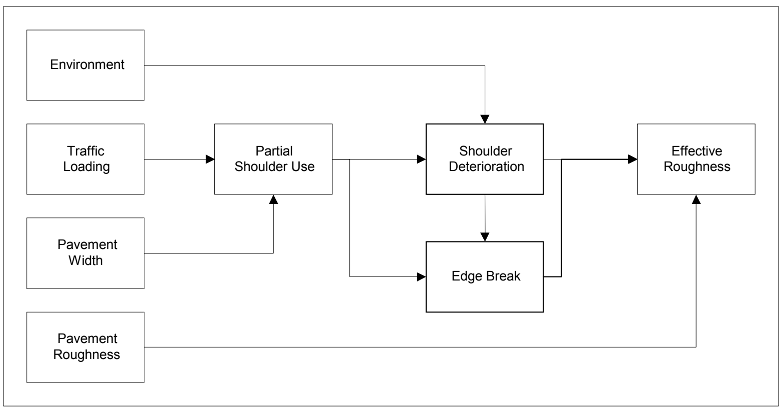

B1.3 Initiation and Progression Phases of Distress

Cracking, ravelling and potholing are modelled in two discrete phases. In the first, initiation, period the distress has not yet become manifest and the area is zero. After initiation the area gradually progresses; in the case of cracking and ravelling this follows a sigmoidal curve as shown in Figure B1-6.

Figure B1-6
Initiation and progression phases of distress

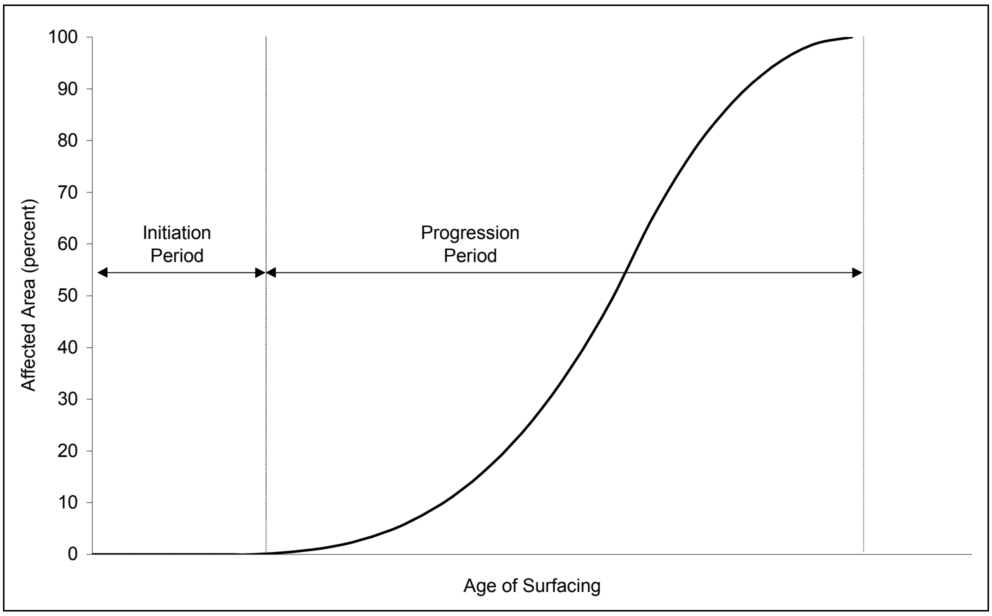

B1.4 Effect of Routine Maintenance

Section B13.2 describes a number of routine maintenance operations that affect the deterioration models described below. The routine operations are crack sealing, crack patching and surface patching of ravelled areas. These operations have a direct effect on the distress parameters – for example, after sealing an open crack, it becomes a sealed crack – and indirect effects on the interaction between parameters. The effects of these works on deterioration are based on the following principles:

- Crack sealing will not restore the loss of structural strength due to cracking of the asphalt layers, but will prevent ingress of water and hence loss of strength in the lower pavement layers.
- Crack patching will restore the structural strength of the asphalt layers and prevent ingress of water.
- Crack sealing and/or patching will not affect the progression of new cracks in the future.
- Sealed or patched cracks will not develop into potholes.
- Crack sealing will reduce roughness effects of cracking to half their unsealed value.
- Surface patching of ravelling will not affect future occurrence of new ravelling but will inhibit development of potholes.

In some of the deterioration and works effects relationships, it is necessary to distinguish between areas of distress that may have been sealed or patched and those that have remained untreated. Using wide structural cracking (ACW) as an example, the following acronyms are used.

ACWu	area of untreated wide structural cracking
ACWs	area of wide structural cracking that has been sealed
ACWp	area of wide structural cracking that has been patched
ACW	total area of wide structural cracking

For routine maintenance, there are three basic scenarios. Again using ACW as an example, these are described below.

i) If no routine maintenance (sealing or patching) has been carried out:

ACW = ACWu (ACWs = 0 & ACWp = 0)

ii) If routine maintenance of 100% of the distress area has been carried out:

a) Sealing 100% of distress area

ACW = ACWs (ACWu = 0 & ACWp = 0)

b) Patching 100% of distress area

ACW = ACWp (ACWu = 0 & ACWs = 0)

iii) If partial routine maintenance has been carried out:

a) Sealing > 0% but <100% of distress area

ACW = ACWu + ACWs (ACWp = 0)

b) Patching > 0% but <100% of distress area

ACW = ACWu + ACWp (ACWs = 0)

As in HDM-III, subscripts 'a' and 'b' are used to denote areas at the start and end of an analysis year respectively and 'd' in front of the acronym is used to denote the incremental change during the analysis year. For example:

$$ACW_b = ACW_a + dACW$$

where

ACW_a = area of wide structural cracking at start of analysis year
ACW_b = area of wide structural cracking at end of analysis year
dACW = incremental change in area of wide structural cracking during analysis year

B2. PAVEMENT CHARACTERISTICS

B2.1 Modified Structural Number

The concept of structural number was first introduced as a result of the AASHO Road Test (Highway Research Board, 1962) as a measure of overall pavement strength (AASHO, 1972). It is essentially a measure of the total thickness of the road pavement weighted according to the ‘strength’ of each layer and calculated as follows:

$$SN = \sum_{i=1}^{n} a_i h_i \qquad \text{. . . (B2.1)}$$

where

SN = structural number of the pavement
n = number of pavement layers
a_i = strength coefficient of the i^{th} layer
h_i = thickness of the i^{th} layer, in inches

In the original analysis of the AASHO Road Test the strength coefficients were treated as model parameters. The pavement performance data were analysed on the basis that sections of road with the same structural number should carry the same total traffic before reaching a defined terminal condition. After deriving the strength coefficients for the various materials, correlation studies were undertaken to relate the coefficients to the more usual engineering tests of material strength such as CBR for granular materials, unconfined compressive strength for cemented materials and Marshall stability for bitumen bound materials.

The AASHO Road Test was constructed on a single subgrade, therefore the effect of different subgrades could not be estimated and the structural number could not include a subgrade contribution. Pavements of a particular structural number but built on different subgrades will therefore not carry the same traffic to a given terminal condition. To overcome this problem and to extend the concept to all subgrades, a subgrade contribution was derived as described by Hodges et al, (1975) and a modified structural number defined as follows:

$$SNC = SN + 3.51 (\log_{10} CBR_s) - 0.85 (\log_{10} CBR_s)^2 - 1.43 \qquad \text{. . . (B2.2)}$$

where

SNC = modified structural number of the pavement
CBR_s = in-situ CBR of the subgrade

The modified structural number, SNC, was used in HDM-III. It has been used extensively and forms the basis for defining pavement strength in many pavement performance models.

B2.2 Adjusted Structural Number

Many road pavements cannot be divided easily into distinct roadbase and sub-base layers with a well-defined and uniform subgrade. Hence, when calculating the structural number according to the equation above, the engineer has to judge which layers to define as roadbase, which as sub-base, and where to define the top of the subgrade. For many roads this has proven quite difficult. There are often several layers that could be considered either as sub-bases or part of the subgrade, especially where capping layers or selected fill have been used. The simple summation over all the apparent layers allows the engineer to obtain almost any value of structural number since the value will depend on where the engineer assumes that the sub-base(s) end and the subgrade begins. In the past this problem has been addressed by simply limiting the total depth of all the layers that are considered to be road pavement. For example, a value of 700 mm was used in HDM-III. However, this is somewhat arbitrary, has not been used universally, and has led to unacceptably large errors in some circumstances.

The problem arises because the contributions of each layer to the structural number are independent of depth. This cannot be correct since logic dictates that a layer that lies very deep within the subgrade can have little or no influence on the performance of the road. To eliminate the problem, a method of calculating the modified structural number has been devised in which the contributions of each layer to the overall structural number decrease with depth. Essentially the contribution, $a_i h_i$ for each layer is reduced by means of a function, f, which decreases with depth.

In order to derive such a function, a conventional three-layer pavement was defined in which the sub-base and subgrade were of the same strength. In such a situation, the calculated modified structural number should be the same irrespective of the choice of depth for the sub-base/subgrade boundary and irrespective of the number and thicknesses of any arbitrary sub-bases that could be defined. In other words, the expression:

$$\sum_j \left[a_{3j}\, h_{3j} \, .f\left(\sum_{i=1}^{j-1} h_{3i} \right) \right] + SNG.f\left(\sum_{i=1}^{j} h_{3i} \right) \qquad ...(B2.3)$$

and its continuous form:

$$\int_0^h a_3\,(Z).f(Z).dZ + SNG.f(h) \qquad ...(B2.4)$$

should be independent of h and j,

where

j	=	number of sub-base layers
h_{3i}	=	thickness of sub-base layer i
f	=	a suitable function

A suitable functional form for *f* has been developed in such a way that this criterion is fulfilled (Rolt and Parkman, 2000). At the same time, the values of modified structural number obtained using the new method for straightforward three and four-layer pavements agree closely with the values obtained using the original form of the equation. The only constraint in using the new equation is that a minimum thickness of total sub-base of 200 mm must be defined. If the sub-base is thinner than this, or is absent, then the top of the subgrade must be redefined as sub-base.

The analysis also showed that the contribution to structural number of weak sub-base material (i.e. coefficient a_3) is not quite compatible with the contribution of the same strength material in the subgrade. To correct this small anomaly, the relationship between a_3 and the CBR of sub-base material has been modified slightly as follows:

$$a_3 = -0.075 + 0.184\,(\log_{10} CBR) - 0.0444\,(\log_{10} CBR)^2 \qquad ...(B2.5)$$

To distinguish the structural number derived from the original Modified Structural Number SNC (equation B2.2), the new structural number is called the Adjusted Structural Number SNP, (Rolt and Parkman, 2000). It is calculated as follows:

$$SNP_s = SNBASU_s + SNSUBA_s + SNSUBG_s \qquad \text{. . . (B2.6)}$$

$$SNBASU_s = 0.0394 \sum_{i=1}^{n} a_{is}\, h_i \qquad \text{. . . (B2.7)}$$

$$SNSUBA_s = 0.0394 \sum_{j=1}^{m} a_{js} \left\{ \left(\frac{b_0 \exp(-b_3 z_j)}{-b_3} + \frac{b_1 \exp(-(b_2+b_3) z_j)}{(b_2+b_3)} \right) - \left(\frac{b_0 \exp(-b_3 z_{j-1})}{-b_3} + \frac{b_1 \exp(-(b_2+b_3) z_{j-1})}{(b_2+b_3)} \right) \right\} \qquad \text{. . . (B2.8)}$$

$$SNSUBG_s = \left(b_0 - b_1 \exp(-b_2 z_m)\right) \left(\exp(-b_3 z_m)\right) \left[3.51 \log_{10} CBR_s - 0.85 (\log_{10} CBR_s)^2 - 1.43\right] \qquad \text{. . . (B2.9)}$$

where

SNP_s	=	adjusted structural number of the pavement for season s
$SNBASU_s$	=	contribution of surfacing and base layers for season s
$SNSUBA_s$	=	contribution of the sub-base or selected fill layers for season s
$SNSUBG_s$	=	contribution of the subgrade for season s
n	=	number of base and surfacing layers (i = 1, n)
a_{is}	=	layer coefficient for base or surfacing layer i for season s
h_i	=	thickness of base or surfacing layer i, in mm
m	=	number of sub-base and selected fill layers (j = 1, m)
a_{js}	=	layer coefficient for sub-base or selected fill layer j for season s
z	=	depth parameter measured from the top of the sub-base (underside of base), in mm
z_j	=	depth to the underside of the jth layer (z_0 = 0), in mm
CBR_s	=	in situ subgrade CBR for season s

The values of the model coefficients b_0 to b_3 are given in Table B2-1 and the values of the layer coefficients a_i and a_j are given in Table B2-2.

Equation B2.9 predicts negative values for the subgrade contribution below CBR values of 3. This is perfectly correct and merely reflects the fact that the subgrade is weaker than that of the AASHO Road Test for which the subgrade contribution is defined as zero. This is different to HDM-III where the subgrade contribution was set to 0 for CBR's less than 3.

Table B2-1
Adjusted structural number model coefficients

Pavement Type	b_0	b_1	b_2	b_3
All pavement types	1.6	0.6	0.008	0.00207

Table B2-2
Pavement layer strength coefficients

Layer	Layer Type	Condition	Coefficient
Surfacing	ST	Usually 0.2	a_i = 0.20 to 0.40
	AM	h_i < 30 mm, low stability and cold mixes	a_i = 0.20
		h_i > 30 mm, MR_{30} = 1500 MPa	a_i = 0.30
		h_i > 30 mm, MR_{30} = 2500 MPa	a_i = 0.40
		h_i > 30 mm, $MR_{30} \geq$ 4000 MPa	a_i = 0.45
Base	GB	Default	$a_i = (29.14\ CBR - 0.1977\ CBR^2 + 0.00045\ CBR^3)\ 10^{-4}$
		CBR > 70, cemented sub-base	$a_i = 1.6\ (29.14\ CBR - 0.1977\ CBR^2 + 0.00045\ CBR^3)\ 10^{-4}$
		CBR < 60, max. axle load > 80kN	a_i = 0
	AB, AP	Dense graded with high stiffness	a_i = 0.32
	SB	Lime or cement	$a_i = 0.075 + 0.039\ UCS - 0.00088(UCS)^2$
Sub-base		Granular	$a_j = -0.075 + 0.184(\log_{10} CBR) - 0.0444(\log_{10} CBR)^2$
		Cemented UCS > 0.7 MPa	a_j = 0.14

Source : Watanatada et al, (1987)

Notes:
1. The table reproduces information from the source, with the exception of the granular sub-base coefficient.
2. If a CBR value for a stabilised (lime or cement) layer is quoted, the corresponding granular coefficient should be used.
3. Unconfined Compressive Strength (UCS) is quoted in MPa at 14 days.
4. MR_{30} is the resilient modulus by the indirect tensile test at 30 °C.
5. CBR is the California Bearing Ratio.

B2.3 Seasonal and Drainage Effects

Even if no deterioration of the pavement takes place, the strength of a pavement still changes during the course of a year due to climatic effects. As rainfall is one of the more influential climatic factors affecting pavement strength, the magnitude of its effect will be influenced by the condition of the drainage. In HDM-4, both seasonal and drainage effects have been included in the modelling of road deterioration.

The road deterioration relationships model the incremental change in the condition of a pavement over a year. Therefore it is important that an average annual strength of the pavement is used in the models that incorporate SNP, rather than the strength measured at a point in time. In HDM-4, it is assumed that a year consists of a dry season and a wet season. The average annual strength is estimated from the strength of the pavement during the dry season and during the wet season, and the duration of each season.

The user is required to input the dry season SNP and the length of the dry season. Also the wet/dry season SNP ratio is required. The average annual SNP is derived as follows:

$$SNP = f_s\, SNP_d \qquad \text{. . . (B2.10)}$$

where

$$f_s = \frac{f}{\left[(1-d) + d(f^p)\right]^{1/p}} \qquad \text{. . . (B2.11)}$$

and

SNP = average annual adjusted structural number
SNP_d = dry season SNP
f = SNP_w / SNP_d ratio

d = length of dry season as a fraction of the year
p = exponent of SNP specific to the appropriate deterioration model (see Table B2-3)

Table B2-3
Values of exponent 'p' for calculating SNP

Distress	Model	p
Cracking	Initiation of Structural Cracking	2.0
Rut Depth	Initial Densification	0.5
	Structural Deformation	1.0
Roughness	Structural Component	5.0

If only one season's SNP value is available then the following relationship (Riley, 1996a & 1999a) should be used to calculate the wet/dry season SNP ratio. This relationship is also used to calculate the wet/dry season SNP ratio for each year of the analysis period, taking into account changes in the drainage and amount of potholing and cracking.

$$f = K_f \left[1 - \frac{(1 - \exp(a_0 MMP))}{a_1} (1 + a_2 DF_a)(1 + a_3 ACRAu_a + a_4 APOT_a) \right] \quad \ldots (B2.12)$$

where
f = SNP_w / SNP_d ratio
SNP_w = wet season SNP
SNP_d = dry season SNP
MMP = mean monthly precipitation, in mm/month
DF_a = drainage factor at start of analysis year
$ACRAu_a$ = total area of untreated cracking at start of analysis year, in per cent
$APOT_a$ = area of potholing at the start of the analysis year, in per cent
K_f = calibration factor for wet/dry season SNP ratio

The HDM-4 coefficient values a_0 to a_4 are given in Table B2-4.

Table B2-4
Coefficient values for the seasonal SNP ratio

Coefficient	a_0	a_1	a_2	a_3	a_4
Default value	-0.01	10	0.25	0.02	0.05

The drainage factor, DF, is a continuous variable whose value can range between 1 (excellent) and 5 (very poor), depending on the type of drain (Paterson, 1998). The user needs to input the type of drain (as listed in Table B2-5) and the condition of the drain as excellent, good, fair, poor or very poor.

The minimum (excellent) and maximum (very poor) values for DF suggested for various types of drain are given in Table B2-5. The value of DF for drains in a good, fair or poor condition is determined by linearly interpolating between these values.

In some instances there may be an absence of drains. In situations where a drain is required the value of DF ranges between 3 and 5, whereas in situations where a drain is unnecessary a value of 1 for DF is suggested.

Table B2-5
Range of drainage factor values

Drain Type	Drain Condition	
	Excellent DF_{min}	Very Poor DF_{max}
Fully lined and linked	1	3
Surface lined	1	3
V-shaped – hard	1	4
V-shaped – soft	1.5	5
Shallow – hard	2	5
Shallow – soft	2	5
No drain - but required	3	5
No drain - not required	1	1

The variation in the wet/dry ratio of SNP is illustrated in Figure B2-1 for a wet climate (rainfall of 200 mm/month), for ranges of cracking and drainage factors. Figure B2-1 illustrates that for very poor drainage (DF = 5) and large amounts of cracking, the wet season SNP is approximately half the value during the dry season, whereas the ratio increases to 0.9 for low levels of cracking and good drainage.

Figure B2-1
Seasonal variation in SNP

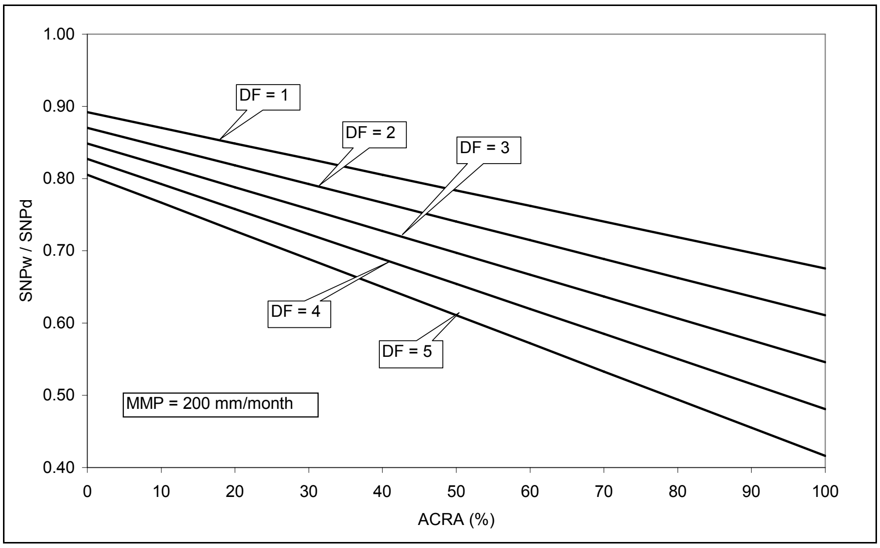

The condition of the drains will deteriorate unless they are maintained through, for example, routine maintenance. The incremental annual change in DF due to deterioration is given below; (the change in DF due to maintenance, ΔDF_w, is detailed in the Road Works Effects section – Section B13.2.4).

$$\Delta DF_d = \max\left\{0,\ \min\left[K_{ddf}\ ADDF,\ (DF_{max} - DF_a)\right]\right\} \qquad \text{. . . (B2.13)}$$

where

$$ADDF = \frac{(DF_{max} - DF_{min})}{\text{Drain Life}} \qquad \text{. . . (B2.14)}$$

and

ΔDF_d = annual change in DF due to deterioration
ADDF = annual deterioration of DF
Drain Life = life of the drain, in years (see Table B2-6)
K_{ddf} = calibration factor for drainage factor

Drain life has been expressed as a function of the terrain as given below. The HDM-4 coefficient values a_0 and a_1 are given in Table B2-6 (Morosiuk, 1998a) for the climatic categories classified by moisture (see Table A2-3 in Section A2.5.2).

$$\text{Drain life} = a_0 (1 + a_1 \, RF) \qquad \text{. . . (B2.15)}$$

where
RF = rise and fall, in m/km

Table B2-6
Coefficient values for drain life

Drain Type	Arid		Semi-arid		Sub-humid		Humid		Per-humid	
	a_0	a_1	a_0	a_1	a_0	a_1	a_0	a_1	a_0	a_1
Fully lined and linked	20	-0.0033	20	-0.0033	13	-0.0031	6	-0.0022	5	-0.0027
Surface lined	20	-0.0033	15	-0.0031	8	-0.0017	5	-0.0027	4	-0.0033
V-shaped - hard	20	-0.0033	15	-0.0031	10	-0.0027	6	-0.0022	4	-0.0033
V-shaped - soft	15	-0.0031	8	-0.0033	6	-0.0022	5	-0.0027	4	-0.0033
Shallow - hard	15	-0.0031	6	-0.0022	5	-0.0027	4	-0.0033	3	-0.0022
Shallow - soft	10	-0.0033	5	-0.0027	4	-0.0033	3	-0.0022	3	-0.0033
No drain - but required	3.5	-0.0029	2.5	-0.0027	2	-0.0033	1.5	-0.0044	1.5	-0.0044
No drain - not required	50	0	50	0	50	0	50	0	50	0

The rates of change in the drainage factor are illustrated in Figure B2-2 for a V-shaped drain in flat and steep terrain in arid and humid climates.

Figure B2-2
Drainage factor deterioration rates

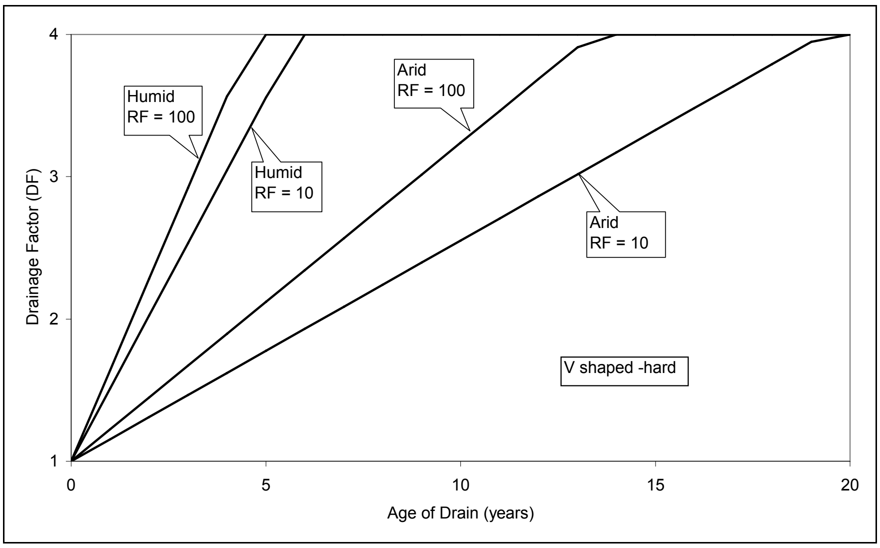

B2.4 Estimating SNP from Deflection Measurements

In HDM-4, the pavement strength can be input directly as SNP or derived through the layer thicknesses, strength coefficients and subgrade CBR as described above (equations B2.6 to B2.9). In addition, SNP can be estimated from either Benkelman beam or Falling Weight Deflectometer (FWD) deflection measurements. Methods of estimating SNP from these deflection measurements are outlined below.

B2.4.1 Benkelman beam deflections

The relationships used in HDM-4 to convert Benkelman beam deflections (DEF) to SNP values are based on those in HDM-III (Paterson, 1987). These relationships distinguish between pavements with cemented bases and those that are not cemented, as follows:

Base is not cemented

$$SNP_s = 3.2\,(DEF_s)^{-0.63} + dSNPK \qquad \text{. . . (B2.16)}$$

Base is cemented

$$SNP_s = 2.2\,(DEF_s)^{-0.63} + dSNPK \qquad \text{. . . (B2.17)}$$

where

$$dSNPK = 0.0000758\,\left[\min(63, ACX_a)HSNEW + \max\left(\min(ACX_a - PACX, 40), 0\right)HSOLD\right] \qquad \text{. . . (B2.18)}$$

and

DEF_s	=	Benkelman beam rebound deflection under 80 kN axle load, 520 kPa tyre pressure and 30°C average asphalt temperature for season s, in mm
dSNPK	=	reduction in adjusted structural number due to cracking
ACX_a	=	area of indexed cracking at start of analysis year, in per cent
PACX	=	area of previous indexed cracking in old surfacing, in per cent i.e. 0.62 (PCRA) + 0.39 (PCRW)
HSNEW	=	thickness of the most recent surfacing, in mm
HSOLD	=	total thickness of previous underlying surfacing layers, in mm

Benkelman beam deflection values are needed by some models. Where these are not user input, DEF values will be derived from SNP values using relationships based on those in HDM-III. These relationships are given below and illustrated in Figure B2-3.

Base is not cemented

$$DEF_s = 6.5\,SNPK_s^{-1.6} \qquad \text{. . . (B2.19)}$$

Base is cemented

$$DEFs = 3.5\,SNPKs-1.6 \qquad \text{. . . (B2.20)}$$

where

$$SNPK_s = SNP_s - dSNPK \qquad \text{. . . (B2.21)}$$

and

$SNPK_s$ = adjusted structural number due to cracking for season s

Figure B2-3
Relationship between SNP and DEF

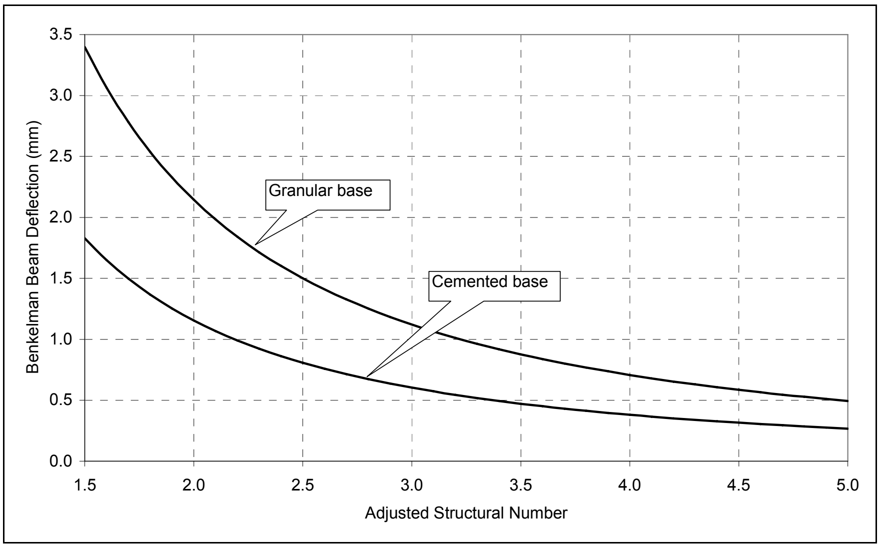

B2.4.2 FWD deflections

During the Highway Development and Management Technical Relationships Study (HTRS) in Malaysia (NDLI, 1995), existing methods of estimating SNP from FWD deflections were evaluated and recommendations made on the most appropriate procedures for use in HDM-4 (Rohde, 1995).

These recommended procedures have since been examined and shown that in certain circumstances anomalies may arise leading to inappropriate SNP values being derived from the FWD deflections. Therefore a method has not been included directly in the HDM-4 software. As an interim measure, the central FWD deflection at 566 kPa is used as the equivalent Benkelman beam deflection in the HDM-4 software. The equations in Section B2.4.1 are then used to calculate SNP.

A recent study by TRL (Rolt, 2000) examined the methods detailed in the NDLI report and other methods that have become more recently available. The methods examined in the TRL study were:

- AASHTO Method A1 - based on layer moduli from back analysis and coefficients scaled by AASHO Road Test moduli (*)
- AASHTO Method A2 - based on layer moduli from back analysis and coefficients calculated from regressions (*)
- AASHTO Method B - based on total pavement depth (*)
- Howard's method (*)
- Rohde's method (*)
- Jameson's method
- Asgari's method
- Salt's method
- Roberts' method
- Rolt's method

Some of the methods determine SNP directly, whilst others determine SN and the subgrade contribution, SNSG, separately. Some of the methods require knowledge of the pavement thickness, others require only the deflection values. The methods identified with an asterisk

(*) require either the thickness of the pavement or the thickness of the individual layers to be known and are therefore unlikely to be suitable for a network level survey and analysis.

The individual methods detailed below, estimate the 'immediate' values of SNP from FWD deflection bowls. The term 'immediate' means that the values are determined at the time and at the condition of measurement. They do not include any corrections for temperature.

AASHTO Method A1

AASHTO (1993) describes several methods of determining structural number. If all layer thicknesses within the pavement are known, back analysis can be used to determine the modulus (E) value of each pavement layer and of the subgrade. These E values can then be related to AASHTO layer coefficients and the SNP calculated, as follows.

For the subgrade:

$$E_{sg} = 17.6(CBR)^{0.68} \qquad \text{. . . (B2.22)}$$

and the subgrade contribution to structural number, SNSG, (Hodges et al, 1975) is given by:

$$SNSG = 3.51[\log_{10}(CBR)] - 0.85[\log_{10}(CBR)]^2 - 1.43 \qquad \text{. . . (B2.23)}$$

The layer coefficients can be related to the layer moduli and the strength coefficients of the road materials in the AASHO Road Test as follows:

$$a_i = a_0(E_i / E_0)^{1/3} \qquad \text{. . . (B2.24)}$$

where a_0 and E_0 are the AASHTO values shown in Table B2-7.

Table B2-7
AASHTO layer coefficients and E values

Layer Type	Layer Coefficient a_0	Layer Modulus E_0 (MPa)
Asphalt surfacing	0.44	3,100
Granular roadbase	0.14	207
Granular sub-base	0.11	104

The structural number (SN) of the constructed pavement layers is determined using equation B2.1 and finally SNP is given by:

$$SNP = SN + SNSG \qquad \text{. . . (B2.25)}$$

AASHTO Method A2

This method is the same as Method A1 except that equations relating the 'a' coefficients to the moduli (in MPa) are used instead of the $(E_i / E_0)^{1/3}$ scaling method as follows:

$$a_1 = 0.412 \log_{10}(E_1/1000) + 0.246 \qquad \text{. . . (B2.26)}$$

$$a_2 = 0.249 \log_{10}(E_2) - 0.439 \qquad \text{. . . (B2.27)}$$

$$a_3 = 0.227 \log_{10}(E_3) - 0.348 \qquad \text{. . . (B2.28)}$$

AASHTO Method B

The 1993 AASHTO Pavement Design Guide provided equations by which the FWD measurements can be used to estimate SNP values. The method operates in two stages. First, the subgrade resilient modulus, E_{sg}, is estimated by use of the outer deflection measurements. Then the central deflection is related to the structural number, the subgrade modulus, the pavement thickness, the applied load and the load plate radius. The equation is cubic in SN and is non-linear in other terms and is usually solved iteratively.

The subgrade modulus is given by an equation of the form:

$$E_{sg} = \frac{0.24(P)}{d_r(r)} \qquad \text{. . . (B2.29)}$$

SN is obtained by finding a value of SN that satisfies:

$$d_0 = 1.5(p)(a)\left[\frac{1}{E_{sg}\sqrt{1+\left(\frac{SN}{0.0045(a)\left(E_{sg}\right)^{1/3}}\right)^2}} + \left(\frac{\left(0.0045H\right)^3}{SN^3}\right) + \left(1-\frac{1}{\sqrt{1+\left(\frac{H}{a}\right)^2}}\right)\right] \qquad \text{. . . (B2.30)}$$

where

E_{sg}	=	subgrade modulus, in psi
d_0	=	measured deflection at the centre of the load plate, in ins
d_r	=	measured deflection at distance r from the centre of the load, in ins
P	=	applied dynamic load, in lbs
p	=	applied pressure, in psi
r	=	radial distance from load centre, in ins
H	=	pavement thickness, in ins
a	=	load plate radius, in ins

Several similar E_{sg} equations have been used, but the exact form is not particularly important in the light of the fact that many subgrades show non-linear stress/strain behaviour and, as a result, the subgrade modulus cannot be estimated very accurately. Indeed, the effective subgrade modulus of the Road Test soil was about one third of the value estimated by back analysis procedures that do not take account of non-linearity. When using Method B (and several other methods) E_{sg} was evaluated using each of the five outer deflection measurements and the lowest value of E_{sg} was adopted.

Howard's Method

Howard (1993) developed two equations for SN, one to be used if SN is less than 2.5 and the other for SN equal to or greater than 2.5. He also provided a formula for E_{sg}. The equations are as follows:

For SN < 2.5

$$SN = 0.88421 + 0.000866(H) + \frac{866.3272}{\left(d_0 - d_{1500}\right)} + \frac{22.6561}{d_{900}} \qquad \text{. . . (B2.31)}$$

For SN $\geq$ 2.5

$$SN = 0.9718761 + 0.002543(H) + \frac{785.4524}{\left(d_0 - d_{1500}\right)} + \frac{69.9904}{d_{900}} \qquad \text{. . . (B2.32)}$$

and

$$E_{sg} = 3036 - 1.661\left(d_{1500}\right) + 0.0108(H) - 0.015\left(d_0\right) - 2607.3\log_{10}\left(d_{900}\right) + 611.3\left[\log_{10}\left(d_{900}\right)\right]^2 \qquad \text{. . . (B2.33)}$$

where

d_0 = peak deflection at 700 kPa, in microns
d_{900} = deflection at 900 mm from centre of loading plate at 700 kPa, in microns
d_{1500} = deflection at 1500 mm from centre of loading plate at 700 kPa, in microns
H = total pavement thickness, in mm

Rohde's Method

Rohde (1994) analysed a large number of theoretical pavements, using the AASHTO Method A as the base against which to judge his results. His method requires deflections to be normalised to 566 kPa and then interpolated using the following formula to calculate equivalent deflections at radial distances of 1.5H and 1.5H + 450 mm.

$$d_x = d_a \frac{(r_x - r_b)(r_x - r_c)}{(r_a - r_b)(r_a - r_c)} + d_b \frac{(r_x - r_a)(r_x - r_c)}{(r_b - r_a)(r_b - r_c)} + d_c \frac{(r_x - r_a)(r_x - r_b)}{(r_c - r_a)(r_c - r_b)} \quad \text{. . . (B2.34)}$$

where
d_x = deflection at offset r_x
x = point at which the deflection is measured
d_i = deflection at sensor i
r_i = offset at sensor i
i = a, b, c are the three offsets closest to point x

Two indices are defined:

$$SIP = d_0 - d_{1.5H} \quad \text{. . . (B2.35)}$$

and

$$SIS = d_{1.5H} - d_{1.5H + 450} \quad \text{. . . (B2.36)}$$

Then SN is estimated from

$$SN = a_0\, SIP^{a1}\, H^{a2} \quad \text{. . . (B2.37)}$$

and E_{sg} is estimated using

$$E_{sg} = 10^{a3}\, SIS^{a4}\, H^{a5} \quad \text{. . . (B2.38)}$$

where
d_0 = peak deflection at 566 kPa, in mm
$d_{1.5H}$ = deflection at offset 1.5 H from centre of loading plate at 566 kPa, in mm
$d_{1.5H + 450}$ = deflection at offset 1.5 H + 450 mm from centre of loading plate at 566 kPa, in mm
H = total pavement thickness, in mm

The coefficients for Rohde's formulae are given in Table B2-8 and Table B2-9.

Table B2-8
Coefficients for SIP formula

Surface Type	a_0	a_1	a_2
AM	0.4728	-0.4810	0.7581
ST	0.1165	-0.3248	0.8241

Table B2-9
Coefficients for SIS formula

Pavement Thickness	a_3	a_4	a_5
H ≤ 380 mm	9.138	-1.236	-1.903
380 < H < 525	8.756	-1.213	-1.708
H > 525 mm	10.655	-1.254	-2.453

Jameson's Method

Jameson (1993) developed the following relationships for SN and subgrade CBR from analysis of a wide range of road pavements in Hong Kong using the AASHTO Method A as the base.

$$\log_{10}(CBR) = 3.264 - 1.018 \log_{10}(d_{900}) \qquad \text{. . . (B2.39)}$$

$$SN = 1.69 + \frac{842.8}{(d_0 - d_{1500})} - \frac{42.94}{d_{900}} \qquad \text{. . . (B2.40)}$$

where

d_0 = peak deflection at 700 kPa, in microns
d_{900} = deflection at 900 mm from centre of loading plate at 700 kPa, in microns
d_{1500} = deflection at 1500 mm from centre of loading plate at 700 kPa, in microns

Equations B2.39 and B2.40 are used with equations B2.23 and B2.25 to estimate SNP.

Asgari's Method

Asgari's method was based on analysis of simulated flexible pavements, created using the BISAR elastic multi-layer program. He derived an equation of the form:

$$SNP = a_0 (d_0)^{a1} \qquad \text{. . . (B2.41)}$$

where the values of a_0 and a_1 may be interpolated from Table B2-10

When using Asgari's formulae, E_{sg} was estimated using Howard's method and regression equations were used to interpolate between the values of the coefficients in Table B2-10. The measured central deflection was normalised linearly to a contact pressure of 700 kPa.

Table B2-10
Asgari's coefficients

Subgrade Modulus (MPa)	a_0	a_1
20	4.710	-1.828
50	2.738	-1.017
100	2.259	-0.905
200	1.844	-0.900

Salt's Method

Salt (1999) developed the following formula for SNP in New Zealand based on using the back-calculated elastic moduli and the AASHTO Method A as the reference.

$$SNP = 112(d_0)^{-0.5} + 47(d_0 - d_{900})^{-0.5} - 56(d_0 - d_{1500})^{-0.5} - 0.4 \qquad \text{. . . (B2.42)}$$

where d_0, d_{900} and d_{1500} are the deflections in microns at the radial offsets 0, 900 and 1500 mm respectively under a standard 40 kN FWD impact load.

Roberts' Method

Roberts (1999) developed the following formulae from data collected in the Philippines and in Australia. It is assumed that he also used the AASHTO Method A to compute the reference SNP.

$$SN = 12.992 - 4.167 \log_{10}(d_0) + 0.936 \log_{10}(d_{900}) \qquad \text{. . . (B2.43)}$$

where the deflections are in microns and the FWD impact pressure is 700 kPa.

The subgrade contribution is calculated from:

$$\log_{10}(CBR) = 3.264 - 1.018 \log_{10}(d_{900}) \qquad \text{. . . (B2.44)}$$

and equation B2.23.

Rolt's Method

Rolt (2000) compared the methods described above and also derived his own models.

i) Using experimental data from studies carried out in Indonesia, Rolt derived the following model:

$$SNP = 1.394 + 4.548(d_0)^{-0.5} - 1.76\left(\frac{d_{900} - d_{1200}}{d_{900}}\right)^{-0.5} \qquad \text{. . . (B2.45)}$$

ii) Rolt also developed a second model using data based on theoretical calculations of deflection bowls for the road structures described in TRL's design guide for roads in tropical regions, Overseas Road Note 31 (TRL, 1993).

$$SNP = -3.325 + 3.084(d_0)^{-0.5} + 0.726\left(\frac{d_0 - d_{300}}{d_0}\right)^{-0.5} - 2.169\left(\frac{d_{300} - d_{600}}{d_{300}}\right)^{-0.5} + 2.45\left(\frac{d_{900} - d_{1200}}{d_{900}}\right)^{-0.5} \qquad \text{. . . (B2.46)}$$

where d_0, d_{300}, d_{600}, d_{900} and d_{1200} are the deflections in mm at the radial offsets 0, 300, 600, 900 and 1200 mm respectively, under a standard 40 kN FWD impact load.

B2.5 Construction Quality

The initiation (and in some cases progression) of certain distresses can be more accurately attributed to problems in material handling, preparation, or construction than to structural weakness in the pavement. In HDM-III, two construction quality indicators were used; a surfacing construction quality indicator (CQ) and a construction compaction indicator (COMP).

The surfacing construction quality code (CQ) was used in HDM-III for modelling crack initiation for surface treatment on granular base and all ravelling models. Construction quality was defined as 0 if there were no identifiable surfacing construction defects and 1 if certain defects were known to exist. In the models where CQ was applied, a zero value had no effect on the model prediction while a CQ of 1 reduced the ravelling initiation period to approximately half. In the crack initiation model, the effect of a CQ value of 1 was most marked at high traffic volumes.

The indicator of the relative compaction in the base, sub-base and selected subgrade layers (COMP) was used in HDM-III to model rut depth in the first year after construction. Paterson (1987) defined relationships for estimating COMP as described below.

A reference profile of nominal compaction (C_{nom}) was defined as:

$$C_{nom,i} = 1.02 - 0.14\, z_i \qquad \text{. . . (B2.47)}$$

and the relative compaction achieved for each layer i (RC_i) was defined by:

$$RC_i = \min\left[1,\ C_i / C_{nom,i}\right] \qquad \text{. . . (B2.48)}$$

where

$$C_i = DD_i / MDD_i \qquad \text{. . . (B2.49)}$$

and

C_i = compaction of layer i
DD_i = in situ dry density of layer i
MDD_i = maximum dry density of material in layer i determined in the laboratory to the relevant compaction standard
$C_{nom,i}$ = nominal specification of compaction to be achieved in layer i with respect to the relevant standard, as a fraction
RC_i = relative compaction, i.e. the ratio of the compaction measured in the field to the nominal compaction, as a fraction
z_i = depth at bottom of layer i, in metres

The relative compaction index for the full pavement (COMP) was then defined as the average relative compaction weighted by layer thickness, over a 1 metre depth as follows:

$$COMP = \sum_{i=2}^{n} RC_i \left(H_i \Big/ \sum_{i=2}^{n} H_i \right) \qquad \text{. . . (B2.50)}$$

where

H_i = thickness of layer, in mm

In HDM-4 the concept of an indicator for construction defects has been extended by using parameters that are continuous variables for the surfacing, the base and relative compaction of the layers. These three indicators are:

- CDS - construction defects indicator for bituminous surfacings
- CDB - construction defects indicator for the base
- COMP - relative compaction of the base, sub-base and selected subgrade layers

CDS is a factor indicating the general level of binder content and stiffness relative to the optimal material design for the specified bituminous mixture. It is used as an indicator to illustrate whether a bituminous surfacing is prone to cracking and ravelling (low value of CDS), or prone to rutting through plastic deformation (high value of CDS).

CDS is a continuous variable, ranging in value between 0.5 and 1.5 as shown in Table B2-11. The HDM-4 default value of CDS is 1.0, i.e. a normal mix with the optimal binder content. Intermediate values are chosen by judgement.

Table B2-11
Construction defects indicator for bituminous surfacings – CDS

Surface Condition		CDS
Dry (Brittle)	nominally about 10% below design optimal binder content	0.5
Normal	optimal binder content	1.0
Rich (Soft)	nominally about 10% above design optimal binder content	1.5

The base construction defects indicator CDB, is a continuous variable ranging between 0 (no construction defects) and 1.5 (several defects). It is used in the potholing models. The type of defects that should be considered in setting a value of CDB are given in Table B2-12. Each of these defects can be assigned a value between 0 and 0.5 and used to estimate the overall CDB value for the pavement (maximum 1.5). The HDM-4 default value of CDB is 0 (no defects).

Table B2-12
Construction defects indicator for the base - CDB

Construction Defect	CDB
Poor gradation of material	0.5
Poor aggregate shape	0.5
Poor compaction	0.5

In HDM-4, COMP is as defined in HDM-III and is used in predicting the initial densification and structural deformation components of the rut depth model. As detailed earlier, Paterson (1987) gives relationships for calculating COMP, but it is proposed that users are also able to estimate it based on the values in Table B2-13.

Table B2-13
Relative compaction values - COMP

	Relative Compaction COMP (per cent)
Full compliance in all layers	100
Full compliance in some layers	95
Reasonable compliance in most layers	90
Poor compliance in most layers	85

B3. CRACKING

B3.1 Introduction

All bituminous pavements crack at some stage of their lives. The direct effects of cracking, as perceived by road users, is minimal; the contribution of cracking to ride quality is small and cracking has few safety implications. What concerns highway engineers are the indirect effects of cracking. One function of a bituminous surfacing is waterproofing, to prevent ingress of water to lower pavement layers with consequent reduction in their strength. Cracking of the surfacing reduces the effectiveness in this regard. Where the bound layers form a significant part of the pavement structure, cracking also directly weakens those layers. Also, if allowed to progress unchecked, cracks increase in severity, spall and become potholes – a distress very noticeable to road users.

Because of its secondary effects, cracking is, in many countries, an important criterion for maintenance intervention, especially where pavement construction comprises unbound base with thin surfacings. Prediction of its occurrence is thus an essential part of pavement performance modelling and has been a major part of many research programmes. Unfortunately, cracking is the most complex of pavement distress modes and the most difficult to model:

- it is not easy to measure using consistent, automated methods
- definition of cracking comprises many parameters, rather than a single one as in the case of mean rut depth
- cracking can have many causes, often inter-related

This document does not attempt to reproduce in detail all the research and resulting models that have been derived over the years, but to present the salient facts about the measurement and mechanisms of cracking and the performance models recommended for use in HDM-4.

B3.2 Measurement of Cracking

The procedures used for measuring and recording cracking data have been frequently modified, reflecting the improved understanding of cracking mechanisms and the individual data needs of each agency. As a result, there are numerous crack measurement procedures used world-wide, with no accepted standard for measuring and reporting cracking data. The need to develop a unified approach for the measurement and reporting of cracking is becoming increasingly important as attempts are made to standardise automated data collection equipment and predictive models for world-wide use.

Some methods of crack measurement require the observer to make a judgement on the cause of the crack (fatigue, thermal, etc), but this is obviously undesirable and does not lend itself to automated data collection. Crack measurement should express what can be observed on the road surface and not attempt to infer the type of crack mechanism.

Paterson (1994) defines the following five attributes used to characterise cracking:

- **Extent**: The area of the pavement covered by cracking, defined by the perimeter bounding all of the area covered by a set of cracks. Expressed in units of either area or as a percentage of the total pavement area.
- **Severity**: A measure of the crack width. It is either defined as the average width of the crack or as a class of crack (e.g. high/low or wide/narrow).

- **Intensity**: The length of cracks per unit area (e.g. m/m^2). Sometimes expressed as crack spacing.
- **Pattern**: This identifies the crack type through the orientation and interconnectedness of the cracks. Typical cracking patterns include crocodile, block and transverse.
- **Location**: This defines the part of the pavement that is cracked. It includes such identifiers as wheelpath, between wheelpaths, edge, and random.

To the above might be added a further attribute; whether the cracks have been sealed, a topic addressed later in this document in the context of works effects.

The most common cracking attributes considered are type, extent, and severity. These three attributes are found in many standardised distress identification procedures, including the World Bank's HDM-III model (Paterson, 1987), the pavement condition index (PCI) procedure (Shahin, et al, 1977), and the SHRP LTPP Distress Identification Manual (SHRP, 1993). Paterson (1994) makes a strong argument for a universal cracking indicator, a single cracking numeric that considers extent, intensity, and severity (through the mean crack width) with the inclusion of modifiers to identify type and location.

One early method employed to standardise crack measurements was used at the AASHO Road Test (Highway Research Board, 1962). This classification was later used by the Texas DOT as part of their Flexible Pavement Design System (Lytton, et al, 1982) and modified for use in the Brazil-UNDP road cost study (GEIPOT, 1982). Paterson (1987) used it as the basis of the formulation of the HDM-III cracking models.

The Brazil study (GEIPOT, 1982) identified cracking by type, severity (class), and extent (area) as follows:

Severity	Class 1:	cracks ≤ 1 mm wide
	Class 2:	cracks 1 to 3 mm wide
	Class 3:	cracks > 3 mm wide without spalling
	Class 4:	spalled cracks
Extent	The sum of rectangular cracked areas reported as a percentage of the total section surface area. For linear cracks, the area was defined by a 0.5 metre wide strip extending the length of the crack.	
Pattern	Crocodile, irregular, block, transverse, longitudinal	

Paterson (1987) defined a cumulative numeric, CR_i, which represents the sum of all areas of cracking with a severity of at least class i as follows:

$$CR_i = \sum_{j=i}^{4} CL_j \qquad \text{. . . (B3.1)}$$

where

CL_j = area cracked of class j, j = 1 to 4

CR_i = cracked area numeric of level i

In HDM-III, CR_2 represented the area of 'all' cracking (the sum of classes 2, 3 and 4) and CR_4 represented the area of 'wide' cracking (class 4 only). Class 1 (hairline cracks) was omitted from the modelling because it was considered as difficult to observe (being visible under some conditions and not under others) and has little mechanical impact on pavement behaviour. HDM-III thus omits the pattern attribute and models only extent and severity.

As the use of separate indices for each severity level of cracking proliferates the number of predictive relationships to be both estimated and applied, an index of cracking, CRX. combining all severities, was defined in HDM-III as follows:

$$CRX = \sum_{i=1}^{4} \left(\frac{(i)\, CL_i}{4} \right) \qquad \text{. . . (B3.2)}$$

i.e.

$$CRX = \frac{(CR_1 + CR_2 + CR_3 + CR_4)}{4} \qquad \text{. . . (B3.3)}$$

where

CRX = area of indexed cracking, in per cent of total surfacing area

As a practical device, to further reduce the number of basic cracking numerics needed to two, CRX was estimated from CR_2 and CR_4 in HDM-III as follows:

$$CRX = 0.62\, CR_2 + 0.39\, CR_4 \qquad \text{. . . (B3.4)}$$

The guidelines for recording cracking on long term pavement performance sections in the Strategic Highway Research Program (SHRP, 1993) use crack pattern, extent and severity as follows:

Severity	**Low**:	Cracks with mean width ≤ 6 mm or sealed cracks with sealant material in good condition.
	Medium:	Cracks with mean width > 6 mm and ≤ 19 mm; or any crack with a mean width ≤ 19 mm and adjacent low severity random cracking.
	High:	Cracks with a mean width > 19 mm; or any crack with a mean width ≤ 19 mm and adjacent to moderate to high severity random cracking.
Extent	m^2 for crocodile, block and map cracking; linear metres for transverse and longitudinal	
Pattern	Crocodile, irregular, block, transverse, longitudinal, map	

It will be noted that the definition of a “wide” crack differs considerably between HDM-III and SHRP – 3 mm against 19 mm.

B3.3 Cracking Mechanisms

For reasons given above, the raw cracking data given by a road condition survey does not directly identify the case of the cracking, but for modelling purposes the cracking mechanisms must be identified and, where possible, discretely modelled. The following cracking mechanisms are the most common:

- fatigue
- ageing
- reflection
- thermal
- shrinkage
- shear

Fatigue cracking has received the most attention, especially in terms of mechanistic modelling. It is also the basis for many pavement design methods. Fatigue cracks normally appear as a crocodile pattern in the wheelpaths and are the result of cumulative traffic loading. The development of this type of cracking is related to pavement structure, materials properties and traffic loading.

Age cracking is caused by the change in property of bituminous binders over time. Oxidation of the binder through exposure to air and heat causes it to become harder and more brittle to the point where it can no longer accommodate the strains caused by daily temperature variations and cracks occur. The crack pattern is typically of irregular or map pattern and affects the whole area of the pavement.

Reflection cracking is the term used to describe cracks in a new surface layer that form immediately above, or very close to, any cracks that exist in the underlying surface. Eventually the pattern of these cracks tends to mirror that of the original cracks hence the term ‘reflection cracks’. The rate of reflection cracking depends principally on the thickness of the new surfacing, but traffic loading, climatic variables, the strength and surface condition of the original pavement prior to overlay, and the characteristics of the overlay material itself are also contributory factors. The formation of reflection cracks can be retarded through the use of crack relieving layers or geomembranes, but the only satisfactory methods of eliminating it completely are removal of the original cracked layer prior to resurfacing or the application of a very thick overlay.

Thermal cracking, like age cracking, is caused by binder stiffening and temperature variations. This mechanism is most common in continental climates with hot summers and cold winters. It most commonly appears as a regularly spaced transverse pattern but can be longitudinal near the centre of the road.

Shrinkage cracks are a form of reflection cracking where shrinkage cracks in the base are propagated through the bituminous surfacing. This normally occurs with cement or lime stabilised bases and the pattern may be block, transverse or longitudinal.

Shear cracks typically appear as a longitudinal pattern near the pavement edge and are caused by shear failure in the underlying layer(s) due to poor shoulder support, drainage or settlement of the embankment.

As shown in Table B3-1, the crack pattern visible to the observer may be the result of several mechanisms and may be difficult to interpret in the modelling process.

Table B3-1
Matrix of crack patterns and mechanisms

Crack Mechanism	Crack Pattern					
	Crocodile	Block	Map	Transverse	Longitudinal	Irregular
Fatigue	✔					
Ageing			✔			
Reflection	✔	✔	✔	✔	✔	✔
Thermal				✔	✔	
Shrinkage		✔		✔	✔	
Shear					✔	

B3.4 Modelling Cracking in HDM-III

The HDM-III cracking models were developed using data collected during the Brazil-UNDP study over the period 1977 to 1982. Descriptions of the test sections used in this study are given in Table B3-2. Greater detail is provided on specific characteristics of these pavements by Paterson (1987).

Separate relationships were derived for ‘all’ cracking and ‘wide’ cracking. As with other distresses in HDM-III, cracking was modelled as having two distinct phases: the time to the development of the distress (the initiation phase) and the progression phase. This two phase approach offers useful information for pavement management purposes, particularly in the situation where the initiation of one distress contributes to initiation or progression of others. Modelling distresses in two distinct phases also has the advantage that there are essentially two opportunities to calibrate the model. Once cracking has initiated one proceeds directly to the progression model, in effect resetting the prediction to zero rather than compounding any errors.

Table B3-2
Characteristics of sections used in the development of the cracking model

Pavement Type	Number of Sections	Range of Surfacing Age, years	Range of Total Surfacing Thickness, mm	Cumulative Traffic Loading MESA	Traffic Volume veh/day
AC on granular base	30	1.6 - 2.0	20 – 103	0.0001 - 4.7	70 – 4800
Chip seal (DBST) on granular base	46	2.7 - 21.0	20 – 50	0.005 - 5.16	100 – 2300
Bituminous surface on cemented base	11	1.6 - 19.4	10 – 40	0.09 - 1.94	300 – 2600
Bituminous overlay on granular base	23	0.2 - 15.0	37 – 187	0.03 - 7.14	360 – 6000
Reseal (chip) on granular base	7	0 - 4.0	43 – 75	0.016 - 0.75	450 – 4500
Reseal (slurry)	32	0 - 13.2	20 – 236	0.001 - 1.16	320 – 4500

B3.4.1 Cracking Initiation

Crack initiation is said to occur when 0.5 per cent of the surface area is cracked. The cracking initiation prediction has a probabilistic form in which the predicted value represents an average and the actual values are distributed about the mean.

Paterson noted that the time to crack initiation was largely affected by ageing, traffic loading, and pavement stiffness. The explanatory variables that emerged from the analysis of the cracking data were traffic (YE4) and modified structural number (SNC). For surface treatments constructed over cracked surfaces, the time to crack initiation was very short and was modelled as a function of thickness or given as a constant. Other explanatory factors that were found to be significant included surface thickness, per cent binder, and binder film thickness. Models were developed based on these other predictive variables; however, the predictive models based on SNC and YE4 were the ones used in HDM-III. They not only explained the performance of the Brazil sections better, they were the easiest to use in a broad range of applications.

The cracking initiation models were further modified by two factors, a user-specified crack initiation factor, K_{ci} (for which the default value was 1.0) and the occurrence distribution factor, F_c, which could be used to break a section into three subsections categorised as weak, medium, and strong. The default in HDM-III was for sections of medium distress, represented by a value of 1.0 for F_c. The crack initiation models further provided the ability to extend the initiation time by taking into consideration the application of preventive treatment. This was done with the crack retardation time factor, CRT (see Section B13.3.3.1). Its default value was zero.

The general form of the cracking initiation model for all cracking is as follows:

$$TYCRA = K_{ci} (F_c\, CRKREL + CRT) \quad \text{. . . (B3.5)}$$

where

TYCRA	=	time to initiation of all cracking, in years
CRKREL	=	appropriate cracking initiation relationship
K_{ci}	=	calibration factor for initiation of cracking (default = 1.0)
F_c	=	occurrence distribution factor (default = 1.0)
CRT	=	crack retardation factor (default = 0)

The appropriate cracking initiation relationships (CRKREL) are detailed in Watanatada, et al, (1987). These relationships have been retained in HDM-4 and are reproduced in Section B3.5.

The model for predicting the initiation of wide cracking, TYCRW, was based on the initiation of narrow cracking and had the following form:

$$TYCRW = K_{ci} (a_0 + a_1\, TYCRA) \quad \text{. . . (B3.6)}$$

The coefficients a_0 and a_1 were defined for the different pavement types (Watanatada, et al, 1987) and have also been retained in HDM-4 (see Section B3.5).

B3.4.2 Cracking Progression

Paterson derived both time-based and traffic-based cracking progression models. Although the traffic-based model was "generally superior" it was not applicable for all surface types and it was the time-based model that was incorporated into HDM-III. This approach is more generally appropriate where specific performance data that would support a different mode of cracking progression is not available. After considering a number of different forms of the model, it was decided to model the progression of cracking as a sigmoidal (S-shaped) function as follows (Paterson, 1987).

The area of cracking at time t, CR_{it}, is derived as follows:

$$CR_{it} = (1 - z)\, 50 + z\, [z\, a_0\, a_1\, t_{ci} + z\, 0.5^{a1} + (1 - z)\, 50^{a1}]^{1/a1} \quad \text{. . . (B3.7)}$$

The incremental change in area of cracking during the period δt, dCR_{it}, is derived as follows:

$$dCR_{it} = z\, z\, \{[\, z\, z\, a_0\, a_1\, \delta t + SCR_{it}^{a1}]^{1/a1} - SCR_{it}\, \} \quad \text{. . . (B3.8)}$$

and the time taken to reach area CR_{it} is derived as follows:

$$t_{ci} = [(1 - z\, z)\, 50^{a1} + z\, z\, SCR_{it}^{a1} - 0.5^{a1}] / a_0\, a_1 \quad \text{. . . (B3.9)}$$

where

CR_{it}	=	area of cracking at time t, in per cent
SCR_{it}	=	min (CR_{it}, 100 – CR_{it})
dCR_{it}	=	incremental change in area of cracking during the period δt, in per cent
t_{ci}	=	time since crack initiation in time-based model, in years
	=	traffic since crack initiation in traffic-based model, in million ESA
δt	=	increment of time in time-based model, in years
	=	increment of traffic loading in traffic-based model, in million ESA
z	=	1, if $t_{ci} \le t_{50}$, otherwise z = -1
t_{50}	=	$(50^{a1} - 0.5^{a1}) / a_0\, a_1$; i.e. time to 50% area

Paterson (1987) details the values of the coefficients a_0 and a_1 and the model statistics. The values of a_0 and a_1 have been reproduced in Table B3-3.

The time-based cracking progression model incorporated into HDM-III (Watanatada, et al, 1987) also included a calibration factor K_{cp} (default of 1.0), and CRP, which was the retardation of cracking progression due to preventive treatment (defined as 1 - 0.12 CRT).

Table B3-3
Coefficient values for the cracking progression models

Cracking class and surfacing	Time-based model		Traffic-based model	
	a_0	a_1	a_0	a_1
All Cracking				
Asphalt Concrete	1.84	0.45	450 $SNC^{-2.27}$	0.65
Surface Treatment	1.76	0.32	1760 $SNC^{-3.23}$	0.28
Cemented Base	2.13	0.36	2.43 $DEF^{0.64}$ $CMOD^{0.90}$	0.41
Asphalt Overlays	1.07	0.28		
Reseals and Slurry Seals	2.41	0.34		
Wide Cracking				
Asphalt Concrete	2.94	0.56	718 $SNC^{-2.52}$	0.72
Surface Treatment	2.50	0.25	4520 $SNC^{-3.19}$	0.39
Cemented Base	3.67	0.38	3.93 $DEF^{0.59}$ $CMOD^{0.74}$	0.30
Asphalt Overlays	2.58	0.45		
Reseals and Slurry Seals	3.4	0.35		

Source: after Paterson (1987)
Note: DEF = Benkelman beam deflection under 80 kN single axle load, in mm
CMOD = resilient modulus of cemented base, in GPa

B3.5 Modelling Cracking in HDM-4

Six crack mechanisms were described in Section B3.3, of which shrinkage and shear cracking are phenomena that can only be explained by, maybe localised, construction or maintenance defects. Such events do not lend themselves to predictive modelling. HDM-III modelled fatigue and ageing mechanisms with some attempt, in the initiation phase, to incorporate reflection cracking.

The models presented below for HDM-4 attempt to improve on the HDM-III models in the following respects:

- inclusion of both traffic and ageing mechanisms in the progression phase of structural cracking
- separate models for initiation and progression of reflection cracks
- a model for the initiation and progression of transverse thermal cracking

B3.5.1 Structural Cracking

Structural cracking is modelled as 'all' and 'wide' cracking (as defined by Paterson, 1987), based on the relationships in HDM-III.

B3.5.1.1 Initiation of All Structural Cracking

The relationships for predicting the time to initiation of all structural cracking on pavements with a stabilised base are of a different form to the relationships for pavements with other types of base. Also the models distinguish between pavements that are original surfacings and those that have been resealed or overlaid. For reseals and overlays, the amount of cracking in the previous bituminous layer prior to resurfacing is taken into account. In the latter category, a further distinction is made between certain types of surface material. A separate relationship is provided for surface types CM (cold mix), SL (slurry seal) and CAPE (cape seal).

In the HDM-4 relationships, the construction defects indicator for bituminous surfacings, CDS has been introduced (see Section B2.5). The use of this variable will enable the user to distinguish between pavements that are more likely to crack and those that are more prone to plastic deformation (see Section B8.4.3) and therefore less likely to crack.

The HDM-4 relationships for predicting the time to initiation of all structural cracking are as follows:

Stabilised Base

if HSOLD = 0 (i.e. Original Surfacings)

$$ICA = K_{cia}\left\{CDS^2\, a_0 \exp\left[a_1 HSE + a_2 \log_e(CMOD) + a_3 \log_e(DEF) + a_4 (YE4)(DEF)\right] + CRT\right\} \quad \text{. . . (B3.10)}$$

if HSOLD > 0 (i.e. Overlays or Reseals)

$$ICA = K_{cia}\left\{CDS^2\left[(0.8\,KA + 0.2\,KW)(1 + 0.1\,HSE) + (1 - KA)(1 - KW)\, a_0 \exp\left(a_1 HSE + a_2 \log_e(CMOD) + a_3 \log_e(DEF) + a_4 (YE4)(DEF)\right)\right] + CRT\right\} \quad \text{. . . (B3.11)}$$

All Other Bases

if HSOLD = 0 (i.e. Original Surfacing)

$$ICA = K_{cia}\left\{CDS^2\, a_0 \exp\left[a_1 SNP + a_2 (YE4/SNP^2)\right] + CRT\right\} \quad \text{. . . (B3.12)}$$

if HSOLD > 0 (i.e. Overlays or Reseals)

i) All surface materials except CM, SL and CAPE

$$ICA = K_{cia}\left\{CDS^2\left[\max\left(a_0 \exp[a_1 SNP + a_2 (YE4/SNP^2)] \max(1 - PCRW/a_3, 0), a_4 HSNEW\right)\right] + CRT\right\} \quad \text{. . . (B3.13)}$$

ii) Surface materials - CM, SL and CAPE

$$ICA = K_{cia}\left\{CDS^2\left[\max\left(a_0 \exp(a_1\, SNP + a_2 (YE4/SNP^2)) \max(1 - PCRA/a_3, 0), a_4\right)\right] + CRT\right\} \quad \text{. . . (B3.14)}$$

where

ICA	=	time to initiation of all structural cracks, in years
CDS	=	construction defects indicator for bituminous surfacings
YE4	=	annual number of equivalent standard axles, in millions/lane
SNP	=	average annual adjusted structural number of the pavement
DEF	=	mean Benkelman beam deflection in both wheelpaths, in mm
CMOD	=	resilient modulus of soil cement, in GPa (range between 0 and 30 GPa for most soils)
HSNEW	=	thickness of the most recent surfacing, in mm
HSOLD	=	total thickness of previous underlying surfacing layers, in mm
PCRA	=	area of all cracking before latest reseal or overlay, in per cent
PCRW	=	area of wide cracking before latest reseal or overlay, in per cent
KW	=	min [0.05 max (PCRW - 10, 0), 1]
KA	=	min [0.05 max (PCRA - 10, 0), 1]
HSE	=	min [100, HSNEW + (1 - KW) HSOLD]

K_{cia} = calibration factor for initiation of all structural cracking
CRT = crack retardation time due to maintenance, in years (see Road Works Effects - Section B13.3.3.1)

The coefficient values a_0 to a_4 for the initiation of all structural cracking are given in Table B3-4.

Table B3-4
Coefficient values for the initiation of all structural cracking models

Pavement Type	Surface Material	HSOLD Value	Equ^n	a_0	a_1	a_2	a_3	a_4
AMGB	All	0	B3.12	4.21	0.14	-17.1		
	All except CM	> 0	B3.13	4.21	0.14	-17.1	30	0.025
	CM	> 0	B3.14	13.2	0	-20.7	20	1.4
AMAB	All	0	B3.12	4.21	0.14	-17.1		
		> 0	B3.13	4.21	0.14	-17.1	30	0.025
AMAP	All	> 0	B3.13	4.21	0.14	-17.1	30	0.025
AMSB	All	0	B3.10	1.12	0.035	0.371	-0.418	-2.87
		> 0	B3.11	1.12	0.035	0.371	-0.418	-2.87
STGB	All	0	B3.12	13.2	0	-20.7		
	All except SL, CAPE	> 0	B3.13	13.2	0	-20.7	20	0.22
	SL, CAPE	> 0	B3.14	13.2	0	-20.7	20	1.4
STAB	All	0	B3.12	13.2	0	-20.7		
	All except SL, CAPE	> 0	B3.13	4.21	0.14	-17.1	20	0.12
	SL, CAPE	> 0	B3.13[1]	4.21	0.14	-17.1	30	0.025
STAP	All	> 0	B3.13	4.21	0.14	-17.1	20	0.12
STSB	All	0	B3.10	1.12	0.035	0.371	-0.418	-2.87
		> 0	B3.11	1.12	0.035	0.371	-0.418	-2.87

Note: 1 - For STAB, equation B3.13 is used for surface material types SL and CAPE

The time to initiation of all structural cracking for an AMGB pavement is illustrated in Figure B3-1 and for an STGB pavement in Figure B3-2 for a range of traffic loadings and pavement structural strengths.

Figure B3-1
Time to initiation of all structural cracking – AMGB

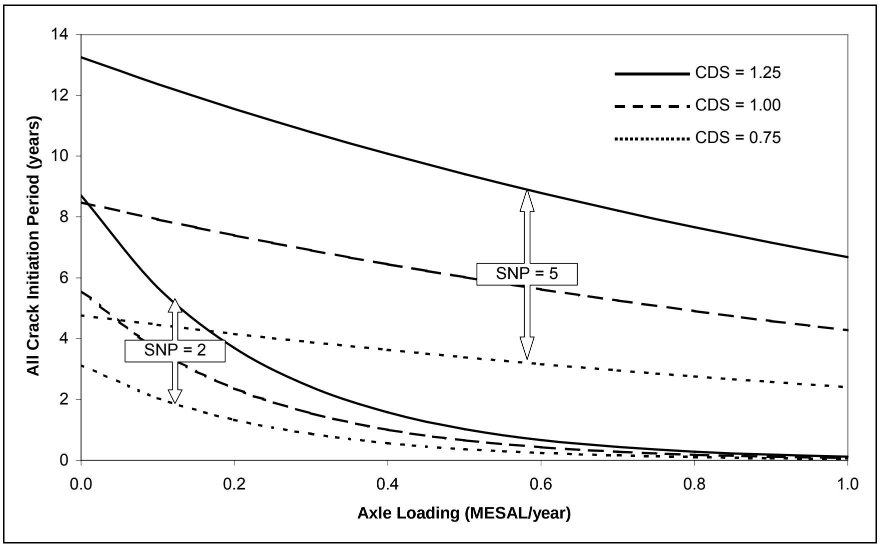

Figure B3-2
Time to initiation of all structural cracking - STGB

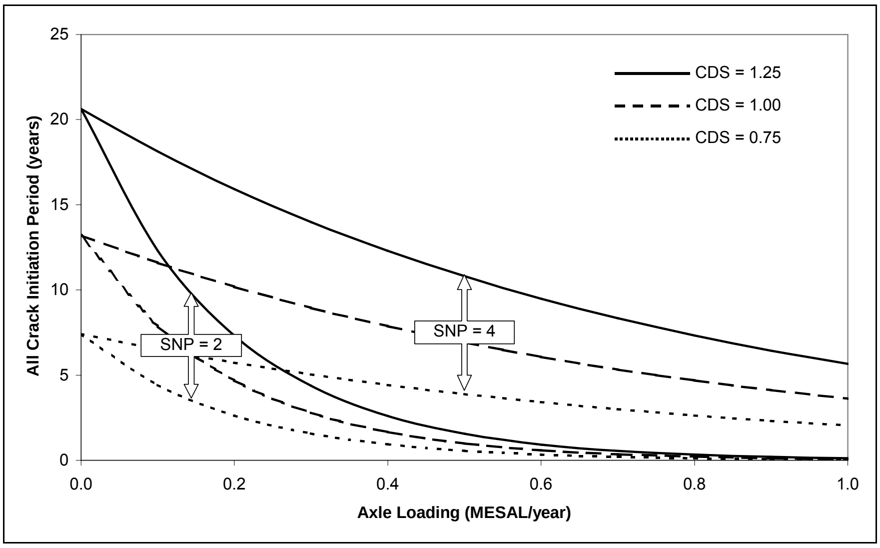

B3.5.1.2 Initiation of Wide Structural Cracking

$$ICW = K_{ciw} \max [(a_5 + a_6 \, ICA), a_7 \, ICA] \qquad \text{. . . (B3.15)}$$

where

ICW = time to initiation of wide structural cracks, in years

K_{ciw} = calibration factor for initiation of wide structural cracking

and the other variables are as defined previously

The coefficient values a_5 to a_7 for the initiation of wide structural cracking are given in Table B3-5.

Table B3-5
Coefficient values for the initiation of wide structural cracking models

Pavement Type	Surface Material	HSOLD	a_5	a_6	a_7
AMGB	All	0	2.46	0.93	0
	All except CM	> 0	2.04	0.98	0
	CM	> 0	0.70	1.65	0
AMAB	All	0	2.46	0.93	0
		> 0	2.04	0.98	0
AMAP	All	> 0	2.04	0.98	0
AMSB	All	0	1.46	0.98	0
		> 0	0	1.78	0
STGB	All	0	2.66	0.88	1.16
	All except SL, CAPE	> 0	1.85	1.00	0
	SL, CAPE	> 0	0.70	1.65	0
STAB	All	0	2.66	0.88	1.16
	All except SL, CAPE	> 0	1.85	1.00	0
	SL, CAPE	> 0	2.04	0.98	0
STAP	All	> 0	1.85	1.00	0
STSB	All	0	1.46	0.98	0
		> 0	0	1.78	0

B3.5.1.3 Progression of All Structural Cracking

The HDM-4 relationships for predicting the progression of structural cracking are based on the time-based models (Paterson, 1987) in HDM-III. The general form of the HDM-4 model for the progression of all structural cracking is given below.

$$dACA = K_{cpa}\left(\frac{CRP}{CDS}\right) z_A \left[(z_A\, a_0\, a_1\, \delta t_A + SCA^{a1})^{1/a1} - SCA\right] \qquad \text{. . . (B3.16)}$$

Progression of all cracking commences when $\delta t_A > 0$ or $ACA_a > 0$

where

$\delta t_A = 1$ if $ACA_a > 0$, otherwise $\delta t_A = \max\{0, \min[(AGE2 - ICA), 1]\}$

if $ACA_a \geq 50$ then $z_A = -1$, otherwise $z_A = 1$

$ACA_a = \max(ACA_a, 0.5)$

$SCA = \min[ACA_a, (100 - ACA_a)]$

$$Y = [a_0\, a_1\, z_A\, \delta t_A + SCA^{a1}] \qquad \text{. . . (B3.17)}$$

i) if $Y < 0$ then

$$dACA = K_{cpa}\left(\frac{CRP}{CDS}\right)(100 - ACA_a) \qquad \text{. . . (B3.18)}$$

ii) if $Y \geq 0$ then

$$dACA = K_{cpa}\left(\frac{CRP}{CDS}\right) z_A (Y^{1/a1} - SCA) \qquad \text{. . . (B3.19)}$$

iii) if $ACA_a \leq 50$ and $ACA_a + dACA > 50$ then

$$dACA = K_{cpa}\left(\frac{CRP}{CDS}\right)(100 - c_1^{1/a1} - ACA_a) \qquad \text{. . . (B3.20)}$$

where

$$c_1 = \max\left\{\left[2\,(50^{a1}) - SCA^{a1} - a_0\, a_1\, \delta t_A\right],\ 0\right\} \qquad \text{. . . (B3.21)}$$

and

dACA	=	incremental change in area of all structural cracking during analysis year, in per cent of total carriageway area
ACA_a	=	area of all structural cracking at the start of the analysis year, in per cent
δt_A	=	fraction of analysis year in which all structural cracking progression applies
AGE2	=	pavement surface age, in years
K_{cpa}	=	calibration factor for progression of all structural cracking
CRP	=	retardation of cracking progression due to preventive treatment, given by CRP = 1 - 0.12 CRT

and the other variables are as defined for crack initiation

The coefficient values a_0 and a_1 for the progression of all structural cracking are given in Table B3-6.

Table B3-6
Coefficient values for the progression of all structural cracking

Pavement Type	Surface Material	HSOLD value	All cracking a_0	All cracking a_1
AMGB	All	0	1.84	0.45
	All except CM	> 0	1.07	0.28
	CM	> 0	2.41	0.34
AMAB	All	0	1.84	0.45
		> 0	1.07	0.28
AMAP	All	> 0	1.07	0.28
AMSB	All	0	2.13	0.35
		> 0	2.13	0.35
STGB	All	0	1.76	0.32
		> 0	2.41	0.34
STAB	All	0	1.76	0.32
	All except SL, CAPE	> 0	2.41	0.34
	SL, CAPE	> 0	1.07	0.28
STAP	All	> 0	2.41	0.34
STSB	All	0	2.13	0.35
		> 0	2.41	0.34

B3.5.1.4 Progression of Wide Structural Cracking

The general form of the HDM-4 model for the progression of wide structural cracking is given below.

$$dACW = K_{cpw}\left(\frac{CRP}{CDS}\right) z_w\,[(z_w\, a_2\, a_3\, \delta t_W + SCW^{a3})^{1/a3} - SCW] \qquad \text{. . . (B3.22)}$$

where

$$dACW = \min\,[ACA_a + dACA - ACW_a,\ dACW] \qquad \text{. . . (B3.23)}$$

Progression of wide structural cracking commences when $\delta t_W > 0$ or $ACW_a > 0$

where

$$\delta t_W = 1 \text{ if } ACW_a > 0, \quad \text{otherwise} \quad \delta t_W = \max\{0,\ \min[(AGE2 - ICW),\ 1]\}$$

The initiation of wide structural cracking is constrained so that it does not commence before the area of all structural cracking (ACA_a) exceeds 5 per cent as follows:

$$\delta t_W = 0 \text{ if } ACA_a \le 5 \text{ and } ACW_a \le 0.5 \text{ and } \delta t_W > 0$$

If patching of wide cracking was performed in the previous analysis year, reducing the area of wide structural cracking to below 1 per cent, but with the area of all structural cracking remaining at over 11 per cent at the start of the current analysis year (i.e. $ACW_a \le 1$ and $ACA_a > 11$), then the rate of progression of wide structural cracking is assumed to begin not at the low initial rate, but at a higher rate similar to the rate before patching.

For this situation a temporary value of wide structural cracking, ACW_{temp} is defined to be 5 per cent less than ACA_a; i.e.

$$ACW_{temp} = ACA_a - 5 \text{ if } ACW_a \le 1 \text{ and } ACA_a > 11$$

This value is then used as the temporary value of ACW_a for the computation of dACW in that analysis year.

dACW is computed each analysis year as follows:

if $ACW_a \ge 50$ then $z_w = -1$, otherwise $z_w = 1$

$$ACW_a = \max(ACW_a,\ 0.5)$$

$$SCW = \min[ACW_a,\ (100 - ACW_a)]$$

$$Y = [a_2\, a_3\, z_W\, \delta t_W + SCW^{a3}] \qquad \text{. . . (B3.24)}$$

i) if Y < 0 then

$$dACW = K_{cpw}\left(\frac{CRP}{CDS}\right)\min\left[(ACA_a + dACA - ACW_a),\ (100 - ACW_a)\right] \qquad \text{. . . (B3.25)}$$

ii) if Y ≥ 0 then

$$dACW = K_{cpw}\left(\frac{CRP}{CDS}\right)\min\left[(ACA_a + dACA - ACW_a),\ z_W\,(Y^{1/a3} - SCW)\right] \qquad \text{. . . (B3.26)}$$

iii) if $ACW_a \le 50$ and $ACW_a + dACW > 50$ then

$$dACW = K_{cpw}\left(\frac{CRP}{CDS}\right)\min\left[(ACA_a + dACA - ACW_a),\ (100 - c_1^{\,1/a3} - ACW_a)\right] \qquad \text{. . . (B3.27)}$$

where

$$c_1 = \max\left\{\left[2\,(50^{a3}) - SCW^{a3} - a_2\, a_3\, \delta t_W\right],\ 0\right\} \qquad \text{. . . (B3.28)}$$

and

$dACW$ = incremental change in area of wide structural cracking during analysis year, in per cent of total carriageway area

ACW_a = area of wide structural cracking at the start of the analysis year, in per cent

δt_W = fraction of analysis year in which wide structural cracking progression applies

K_{cpw} = calibration factor for progression of wide structural cracking

and the other variables are as defined previously

The coefficient values a_2 and a_3 for the progression of wide structural cracking are given in Table B3-7.

Table B3-7
Coefficient values for the progression of wide structural cracking

Pavement Type	Surface Material	HSOLD value	Wide cracking a_2	Wide cracking a_3
AMGB	All	0	2.94	0.56
	All except CM	> 0	2.58	0.45
	CM	> 0	3.40	0.35
AMAB	All	0	2.94	0.56
		> 0	2.58	0.45
AMAP	All	> 0	2.58	0.45
AMSB	All	0	3.67	0.38
		> 0	3.67	0.38
STGB	All	0	2.50	0.25
		> 0	3.40	0.35
STAB	All	0	2.50	0.25
	All except SL, CAPE	> 0	3.40	0.35
	SL, CAPE	> 0	2.58	0.45
STAP	All	> 0	3.40	0.35
STSB	All	0	3.67	0.38
		> 0	3.40	0.35

The rates of progression of all and wide structural cracking are illustrated in Figure B3-3 for an AMGB pavement.

Figure B3-3
Progression of all and wide structural cracking – AMGB

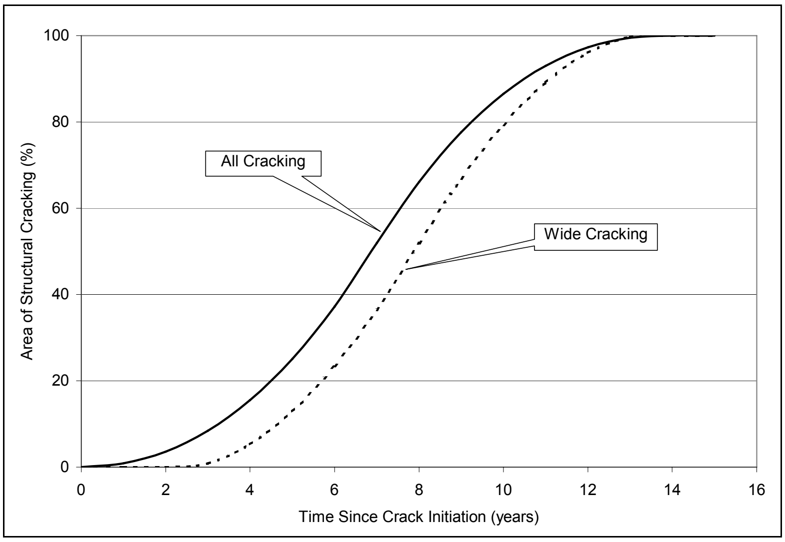

B3.5.1.5 Proposed Modifications to the Cracking Progression Model

It is generally accepted that the structural cracking relationships were originally derived using observed cracking caused by a combination of traffic loading and environmental (age) effects. For this reason the Brazil research showed similar correlations for the time and traffic based models (Paterson, 1987). Therefore both time (age) and traffic should be represented in the crack progression models.

NDLI (1995) proposed the adoption of the traffic-based model, but due to apparent anomalies in the model the original time-based models were used in version 1 of the HDM-4 software. Subsequently a modified traffic-based model was formulated (Paterson, 1999), based on the following principles:

1. The time to 100% cracking for the time-based models are assumed to be representative for “normally designed” pavements.
2. The annual traffic loading (YE4) causing the expected initiation period of “normally designed” pavements (typically 12 years for AMGB, 9 years for STGB) is estimated for a chosen SNP (or deflection for SB pavements).
3. The cumulative loading from 0 to 100% cracking is read from the prediction graphs in Paterson, 1987 and the implied time is derived by dividing the cumulative loading by the annual loading for the “normal design”.
4. The implied time of the “biased” traffic model is compared with the time based period and the suppression factor is calculated as biased time divided by expected time.
5. This is repeated for three values of SNP for each of the three dominant pavement types.

The time to 50% cracking is given in Paterson (1987) as:

$$T_{50} = \frac{(50^b - 0.5^b)}{a\,b} \qquad \text{. . . (B3.29)}$$

where

T_{50} = time to 50% cracking, in years
a and b = model coefficients

In the traffic-based model, the coefficient a has the form:

$a = a_0(YE4)(SNP)^{a1}$ granular bases
$a = a_0(YE4)(DEF)a_1(CMOD)a_2$ cemented bases

The values derived for the traffic-based model coefficients by Paterson (1999) are shown in Table B3-8.

Table B3-8
Model coefficients from Paterson (1999)

Pavement Type	Cracking	a_0	a_1	a_2	b
AMGB	All	200	-2.27		0.65
	Wide	320	-2.52		0.72
STGB	All	520	-3.23		0.28
	Wide	1360	-3.19		0.39
STSB	All	1.5	0.64	0.90	0.41
	Wide	2.3	0.59	0.74	0.30

Figure B3-4 and Figure B3-5 show the times to 100% cracking given by these models for ranges of traffic loading and pavement strength. These graphs illustrate that for low traffic loading, crack progression predictions can be very low. While the model predictions may be valid for “normal” combinations of traffic and pavement strength, deviation from these may give unreasonable values, either high or low.

Figure B3-4
Crack progression after Paterson (1999) - AMGB

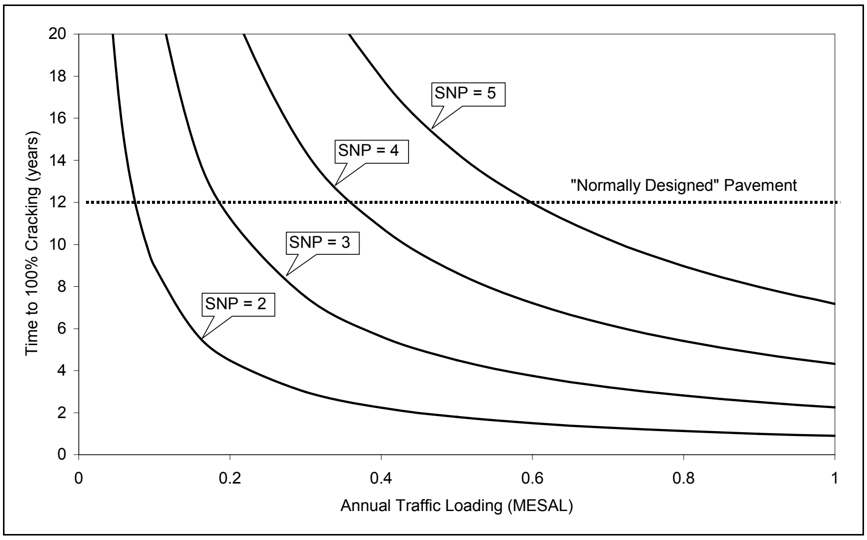

Figure B3-5
Crack progression after Paterson (1999) - STGB

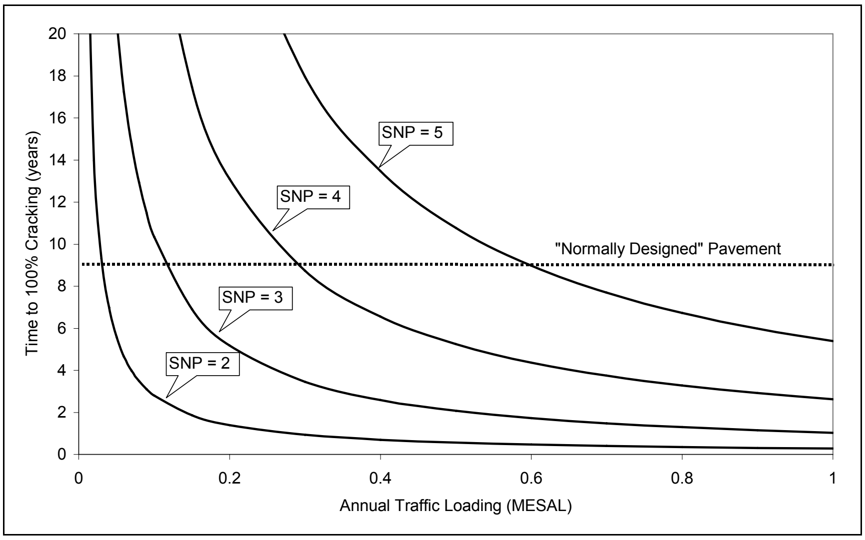

Riley (2000b) proposed defining term “a” in the above model in the following form:

$$a = a_0 + a_1(YE4)(SNP)^{a2}$$

Using values of a_0 = 1.5 and a_1 = 100 for AMGB pavements (other coefficients as before) gives the results shown in Figure B3-6. This gives a maximum period to 100% cracking of about 25 years at little or no traffic and around 12 years for the “normally designed” pavements defined in Paterson (1999). Abnormally high ratios of traffic loading to strength result in rapid crack progression as might be expected.

Figure B3-6
Crack progression after Riley (2000b) - AMGB

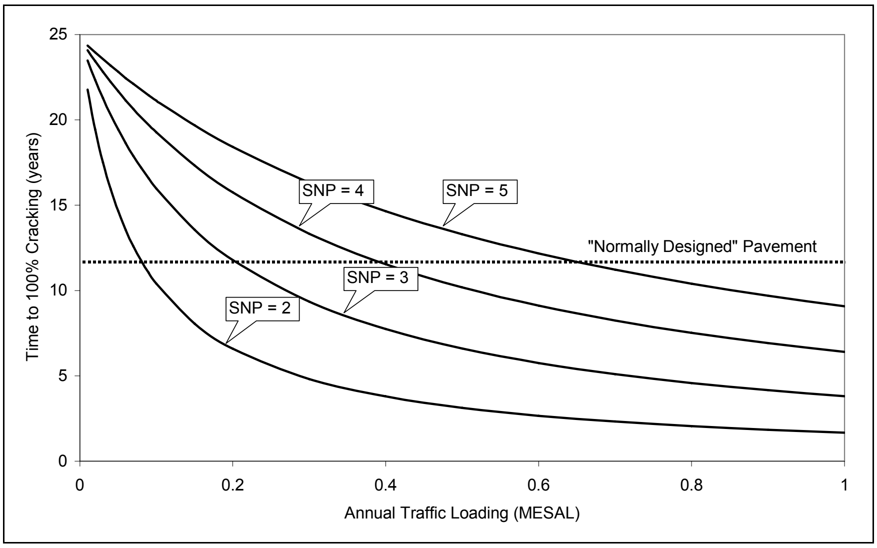

By comparing the Paterson (1987) models for cracking initiation and progression, coefficients can be derived for other pavement types.

B3.5.2 Reflection Cracking

No fully satisfactory models for the prediction of reflection cracking have been identified, but there have been a number of studies in which methods of reducing reflection cracking have been explored and some studies where a limited range of the key variables have been investigated. A comprehensive research study in Malaysia on the performance of relatively thin overlays (Rolt, et al, 1996) showed how reflection cracking depends on traffic, existing structural strength and surface condition. No studies could be found where the effect of climatic variables, in particular the effect of the daily temperature range, could be isolated.

The results from the Malaysia study were used to derive the following models for predicting the initiation and progression of reflection cracking (Rolt, 2000).

B3.5.2.1 Initiation of Reflection Cracking

The Malaysia study showed that initiation of reflection cracking depended on the thickness of the overlay and the deflection before overlay. The relationship for predicting the time to initiation of reflection cracking is as follows:

$$ICF = K_{cif}\left(\frac{a_0}{ADH}\right)(DEF)^{a1}\left(1-\frac{\min\left[HSNEW,\,(a_2-1)\right]}{a_2}\right)^{a3} \qquad \text{. . . (B3.30)}$$

where

ICF	=	time to initiation of reflection cracking, in years
ADH	=	average daily number of heavy vehicles in both directions
DEF	=	Benkelman beam deflection, in mm
HSNEW	=	thickness of most recent surfacing, in mm
K_{cif}	=	calibration factor for initiation of reflection cracking

The coefficient values a_0 to a_3 for the initiation of reflection cracking are given in Table B3-9.

Table B3-9
Coefficient values for the initiation of reflection cracking

Pavement Type	a_0	a_1	a_2	a_3
All pavement types	685	-0.5	200	-2.0

The time to initiation of reflection cracking given by the above model is plotted against ADH in Figure B3-7, against HS in Figure B3-8 and against DEF in Figure B3-9.

Figure B3-7
Time to initiation of reflection cracking vs traffic

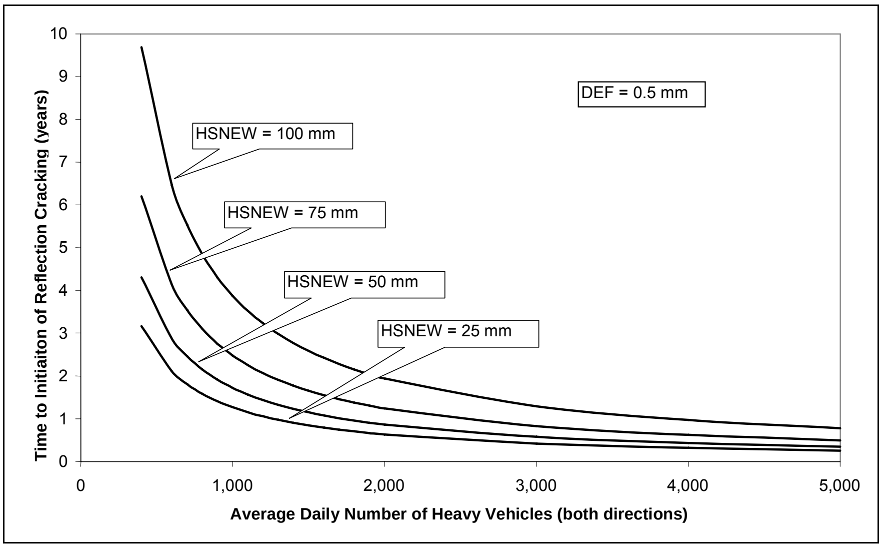

Figure B3-8
Time to initiation of reflection cracking vs surfacing thickness

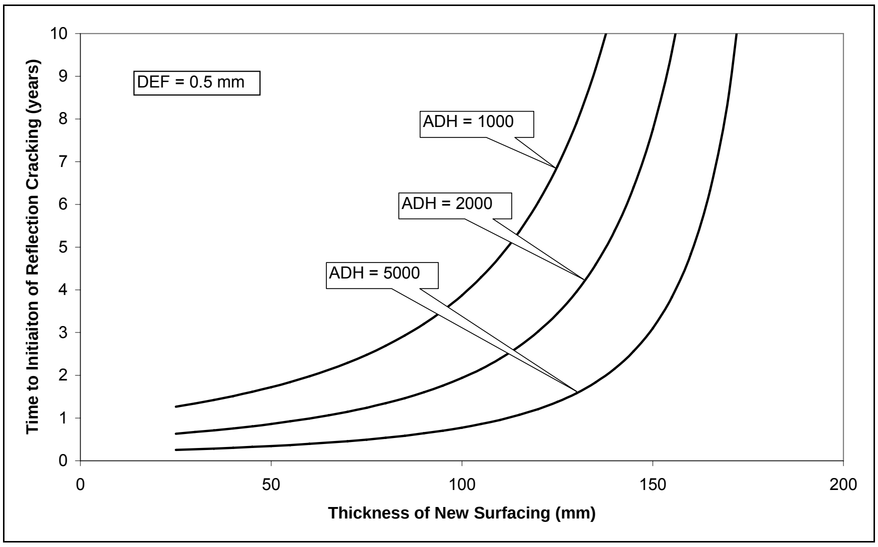

Figure B3-9
Time to initiation of reflection cracking vs deflection

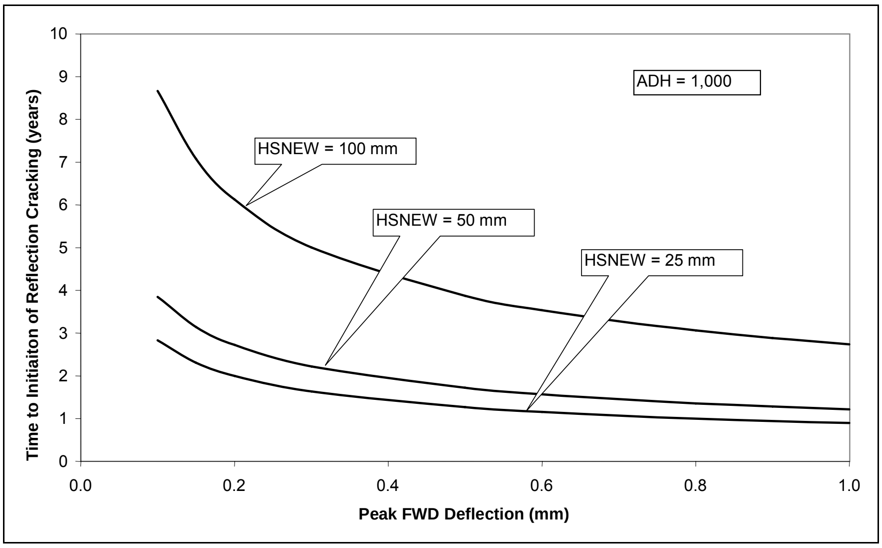

B3.5.2.2 Progression of Reflection Cracking

Progression of reflection cracking commences when $\delta t_F > 0$

where $\delta t_F = 1$ if $ACF_a > 0$,

otherwise $\delta t_F = \max\{0, \min[(AGE2 - ICF), 1]\}$

The model proposed for predicting the rate of progression of reflection cracking is:

$$dACF = K_{cpf} a_0 (ADH)(DEF)^{a1} \max\left[0, \left(1 - \frac{HSNEW}{a_2}\right)\right]^{a3} \delta t_F \qquad \text{. . . (B3.31)}$$

and

$ACF_b = \min[(ACF_a + dACF), PCRA]$

where

$dACF$ = incremental change in area of reflection cracking during analysis year, in per cent of total carriageway area

ACF_a = area of reflection cracking at start of analysis year, in per cent of total carriageway area

ACF_b = area of reflection cracking at end of analysis year, in per cent of total carriageway area

$PCRA$ = area of cracking before latest reseal or overlay, in per cent of total carriageway area

δt_F = fraction of analysis year in which reflection cracking progression applies

K_{cpf} = calibration factor for progression of reflection cracking

and the other variables are as defined previously

The coefficient values a_0 to a_3 for the progression of reflection cracking are given in Table B3-10.

The rate of progression of reflection cracking is illustrated in Figure B3-10 for a range of new surfacing thicknesses and in Figure B3-11 for a range of traffic levels.

Table B3-10
Coefficient values for the progression of reflection cracking

Pavement Type	a_0	a_1	a_2	a_3
All pavement types	0.0182	0.5	200	2.0

Figure B3-10
Progression of reflection cracking for a range of surfacing thicknesses

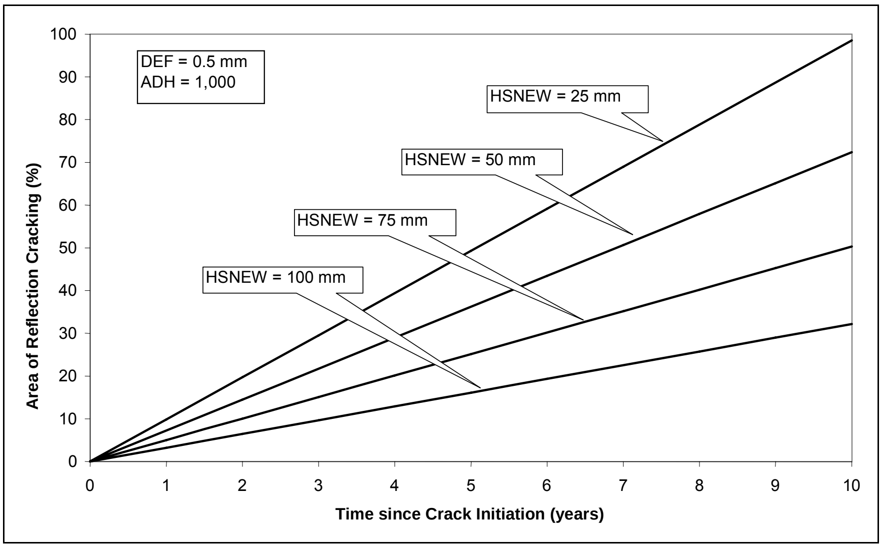

Figure B3-11
Progression of reflection cracking for a range of traffic

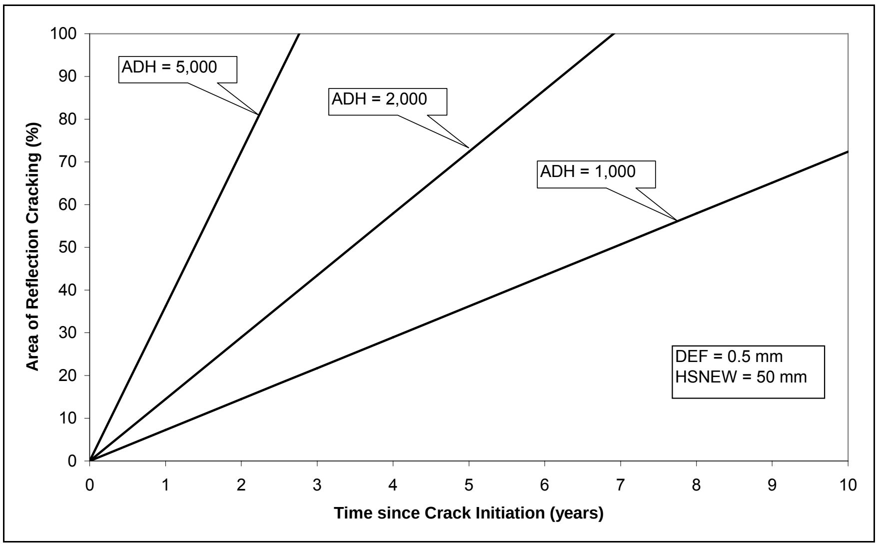

The reflection cracking model has been derived from observations of 'previous' wide cracking reflecting through an overlay and in turn becoming wide cracking in the new surfacing within a relatively short time. It is therefore proposed that reflection cracking is treated as wide cracking in HDM-4.

B3.5.3 Transverse Thermal Cracking

Transverse thermal cracking has been introduced as a new type of distress in HDM-4. It is modelled as cracking intensity expressed as the number of cracks per km (Riley, 1997). A coefficient of thermal cracking (CCT) is used as a variable to predict time to initiation of thermal cracks for the various climate zones. The default values of CCT set in HDM-4 are given in Table B3-11. These values effectively allow transverse thermal cracking to be initiated only in sub-tropical hot (arid and semi-arid) and temperate freeze climate zones (i.e. CCT $\neq$ 100).

Also given in Table B3-11 are the default values in HDM-4 of the maximum number of thermal cracks (NCT_{eq}) per kilometre of road and the time since crack initiation to reach this level of cracking (T_{eq}), for the various climate zones. As for CCT, the default values of NCT_{eq} and T_{eq} have been set in the HDM-4 program such that the progression of transverse thermal cracking is inhibited for various climate zones (i.e. where NCT_{eq} = 0 and T_{eq} = 50).

Table B3-11
HDM-4 default values of CCT, NCT_{eq} and T_{eq}

	Coefficient of Thermal Cracking (CCT)				
	Tropical	**Sub-tropical hot**	**Sub-tropical cool**	**Temperate cool**	**Temperate freeze**
Arid	100	5	100	100	2
Semi-arid	100	8	100	100	2
Sub-humid	100	100	100	100	1
Humid	100	100	100	100	1
Per-humid	100	100	100		
NCT_{eq}	0	100	0	0	20
T_{eq}	50	7	50	50	7

The conceptual model for transverse thermal cracking is illustrated in Figure B3-12. This figure shows that after an initiation period of ICT years, the progression of transverse thermal cracking occurs over a further period of time, T_{eq}, at which point the maximum number of cracks, NCT_{eq}, have been reached.

Figure B3-12
Conceptual model for transverse thermal cracking

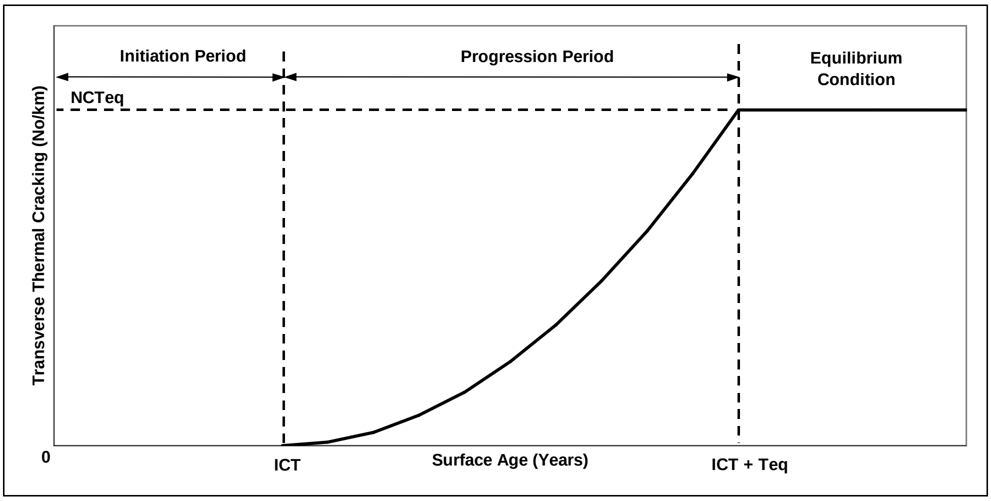

B3.5.3.1 Initiation of Transverse Thermal Cracking

A distinction is made between the time to initiation of transverse thermal cracking in original surfacings and in overlays or reseals. The relationships for predicting the time to initiation, ICT, in years are as follows:

a) if HSOLD = 0 (i.e. Original Surfacings)

$$ICT = K_{cit} \max [1, (CDS)(CCT)] \qquad \text{. . . (B3.32)}$$

b) if HSOLD > 0 (i.e. Overlays or Reseals)

$$ICT = K_{cit} \, CDS \, (CCT + a_0 + a_1 \, HSNEW) \qquad \text{. . . (B3.33)}$$

where

ICT = time to initiation of transverse thermal cracks, in years
CCT = coefficient of thermal cracking (see Table B3-11)
HSNEW = thickness of the most recent surfacing, in mm
CDS = construction defects indicator for bituminous surfacings
K_{cit} = calibration factor for initiation of transverse thermal cracking

The coefficient values a_0 to a_1 for the initiation of transverse thermal cracks are given in Table B3-12.

Table B3-12
Coefficient values for the initiation of transverse thermal cracking

Pavement Type	HSOLD value	a_0	a_1
All pavement types	> 0	-1.0	0.02

B3.5.3.2 Progression of Transverse Thermal Cracking

As in the initiation models, a distinction is made between the rates of progression of transverse thermal cracking in original surfacings and in overlays or reseals.

Progression of transverse thermal cracking commences when $\delta t_T > 0$

where $\delta t_T = 1$ if $ACT_a > 0$,

otherwise $\delta t_T = \max \{0, \min [(AGE2 - ICT), 1]\}$

i) if HSOLD = 0 (i.e. Original Surfacings)

$$dNCT = K_{cpt} \left(\frac{1}{CDS}\right) \max\left\{0, \min\left[(NCT_{eq} - NCT_a), \left(\frac{2\,NCT_{eq}(AGE3 - ICT - 0.5)}{T_{eq}^{\;2}}\right)\right]\right\}\delta t_T \qquad \text{. . . (B3.34)}$$

ii) if HSOLD > 0 (i.e. Overlays or Reseals)

$$dNCT = K_{cpt} \left(\frac{1}{CDS}\right) \min\left\{(NCT_{eq} - NCT_a), \max\left[\min\left(a_3\,PNCT, (PNCT - NCT_a)\right), \left(\frac{2\,NCT_{eq}(AGE3 - ICT - 0.5)}{T_{eq}^{\;2}}\right), 0\right]\right\}\delta t_T \qquad \text{. . . (B3.35)}$$

where

dNCT = incremental change in number of transverse thermal cracks during analysis year, in no/km

PNCT = number of transverse thermal cracks before latest overlay or reseal, in no/km

NCT_a = number of (reflected) transverse thermal cracks at the start of the analysis year, in no/km

NCT_{eq} = maximum number of thermal cracks, in no/km (see Table B3-11)

T_{eq} = time since crack initiation to reach maximum number of thermal cracks, in years (see Table B3-11)

AGE3 = age since last overlay or reconstruction, in years

δt_T = fraction of analysis year in which transverse thermal cracking progression applies

K_{cpt} = calibration factor for progression of transverse thermal cracking

and the other variables are as described in transverse thermal cracking initiation

The coefficient value for the progression of transverse thermal cracks is given in Table B3-13.

Table B3-13
Coefficient value for the progression of transverse thermal cracking

Pavement Type	HSOLD value	a_2
All pavement types	> 0	0.25

The model is illustrated in Figure B3-13 using the default values in Table B3-11 for two climates. For a sub-tropical hot, arid climate, the model predicts that cracks will initiate after 5 years and reach an equilibrium state of 100 cracks/km after a further period of 7 years. Similarly for a temperate freeze, humid climate, the model predicts that cracks will initiate after one year and reach an equilibrium state of 20 cracks/km after 8 years.

Figure B3-13
Transverse thermal cracking progression for two climates

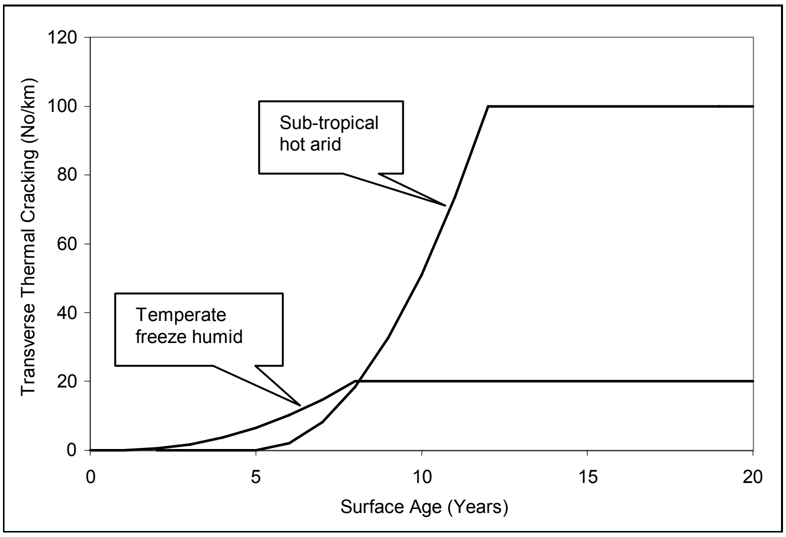

The rate at which transverse thermal cracks reflect through overlays has been plotted in Figure B3-14 for overlay thicknesses of 50, 100, and 150 mm. This figure shows that the model predicts that all transverse thermal cracks will reflect through a 50 mm overlay after 4 years and that it will take 6 years for all the cracks to reflect through a 150 mm overlay.

The default value of 1.0 was used for the calibration factors in both Figure B3-13 and Figure B3-14. The predicted time to initiation and subsequent progression can be adjusted by altering the values of the calibration factors.

Figure B3-14
Reflection of transverse thermal cracking

B3.5.3.3 Area of Transverse Thermal Cracking

The transverse thermal cracking model predicts the incremental change in the number of cracks, rather than as a percentage of the carriageway area that is cracked.

The influence of a single crack in HDM-4 is assumed to be 0.25 metres each side of the crack (as in HDM-III). Therefore the area of a single crack in square metres is calculated as the length of the crack in metres multiplied by 0.5 metres. In HDM-4, a transverse thermal crack is assumed to traverse the full width of the carriageway. Thus the area of transverse cracking in m^2 can be simply calculated as the number of cracks multiplied by 0.5.

The area of transverse thermal cracking, as a percentage of the carriageway area, is therefore given by:

$$dACT = dNCT / 20 \qquad \text{. . . (B3.36)}$$

where

dACT = incremental change in area of transverse thermal cracking during analysis year, in per cent of total carriageway area

dNCT = incremental change in number of transverse thermal cracks during analysis year, in no/km

B3.5.4 Total Areas of Cracking

The above cracking models predict areas of ‘all’ and ‘wide’ structural cracking (ACA and ACW respectively), reflection cracking (ACF) and transverse thermal cracking (ACT). In several of the deterioration and works effects models, areas of cracking other than ACA, ACW, ACF or ACT are required. These are defined below.

Area of Structural and Reflection Cracking

The total area of structural and reflection cracking (i.e. excluding transverse thermal cracking) is defined as follows:

$$ACAT = ACA + ACF \qquad ...(B3.37)$$

where

ACAT = total area of all structural and reflection cracking, in per cent
ACA = area of all structural cracking, in per cent
ACF = area of reflection cracking, in per cent

Area of Wide Cracking

It is proposed that in HDM-4, reflection cracking is treated as 'wide' cracking. The total area of wide structural and reflection cracking, ACWT, is defined as follows:

$$ACWT = ACW + ACF \qquad ...(B3.38)$$

where

ACWT = total area of wide structural and reflection cracking, in per cent
ACW = area of wide structural cracking, in per cent

Area of Indexed Cracking

The area of indexed cracking, ACX is a weighted average of 'all' and 'wide' cracking and is defined by Paterson (1987) as follows:

$$ACX = 0.62\ ACAT + 0.39\ ACWT \qquad ...(B3.39)$$

where

ACX = area of indexed cracking, in per cent

Total Area of Cracking

The total area of cracking combines the structural, reflection and transverse thermal cracking and is defined as follows:

$$ACRA = ACA + ACF + ACT \qquad ...(B3.40)$$

where

ACRA = total area of carriageway cracked, in per cent
ACT = area of transverse thermal cracking, in per cent

B3.5.5 Initial Values of Cracking

In HDM-4, cracking is measured as in HDM-III as extent and severity (all, wide). In addition, transverse thermal cracks are discretely measured in terms of extent but not severity. An additional attribute is included to denote the extent of cracks which are sealed.

At the start of an analysis, the data for a pavement section will comprise:

- extent of all crocodile and map cracking as per cent of pavement area
- extent of wide crocodile and map cracking as per cent of pavement area
- extent of transverse cracking as number of cracks per km
- extent of cracks that are sealed as per cent of wide cracks

To an observer, structural and reflection cracking appears indistinguishable, and therefore recorded cracking data for a pavement will be an aggregated total for the two mechanisms. In order to apply the cracking prediction models, it is necessary to disaggregate the total observed area of cracking into structural and reflection types at the start of an analysis.

- If the area of previous cracking (PCRA) is zero or unknown, then it is assumed that all observed cracks (ACO) are structural; reflection cracking is zero.
- If PCRA is known, it is compared with the area of reflection cracking calculated using the above models (ACF').
- If the calculated prediction of reflection cracking (ACF') is less than the total observed (ACO), it is assumed that the predicted value for ACF is correct and the difference between that and ACO is structural cracking. Both reflection and structural cracking are thereafter progressed in accordance with the relevant models.
- If ACF' is greater than ACO, then ACF is assumed to be equal to ACO. Thereafter ACF is progressed using the model for reflection cracking. Structural cracking progresses once the initiation period is exceeded.

This logic is shown in the flow chart in Figure B3-15.

If sealed cracks are present the age spectrum of the sealing must also be determined. Crack sealing is described under road works effects in Section B13.2 on routine maintenance.

Figure B3-15
Initiating cracking values

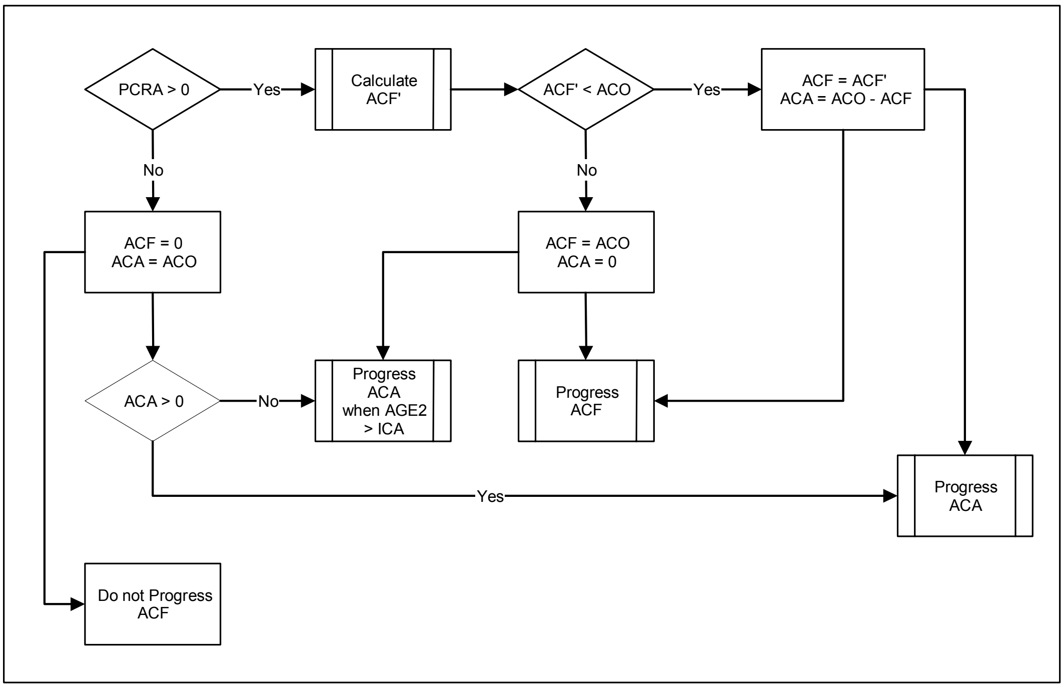

B4. Ravelling

Ravelling is the loss of surface aggregate particles from the bitumen-aggregate matrix. The occurrence of ravelling varies considerably between regions and from country to country according to construction methods, specifications, available materials, and local practice. Ravelling is a common distress in poorly constructed, thin bituminous layers, such as surface treatments, but is rarely seen in high quality, hot-mix asphalt.

Ravelling is one of a number of bituminous pavement deterioration modes that is grouped under the general heading of "disintegration." Also included in this category are potholing and edge breaking. Ravelling is typically limited to the pavement's surface, and as such contributes to a reduction in the functional rather than the structural performance of a pavement. However, in severe cases, ravelling of a thin surface treatment may contribute to potholing, which does affect the structural performance of the pavement.

B4.1 Mechanisms of Ravelling

In broad terms, ravelling can be defined as "the progressive loss of surface material by weathering and/or traffic abrasion" (Asphalt Institute, 1989). While surface material loss occurs as a result of a number of causes, the two primary causes of ravelling are mechanical fracture of the binder film and loss of adhesion between binder and stone (which in the presence of water, is also known as 'stripping') (Paterson, 1987). This definition is preferable to the more restrictive one used in the Long Term Pavement Performance (LTPP) program (SHRP, 1993): "wearing away of the pavement surface in high-quality hot mix asphalt concrete". This latter definition over-emphasises hot mix pavements and only addresses one of the several possible causes of ravelling.

Bituminous layers are meant to be resilient and resistant to the applied stresses of environment and load. Mechanical fracture of the binder film around a stone particle occurs when the binder has become too brittle or the film is too thin to sustain the stresses imposed through the tyre contact area of a moving vehicle.This loss in the binder's resilience and resistance to applied stresses is a natural part of the ageing of bituminous pavements.

There are two types of ageing that take place, short-term ageing and long-term ageing. Short-term ageing occurs in the processing of hot-mix asphalt (at the plant) or during construction operations (in the field). The hardening that occurs during this process is a result of the loss of the volatile portions of the bitumen. Long-term ageing typically occurs as a result of exposure to ambient temperatures and ultraviolet light. It is primarily caused by oxidation and the formation of oxidative products. Factors that affect long-term ageing include: the type of bitumen and additives, the type of aggregate, per cent air voids content, amount of solar (ultraviolet) radiation, and ambient temperatures.

In either case, as the viscosity of the binder increases, the likelihood of mechanical fracture also increases. The process of mechanical fracture is then actually caused by the action of vehicle tyres passing over the pavement surface: the lateral force of tyres on the aggregate helps to dislodge the aggregate that rests in a brittle matrix.

Loss of adhesion between the binder and aggregate also occurs when the bond between binder and aggregate is broken (or may not even develop) due to the presence in the aggregate of an excess of deleterious materials such as fine-grained (< 0.425 mm) particles. When an excess of fines is present, and especially when the larger aggregate particles are coated with fines, the bitumen coats the fines rather than the coarse aggregate. There may thus be insufficient binder to form the bitumen-aggregate matrix or the aggregate may never actually get coated with a film of bitumen. The deterioration that occurs in this form of ravelling can develop quite rapidly.

B4.2 Modelling Ravelling in HDM-III

The development of the ravelling model in HDM-III was based on data collected during the Brazil-UNDP paved road deterioration study. Ravelling was quantified by the sum of areas of ravelling on a test section. As ravelling was not considered a problem on asphalt surfaces, data were recorded only for surface treatment surfacings. Therefore the HDM-III ravelling model predicts the time to initiation of ravelling and its subsequent rate of progression only for surface treated pavements. No definition of severity of ravelling was included.

In this study, the various phenomena included under the category of ravelling were:

1) Stone loss by mechanical fracture (true ravelling)
2) Stone loss by loss of adhesion (stripping or contamination)
3) Scabbing – loss of a fragment of surfacing, such as a slurry seal, exposing the underlying bituminous surfacing
4) Stone loss through lack of binder – where narrow longitudinal strips of basecourse or underlying surfacing had become exposed, attributable to faulty binder distribution at the time of construction
5) Ravelling of either the top or bottom layer of surfacing, without distinction

As it was clear that some of these categories of ravelling could quite confidently be attributed to problems that manifestly had occurred during construction and had resulted in premature ravelling distress, the construction quality code (CQ) was used. CQ was assigned a value based on the following:

CQ = 1 In the cases where the seal appeared to be streaky due to faulty binder distribution, or 100 per cent loss of stone occurred within one to three years due apparently to loss of adhesion

CQ = 0 In the absence of identifiable surfacing construction problems

Three types of surface treated pavements were included in the database for the development of the HDM-III ravelling model. The number of sections of each surface type are shown in Table B4-1 and some key characteristics of the sections are shown in Table B4-2.

Of the 96 sections of slurry seal, only 15 were observed to “ravel”, and of those most of the distress was delamination. The chip seals usually consisted of a top layer of 10 mm stone placed on top of a lower layer of 16 or 19 mm stone (a double surface treatment). Most of the ravelling in the chip seals often consisted of the loss of the top layer (10 mm) aggregate in the two-layer applications.

The general trend of ravelling was suggested by Paterson (1987) to be similar to the other time-based deterioration models. That is, ravelling deterioration is divided into two phases: an initiation period, defined as the time from construction of the surfacing to the first development of ravelling, and the progression period, which is the increase in the per cent ravelled area over time once the distress has appeared.

Table B4-1
Pavement sections used to develop HDM-III ravelling models

Surface Type	Number of Sections
Double Surface Treatment	116
Slurry Seal Reseal	96
Open-Graded Cold Mix	16

Table B4-2
Characteristics of pavements used to develop HDM-III ravelling models

Parameter	Minimum	Maximum	Mean
Traffic, vehicles per day	100	4,500	1,700
Equivalent Axle Loads, MESA/lane/yr	0.007	2.810	0.194
Construction Quality, CQ (0 = no faults, 1 = faulty)	0 (191)	1 (37)	0.162
Deflection, mm	0.26	2.02	0.79
Modified Structural Number, SNC	2.71	7.72	3.86

B4.2.1 Initiation of Ravelling

Initiation of ravelling is said to occur when 0.5 per cent of a test section's area is classified as ravelled. In examining the explanatory variables, it was found that traffic volume had a significant effect when sections were differentiated by pavement type. Therefore, a model for the initiation period was developed that predicted the mean time to the onset of ravelling (for the three different types of pavements that exhibited ravelling) based on the annual vehicle loadings. Factors that were found not to have an effect on the initiation of ravelling included base type (although cemented bases were excluded from the study) and pavement strength (Paterson, 1987).

A significant portion of the ravelling could be attributed to poor quality work during the surface layer application or construction phase and consequently the construction quality indicator (CQ) was introduced as an explanatory variable as described earlier. As for cracking initiation, two factors were introduced in the ravelling initiation model; a user-specified ravelling initiation factor, K_{vi} and the occurrence distribution factor, F_r, (both default values of 1.0).

Also similarly, a ravelling retardation factor, RRF, was introduced to provide the ability to extend the initiation time by taking into consideration the application of preventive treatment. However, whereas CRT was additive in the cracking initiation model, in the ravelling initiation model, RRF is multiplicative of the initiation time. This is discussed in more detail in the Road Works Effects – Section B13.3.3.1.

The HDM-III model for the initiation of ravelling is as follows:

$$TYRAV = K_{vi} \{F_r [a_0 \exp(-0.655\ CQ - 0.156\ YAX)]\ RRF\} \quad \text{. . . (B4.1)}$$

where

TYRAV	=	time to initiation of ravelling, in years
K_{vi}	=	calibration factor for initiation of ravelling (default = 1.0)
F_r	=	occurrence distribution factor (default = 1.0)
RRF	=	ravelling retardation factor (see Section B13.3.3.1)
CQ	=	construction quality factor (0 if no faults, 1 if faulty)
YAX	=	annual number of axles of all vehicle classes in the analysis year, in millions/lane

a_0 = constant related to surfacing type;
(10.5 for surface treatment, 14.1 for slurry seal, 8.0 for cold mix)

B4.2.2 Progression of Ravelling

As in the case of cracking progression, Paterson (1987) found that the time-series data of ravelled area was best represented by a sigmoidal (S-shaped) function. The integrated model for the prediction of the area of ravelling at a time, t, since initiation is expressed as follows:

$$ARAV_t = (1 - z)\,50 + z[z\,a_0\,a_1\,t + z\,0.5^{a1} + (1 - z)\,50^{\,a1}]^{1/a1} \qquad \text{. . . (B4.2)}$$

and for the time to reach a given area, since initiation is given by:

$$t = [(1 - z)\,50^{a1} + z\,SRAV_t^{a1} - 0.5^{a1}]\,/\,a_0\,a_1 \qquad \text{. . . (B4.3)}$$

where

- ARV_t = area of ravelling at time t, in per cent
- $SRAV_t$ = min (ARV_t, 100 – ARV_t)
- t = time since initiation of ravelling, in years
- z = 1, if $t \le t_{50}$, otherwise z = -1
- t_{50} = $(50^{a1} - 0.5^{a1}) / a_0\,a_1$ (i.e. time to 50% area)
- a_0 = 4.42
- a_1 = 0.352

In the HDM-III incremental model, the factors K_{vi} and RRF used in the initiation model are also used in the progression model but in a reciprocal form. The HDM-III incremental ravelling progression model is as follows:

$$\delta ARAV = \left(\frac{1}{K_{vi} RRF}\right) z\left\{\left[z\ 1.56\ \delta TRAV + SRAV^{0.352}\right]^{2.84} - SRAV\right\} \qquad \text{. . . (B4.4)}$$

where

- $\delta ARAV$ = predicted change in area of ravelling during an analysis year, in per cent
- $\delta TRAV$ = fraction of analysis year during which ravelling progression applies, in years

and the other variables are as defined previously

B4.3 Modelling Ravelling in HDM-4

The models for predicting the initiation and progression of ravelling in HDM-4 are based on those in HDM-III. The initiation model is basically as proposed by Paterson (1987), with the construction defects indicator for bituminous surfacings, CDS, (see Section B2.5) replacing the original construction quality variable CQ. The progression model is also based on that proposed by Paterson (1987) but with a traffic variable introduced as proposed by Riley (1999b). The variable CDS has also been included in the progression model.

B4.3.1 Initiation of Ravelling

In version 1 of HDM-4, the ravelling initiation model was as follows:

$$IRV = K_{vi}\,(CDS)^2\,a_0\,(RRF)\,\exp[a_1(YAX)] \qquad \text{. . . (B4.5)}$$

where

- IRV = time to ravelling initiation, in years
- CDS = construction defects indicator for bituminous surfacings
- YAX = annual number of axles of all vehicle classes in the analysis year, in millions/lane

K_{vi} = calibration factor for ravelling initiation
RRF = ravelling retardation factor due to maintenance (see Road Works Effects – Section B13.3.3.1)

The coefficient values a_0 and a_1 for the ravelling initiation model are given in Table B4-3.

Table B4-3
Coefficient values for the ravelling initiation model

Surface Type	Surface Material	a_0	a_1
AM	All except CM	100.0	-0.156
	CM	8.0	-0.156
ST	All except SL, CAPE	10.5	-0.156
	SL, CAPE	14.1	-0.156

Ravelling of AM pavements (other than cold mixes) was effectively inhibited in version 1 of HDM-4 by setting the value of the coefficient a_0 = 100 in the ravelling initiation model, as illustrated in Figure B4-1 for a normal (CDS = 1.0) road.

Figure B4-1
Ravelling initiation – HDM-4 version 1

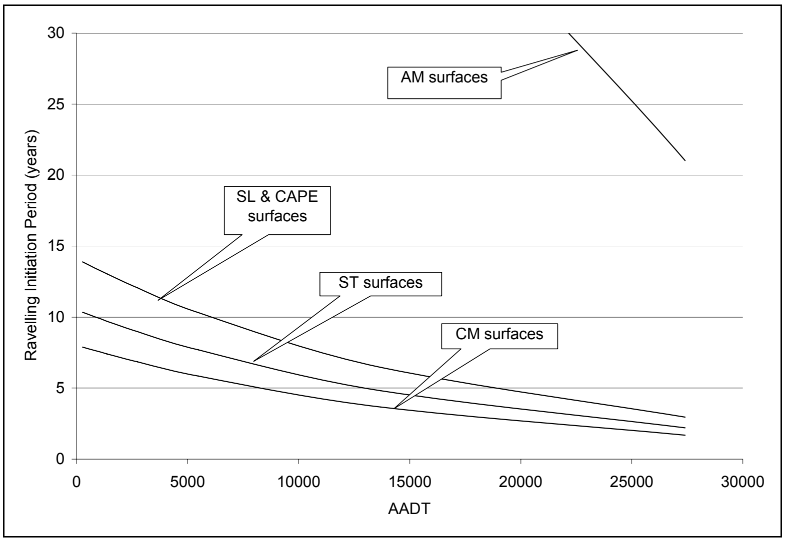

As users of HDM-4 have expressed a wish to have the option of being able to model ravelling on AM surfaces, various options were examined. Morosiuk (2003a) proposed lowering the value of a_0, whereas ARRB (Toole, et al, 2003) proposed adoption of a common intercept by removing the effect of traffic. The ARRB option was selected by PIARC (2004) and has been implemented in version 2 of HDM-4.

The coefficient values a_0 and a_1 for the ravelling initiation model implemented in version 2 of HDM-4 are given in Table B4-4 and the ravelling initiation periods for the various types of surface are illustrated in Figure B4-2.

Table B4-4
Coefficient values for the ravelling initiation model

Surface Type	Surface Material	a_0	a_1
AM	All except CM	10.0	0
	CM	8.0	-0.156
ST	All except SL, CAPE	10.0	0
	SL, CAPE	12.0	0

Figure B4-2
Ravelling initiation – HDM-4 version 2

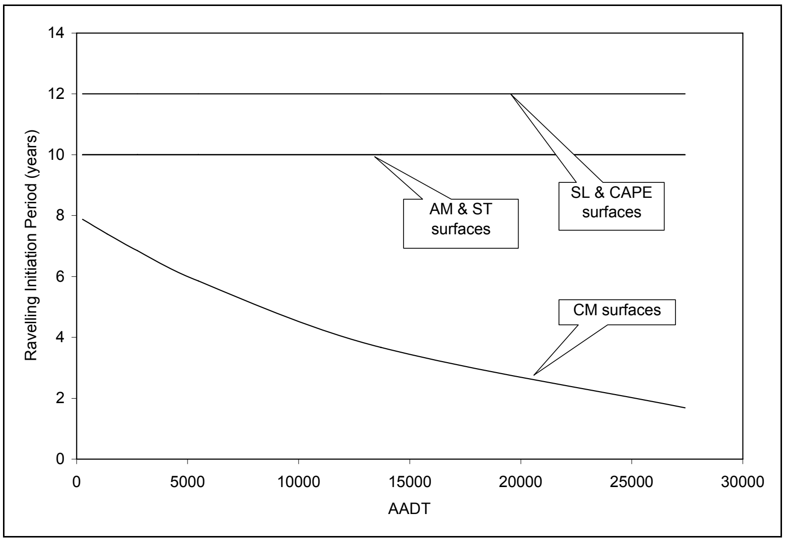

B4.3.2 Progression of Ravelling

A traffic variable, YAX, has been introduced in the HDM-4 ravelling progression model to indicate the differences in the rates of ravelling progression on low volume roads and on highly trafficked roads.

In version 1 of HDM-4, once ravelling initiation occurred, the effect of YAX was to extend the time to 100 per cent ravelling on low volume roads to 20 years, reducing to 5 years for highly trafficked roads (Riley 1999b). As this rate was considered to be too rapid, the effect of YAX was amended in version 2 of HDM-4 to extend the time to 100 per cent ravelling on low volume roads to 40 years, reducing to 10 years for highly trafficked roads (Morosiuk, 2003a). The effect of YAX has been limited to values ranging between 0.1 (AADT of 275) and 1.0 (AADT of 2750). This conceptual model is illustrated in Figure B4-3.

Figure B4-3
Effect of traffic on time to reach 100% ravelling

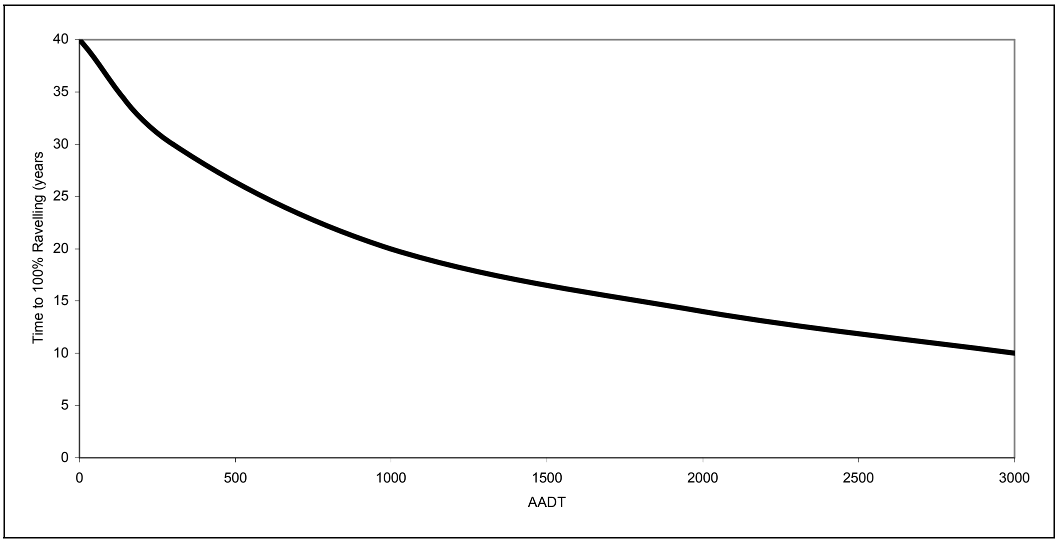

The general form of the model for the progression of ravelling is given below.

$$dARV = \left(\frac{K_{vp}}{RRF}\right)\left(\frac{1}{CDS^2}\right) z \left[\left(z\,(a_0 + a_1 YAX)\, a_2\, \delta t_v + SRV^{a2}\right)^{1/a2} - SRV\right] \quad \text{. . . (B4.6)}$$

Progression of ravelling commences when $\delta t_v > 0$ or $ARV_a > 0$

where $\delta t_v = 1$ if $ARV_a > 0$

otherwise $\delta t_v = \max\{0, \min[(AGE2 - IRV), 1]\}$

if $ARV_a \geq 50$ then $z = -1$, otherwise $z = 1$

$ARV_a = \max(ARV_a, 0.5)$

$SRV = \min[ARV_a, (100 - ARV_a)]$

$YAX = \max[\min(YAX, 1), 0.1]$

$$Y = [(a_0 + a_1 YAX)\, a_2\, z\, \delta t_v + SRV^{a2}] \quad \text{. . . (B4.7)}$$

i) if Y < 0 then

$$dARV = \left(\frac{K_{vp}}{RRF}\right)\left(\frac{1}{CDS^2}\right)(100 - ARV_a) \quad \text{. . . (B4.8)}$$

ii) if Y ≥ 0 then

$$dARV = \left(\frac{K_{vp}}{RRF}\right)\left(\frac{1}{CDS^2}\right) z\,(Y^{1/a2} - SRV) \quad \text{. . . (B4.9)}$$

iii) if ARVa ≤ 50 and ARVa + dARV > 50 then

$$dARV = \left(\frac{K_{vp}}{RRF}\right)\left(\frac{1}{CDS^2}\right)(100 - c_1^{1/a2} - ARV_a) \quad \text{. . . (B4.10)}$$

where

$c_1 = \max \{[2 (50^{a2}) - SRV^{a2} – (a_0 + a_1 YAX) a_2 \delta t_v], 0\}$ . . . (B4.11)

and

dARV = change in area of ravelling during analysis year, in per cent of total carriageway area

ARV_a = area of ravelling at the start of the analysis year, in per cent

δt_v = fraction of analysis year in which ravelling progression applies

AGE2 = pavement surface age, in years

K_{vp} = calibration factor for ravelling progression

and the other variables are as defined for ravelling initiation

The coefficient values a_0 to a_2 for the ravelling progression model are given in Table B4-5.

Table B4-5
Coefficient values for the ravelling progression model

Pavement Type	a_0	a_1	a_2
All pavement types	0.3	1.5	0.352

The rates of ravelling progression are illustrated in Figure B4-4 for a range of construction defect indicators, CDS.

Figure B4-4
HDM-4 rates of ravelling progression

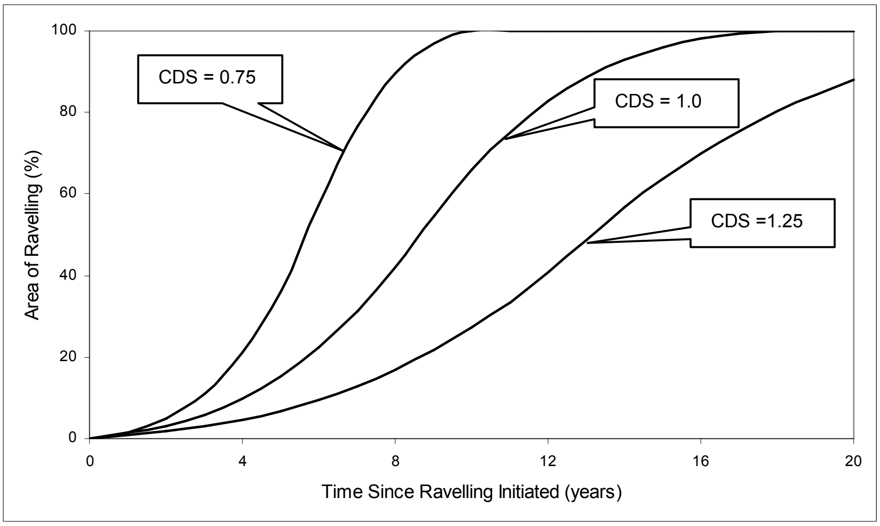

B5. POTHOLING

Potholes are the most visible and severe form of pavement distress. Paterson (1987) defined a pothole as a cavity in the road surface which is 150 mm or more in average diameter and 25 mm or more in depth, in order to distinguish between potholing and ravelling.

B5.1 Measurement of Potholes

Most methods of recording surface defects include potholing as a distress mode. The expression of extent and severity takes many forms but, in general, uses combinations of the following:

Extent:

- total potholed area (e.g. m^2) per unit length of road
- number of potholes per unit length of road
- per cent of the pavement area that is potholed

Severity:

- average depth
- average area of individual potholes
- combination of depth and area, for example small and shallow, large and deep

In the Brazil study (GEIPOT, 1982) potholing was recorded as volume per unit length. This was converted to per cent area by applying a standard depth of 80 mm in the HDM-III model (Paterson, 1987). The use of volume as a unit of measurement had the virtue that it related to maintenance needs (m^3 of asphalt for patching) and was highly correlated with simulations of roughness effects.

The unit of measurement of any distress mode should take into account the ease and accuracy of recording under field conditions. The use of per cent area, or recording the potholed area in m^2, invariably leads to over-estimation of potholing by an observer. For example, a pothole of diameter 300 mm has a surface area of 0.07 m^2. If such a pothole existed every 50 metres on a 6 metre wide carriageway, the pavement would probably be considered as being in a very poor condition. Yet the area of potholing would be 1.4 m^2 per kilometre length of road or 0.02 per cent of the surface area.

It is not uncommon for values of 10 per cent or more to be applied in HDM-III analyses even though the roughness of the roads is specified as relatively low. If 10 per cent of a pavement area is potholed it can be considered as almost totally destroyed.

In HDM-4 therefore, the extent of potholing is expressed in terms of 'pothole units'. Each pothole unit has a surface area of 0.1 m^2, i.e. approximately 300 mm in diameter and therefore can be adequately estimated by reference to a person's foot. For estimating maintenance requirements in HDM-4, the depth of a 'pothole unit' has been assumed to be 100 mm, i.e. a volume of 10 litres.

B5.2 Mechanisms of Potholing

Potholes develop in a surface that is either cracked, ravelled, or both. In the case of cracking, the crack width increases to the point where material spalls from the edge of the crack under the action of traffic and environment. Ravelling, most common in surface treatments, exposes the unbound base; material loss continues downwards to form potholes. In both cases, the development/enlargement of the pothole is dependent on the ability of the materials to resist disintegration as wheels hit the edge of the pothole or spalled crack. Thus, thick asphalt surfacings will pothole more slowly than thin surfacings and cemented bases will be more resistant than granular bases.

The presence of water accelerates pothole formation both through a general weakening of the pavement structure and lowering the resistance of the surface and base materials to disintegration.

B5.3 Modelling Potholing in HDM-III

The HDM-III pothole model was derived from studies in Brazil, St. Vincent, Ghana and Kenya and predicts the initiation and progression of potholing resulting from wide cracking or ravelling (Paterson, 1987). As with other distress modes (cracking, ravelling) the model first defines an initiation period (the delay between the onset of wide cracking or ravelling and the start of potholing) followed by the annual occurrence of new potholes. It also models the enlargement of existing potholes if no patching is carried out.

B5.3.1 Initiation of Potholing

HDM-III defined a period (TMIN) between the initiation of either wide cracking or ravelling and the occurrence of the first pothole. This period is a function of traffic flow and the thickness of the asphaltic layers. Potholing initiation occurs typically 2 to 6 years after wide cracking and 3 to 6 years after ravelling of thin surface treatments. The equations are given below and illustrated in Figure B5-1.

cemented base

$$TMIN = \max[(6 - YAX),\ 2) \qquad \text{. . . (B5.1)}$$

base is not cemented

$$TMIN = \max[(2 + 0.04\ HS - 0.5\ YAX),\ 2) \qquad \text{. . . (B5.2)}$$

where

TMIN = time to initiation of potholing, in years
HS = total thickness of bituminous layers, in mm
YAX = annual number of axles of all vehicle classes in the analysis year, in millions/lane

The time TMIN is further constrained by the cumulative area of wide cracking and ravelling; pothole initiation cannot take place before the area of wide cracking exceeds 20 per cent or the area of ravelling exceeds 30 per cent.

Figure B5-1 shows the pothole initiation period for different traffic volumes and asphalt thicknesses for pavements with cemented bases and non cemented bases.

B5.3.2 Progression of Potholing

In HDM-III the progression of potholing is computed firstly as a volume, in m^3/lane-km, because the effect on roughness has been shown to be linearly related to pothole volume (Paterson, 1987). For consistency with accounting of other distress types, potholing is then converted to an equivalent percentage area, assuming an average pothole depth of 80 mm.

Figure B5-1
HDM-III predicted time to initiation of potholes

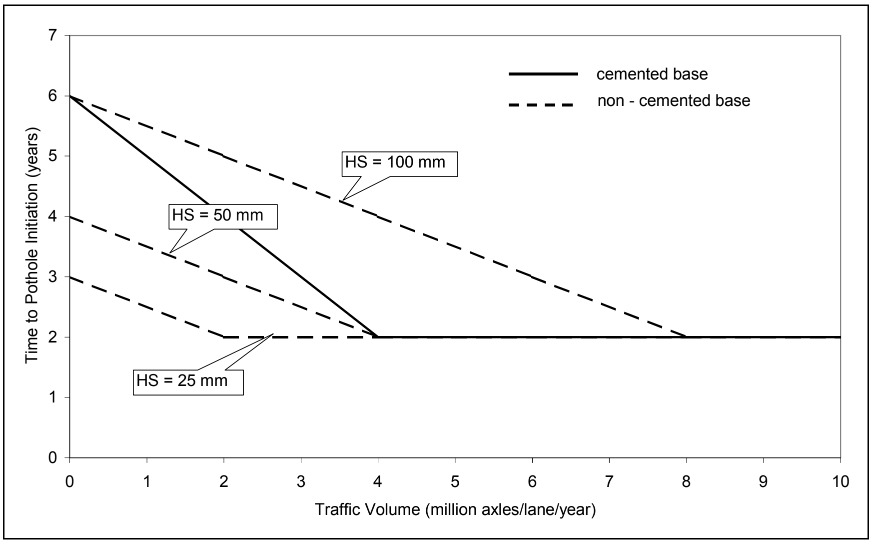

The potholing progression comprises three components; i.e. new potholes caused by wide cracking, new potholes caused by ravelling and the enlargement of existing potholes, defined as follows:

$$\Delta APOT = \min[\Delta APOTCR + \Delta APOTRV + \Delta APOTP,\ 10] \qquad \text{. . . (B5.3)}$$

where

$$\Delta APOTCR = K_{pp} \min[2(ACRW)(U),\ 6] \quad \text{if } ACRW > 20 \qquad \text{. . . (B5.4)}$$
$$= 0 \quad \text{otherwise}$$

$$\Delta APOTRV = K_{pp} \min[0.4(ARAV)(U),\ 6] \quad \text{if } ARAV > 30 \qquad \text{. . . (B5.5)}$$
$$= 0 \quad \text{otherwise}$$

$$\Delta APOTP = \min\{APOT_a [(KBASE)(YAX)(MMP + 0.1)],\ 10\} \qquad \text{. . . (B5.6)}$$

$$U = \frac{(1+CQ)(YAX/SNC)}{(HS)(0.8W/ELANES)} \qquad \text{. . . (B5.7)}$$

$$KBASE = \max[2 - 0.02(HS),\ 0.3] \quad \text{if base is granular} \qquad \text{. . . (B5.8)}$$
$$= 0.6 \quad \text{if base is cemented}$$
$$= 0.3 \quad \text{otherwise}$$

and

ΔAPOT	=	total annual increase in area of potholes, in per cent
ΔAPOTCR	=	annual increase in potholes due to wide cracking, in per cent
ΔAPOTRV	=	annual increase in potholes due to ravelling, in per cent
ΔAPOTP	=	annual increase in potholes due to enlargement, in per cent
ACRW	=	area of wide cracking, in per cent
ARAV	=	area of ravelling, in per cent
HS	=	total thickness of bituminous surfacing, in mm
YAX	=	annual number of axles of all vehicle classes in the analysis year, in millions/lane
SNC	=	modified structural number of the pavement
CQ	=	construction quality indicator (1 = faulty construction, 0 = no faults)
W	=	carriageway width, in m
MMP	=	mean monthly precipitation, in metres/month

ELANES	=	effective number of lanes	
	=	1.0	if W < 4.5
	=	1.5	if 4.5 < W < 6.0
	=	2.0	if 6.0 < W < 8.0
	=	3.0	if 8.0 < W < 11.0
	=	4.0	if W > 11.0
K_{pp}	=	calibration factor for potholing progression	

The rates of potholing progression predicted by HDM-III are illustrated in Figure B5-2 for a thin (20 mm) and thick (100 mm) bituminous surfacing, and for a range of pavement structural strengths. The rates of potholing enlargement are illustrated in Figure B5-3.

Figure B5-2
HDM-III predicted rates of potholing progression

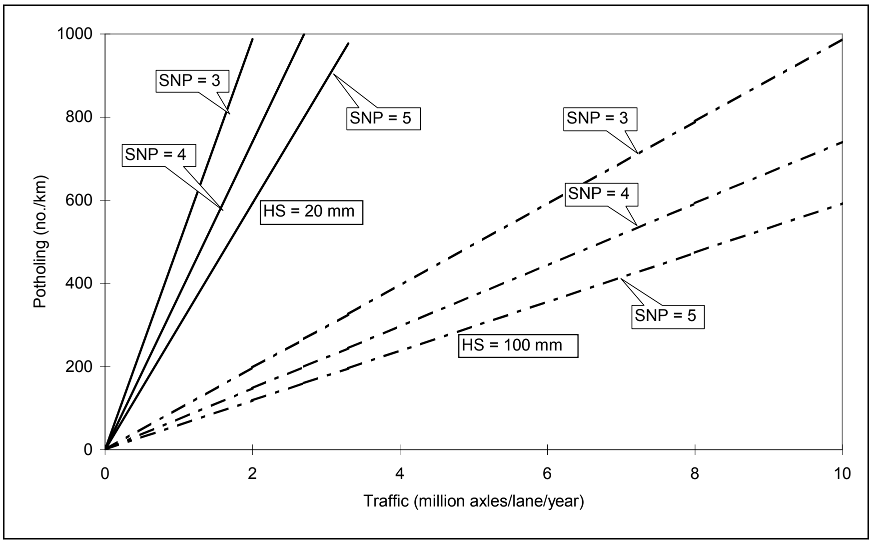

Figure B5-3
HDM-III predicted rates of potholing enlargement

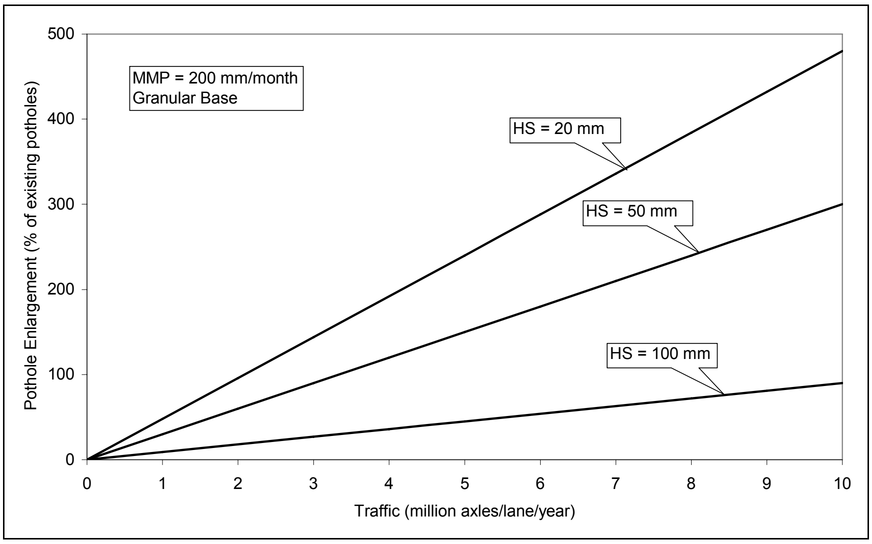

B5.4 Modelling Potholing in HDM-4

The potholing models in HDM-4 use the construction defects indicator for the base, CDB, as a variable (see Section B2.5). In the models potholing is expressed in terms of the number of ‘pothole units’ of area 0.1 m^2. In HDM-4 the volume of each of these pothole units is assumed to be 10 litres (i.e. 100 mm in depth). The relationships for the initiation and progression of potholing have been modified (Riley, 1996b) from those originally proposed for inclusion in HDM-4 in the NDLI report (NDLI, 1995).

B5.4.1 Initiation of Potholing

As in HDM-III, potholes are predicted to initiate from either wide cracking or ravelling. The HDM-III restrictions of ACW > 20% and ARV > 30% before the initiation of potholes can occur from cracking and ravelling, have been made user specified (Morosiuk, 2003a). The HDM-4 default values remain as ACA > 20% and ARV > 30%.

$$IPT = K_{pi}\, a_0 \left[\frac{(1+a_1 HS)}{(1+a_2 CDB)\,(1+a_3 YAX)\,(1+a_4 MMP)} \right] \qquad \text{. . . (B5.9)}$$

where

IPT	=	time between the initiation of wide cracking or ravelling and the initiation of potholes, in years
HS	=	total thickness of bituminous surfacing, in mm
CDB	=	construction defects indicator for the base
YAX	=	annual number of axles of all vehicle classes in the analysis year, in millions/lane
MMP	=	mean monthly precipitation, in mm/month
K_{pi}	=	calibration factor for pothole initiation

The values for IPT are calculated separately for potholing due to cracking and due to ravelling. The separation between these two mechanisms of potholing is maintained throughout the analysis with the progression being modelled differently for potholes due to cracking, due to ravelling and due to the enlargement of existing potholes.

The coefficient values a_0 to a_4 for the potholing initiation model are given in Table B5-1.

Table B5-1
Coefficient values for potholing initiation model

Cause of Pothole Initiation	Pavement Type	a_0	a_1	a_2	a_3	a_4
Cracking	AMGB, STGB	2.0	0.05	1.0	0.5	0.01
	All except GB bases	3.0	0.05	1.0	0.5	0.01
Ravelling	AMGB, STGB	2.0	0.05	1.0	0.5	0.01
	All except GB bases	3.0	0.05	1.0	0.5	0.01

The time to initiation of potholes as predicted by HDM-4 is illustrated in Figure B5-4 for a pavement with a granular base for a range of surfacing thicknesses. A comparison between Figure B5-4 and Figure B5-1 shows the difference between the HDM-III and HDM-4 predicted initiation times for potholes.

Figure B5-4
HDM-4 predicted time to initiation of potholes

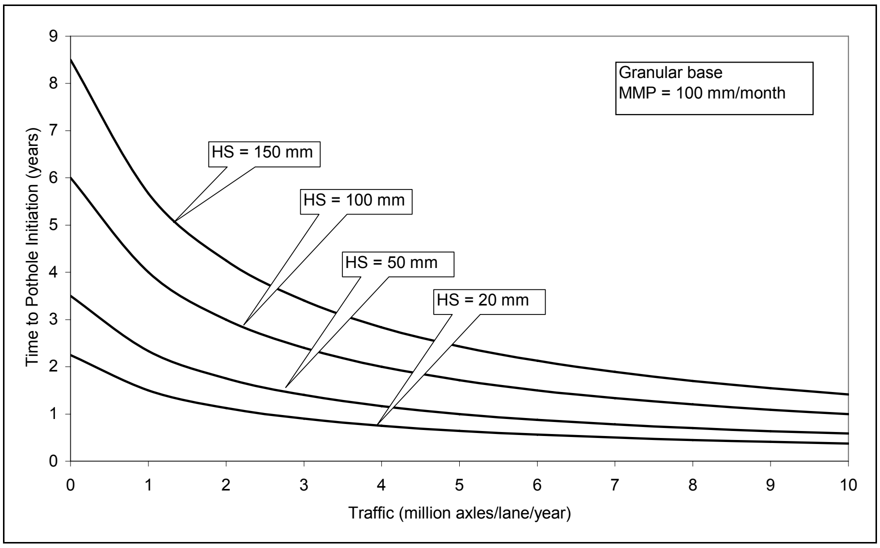

B5.4.2 Progression of Potholing

Pothole progression arises from potholes due to cracking, ravelling and the enlargement of existing potholes. The progression of potholes is affected by the time lapse between the occurrence and patching of potholes; i.e. the frequency of pothole patching. For example, a response time of say 2 weeks between the occurrence of potholes and patching them will result in a smaller area of potholes occurring during the course of a year than if the frequency of patching potholes was say 6 months because if patching is delayed, potholes will grow larger.

In version 1 of HDM-4, a time lapse factor (TLF) was introduced as an indicator of the response time of patching potholes (Odoki, 1997). TLF is defined as a function of the frequency of pothole patching (Fpat) as follows:

$$TLF = 1.541\left[\exp\left(\frac{Fpat}{730}\right) - 1\right] \qquad \text{. . . (B5.10)}$$

where

TLF = time lapse factor ($0 < TLF \leq 1$)
Fpat = frequency of pothol patching, in days

In version 2 of HDM-4, a patching policy factor (PEFF) has been introduced in the potholing progression model in HDM-4 in place of TLF (PIARC, 2004). This modification recognises that a new pothole has to reach a certain size before it is deemed to need repair, that patching may be performed at regular intervals during the year, and that for each patching campaign, partial patching can be carried out. The patching policy factor is calculated as:

$$PEFF = 1 - \frac{Ppt}{100}(1 - TLF) \qquad \text{. . . (B5.11)}$$

where

PEFF = patching policy factor ($0 < PEFF \leq 1$)
Ppt = percentage of potholes to be patched ($0 < Ppt \leq 100$)

In order to differentiate between new potholes (created from cracked or ravelled areas) which have to reach a certain size before they are deemed to need repair, and enlargement of existing potholes, the TLF function has been modified (Riley, 2000c) as follows:

$$TLF = a_0 + (1 - a_0)\left(\frac{Fpat}{365}\right)^{a1} \qquad \text{. . . (B5.12)}$$

The TLF coefficient values of a_0 and a_1 are given in Table B5-2.

Table B5-2
Coefficient values for TLF relationship

Cause of pothole progression	a_0	a_1
Cracking & Ravelling	0.2	1.5
Enlargement	0	1.5

Values of TLF for cracking & ravelling and for enlargement, for a range of pothole patching frequencies, have been tabulated in Table B5-3 and plotted in Figure B5-5.

Table B5-3
Values of TLF

Frequency of pothole patching	TLF	
	Cracking & Ravelling	Enlargement
< 2 weeks	0.21	0.01
1 month	0.22	0.02
2 months	0.25	0.07
3 months	0.30	0.12
4 months	0.35	0.19
6 months	0.48	0.35
12 months	1.0	1.0

Figure B5-5
Plot of TLF for a range of pothole patching frequencies

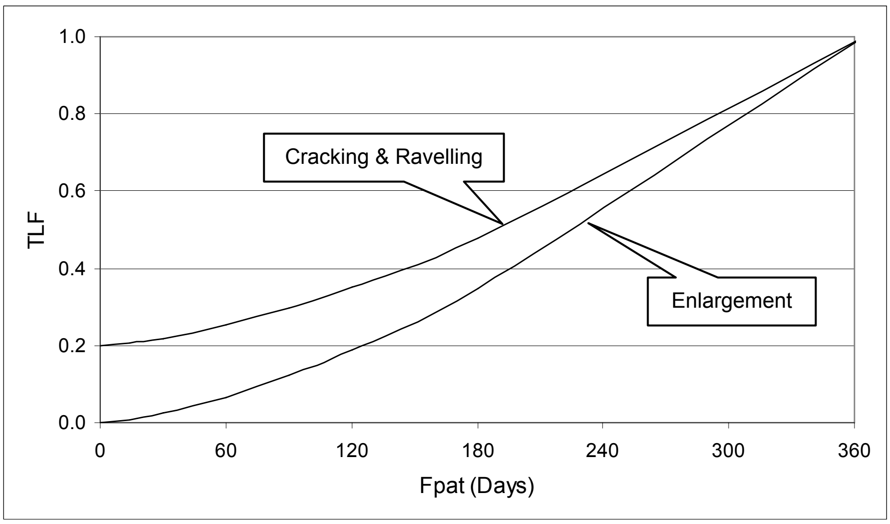

The default value of 0.2 for a_0 has been set, but is likely to vary from agency to agency. In the case of enlargement of potholes existing at the start of the year, there is no intercept in the function as enlargement will be a continuous process until repairs are executed. As illustrated in Figure B5-5, a value of 0.2 for a_0 equates to a 4-month delay in initiation of potholing and patching for new potholes compared with existing potholes.

The values of TLF listed in Table B5-3 show that if pothole patching is carried out only once a year, then potholing progression is unaffected by maintenance (TLF = 1.0). However, if potholes are effectively patched as soon as they occur (i.e. in less than 2 weeks), then a much smaller proportion of the expected number of potholes are likely to have appeared over the course of the year.

The HDM-4 user needs to choose one of the frequencies of pothole patching listed in Table B5-3. The corresponding value of TLF is then used for PPF in the potholing progression model to predict the incremental increase in the number of pothole units during the analysis year.

The potholing progression model contains YAX which is the number of axles per lane. It is possible to have the same YAX on each lane of a 2-lane road and on each lane of a 4-lane road. The model therefore will predict the same number of potholes for both roads (assuming all other variables are the same). Therefore in version 2 of HDM-4, the model has been modified to include the variable ELANES to take into account the number of lanes of a section of road (Morosiuk, 2003a).

The HDM-4 annual incremental increase in the number of pothole units is calculated as:

$$dNPT_i = K_{pp}\, a_0\, ADIS_i\, (PEFF)\left(\frac{ELANES}{2}\right)\left[\frac{(1+a_1 CDB)(1+a_2\, YAX)(1+a_3\, MMP)}{(1+a_4\, HS)}\right] \qquad \ldots (\text{B5.13})$$

Pothole progression from wide cracking or ravelling commences as follows:

i) if at the start of the first year of the analysis period $ACW_a = 0$, then potholing progression from wide cracking commences when

$AGE2 > ICW + IPT$ and $ACW_a > ACW_{pi}$

or

if at the start of the first year of the analysis period $ARV_a = 0$, then potholing progression from ravelling commences when

$AGE2 > IRV + IPT$ and $ARV_a > ARV_{pi}$

ii) if at the start of the first year of the analysis period $0 < ACW_a \leq ACW_{pi}$ then potholing progression from wide cracking commences when $ACW_a > ACW_{pi}$

or

if at the start of the first year of the analysis period $0 < ARV_a \leq ARV_{pi}$ then potholing progression from ravelling commences when $ARV_a > ARV_{pi}$

iii) if at the start of the first year of the analysis period $ACW_a > ACW_{pi}$ then potholing progression from wide cracking commences immediately

or

if at the start of the first year of the analysis period $ARV_a > ARV_{pi}$ then potholing progression from ravelling commences immediately

iv) if during the analysis period ARV_a becomes $< ARV_{pi}$ because of ravelling areas reverting to cracked areas, then potholing still progresses from ravelling

Pothole progression from enlargement commences if $NPT_a > 0$ at the start of an analysis year.

The total annual increase in the number of pothole units per kilometre of road length is given by:

$$dNPT = \sum_{i=1}^{3} dNPT_i \qquad \text{. . . (B5.14)}$$

where

$dNPT$	=	total number of additional pothole units per km during analysis year
$dNPT_i$	=	additional number of pothole units per km derived from distress type i (wide cracking, ravelling, enlargement) during analysis year
$ADIS_i$	=	per cent area of wide cracking at start of the analysis year, or per cent area of ravelling at start of the analysis year, or number of existing pothole units per km at start of the analysis year
ACW_{pi}	=	user specified minimum area of wide cracking before potholes can occur (default = 20)
ARV_{pi}	=	user specified minimum area of ravelling before potholes can occur (default = 30)
ELANES	=	effective number of lanes for the road section
PEFF	=	patching policy factor (see Table B5-3)
K_{pp}	=	calibration factor for pothole progression

and the other variables are as defined for potholing initiation

The coefficient values a_0 to a_4 for the potholing progression model are given in Table B5-4.

Table B5-4
Coefficient values for potholing progression model

Cause of Pothole Progression	Pavement Type	a_0	a_1	a_2	a_3	a_4
Cracking	AMGB, STGB	1.0	1.0	10	0.005	0.08
	All except GB bases	0.5	1.0	10	0.005	0.08
Ravelling	AMGB, STGB	0.2	1.0	10	0.005	0.08
	All except GB bases	0.1	1.0	10	0.005	0.08
Enlargement	AMGB, STGB	0.07	1.0	10	0.005	0.08
	All except GB bases	0.035	1.0	10	0.005	0.08

The rates of potholing progression with no pothole patching (PEFF = 1.0) predicted by HDM-4 are illustrated in Figure B5-6.

The predicted rates of potholing progression with a patching frequency of 2 months are illustrated in Figure B5-7 for new potholes (cracking & ravelling) and for enlargement of existing potholes. Also plotted in Figure B5-7 are the rates with the 'no patching' policy, for comparison.

Figure B5-6
HDM-4 predicted rates of potholing progression – no patching

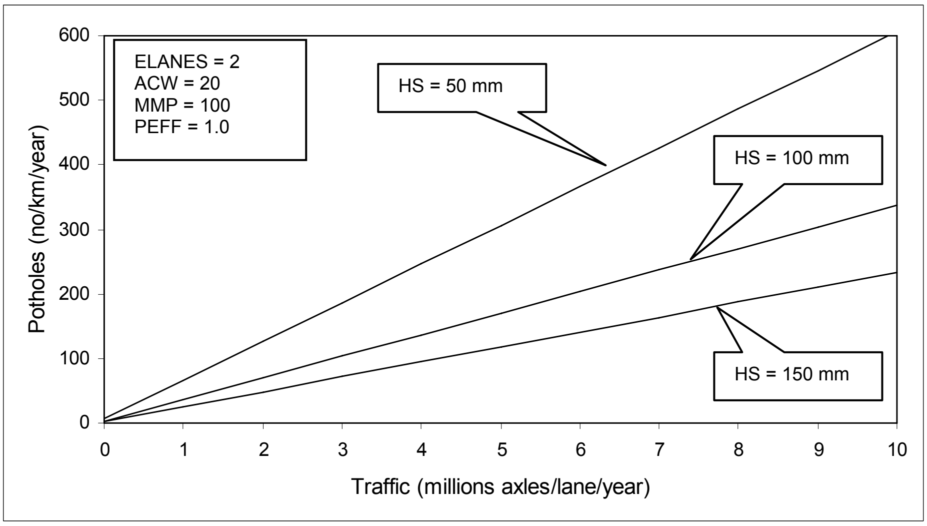

Figure B5-7
HDM-4 predicted rates of potholing progression – with patching

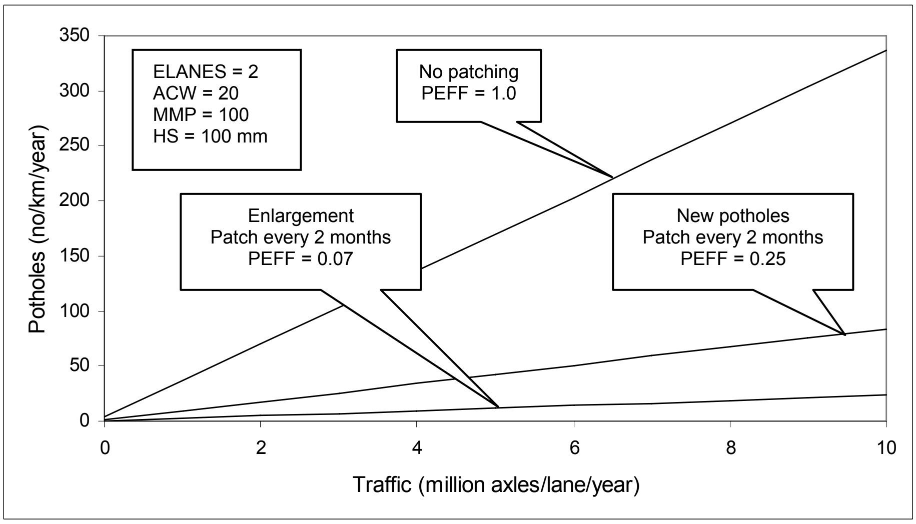

B6. EDGE BREAK

Edge break can be defined as the loss of surface, and possibly base materials, from the edge of the pavement, and commonly arises on narrow roads with unsealed shoulders. Ideally, three parameters are needed to define edge break:

- the length of the occurrence
- the width of the lost material
- the depth of the lost material

To record the data in this way for both sides of the road is arduous and a single unit of measurement is desirable. Average width of edge break is often used in pavement surveys but this omits the depth of edge break, and hence the volume of material needed for repair.

B6.1 Mechanisms of Edge Break

Loss of material at the pavement edge can be caused by two mechanisms; shear failure and attrition. Shear failure occurs in the upper layers due to vertical wheel loads at, or close to, an edge that is lacking lateral support from the shoulder. Parameters governing this mechanism are the drop height from pavement to shoulder, the strength of the pavement material and the number of wheel loads that pass close to or over the pavement edge.

Attrition occurs when wheels travel on and off the pavement edge, as happens when vehicles pass on narrow roads (carriageway width less than 4 - 5 m) or when parking on the shoulder. As with shear failure, the extent of material loss is a function of wheel passes, edge step and, possibly, the speed of the vehicles.

B6.2 Conceptual Models for Edge Break

Many countries, especially in Asia, have a significant length of narrow, often single lane, roads where traffic volumes have grown at a high rate over the last 20 years. On such roads, edge break can be a serious problem. However, little research data has been available with which to produce validated models that relate edge break to traffic volume, road geometry and condition. Edge break was not modelled in HDM-III.

Hoban (1987) provided an approach to modelling edge break which was subsequently adapted and modified for use in Indonesia (Hoff and Overgaard, 1994). The model proposed by Hoban derived an expression for the number of edge crossings by vehicles on narrow pavements due to vehicles meeting and overtaking as follows:

$$ERATE = \frac{26.5(PSH)(AADT)^2}{S} \quad \text{. . . (B6.1)}$$

where

$$PSH = \max\{\min[(2.65 - 0.425\ CW),\ 1],\ 0\} \quad \text{. . . (B6.2)}$$

and

ERATE = number of edge crossing per km per year
PSH = proportion of shoulder use time due to width
S = average traffic speed, in km/h
CW = carriageway width, in m
AADT = annual average daily traffic, in veh/day

Hoban (1987) used data from Hide and Keith (1979) for annual patching quantities in St. Vincent to estimate edge repair needs and tentatively concluded that it represented 30 m^3 per million edge crossings to give the following:

$$VEB = \frac{0.0008(PSH)(AADT)^2}{S} \qquad \text{. . . (B6.3)}$$

where

VEB = loss of edge material, in m^3 per km per year

Figure B6-1 shows the predictions of this model for a carriageway width of 3.5 m and traffic speeds of 50 km/h and 100 km/h.

Figure B6-1
Edge break derived from Hoban (1987)

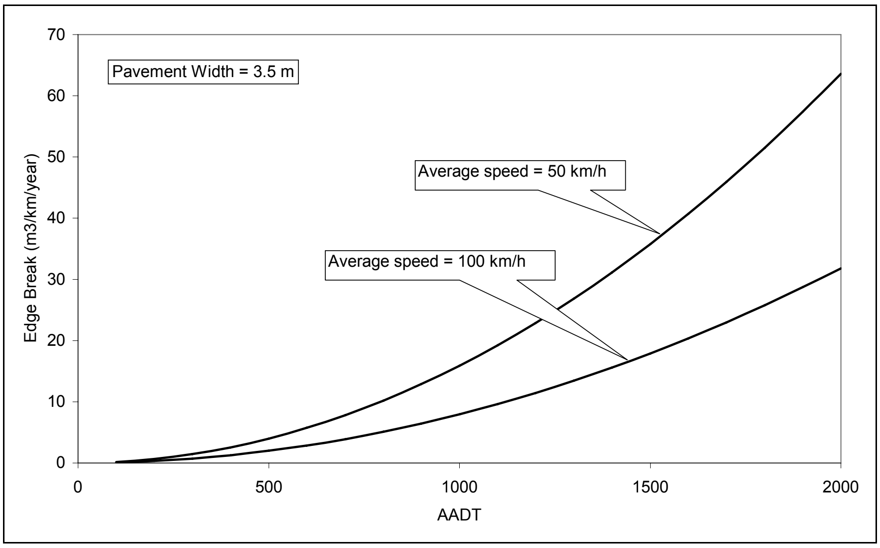

The relationship shown in Figure B6-1 is, in some ways, counter-intuitive, being inversely related to vehicle speed. The speed effect is due to the number of inter-actions per unit of time and length: at higher speeds there are fewer vehicle inter-actions. It might be expected that vehicles passing between the pavement and the shoulder would cause greater damage at higher speeds with the impact of the tyres on the edge of the asphalt, however, there is no research to substantiate this.

Hoff and Overgaard (1994) proposed some refinement of the Hoban model by incorporating edge step and the damaging effects of vehicle speed. It was assumed that, with no edge step, edge break would not occur and that the roads studied in St. Vincent had an average edge step of 80 mm. The damaging effect of speed was represented by the square root of speed and the average speed in St. Vincent was assumed to be 50 km/h. This resulted in the following model:

$$VEB = \frac{0.7(PSH)(AADT)^2(ESTEP)}{\sqrt{S}} \times 10^{-6} \qquad \text{. . . (B6.4)}$$

where

$$PSH = \max\{[-3.41 + 14.51/CW + 0.0295\,(CW)^2],\ 0\} \qquad \text{. . . (B6.5)}$$

and

ESTEP = elevation difference from pavement to shoulder, in mm

The above model is illustrated in Figure B6-2 for a carriageway width of 3.5 m and average speed of 50 km/h.

Figure B6-2
Edge break derived from Hoff and Overgaard (1994)

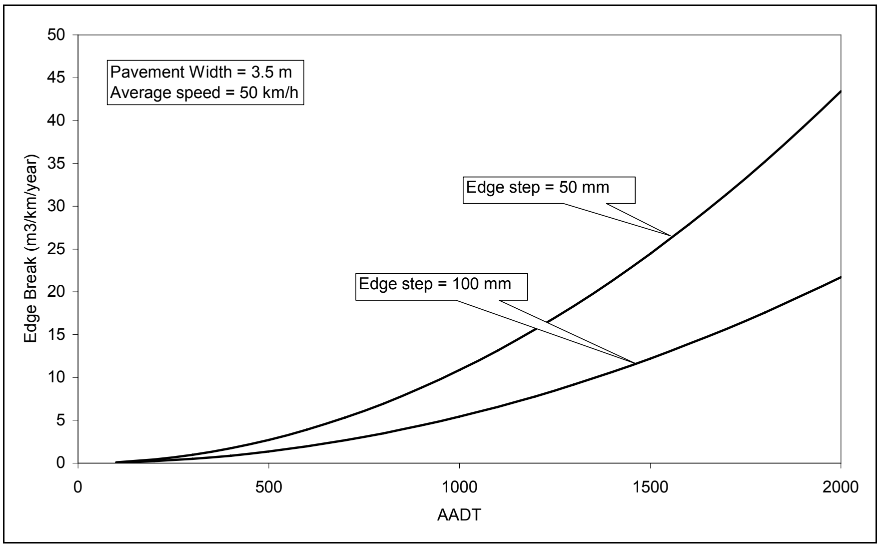

Both the Hoban model and the Hoff and Overgaard model are conceptual and, apart from very tenuous data from the Caribbean study, lack any validation. It is reasonable to expect that there would be a strong effect from moisture as it will weaken both the shoulder material that provides support to the edge of the surfacing and the base of the pavement. However, neither model includes a rainfall term.

In 1995 a survey was made of selected rural roads in Indonesia, which included the collection of data on various forms of distress, traffic and pavement history. The database (Hoff and Overgaard, 1995) also contained data on the amount of edge break. A preliminary analysis of this database was made by the original HDM-4 study team based in Malaysia (NDLI, 1995), using bands of pavement width.

For a carriageway width less than 4.0 m (PSH = 1 based on Hoban, 1987), the assumption was made that vehicle speeds were 30 km/h in hilly terrain and 50 km/h in flat terrain. The following expression was obtained for this carriageway width band:

$$VEB = \frac{30(ESTEP)(AADT)^2}{S} \times 10^{-6} \qquad \text{. . . (B6.6)}$$

Figure B6-3 compares the observed and predicted values of edge break obtained using this relationship.

For width bands above 4.0 m very little edge break was recorded which suggests that shoulder use is minimal. On rural roads in Indonesia heavy vehicles are rare: trucks are 2 - 3 tonne capacity and buses typically have 10 - 20 seats. Speeds are also low and vehicles can generally pass each other on a 4.5 m wide pavement without using the shoulders.

Figure B6-3
Observed and predicted edge break from Indonesia

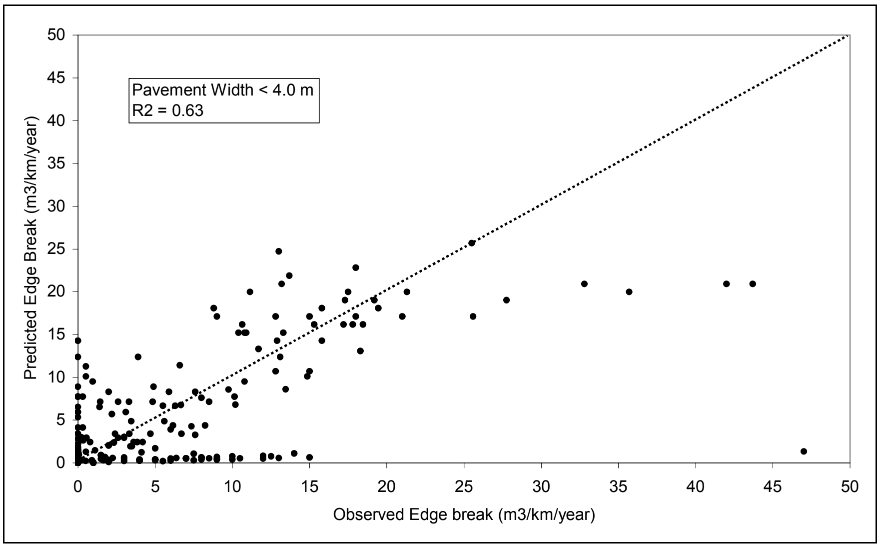

B6.3 Modelling Edge Break in HDM-4

As edge break was not modelled in HDM-III and little data exists for an empirical model to be developed, the conceptual model presented by Hoban (1987) was used as a starting point in the development of an edge break model for HDM-4. As noted earlier, this model omits two possibly important explanatory variables, edge step and rainfall. Analysis of the data from Hoff and Overgaard (1995) showed that edge step seemed to be well correlated with volume of edge break. Although it was not possible to quantify rainfall effects, it is considered that this parameter should be included in the model to allow for calibration by users.

The following conceptual edge break model has been included in HDM-4.

$$dVEB = K_{eb}\ a_0\ PSH\ (AADT)^2\ ESTEP\ (S)^{a1}\ (a_2 + MMP/1000)\ 10^{-6} \qquad \ldots (B6.7)$$

where

$$PSH = \max\left\{\min\left[\max\left(a_3 + a_4\ CW,\ \frac{CW_{max} - CW}{a_5}\right),\ 1\right],\ 0\right\} \qquad \ldots (B6.8)$$

and

dVEB	=	annual loss of edge material, in m^3/km
PSH	=	proportion of time using shoulder
AADT	=	annual average daily traffic
ESTEP	=	elevation difference from pavement to shoulder, in mm
MMP	=	mean monthly precipitation, in mm/month
S	=	average traffic speed, in km/h
CW	=	carriageway width, in metres
CW_{max}	=	user definable maximum carriageway width for the occurrence of edge break, in metres (default = 7.2, maximum = 7.5)
K_{eb}	=	calibration factor for edge break progression

The coefficient values a_0 to a_5 for the edge break model are given in Table B6-1.

The edge break model is illustrated in Figure B6-4 for a surface treatment on a granular base pavement and three carriageway widths.

Table B6-1
Coefficient values for edge break model

Pavement Type	a_0	a_1	a_2	a_3	a_4	a_5
AMGB	50	-1.0	0.2	2.65	-0.425	10
AMAB, AMSB, AMAP	25	-1.0	0.2	2.65	-0.425	10
STGB	75	-1.0	0.2	2.65	-0.425	10
STAB, STSB, STAP	50	-1.0	0.2	2.65	-0.425	10

Figure B6-4
Edge break model – pavement type STGB

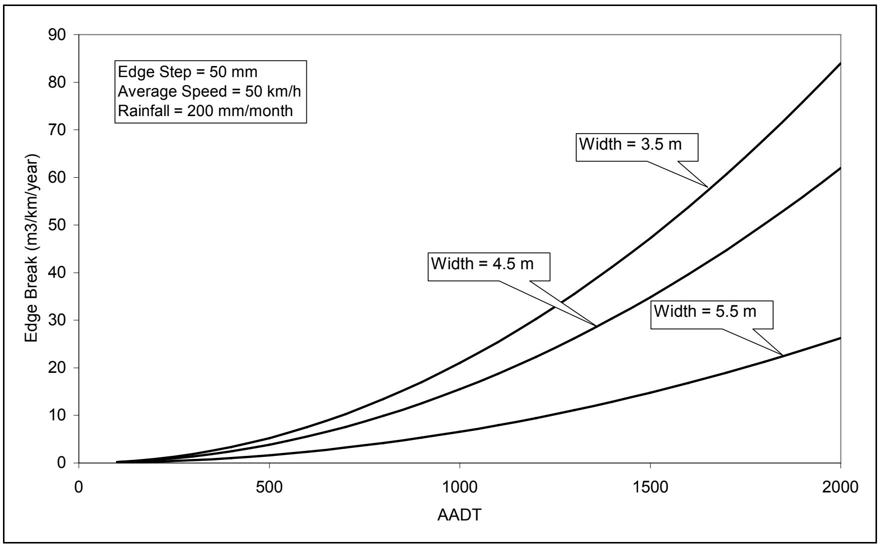

The variable PSH ranges between 0 and 1, indicating the proportion of time that vehicles use the shoulder and are therefore likely to cause edge break. In HDM-4 the value of PSH is equal to 1 when CW < 4 metres. The value of PSH then reduces as CW increases, reducing finally to zero, at which point HDM-4 predicts that edge break will not occur.

Originally the value of PSH was zero for carriageway widths in excess of 6.2 metres (NDLI, 1995), but has subsequently been amended so that the user is able to define the upper limit of carriageway width (CW_{max}) at which edge break ceases to be predicted by HDM-4 (Morosiuk, 1998b). The default value of CW_{max} in HDM-4 has been set to 7.2 metres with the upper limit of CW_{max} set to 7.5 metres. These limits effectively mean that HDM-4 predicts edge break will occur on pavements where CW < 6.2 metres, will not occur on pavements where CW > 7.5 metres, and the user has the flexibility to inhibit the occurrence of edge break between these carriageway limits.

B6.4 Proposed Modifications to the Edge Break Model

Modifications have been proposed (Riley, 2000a) to the edge break model currently in the HDM-4 software and the use of the model in reducing the effective width of the pavement. Edge break occurs when a wheel load is applied to a pavement edge that has inadequate support. It is a shear failure described in Yoder (1959) as “resistance to movement under load is made up of shearing resistance along a logarithmic spiral plus weight outside the loaded area.” This is illustrated in Figure B6-5. It is clear that loss of shoulder material reduces both the shear resistance and the counterweight to the wheel loading.

Figure B6-5
Shear planes at pavement edge

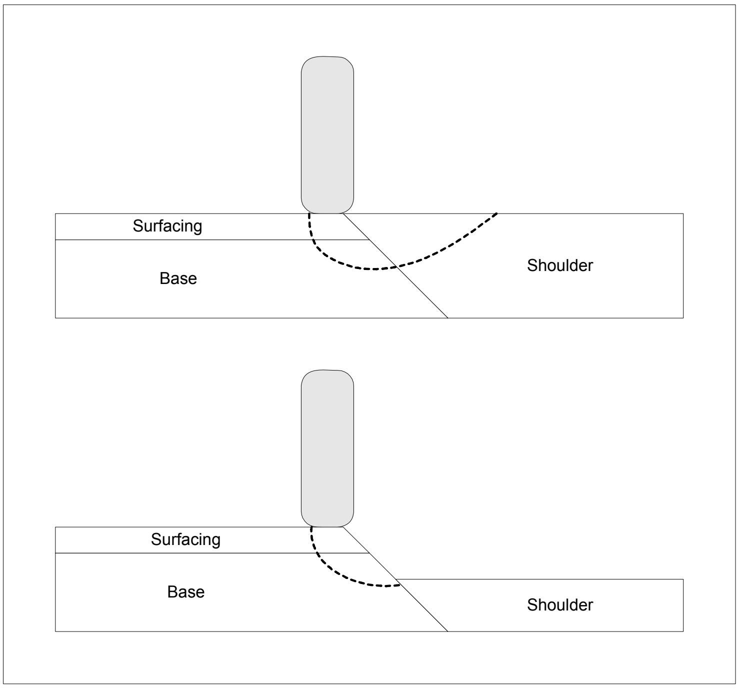

Adopting a mechanistic approach, the model parameters for edge break are:

1. the wheel loading and number of applications
2. the distance of the wheel from the pavement edge
3. the shear resistance of the surfacing, base and shoulder materials
4. the elevation difference between pavement and shoulder

The first of these can be characterised by the axle loading variable used in other deterioration models, YE4. A surrogate for the second is the number of times that a wheel passes from pavement to shoulder and for the third the thickness of bound layers. The fourth, edge step, is already explicitly modelled.

Hoban (1987) gives an expression for the frequency of edge crossings which can be expressed as:

$$ERATE = 3\left[\frac{(PSH)(AADT)^2}{S}\right]10^{-3} \qquad \text{. . . (B6.9)}$$

where

ERATE	=	edge crossings per km per hour
PSH	=	proportion of time using shoulder
AADT	=	annual average daily traffic
S	=	average traffic speed, in km/h

The model for frequency of edge crossings is illustrated in Figure B6-6 for a range of carriageway widths and vehicle speeds.

The model for edge break is proposed as:

$$dVEB = a_0 \frac{(YE4)(ERATE)(ESTEP)}{1 + a_1(HS)} \qquad \text{. . . (B6.10)}$$

where

dVEB = annual loss of edge material, in m^3/km
HS = thickness of bound layers in mm
YE4 = annual number of equivalent standard axles, in millions/lane
ESTEP = elevation difference from pavement to shoulder, in mm

Adopting values of a_0 = 2 and a_1 = 0.1 gives the results shown in Figure B6-7 where heavy vehicles are assumed to be 10% of the total traffic and have an axle load equivalency of 1.

Figure B6-6
Frequency of edge crossings

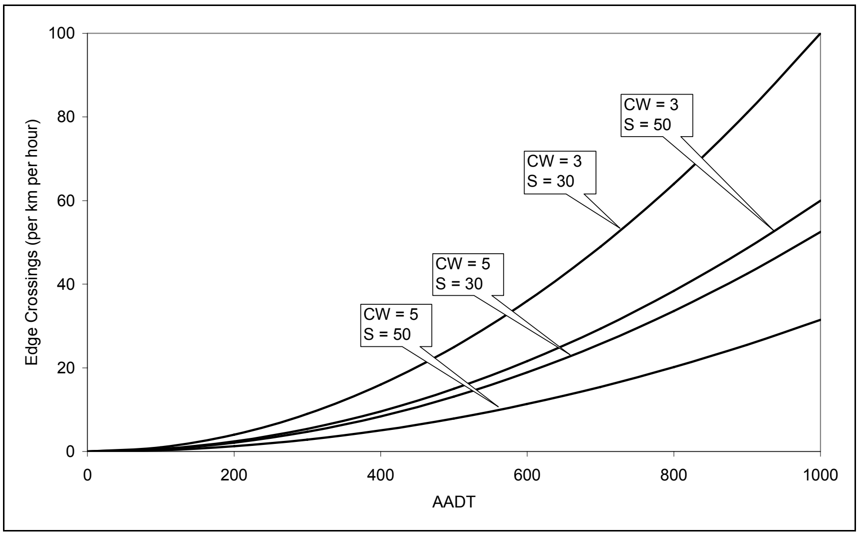

Figure B6-7
Volume of edge break

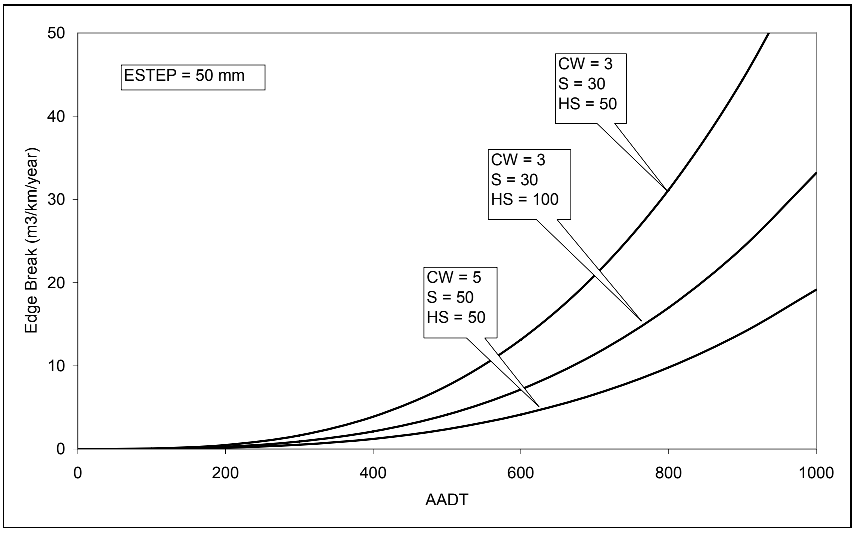

Edge break will reduce the effective width of the pavement by:

$$dCW = \frac{dVEB}{HS} \qquad \text{. . . (B6.11)}$$

where
dCW = annual reduction in effective pavement width, in metres

B7. TOTAL DAMAGED SURFACE AREA

The total road surface consists of the following:

(i) cracking

(ii) ravelling

(iii) potholing

(iv) edge break

(v) undamaged: this area consists of the original road surface which is still in good condition since the last surfacing and the area which has been patched.

The HDM-4 models described in this section calculate the incremental increase in areas of cracking, ravelling, potholing and edge break during an analysis year. For each distress, the incremental increase in area is added to the respective distress area at the beginning of the analysis year to give the area of each distress at the end of the analysis year.

In modelling pavement deterioration, it is important to ensure that the sum of damaged and undamaged surface area must be equal to 100 per cent, in any given analysis year. If, for example, the area of cracking at the end of the year is predicted to be 60%, the area of ravelling to be 35%, the area of potholing 5% and the area of edge break 10%, then the total damaged area is predicted to be 110%. As each distress is treated as mutually exclusive in HDM-4, then the predicted end of year values need to be adjusted to ensure that the total damaged area cannot exceed 100%.

A logic has therefore been devised in HDM-4 for calculating the distress values at the end of an analysis year which ensures that the total damaged area does not exceed 100 per cent. This logic is described in detail in Volume 4, of the HDM-4 Series - Analytical Framework and Model Descriptions (Odoki and Kerali, 2000), together with the relationships for computing the damaged areas at the end of each analysis year and before road works.

B8. RUTTING

Rutting is defined as the permanent or unrecoverable traffic-associated deformation within pavement layers which, if channelised into wheelpaths, accumulates over time and becomes manifested as a rut (Paterson, 1987). Rutting may arise because of material weakness, surface wear or structural inadequacy. Furthermore, the monitoring and control of rutting has important performance implications because of its influence on vehicle operation (affecting vehicle tracking), safety (hydroplaning on ponded water), and dynamic loading (through surface profile variations).

B8.1 Mechanisms of Rutting

The causes of permanent deformation can be classified into traffic-associated and non-traffic-associated causes. Traffic associated permanent deformation results from a rather complex combination of densification and plastic flow mechanisms. Densification is defined by Paterson (1987) as the change in the volume of material as a result of the tighter packing of the material particles and sometimes also the degradation of particles into smaller sizes. Rutting due to densification is usually fairly wide and uniform in the longitudinal direction with heaving on the surface rarely occurring, as shown in Figure B8-1.

Figure B8-1
Typical rut profile as a result of densification

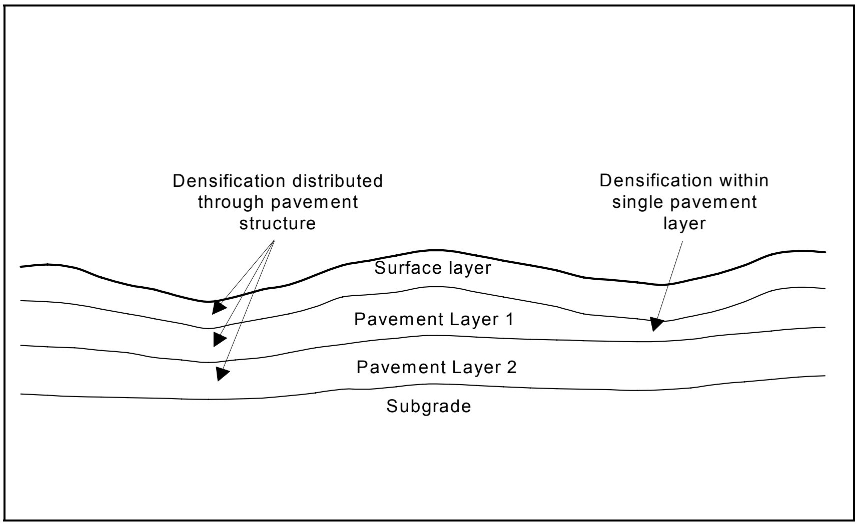

The degree of densification depends greatly on the compaction achieved during construction. The density specification should be selected in accordance with the expected loadings and pavement type. Failure to reach the specified compaction during construction results in an increase in densification under heavy traffic, most of which will occur early in the life of the pavement. It is important to note that for similar rut depth values, the deformation within the pavement may be located within a single weak layer, or more evenly distributed through the depth of the pavement, as illustrated in Figure B8-1.

Plastic flow essentially involves no volume changes, and gives rise to shear displacements in which both depression and heave are usually manifest. Plastic flow occurs when the traffic induced stresses exceed the shear strength of the material, or are sufficient to induce creep (Paterson, 1987). The rutting in this case is usually characterised by heaving on the surface alongside the wheelpaths, as illustrated Figure B8-2.

Figure B8-2
Typical rut profile as a result of plastic flow (shoving)

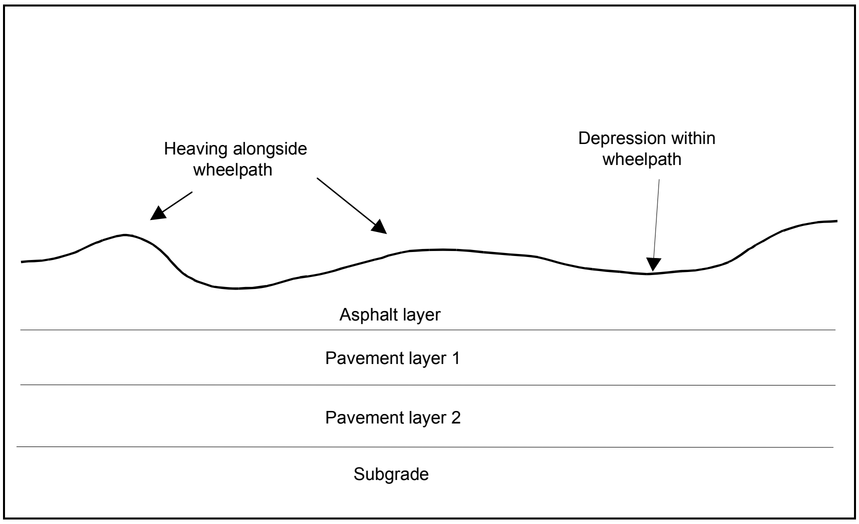

B8.2 Phases of Rutting

The resistance of pavement structures to rutting is dependent on a number of factors which relate to applied loads (traffic type, volume and speed), the environment (temperature, rainfall), the pavement structure (thickness and design), the construction process. In general, this resistance to permanent deformation of pavement materials may be divided into the following three phases:

Initial densification

This phase, also referred to as bedding in, secondary or post construction compaction, describes the relatively rapid initial increase in rutting on a newly constructed pavement once it is opened to traffic. The phase is characterised by a decreasing deformation (strain) rate, and the amount of initial densification is mainly influenced by the compaction achieved during construction and traffic load.

Constant rate of deformation

During this phase the rate of deformation (strain) tends to stabilise, resulting in a constant rate of increase in deformation with traffic. The rate of deformation is mainly influenced by traffic loading, pavement strength and environmental factors.

Accelerating deformation

This is the third and final phase in the development of deformation and it is characterised by an increased rate of deformation. This increase is mainly influenced by traffic loading, pavement strength and environmental factors.

The factors influencing the three phases are discussed in more detail for the bituminous pavement types included in HDM-4, defined in terms of base course material; i.e. granular base (GB), cement-treated base (SB) and asphalt base (AB) pavements.

B8.2.1 Granular Base Pavements

The general trends in deformation of granular base pavements are shown in Figure B8-3.

Figure B8-3
Relative behaviour of granular materials (after Freeme, 1983)

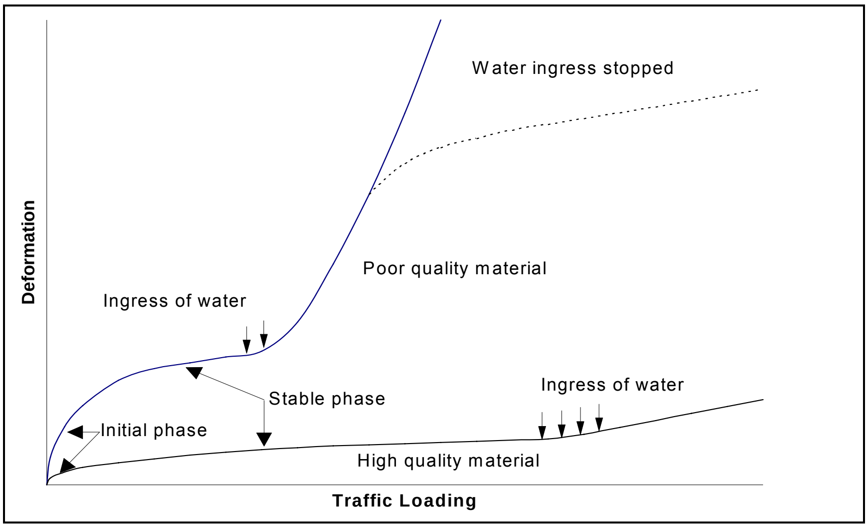

The factors influencing the magnitude and duration of various phases are:

Construction compaction: The amount of early deformation, also referred to as post-construction compaction, depends on the densification achieved during the construction of the pavement layers and the quality of the pavement layers. The higher the level of compaction and the better the quality of material in the pavement layers, then the expected initial densification will be lower, as illustrated in Figure B8-3.

Material quality: The rate of increase in deformation during the stable phase also depends on the initial quality of the material. Where the initial quality of the material is poor, high traffic loadings may result in quick shear failure, and the stable phase may be non-existent or very brief, as illustrated in Figure B8-3. For relatively high quality materials, the performance under traffic is much better, partly because good material is stronger and partly because it is less susceptible to water.

Moisture content: Over time the pavement surface may crack. The increased moisture content due to ingress of water through a cracked surface layer will result in a decrease in shear strength of granular pavement layers which, when over-stressed will increase deformation, especially in the final phase. The rate of increase is dependent on material quality (high quality materials are less susceptible to ingress of water), the amount of water ingress (rainfall), and traffic loading.

Traffic loading: Traffic loading is a combination of the magnitude and number of applied loads (number of equivalent standard axles), and is one of the most important factors contributing to rutting. Traffic induces stresses within the pavement structure and this determines the quality of materials required as well as the behaviour of the pavement. It is important to note that a few excessive loads or tyre pressures for which the pavement was not designed may cause stresses exceeding the shear strength of the material, resulting in the premature failure of the layer.

B8.2.2 Cement-treated Base Pavements

The general deformation trends of cement-treated base pavements are shown in Figure B8-4.

Figure B8-4
Relative behaviour of cement-treated materials

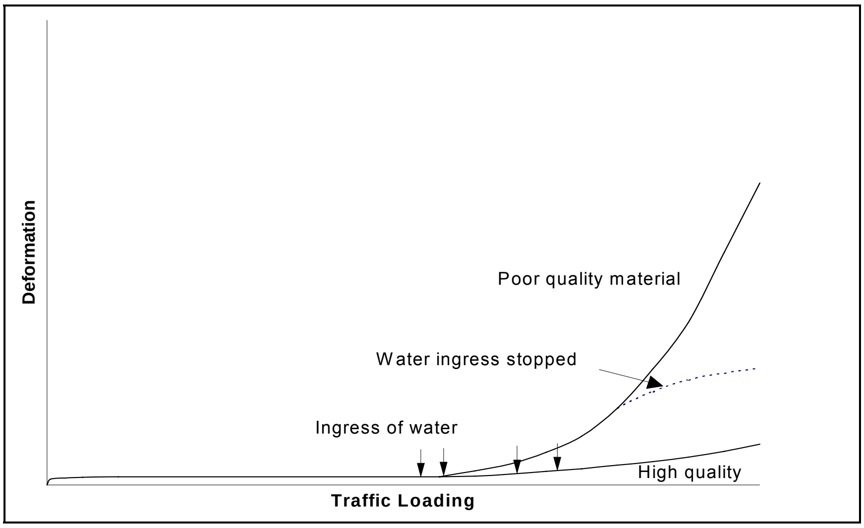

after Freeme, 1983

For these pavements, the expected initial increase in deformation due to post-construction compaction is much lower and usually negligible in most cases. This is followed by a stable phase during which little or no deformation occurs. Under some circumstances a third phase may occur during which the rate of deformation increases. This phase only occurs if the integrity of the cemented material is compromised through very heavy traffic, severe environmental effects or very poor materials. In the latter case, the pavement will behave in a similar way to a pavement with unbound base layers. For cement-treated base pavements, most of the pavement strength is usually concentrated within these layers, and construction quality has a considerable influence on the performance of the layer.

B8.2.3 Asphalt Base Pavements

The general deformation trends of asphalt base pavements are illustrated in Figure B8-5.

The behaviour during the various phases is similar to that of granular base pavements. The main difference in behaviour between asphalt layers and granular layers occurs in the final phase, where asphalt layers are far more water-resistant than granular layers, but as a result of their visco-elastic behaviour they are more temperature susceptible. The factors influencing the magnitude and duration of various phases are construction compaction, material quality (which, for asphalt layers, refers to the mix properties of binder content, air voids and aggregate type), traffic loading and most importantly, the speed of loading. Thus climbing lanes are very susceptible to deformation.

The influence of the asphalt's characteristics is discussed below (Verhaeghe, et al, 1993):

Binder content: The selection of a suitable binder content for a given grading of aggregate is one of the main problems in the design of a bituminous mixture. From the point of view of deformation, asphalt mixes should contain just enough binder to give cohesion and to enable adequate compaction to be achieved, without undue risk to plastic deformation under the prevailing conditions of traffic and temperature. Too much binder will lubricate the mix to such an extent that the mixture will lack internal friction and become unstable.

Air voids content: The level of air voids within an asphalt mix influences the behaviour of the mix. The higher the air voids after trafficking, the more resistant the mix is to deformation. As a result, however, an increased rate of hardening of the binder occurs due to the increased permeability to air, making the surfacing stiffer and more liable to cracking. If the air voids content is too low, the asphalt mix will become unstable, resulting in plastic flow of the layer under heavy trafficking, slow moving loads or high maximum temperature. According to Road Note 31 (TRL, 1993), numerous studies indicate that the minimum air voids after heavy trafficking should always exceed 3 per cent to avoid potential plastic flow, but should be less than 5 per cent to keep hardening of the binder (under tropical conditions) to a minimum.

Aggregate type and quantity: The resistance to permanent deformation of certain asphalt mixes (asphalt concrete and bitumen macadam) is dependent upon the interaction between particles of the coarse aggregate to form a mechanical interlocking structure; the higher the particle to particle contact within the mix, the more resistant the mix will be to deformation. Thus both the shape and texture of coarse aggregate is of importance. Also the higher the stone content the lower the deformation, but the more difficult it is to achieve the required compaction during construction.

Temperature: The dependence of the deformation properties of bituminous mixtures on temperature is due to the strong dependence of the viscosity of the bitumen on temperature. Typically, an increase in temperature from 25°C to 50°C will decrease the viscosity by a factor of five, although this will depend on loading time. Such a change in viscosity reduces the resistance to deformation by a much lower factor, but designing mixtures to resist deformation under severe conditions of high temperatures and slow moving heavy traffic is difficult.

Figure B8-5
Relative behaviour of asphalt materials

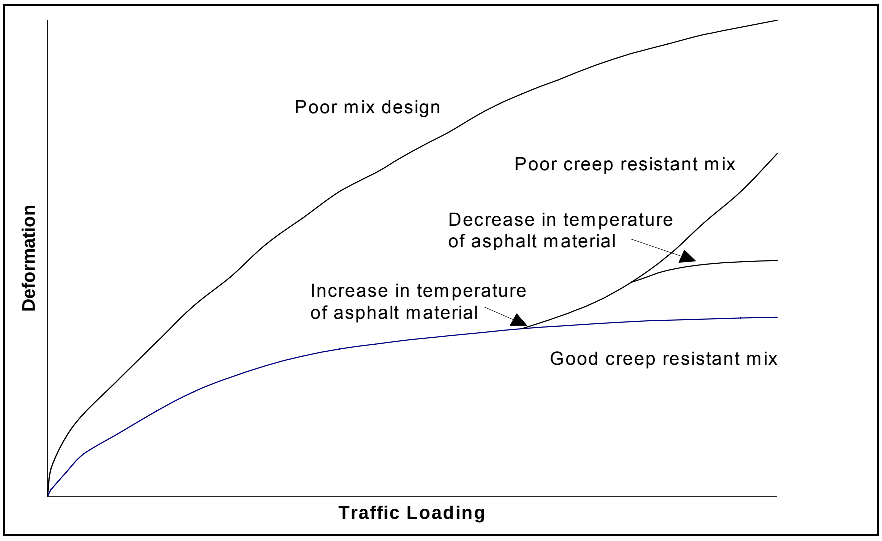

after Freeme, 1983

B8.3 Modelling Rutting in HDM-III

The HDM-III rut depth models were derived from data collected during the Brazil-UNDP study. Rut depth in this study was measured with a 1.2m straight-edge at four locations at 80 metre intervals in each wheelpath of a 320-metre section. A total of 2,546 sections were surveyed, of which 1215 were surface treatment and 797 were asphalt concrete. For analytical purposes, the measurements were reduced to a mean and standard deviation for each section.

Rut depth values were generally low in the Brazil-UNDP study (95 per cent of the rut depth values were less than 8 mm) on account of the design standards of the pavements, and predominantly thin asphalt surfacings (generally less than 100 mm). Thus the validity of these models may be restricted for cases of high levels of rutting. Further details of the sections and ranges of measurements are given in Paterson (1987).

Two separate models, one for the mean rut depth and one for the standard deviation of rut depth were developed by Paterson (1987) as 'absolute' models; i.e. they predict the rutting at a point in time rather than the incremental change over a period of time. These relationships are given below:

Mean rut depth

$$RDM = AGE3^{0.166}\ SNC^{-0.502}\ COMP^{-2.3}\ NE_4^{ERM} \qquad \text{. . . (B8.1)}$$

Standard deviation of rut depth

$$RDS = 2.063\ RDM^{0.532}\ SNC^{-0.422}\ COMP^{-1.664}\ NE_4^{ERS} \qquad \text{. . . (B8.2)}$$

where

$$ERM = 0.0902 – 0.009(RH) + 0.0384(DEF) + 0.00158(MMP)(CRX) \qquad \text{. . . (B8.3)}$$

$$ERS = 0.00116\ (MMP)\ (CRX) – 0.009\ (RH) \qquad \text{. . . (B8.4)}$$

and

RDM = mean rut depth, in mm
RDS = standard deviation of rut depth, in mm
NE_4 = cumulative number of equivalent standard axles (esa)
SNC = modified structural number of the pavement
DEF = mean Benkelman beam deflection in both wheelpaths, in mm
AGE3 = age of pavement since last overlay or construction, in years
COMP = relative compaction in the base, sub-base and selected subgrade layers, as a fraction (see Section B2.5)
MMP = mean monthly precipitation, in m/month
CRX = area of indexed cracking, in per cent
RH = rehabilitation factor (RH = 1 for overlaid pavements and RH = 0 for original pavements)

The mean rut depth was found to be a non-linear function and the rut depth standard deviation was expected to depend on the uniformity of the pavement, e.g., either the variation in stiffness (deflection) or in compaction. However, a satisfactory relationship could not be identified from the data available. Since the rut depth standard deviation was identified as one component of the roughness prediction model, a model was then developed as a function of the mean rut depth, plus a few other explanatory variables which were expected to represent non-uniformity in the pavement.

The 'absolute' models developed by Paterson (1987) were modified in HDM-III (Watanatada, et al, 1987) to convert the absolute rut depth model to an incremental one, in order to be compatible with the incremental model structure in HDM-III. The rut depth models in HDM-III are as follows:

Mean rut depth (RDM)

The progression of mean rut depth is given by:

$$RDM = K_{rp} \frac{39800\,[(YE4)\,(10^6)]^{ERM}}{(SNC^{0.502})(COMP^{2.3})} \qquad \text{. . . (B8.5)}$$

In the first year when the mean rut depth at the start of the year (RDM_a) is zero, equation B8.5 is used directly to estimate the incremental change in RDM (dRDM), but subsequently dRDM is derived as follows:

$$dRDM = K_{rp}\left\{\frac{0.166 + ERM}{AGE3} + 0.0219(MMP)(dCRX)\log_e[\max(1,\ AGE3\ YE4)]\right\}RDM_a$$

. . . (B8.6)

where

$$ERM = 0.09 - 0.009(RH) + 0.0384(DEF) + 0.00158(MMP)(CRX_a) \qquad \text{. . . (B8.7)}$$

and

dRDM = incremental change in the mean rut depth during analysis year, in mm
RDM_a = mean rut depth at the beginning of the analysis year, in mm
YE4 = annual number of equivalent standard axles, in millions/lane
COMP = relative compaction in the base, sub-base and selected subgrade layers, in per cent (see Section B2.5)
CRX_a = area of indexed cracking at the beginning of analysis year, in per cent
dCRX = incremental change in indexed cracking during analysis year, in per cent
K_{rp} = calibration factor for rut depth progression
and the other variables are as defined previously

Standard Deviation of Rut Depth (RDS)

$$RDS = K_{rp} \frac{4390\,(dRDM^{0.532})(YE4\ 10^6)^{ERS}}{(SNC^{0.422})(COMP^{1.66})} \qquad \text{. . . (B8.8)}$$

In the first year when RDM_a = 0, equation B8.8 is used to estimate the change in the standard deviation of rut depth (dRDS), and the prediction is halved as an explicit suppression of the sharp initial increase. Subsequently the incremental change in rut depth standard deviation is derived as follows:

$$dRDS = K_{rp}\left\{\frac{0.532(dRDM)}{RDM_a} + \frac{ERS}{AGE3} + 0.0159(MMP)(dCRX)\log_e[\max(1,\ AGE3\ YE4)]\right\}$$

. . . (B8.9)

where

$$ERS = 0.00115\,(MMP)\,(CRX_a) - 0.0086\,(RH) \qquad \text{. . . (B8.10)}$$

and

dRDS = incremental change in standard deviation of rut depth during the analysis year, in mm

The prediction of first-year mean rut depth by the HDM-III model is illustrated in Figure B8-6.

From Figure B8-6 it is evident that the expression for first-year mean rut depth development is the most sensitive to pavement strength (at lower strengths), and to a lesser degree to compaction, with virtually no sensitivity to axle loading. The sensitivity to the other terms within the expression, namely rainfall and cracking, was assumed to be negligible in this example since the pavement was new and assumed to be uncracked.

Figure B8-6
First year mean rut depth (RDM) prediction by HDM-III

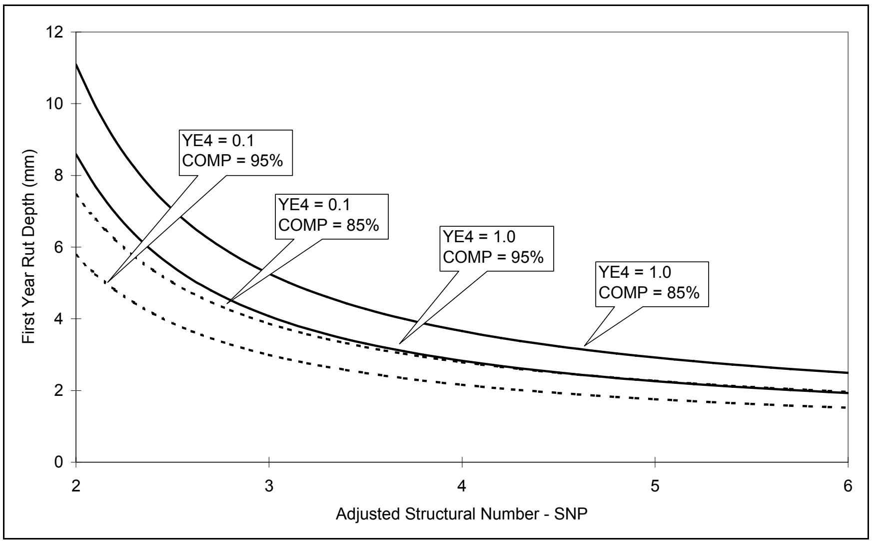

In order to illustrate the progression of rutting over the life of a pavement, the HDM-III deterioration model needs to be run to enable the progression of variables such as cracking to be estimated for use in the rutting model. The HDM-III predicted mean rut depth progressions over the life of a pavement are illustrated in Figure B8-7 for various levels of rainfall. No maintenance was allowed over the life (20 years) of a pavement with a granular base with a structural strength of 4.0, under an annual traffic loading of 0.5 million ESA.

Figure B8-7
HDM-III predicted rates of rut depth progression

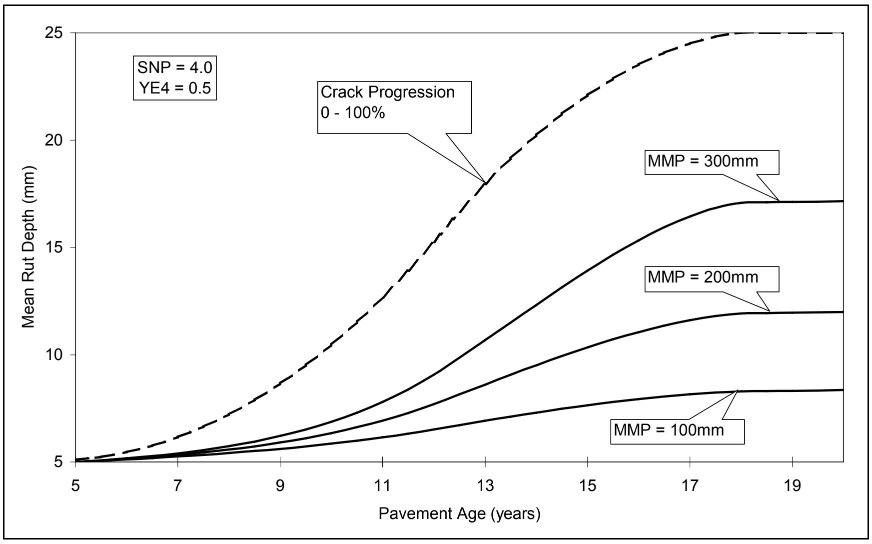

B8.4 Modelling Rutting in HDM-4

Some of the limitations of the HDM-III rutting model have been addressed in the model incorporated in HDM-4. In particular these are:

- separate relationships to model the various phases of the progression of structural deformation
- a new relationship for modelling the plastic deformation of pavements

- a new relationship for modelling the seasonal surface wear which occurs in countries where vehicles use snow chains or studded tyres on roads covered with snow and ice
- standardise the rut depth predictions to those measured under a 2.0m straight-edge

Rut depth modelling is performed after the values of all the surface distresses (cracking, ravelling, potholing and edge break) at the end of the year have been calculated (i.e. after checking the total damaged surface area does not exceed 100 per cent – see Section B7).

The HDM-4 rut depth model is based on four components of rutting, the rut depth at any time being the sum of the four components. These four components are as follows:

- initial densification
- structural deformation
- plastic deformation
- wear from studded tyres

B8.4.1 Initial Densification

The relationship for the initial densification component of rutting is based on the HDM-III model for predicting the rutting in the first year of a new pavement (equation B8.5). The HDM-III model predicts rut depths measured under a 1.2m straight-edge. In order to predict ruts measured under a 2.0m straight-edge, the coefficient values in the HDM-4 relationship have been changed using the following relationship (NDLI, 1995).

$$RDM_{2.0} = 1.3\,(RDM_{1.2}) \qquad \text{. . . (B8.11)}$$

where

$RDM_{2.0}$ = rut depth under a 2.0 metre straight-edge
$RDM_{1.2}$ = rut depth under a 1.2 metre straight-edge

The initial densification depends upon the degree of relative compaction of the base, sub-base and selected subgrade layers applied to these layers at construction. The variable used to describe this compaction, COMP, has been described in detail in Section B2.5 with suggested values of COMP given in Table B2-13.

As initial densification only applies to new construction or reconstruction that involves the construction of a new base layer, this component of rutting is modelled in HDM-4 for only the first year after such construction. AGE4 is used in HDM-4 to denote the time since such construction (see Section A2.5.3). For an existing pavement that is older than one year at the start of an analysis period (i.e. AGE4 > 1), initial densification is not modelled.

The HDM-4 initial densification model is:

$$RDO = K_{rid}\,[a_0\,(YE4\;10^6)^{(a1 + a2\,DEF)}\,SNP^{a3}\,COMP^{a4}] \qquad \text{. . . (B8.12)}$$

where

RDO = rutting due to initial densification, in mm
YE4 = annual number of equivalent standard axles, in millions/lane
DEF = average annual Benkelman beam deflection, in mm
SNP = average annual adjusted structural number of the pavement
COMP = relative compaction, in per cent (see Section B2.5)
K_{rid} = calibration factor for initial densification

The coefficient values a_0 to a_4 for the initial densification model are given in Table B8-1.

Table B8-1
Coefficient values for initial densification model

Pavement Type	a_0	a_1	a_2	a_3	a_4
AMGB, AMAB, AMSB, STGB, STAB, STSB	51740	0.09	0.0384	-0.502	-2.30
AMAP, STAP	0	0	0	0	0

B8.4.2 Structural Deformation

The structural deformation component of rutting in HDM-4 is based on the rutting progression model in HDM-III, but has been simplified into a linear form (Morosiuk, 1998c). Structural deformation is assumed to progress linearly until cracking occurs, at which point the progression of rutting is assumed to increase at a faster rate as illustrated conceptually in Figure B8-8.

A linear model was derived by fitting straight lines to the progressions of rutting predicted by the original 'absolute' model derived by Paterson (equation B8.1). Cracking was set to zero in equation B8.1 to derive the structural deformation without cracking component. In order to derive the structural deformation after cracking component, cracking was included in the analysis. The HDM-III cracking initiation and progression models were used to estimate when cracking would start and the amount of cracking in each of the following years.

Figure B8-8
Linear structural deformation model

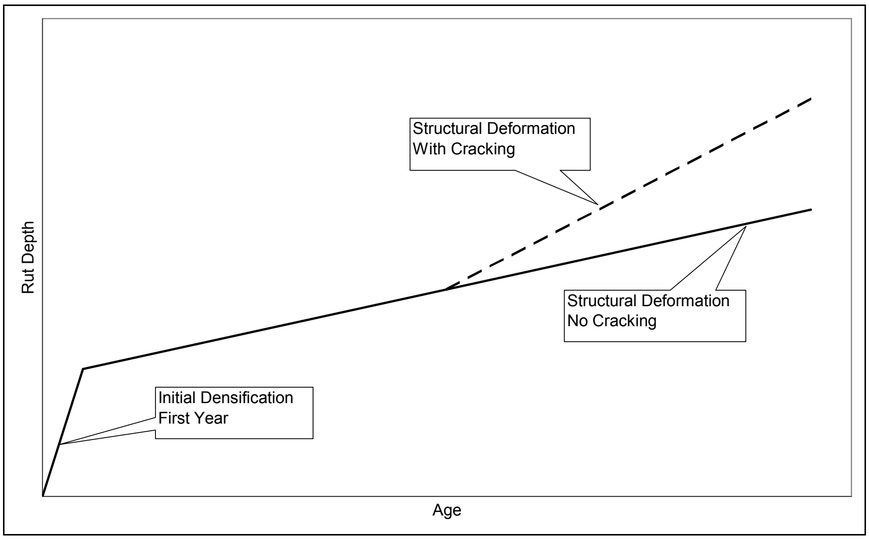

The two components for structural deformation derived from this analysis are given below:

Structural deformation without cracking

$$\Delta RDST_{uc} = K_{rst}\,(a_0\ SNP^{a1}\ YE4^{a2}\ COMP^{a3}) \qquad \text{. . . (B8.13)}$$

Structural deformation after cracking

$$\Delta RDST_{crk} = K_{rst}\,[a_0\ SNP^{a1}\ YE4^{a2}\ MMP^{a3}\ ACX_a^{a4}] \qquad \text{. . . (B8.14)}$$

The total annual incremental increase in structural deformation is as follows:

i) if ACRA = 0

$\Delta RDST = \Delta RDSTuc$ . . . (B8.15)

ii) if ACRA > 0

$\Delta RDST = \Delta RDST_{uc} + \Delta RDST_{crk}$ . . . (B8.16)

where

$\Delta RDST$ = total incremental increase in structural deformation in analysis year, in mm

$\Delta RDST_{uc}$ = incremental rutting due to structural deformation without cracking in analysis year, in mm

$\Delta RDST_{crk}$ = incremental rutting due to structural deformation after cracking in analysis year, in mm

MMP = mean monthly precipitation, in mm/month

ACX_a = area of indexed cracking at the beginning of analysis year, in per cent

K_{rst} = calibration factor for structural deformation

and the other variables are as defined for initial densification

The coefficient values a_0 to a_4 for the structural deformation models are given in Table B8-2.

Table B8-2
Coefficient values for structural deformation model

	Pavement Type	a_0	a_1	a_2	a_3	a_4
Without Cracking	All pavement types	44950	-1.14	0.11	-2.3	
After Cracking	All pavement types	0.0000248	-0.84	0.14	1.07	1.11

B8.4.3 Plastic Deformation

Plastic flow is not adequately modelled in HDM-III. The HDM-III model is only based on the plastic flow resulting from the shear failure of pavement layers when over-stressed, and does not represent the plastic flow (shoving) of asphalt layers (soft asphalt at high road temperatures) or long-term plastic deformation (creep) of thick asphalt (> 150 mm) pavements. This limitation was identified by Paterson (1987) during the initial validation of the rut models on rut data obtained on thick asphalt pavements, and can result in the under prediction of rutting for these pavements.

According to Road Note 31 (TRL, 1993) severe conditions will typically consist of a combination of two or more of the following:

- high maximum temperatures
- very heavy axle loads
- channellised traffic
- stopping or slow moving traffic

It should be borne in mind, however, that the occurrence of a combination of any of the above mentioned factors does not necessarily result in plastic deformation or flow, since the asphalt mix could have been designed to withstand such conditions. Thus, any attempt to predict the occurrence of plastic deformation should not only include the influence of the above mentioned factors, but also consider the properties of the asphalt layer.

There are many mix properties that affect the performance of an asphalt layer. To ensure that only the necessary properties are included in a plastic deformation model, the following criteria were used to select the asphalt mix properties (NDLI, 1995):

- ability to quantify changes in performance
- obtainable without specialised equipment
- availability in a typical application
- familiarity to the users

After the evaluation of the test results of studies conducted around the world, the two asphalt mix properties selected by the HTRS team in Malaysia for inclusion into the plastic deformation model, were binder viscosity and air voids.

Binder viscosity: Binder viscosity was identified as a factor with a strong influence on the stability of an asphalt mix at high road temperatures. As it is not convenient to measure viscosity directly, the Ring and Ball Softening Point Test can be used as an indication of equi-viscous conditions close to that temperature range. Softening Point (SP) is defined as the temperature at which the bitumen attains a particular degree of softness or a particular consistency.

Before incorporating softening point (SP) into a model, the change (increase) in softening point of the binder in an asphalt mix over time needs to be considered. The main factors influencing this increase in softening point are:

- **Mixing and placement**: It is usual for bitumens to harden by up to one grade during mixing and placement (Daines, 1992). This results in a typical increase in softening point of about 4°C, but is dependent on the mixing temperature.
- **Voids in mix**: The higher the void content of an asphalt mix, the more permeable the mix is to air and thus susceptible to age hardening (Daines, 1992). This hardening of the binder, results in an increase in its softening point over time, the amount of increase being a linear function of the voids within the mix;
- **Pavement Temperature**: In combination with the voids, the pavement temperature will also affect the rate of hardening of the bitumen within the mix. The higher the pavement temperature, the higher the temperature of air within the voids, and thus the evaporation of volatiles from the bitumen.

To quantify this expected increase in the softening point (hardening) of the binder within an asphalt mix the following models were derived from data obtained from long term performance studies in England (Daines, 1992) and Malaysia (Harun and Morosiuk, 1995):

$$SP = SP_i + SP_m + \Delta SP \qquad \text{. . . (B8.17)}$$

where

$$\Delta SP = a_0 \, VIM_a \, PT^{a1} \qquad \text{. . . (B8.18)}$$

and

SP	=	softening point of binder in the mix at the end of analysis period, in °C
SP_i	=	initial softening point of binder from Ring and Ball test, in °C
SP_m	=	increase in softening point of binder due to mixing and placement, in °C
ΔSP	=	incremental increase in softening point during analysis year, in °C
VIM_a	=	voids in the mix at the start of the analysis year, in per cent
PT	=	pavement temperature at depth of 20 mm below surface during analysis year, in °C

The coefficient values a_0 and a_1 proposed by the HTRS team are given in Table B8-3.

Table B8-3
Coefficient values for softening point model

a_0	a_1
0.017	0.076

This shows that SP increases sharply during mixing and placement, followed by a relatively high increase due to the high voids (VIM) content early in the life of the asphalt mix. As the road ages, VIM tends to decrease with load applied, and SP increases. This can be explained by the fact that as the voids decrease, the asphalt mix becomes more impermeable to air, and thus the binder to hardening. Studies have indicated that once VIM is less than 4 per cent, in-situ hardening of the binder is negligible (Daines, 1992). Analysis of data indicates an increase in SP within the range 0.5°C to 4°C for an increase in mixing temperature from 140°C to 170°C. The increase over time seems to be within the range of 0.1°C to 2.9°C per year for a VIM range from 2.4 to 9 per cent. Only the first 10 years are illustrated because after 10 years the change is negligible.

Figure B8-9
Expected increase in softening point over time

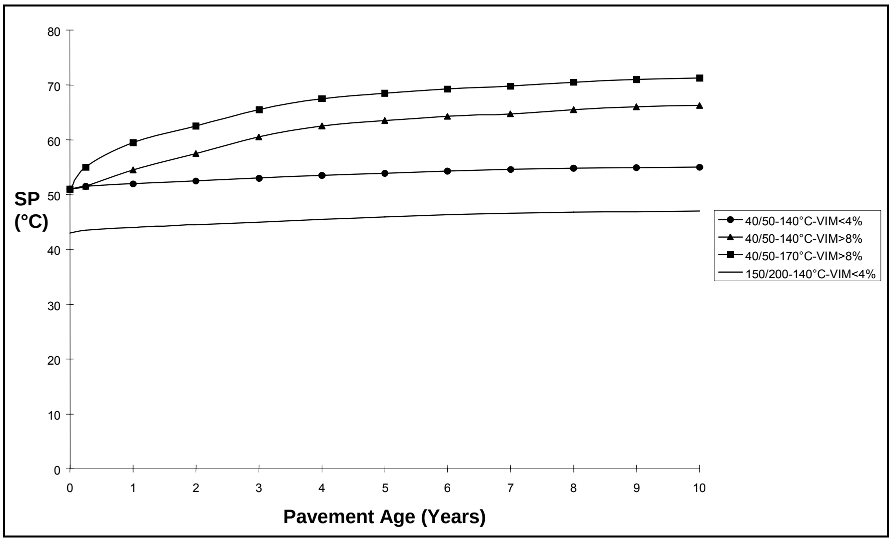

Air Voids (VIM): The voids in the mix (VIM) is calculated as the difference between the bulk volume of the mix and the sum of the volumes of the aggregate and the effective bitumen, and expressed as a percentage of the total volume of constituents as follows:

$$VIM = 100 - (V_a + V_b) \quad \text{. . . (B8.19)}$$

where

VIM = voids in mix, in per cent
V_a = volume of aggregate, in per cent
V_b = volume of effective binder in mix, in per cent

Voids in the mix was selected because various studies showed that once VIM dropped below 3% (2% for less severe conditions, i.e. higher speeds, lower temperatures), the mix became unstable and plastic flow occurred. Furthermore, VIM was selected instead of voids in mineral aggregate (VMA) because VIM includes both the effective volume of binder and the volume of aggregate, thus also allowing the quantification of the influence of excess binder within the mix. As with SP, VIM also changes (decreases) over time. The factors influencing this change in voids are:

- **Axle loads and average speed of heavy vehicles**: Axle loads have an influence on plastic deformation that is not only dependent on the magnitude of the axle loads but also on the duration of the load application, and thus the speed of the heavy vehicles. A typical example of this is the difference in behaviour of the same asphalt mix on a relatively flat section of road compared with a section on a climbing lane.
- **Ratio between pavement temperature and softening point of the binder**: The influence of pavement temperature on the rheological properties of the asphalt mix, especially the viscosity, is well studied and documented, and as such would have an influence on the change in VIM over time.

To quantify the expected decrease of VIM the following proposed models were derived from data obtained from long term performance studies in Malaysia (Harun and Morosiuk, 1995).

The decrease in VIM during the first year is given by:

$$\Delta VIM = a_0 \, YE4 \, Sh^{a1} \left(\frac{PT}{SP} \right)^{a2} \qquad \text{. . . (B8.20)}$$

Subsequent incremental decrease in VIM is given by:

$$\Delta VIM = a_3 \, YE4 \, Sh^{a4} \left(\frac{PT}{SP} \right)^{a5} \qquad \text{. . . (B8.21)}$$

where

ΔVIM	=	decrease in voids during an analysis year, in per cent
YE4	=	annual number of equivalent standard axles, in millions/lane
Sh	=	speed of heavy vehicles, in km/h
PT	=	pavement temperature at a depth of 20 mm during analysis year, in °C
SP	=	softening point of binder in the mix, in °C

The coefficient values a_0 to a_5 proposed by the HTRS team are given in Table B8-4

Table B8-4
Coefficient values for air voids model

a_0	a_1	a_2	a_3	a_4	a_5
43.558	-0.616	2.231	5.27	-0.716	3.225

A typical change in VIM as would be predicted by the model is illustrated in Figure B8-10. The plot in Figure B8-10 shows that there is a sharp initial decrease in VIM in the first year (equation B8.20), followed by a lower rate of change in VIM (equation B8.21). Studies have indicated that the sharp initial decrease is in the range of 2 to 3 per cent, followed by a more or less constant but lower rate of decrease over time.

Figure B8-10
Expected decrease of the voids in mix over time

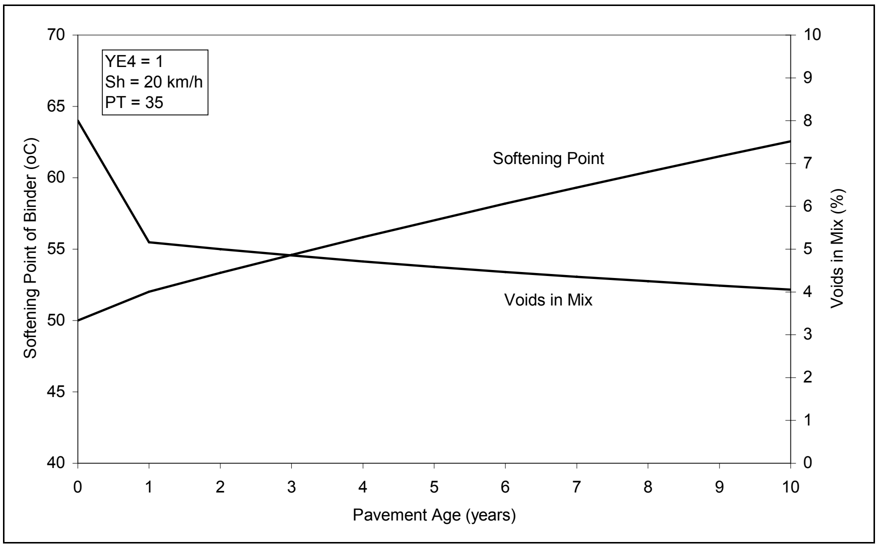

With the mix properties and their change over time quantified, the HTRS team derived the following model for predicting the plastic deformation within asphalt layers:

$$\Delta RDPD = K_{rpd}\ a_0\ YE4\ Sh^{a1}\ HS^{a2} \left(\frac{PT}{SP}\right)^{a3} VIM^{a4} \qquad \text{. . . (B8.22)}$$

where

ΔRDPD = incremental increase in plastic deformation within the asphalt layers of the pavement, in mm

HS = thickness of the bituminous layer, in mm

K_{rpd} = calibration factor for plastic deformation

and the other variables are as defined previously

The coefficient values a_0 to a_4 for this plastic deformation model are given in Table B8-5

Table B8-5
Coefficient values for the HTRS plastic deformation model

a_0	a_1	a_2	a_3	a_4
2.46	-0.78	0.71	1.34	-1.26

The first part of the model predicts the creep within asphalt layers. For reasonable values of VIM (approx > 3%), then effectively only creep is predicted by the model. Creep will be a relatively constant annual increase within the layer as a function of the traffic load, speed of heavy vehicles, temperature and thickness, with voids not having a substantial influence on creep. However, should the voids decrease below a critical value (approx < 3%), the model will respond with an increased rate of deformation as illustrated in Figure B8-11.

Although the above plastic deformation model appeared to predict reasonable rates of plastic flow, it was considered that for most applications of HDM-4, users would not have data for the asphalt mix properties to model the annual changes in SP and VIM. Therefore a model was proposed for inclusion in HDM-4 that did not require the user to specify asphalt mix properties. However, the more accurate method of determining the plastic deformation of a bituminous surfacing using these mix properties is detailed in Volume 5 of the HDM-4 Series - A Guide to Calibration and Adaptation (Bennett and Paterson, 2000).

Figure B8-11
Typical prediction of plastic deformation (creep and flow)

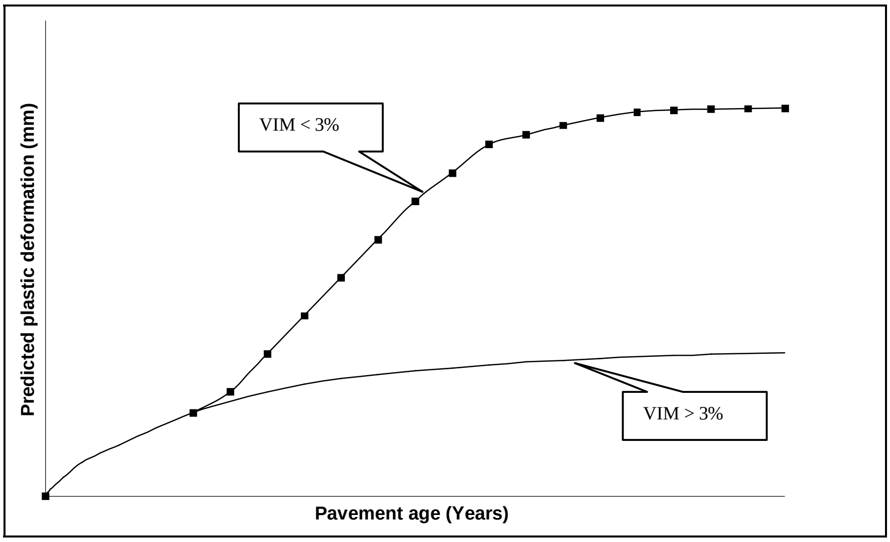

The HDM-4 general plastic deformation model (i.e. without material properties) includes the construction defects indicator, CDS, to indicate whether a surfacing is prone to plastic deformation. CDS is described in Section B2.5 with guidelines on suggested values of CDS given in Table B2-11. The CDS variable has been used as a substitute for the mix properties variables omitted from the NDLI original model (equation B8.22) (Morosiuk, 2003a).

The HDM-4 plastic deformation component of rutting is given by:

$$\Delta RDPD = K_{rpd}\ a_0\ CDS^{a1}\ YE4\ Sh^{a2}\ HS^{a3} \qquad \text{. . . (B8.23)}$$

where

$\Delta RDPD$ = incremental increase in plastic deformation in analysis year, in mm
CDS = construction defects indicator for bituminous surfacings
$YE4$ = annual number of equivalent standard axles, in millions/lane
Sh = speed of heavy vehicles, in km/h
HS = total thickness of bituminous surfacing, in mm
K_{rpd} = calibration factor for plastic deformation

The coefficient values a_0 to a_3 for the plastic deformation model are given in Table B8-6.

Table B8-6
Coefficient values for the plastic deformation model

Surface Type	a_0	a_1	a_2	a_3
AM	0.3	3.27	-0.78	0.71
ST	0	3.27	-0.78	0.71

The rate of progression of the plastic deformation component of rutting predicted by HDM-4 is illustrated in Figure B8-12.

Figure B8-12
HDM-4 predicted rate of plastic deformation

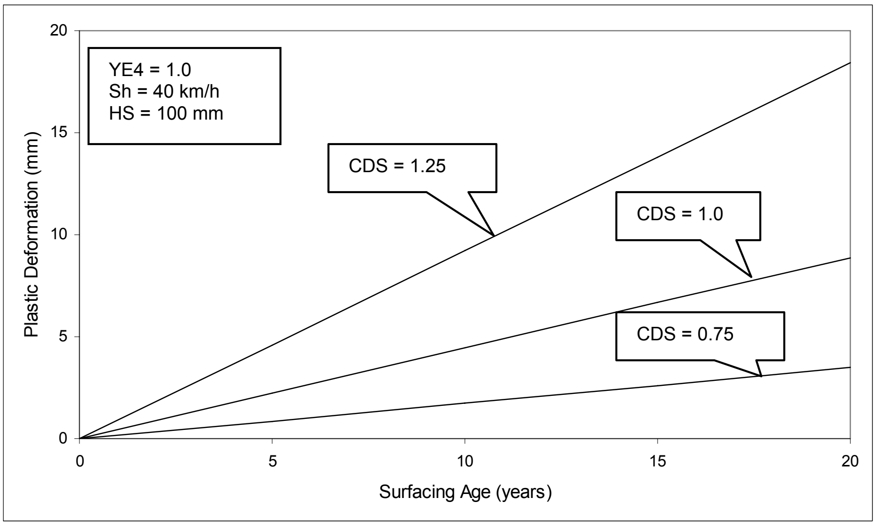

B8.4.4 Surface Wear

A model for predicting rutting resulting from studded tyre wear was developed by Djarf (1995) based on data from Sweden. This model predicts the seasonal surface wear which occurs in countries where vehicles use snow chains or studded tyres on roads covered with snow and ice. To enable users to predict this additional rutting that may occur in cold climates, this model has been incorporated in HDM-4 as the fourth component of rutting.

The HDM-4 surface wear component of rutting is given by:

$$\Delta RDW = K_{rsw} [a_0 \, PASS^{a1} \, W^{a2} \, S^{a3} \, SALT^{a4}] \qquad \text{. . . (B8.24)}$$

where

ΔRDW = incremental increase in rut depth due to studded tyres in analysis year, in mm

PASS = annual number of vehicle passes with studded tyres in one direction, in thousands

S = average traffic speed, in km/h

SALT = variable for salted or unsalted roads (2 = salted; 1 = unsalted)

W = road width, in m (carriageway plus total shoulder width)

K_{rsw} = calibration factor for surface wear

The coefficient values a_0 to a_4 for the surface wear model are given in Table B8-7.

Table B8-7
Coefficient values for surface wear model

Pavement Type	a_0	a_1	a_2	a_3	a_4
All pavement types	0.0000248	1.0	-0.46	1.22	0.32

The predictions of surface wear progression form this model are given in Figure B8-13.

Figure B8-13
HDM-4 surface wear model

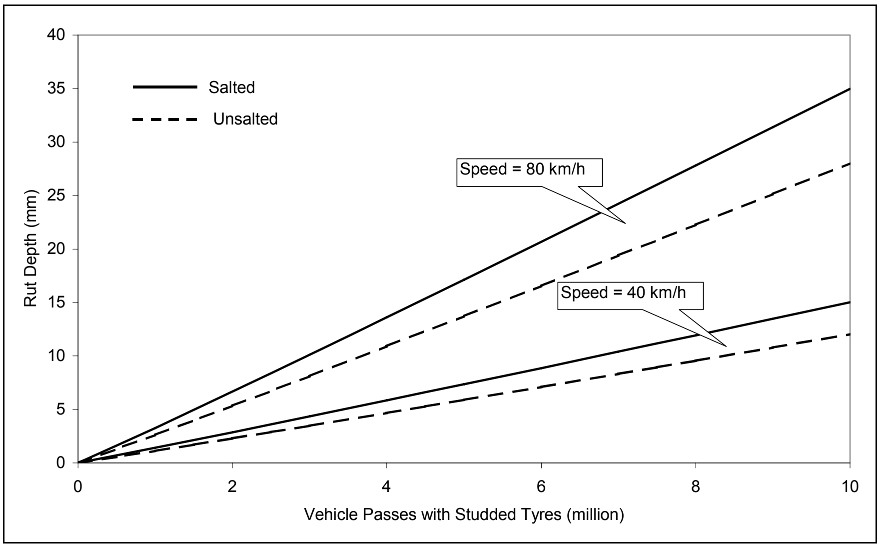

B8.4.5 Total Rut Depth

The annual incremental increase in total rut depth, ΔRDM, is derived as follows:

if $AGE4 \leq 1$

$$\Delta RDM = RDO + \Delta RDPD + \Delta RDW \qquad ...(B8.25)$$

otherwise

$$\Delta RDM = \Delta RDST + \Delta RDPD + \Delta RDW \qquad ...(B8.26)$$

where

ΔRDM = incremental increase in total mean rut depth in both wheelpaths in analysis year, in mm
RDO = initial densification, in mm
$\Delta RDST$ = incremental increase in structural deformation in analysis year, in mm
$\Delta RDPD$ = incremental increase in plastic deformation in analysis year, in mm
ΔRDW = incremental increase in wear by studded tyres in analysis year, in mm

The maximum mean rut depth at the end of the year has been increased to 100 mm in HDM-4 from the 50 mm limit in HDM-III.

The total rut depth, RDM_b, at any given time is given as:

$$RDM_b = \min[(RDM_a + \Delta RDM), 100) \qquad ...(B8.27)$$

where

RDM_b = total mean rut depth in both wheelpaths at end of analysis year, in mm
RDM_a = total mean rut depth in both wheelpaths at start of analysis year, in mm

B8.4.6 Standard Deviation of Rut Depth

Only the rut depth standard deviation, calculated as a function of the mean rut depth, is incorporated within the roughness model. Although the standard deviation of rut depth can be readily quantified by taking frequent samples along a pavement, many HDM-III users reported difficulties in estimating this parameter. Therefore an evaluation was undertaken (NDLI, 1995) to examine whether a simple relationship between mean rut depth and rut depth standard deviation could be optionally used instead of the HDM-III model.

The results of the evaluation (NDLI, 1995), found that depending upon the phase of life for a road section there are different distributions of rut depths. During the early years the data follow an exponential distribution, then as ruts begin to manifest themselves they transition to a log-normal distribution. During the latter stages of life the data are normally distributed.

Since the central limit theorem upon which the normal distribution is based does not extend to the standard deviation, it is important to know what rut depth distribution applies to the pavement before calculating the standard deviation. If this is not done, the resulting value will not be correct.

For situations where the actual standard deviation of the rut depth has not been calculated, the following model was proposed for predicting rut depth standard deviation within HDM-4 (NDLI, 1995):

$$RDS = a_0 \, RDM \qquad \text{. . . (B8.28)}$$

where

RDS = rut depth standard deviation at start of an analysis period, in mm

RDM = mean rut depth at start of an analysis period, in mm

The values recommended for the coefficient a_0 based on an analysis of the available data are given in Table B8-8.

Table B8-8
Coefficient values for determining RDS from RDM

Range of mean rut depth (mm)	a_0
0 – 5	0.8
5 – 15	0.5
> 15	0.3

Using these values of a_0 in equation B8.28, a regression equation can be derived between RDS and RDM. Taking the first differential of the regression equation then gives an incremental relationship for RDS (Riley, 2000d). The generalised form for predicting the incremental change in RDS is given as:

$$\Delta RDS = K_{rds} \max [a_0, \; a_1 - a_2(RDM_b)] \; \Delta RDM \qquad \text{. . . (B8.29)}$$

where

ΔRDS = incremental change in rut depth standard deviation in analysis year, in mm

RDM_b = mean rut depth at end of analysis year, in mm

ΔRDM = change in mean rut depth during analysis year, in mm

K_{rds} = calibration factor for rut depth standard deviation

The coefficient values a_0 to a_2 for the rut depth standard deviation model are given in Table B8-9.

Table B8-9
Coefficient values for rut depth standard deviation model

Pavement Type	a_0	a_1	a_2
All pavement types	0.2	0.65	0.03

The rut depth standard deviation model is plotted in Figure B8-14.

Figure B8-14
Rut depth standard deviation model

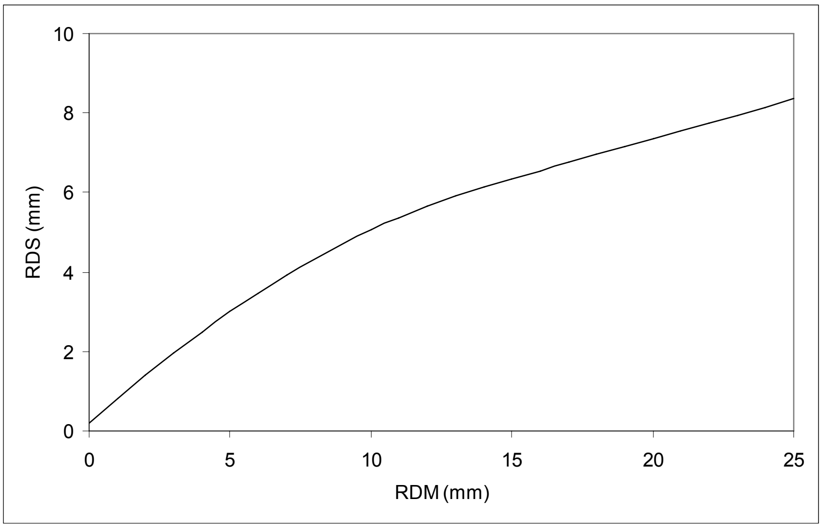

The rut depth standard deviation at the end of an analysis year is given by:

$$RDS_b = RDS_a + \Delta RDS \qquad \text{. . . (B8.30)}$$

where

RDS_b = rut depth standard deviation at end of analysis year, in mm
RDS_a = rut depth standard deviation at start of analysis year, in mm
ΔRDS = incremental change in rut depth standard deviation in analysis year, in mm

B9. SHOULDERS

A discussion note was produced by Riley (2000a) on shoulder deterioration and has been used as the basis for deriving the proposed shoulder deterioration models described in this Section. The letters 'sh' have been added to the acronyms of distresses and parameters related to shoulders to distinguish them from those related to the pavement. Similarly the 'K' calibration factors have 'sh' added to them.

Deterioration models for shoulders have not been included in version 2 of HDM-4. However, they are documented in this volume, primarily for discussion and review purposes, with a view of including shoulder deterioration models in a future version of the software.

B9.1 Unsealed Shoulders

B9.1.1 Edge Step – Material Loss

The loss of material from an unsealed shoulder is similar to that of an unsealed pavement, being caused by environment and traffic. The HDM-4 model for material loss of unsealed roads is (see Section E3.5 for details):

$$MLA = K_{gl}\, 3.65\, [3.46 + 0.246(MMP/1000)(RF) + (KT)(AADT)] \qquad \ldots (B9.1)$$

where

$$KT = K_{kt} \max [0,\ 0.022 + 0.969(HC/57300) + 0.00342(MMP/1000)(P075) - 0.0092(MMP/1000)(PI) - 0.101(MMP/1000)] \qquad \ldots (B9.2)$$

and

MLA = annual material loss, in mm/year
KT = traffic-induced material whip-off coefficient
AADT = annual average daily traffic, in veh/day
MMP = mean monthly precipitation, in mm/month
RF = average rise plus fall of the road, in m/km
HC = average horizontal curvature of the road, in deg/km
PI = plasticity index of the material, in per cent
K_{gl} = calibration factor for material loss
K_{kt} = calibration factor for traffic-induced material whip-off coefficient

For granular materials with low percentages of fines and low PI, the term KT tends to zero and thus for typical shoulders, materials might be ignored. This removes the need to provide material properties for the shoulder. In addition the AADT on an unsealed shoulder is likely to be negligible. Therefore the (KT)(AADT) component can be assumed to be zero for unsealed shoulders and the model for material loss becomes:

$$MLA = 12.5 + 0.0009(MMP)(RF) \qquad \ldots (B9.3)$$

This gives annual loss of material in the range 13 – 40 mm as shown in Figure B9-1.

The loss of material from a shoulder is not transversely uniform. Figure B9-2 shows typical cross sections for an unsealed shoulder when new and after deterioration. There is normally a transfer of material from the inside to the outside when the shoulder is trafficked and this depression can act as a gutter on a gradient with consequent erosion. One of the parameters in the edge break model is the edge step between the edge of the pavement and the shoulder. It is postulated that this will be greater than the average material loss.

It is suggested that the edge step might be twice the average material loss. In the case of cement stabilised bases, the stabilisation typically extends for 0.3 – 0.5 m from the pavement edge and the guttering effect shown in Figure B9-2 may be much reduced.

Figure B9-1
Annual material loss

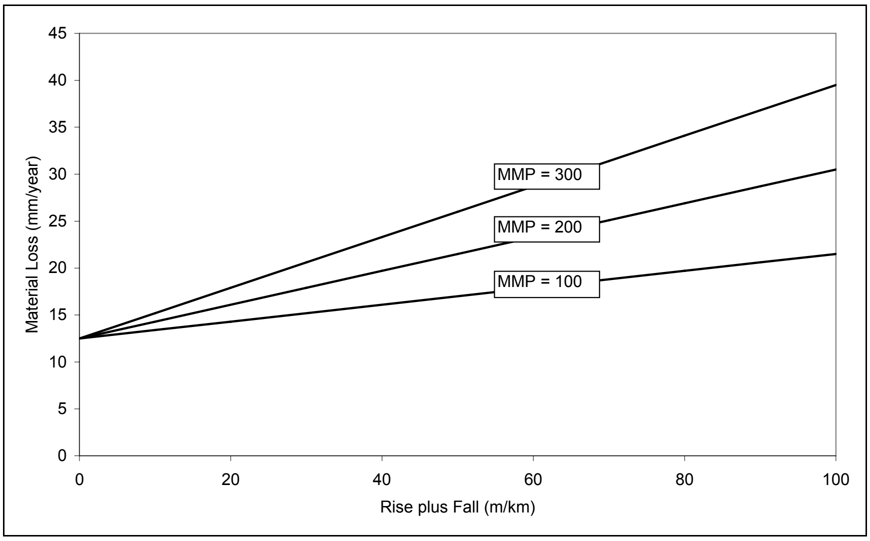

Figure B9-2
Transverse shoulder profiles

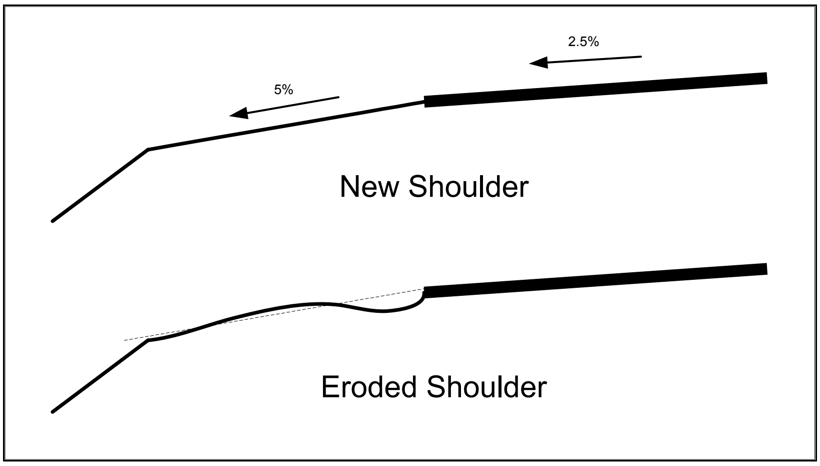

The model for edge step would therefore be:

$$\Delta ESTEP = a_0 + a_1(MMP)(RF) \qquad \text{. . . (B9.4)}$$

$$ESTEP_b = \min[100,\ ESTEP_a + \Delta ESTEP] \qquad \text{. . . (B9.5)}$$

where

$\Delta ESTEP$ = annual increment of edge step, in mm
$ESTEP_a$ = edge step at start of analysis year, in mm
$ESTEP_b$ = edge step at end of analysis year, in mm

Proposed coefficient values a_0 and a_1 for this ESTEP model are given in Table B9-1.

Table B9-1
Coefficients for ESTEP model

Pavement Type	a_0	a_1
STSB, AMSB	12	0.001
Others	25	0.002

For unsealed shoulders it is proposed that the default value of $ESTEP_a$ at the start of the analysis period is set to 5 mm if the pavement type selected is STSB or AMSB, and set to 10 mm for all other pavement types. The above model is then used to increment the increase in ESTEP on an annual basis for use in the Edge Break model. Reduction in the value of ESTEP occurs through maintenance of unsealed shoulders.

B9.1.2 Roughness

The roughness of an unsealed shoulder is of interest when partial shoulder use is required by motorised traffic on narrow pavements and by non-motorised traffic where high motorised volumes force them off the carriageway.

The HDM-4 unsealed models use a minimum and a maximum roughness. The same could be applied to shoulders with a convex curve representing the change from minimum to maximum (without maintenance) over time.

If the shoulder is not used by motorised traffic, increases in roughness will be due to environmental causes, often in the form of transverse erosion gullies. Deterioration can in this case be predicated on rainfall and time since last shoulder rehabilitation. With narrow pavements and partial traffic use, other deterioration modes may take place, such as formation of potholing, depressions or corrugations in loose material. The last is less likely with unsealed shoulders than with unsealed pavements as loose material will tend to be removed by rainfall run-off.

To allow for user input of initial shoulder roughness, an incremental model is desirable. Paterson (1987) gave a form in which the rate of roughness progression reduced as roughness approached the maximum value:

$$\Delta RI = \gamma(RI_{max} - RI_a) \qquad \text{. . . (B9.6)}$$

where

ΔRI = change in roughness during the year
RI_{max} = maximum roughness
RI_a = roughness at start of year
γ = vector of explanatory variables

For simplicity, it is proposed that explanatory variables are limited to rainfall, traffic volume and proportion of shoulder use. With a linear relationship, the model form is:

$$\Delta RIsh = Ksh_{gp}\, a_0[1 + a_1(MMP) + a_2(AADT)(\delta t_{sh})]\,(RIsh_{max} - RIsh_a) \qquad \text{. . . (B9.7)}$$

where

$$\delta t_{sh} = a_3(PSH)(AADT)\, 10^{-6} \qquad \text{. . . (B9.8)}$$

$$PSH = \max\left\{\min\left[\max\left(a_4 + a_5\, CW,\ \frac{CW_{max} - CW}{a_6}\right),\ 1\right],\ 0\right\} \qquad \text{. . . (B9.9)}$$

and

$\Delta RIsh$	=	incremental change in shoulder roughness during analysis year, in m/km IRI
$RIsh_{max}$	=	maximum allowable shoulder roughness, in m/km IRI (default = 20)
$RIsh_a$	=	roughness of the shoulder at start of analysis year, in m/km IRI
AADT	=	annual average daily traffic, in veh/day
MMP	=	mean monthly precipitation, in mm/month
δt_{sh}	=	proportion of time vehicles use the shoulder due to road width and traffic volume
PSH	=	proportion of time vehicles use the shoulder due to road width
CW	=	carriageway width, in metres
CW_{max}	=	maximum carriageway width where vehicles use the shoulder, in metres (default = 7.2)
Ksh_{gp}	=	calibration factor for roughness progression of unsealed shoulders, in m/km IRI

Proposed coefficient values a_0 to a_6 for the unsealed shoulder roughness model are given in Table B9-2.

Table B9-2
Coefficients for unsealed shoulder roughness model

Pavement Type	a_0	a_1	a_2	a_3	a_4	a_5	a_6
All	0.1	0.01	0.02	58	2.65	-0.425	10

Rates of roughness progression of unsealed shoulders are shown in Figure B9-3. With no rainfall or traffic, the model will give 75% of maximum roughness in about 10 years. With rainfall of 100 mm/month and low traffic, this level of roughness is reached after 6 years. With the same rainfall and 1,000 veh/day and a pavement width of 3 m the 75% level is reached after 3 years. This is of course with zero maintenance.

Figure B9-3
Unsealed shoulder roughness progression

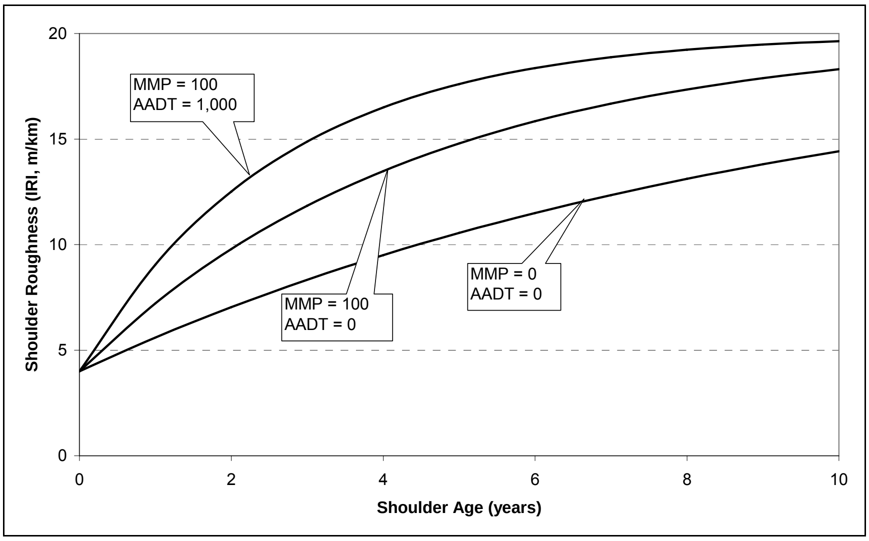

B9.2 Sealed Shoulders

B9.2.1 Types of Sealed Shoulders

The term “sealed shoulder” covers a broad range of construction standards. At the lowest level, a surface dressing is applied to an existing gravel shoulder while at the higher end the sealed shoulder is an extension of the carriageway with the same base and surfacing materials types and thickness.

To avoid undue complication in the modelling of shoulder deterioration, it is proposed that three construction standards are defined:

1. Light - thin surfacing, typically surface dressing, with a base that is made of naturally occurring gravel with properties below the normal standard for a road base.
2. Intermediate – double surface dressing or thin asphalt on a base that is extended from the carriageway.
3. Full – the shoulder is an extension of the main carriageway.

It can be assumed that a sealed shoulder would not be provided on roads with narrow carriageways (single or intermediate lane roads) and that use by heavy vehicles would be occasional in the case of types 1 and 2.

The amount of traffic loading on shoulders can be assumed to be so small as to be negligible. Therefore it is proposed to consider only deterioration models that are environmentally related – cracking, ravelling and roughness.

B9.2.2 Cracking of Sealed Shoulders

The models for initiation and progression of structural cracking contain terms to represent fatigue as a function of traffic loading, pavement strength and ageing. If traffic loading is assumed to be zero for light and intermediate shoulder types, only the pavement strength and age terms will apply.

B9.2.2.1 Initiation of Cracking

The time to initiation of cracking of sealed shoulders is given by the following relationships:

a) Non Stabilised Shoulder Bases

$$ICAsh = Ksh_{cia}\ a_0 \exp(a_1 SNPsh) \qquad \text{. . . (B9.10)}$$

b) Stabilised Shoulder Base

$$ICAsh = Ksh_{cia}\left\{a_0 \exp\left[a_1 HSsh + a_2 \log_e(CMOD) + a_3 \log_e(DEFsh)\right]\right\} \qquad \text{. . . (B9.11)}$$

where

ICAsh	=	time to initiation of shoulder cracks, in years
SNPsh	=	average annual adjusted structural number of the shoulder
DEFsh	=	Benkelman beam deflection of the shoulder, in mm
CMOD	=	resilient modulus of soil cement, in GPa (range between 0 and 30 GPa for most soils)
HSsh	=	thickness of the shoulder surfacing, in mm
Ksh_{cia}	=	calibration factor for initiation of shoulder cracking

The coefficient values a_0 to a_3 are given in Table B9-3.

Table B9-3
Coefficient values for the initiation of shoulder cracking model

Shoulder Base	a_0	a_1	a_2	a_3
Stabilised	1.12	0.035	0.371	-0.418
Non Stabilised	4.21	0.14		

It is unlikely that users will have values for the variables in the above relationships that are relevant for the shoulder. It will therefore be necessary to assign default values for these variables that the user can amend if necessary. The proposed default values are given in Table B9-4.

Table B9-4
Default values for variables in the initiation of shoulder cracking model

Shoulder Type	Shoulder Base	SNPsh	HSsh	CMOD	DEFsh
1	Non Stabilised	1.5			
2	Non Stabilised	Note 1			
	Stabilised		25	Note 2	Note 3

Note 1 SNPsh = min(2, carriageway SNP)
Note 2 As specified by the user for the carriageway
Note 3 DEFsh = $3.5[\text{carriageway SNP-}a_0(\text{HSOLD})]^{-1.6}$
where a_0 = 0.008 if shoulder surfacing is ST, a_0 = 0.014 if shoulder surfacing is AM

B9.2.2.2 Progression of Cracking

The structural cracking progression models for bituminous pavements in HDM-4 were originally derived using cracking caused by a combination of traffic loading and environmental effects. For sealed shoulder types 1 & 2, the effect of traffic loading is negligible. Therefore it is proposed that the time to reach 50% cracking is doubled from that predicted for bituminous pavements.

The time to 50% cracking is given by

$$t_{50} = (50^{a1} - 0.5^{a1}) / a_0\, a_1 \qquad \text{. . . (B9.12)}$$

The coefficient values for a_0 and a_1 in the HDM-4 structural cracking progression model are given in Table B9-5 together with values of t_{50}.

Table B9-5
HDM-4 crack progression coefficient values for bituminous roads

Pavement Type	a_0	a_1	t_{50}
AMGB	1.84	0.45	6.1
STGB	1.76	0.32	4.8
AMSB, STSB	2.13	0.35	4.2

By halving the value of a_0, the value of t_{50} is doubled. The coefficient values a_0 and a_1 proposed for the cracking progression of sealed shoulder types 1 & 2 are given in Table B9-6.

Table B9-6
Proposed coefficient values for cracking progression model for sealed shoulders

Shoulder Base	Shoulder Surfacing	a_0	a_1
Non Stabilised	AM	0.92	0.45
	ST	0.88	0.32
Stabilised	AM	1.07	0.35
	ST	1.07	0.35

It is proposed that the coefficient values listed in Table B9-6 should be used in the existing structural cracking progression model to predict the rate of cracking on sealed shoulder types 1 & 2.

The general form of the model for the progression of shoulder cracking is as follows.

$$dACAsh = Ksh_{cpa}\, z \left[(z\, a_0\, a_1\, \delta t_c + SCA^{a1})^{1/a1} - SCA\right] \qquad \text{. . . (B9.13)}$$

Progression of shoulder cracking commences when $\delta t_c > 0$ or $ACAsh_a > 0$

where

$\delta t_c = 1$ if $ACAsh_a > 0$, otherwise $\delta t_c = \max\{0, \min[(AGEsh - ICAsh), 1]\}$

if $ACAsh_a \geq 50$ then $z = -1$, otherwise $z = 1$

$ACAsh_a = \max(ACAsh_a, 0.5)$

$SCA = \min[ACAsh_a, (100 - ACAsh_a)]$

$Y = [a_0\, a_1\, z\, \delta t_c + SCA^{a1}]$

i) if $Y < 0$ then

$$dACAsh = Ksh_{cpa}\, (100 - ACAsh_a) \qquad \text{. . . (B9.14)}$$

ii) if $Y \geq 0$ then

$$dACAsh = Ksh_{cpa}\, z\, (Y^{1/a1} - SCA) \qquad \text{. . . (B9.15)}$$

iii) if $ACAsh_a \leq 50$ and $ACAsh_a + dACAsh > 50$ then

$$dACAsh = Ksh_{cpa}\, (100 - c_1^{1/a1} - ACAsh_a) \qquad \text{. . . (B9.16)}$$

where

$$c_1 = \max\left\{\left[2\,(50^{a1}) - SCA^{a1} - a_0\, a_1\, \delta t_c\right],\ 0\right\} \qquad \text{. . . (B9.17)}$$

and

$dACAsh$	=	incremental change in area of shoulder cracking during analysis year, in per cent of total carriageway area
$ACAsh_a$	=	area of all shoulder cracking at the start of the analysis year, in per cent
δt_c	=	fraction of analysis year in which shoulder cracking progression applies
$AGEsh$	=	shoulder surface age, in years
Ksh_{cpa}	=	calibration factor for progression of shoulder cracking

and the other variables are as defined for crack initiation

B9.2.3 Ravelling of Sealed Shoulders

As for cracking, the models for initiation and progression of ravelling include traffic and age terms and can be applied to sealed shoulders with the traffic loading terms set to zero.

B9.2.3.1 Initiation of Ravelling

The ravelling initiation model for sealed shoulders is as follows:

$$IRVsh = Ksh_{vi}\, a_0$$

where

IRVsh = time to initiation of shoulder ravelling, in years
Ksh_{vi} = calibration factor for shoulder ravelling initiation

The coefficient values for a_0 for the ravelling initiation of sealed shoulders are based on the values for bituminous pavements (see Section B4.3.1) and are given in Table B9-7.

Table B9-7
Coefficient values for the ravelling initiation of sealed shoulders model

Shoulder Surface	a_0
AM	16.0
ST	10.5

B9.2.3.2 Progression of Ravelling

The ravelling progression model for bituminous pavements includes both traffic and environment effects. Therefore, as for cracking, it is proposed that the time to reach 50% ravelling on sealed shoulders is doubled, by halving the revised value of a_0. Setting a value of a_0 = 1.105 and leaving the other coefficient value as 0.352, the proposed rate of progression of ravelling of sealed shoulder is given as follows.

The general form of the model for the progression of ravelling on sealed shoulders is given below.

$$dARVsh = Ksh_{vp} z \left[\left(z\, a_0\, a_1\, \delta t_v + SRV^{a1}\right)^{1/a1} - SRV\right] \qquad \text{. . . (B9.18)}$$

Progression of ravelling commences when $\delta t_v > 0$ or $ARVsh_a > 0$

where $\delta t_v = 1$ if $ARVsh_a > 0$

otherwise $\delta t_v = \max \{0, \min [(AGEsh - IRVsh), 1]\}$

if $ARVsh_a \geq 50$ then $z = -1$, otherwise $z = 1$

$ARVsh_a = \max (ARVsh_a, 0.5)$

$SRV = \min [ARVsh_a, (100 - ARVsh_a)]$

$Y = [a_0\, a_1\, z\, \delta t_v + SRV^{a1}]$

i) if $Y < 0$ then

$$dARVsh = Ksh_{vp} (100 - ARVsh_a) \qquad \text{. . . (B9.19)}$$

ii) if $Y \geq 0$ then

$$dARVsh = Ksh_{vp} z (Y^{1/a1} - SRV) \qquad \text{. . . (B9.20)}$$

iii) if $ARVsh_a \leq 50$ and $ARVsh_a + dARVsh > 50$ then

$$dARVsh = Ksh_{vp} (100 - c_1^{1/a1} - ARVsh_a) \qquad \text{. . . (B9.21)}$$

where

$$c_1 = \max \{[2 (50^{a1}) - SRV^{a1} - a_0\, a_1\, \delta t_v], 0\} \qquad \text{. . . (B9.22)}$$

and

- dARVsh = change in area of shoulder ravelling during analysis year, in per cent of total shoulder area
- $ARVsh_a$ = area of shoulder ravelling at the start of the analysis year, in per cent
- δt_v = fraction of analysis year in which shoulder ravelling progression applies
- AGEsh = shoulder surface age, in years
- Ksh_{vp} = calibration factor for ravelling progression of sealed shoulders

The coefficient values a_0 and a_1 for the ravelling progression model for sealed shoulders are given in Table B9-8.

Table B9-8
Coefficient values for the ravelling progression model for sealed shoulders

Pavement Type	a_0	a_1
All pavement types	1.105	0.352

B9.2.4 Edge Break of Sealed Shoulders

In general, edge break does not occur when the shoulder is sealed. Therefore if the user specifies that the shoulders are sealed, then the default value of ESTEP should be set to zero.

B9.2.5 Roughness of Sealed Shoulders

For the prediction of roughness of sealed shoulders, only the cracking and environmental components need to be considered.

The cracking component of roughness is given by:

$$\Delta RIsh_c = Ksh_{gc}\ a_0\ \Delta ACAsh \qquad \text{. . . (B9.23)}$$

where

- $\Delta RIsh_c$ = incremental change in shoulder roughness due to cracking during analysis year, in m/km IRI
- $\Delta ACAsh$ = incremental change in area of cracking of the shoulder during analysis year, in per cent
- a_0 = 0.0066
- Ksh_{gc} = calibration factor for the cracking component of shoulder roughness

The environmental component of roughness is given by:

$$\Delta RIsh_e = Ksh_{gm}\ m\ RIsh_a \qquad \text{. . . (B9.24)}$$

where

- $\Delta RIsh_e$ = incremental change in shoulder roughness due to environment during analysis year, in m/km IRI
- $RIsh_a$ = shoulder roughness at the start of the analysis year, in m/km IRI
- m = environmental coefficient
- Ksh_{gm} = calibration factor for the environmental coefficient

The roughness of the shoulder at the end of an analysis year is given by:

$$RIsh_b = \min\left[(RIsh_a + \Delta RIsh),\ a_0\right] \qquad \text{. . . (B9.25)}$$

where

$$\Delta RIsh = \Delta RIsh_c + \Delta RIsh_e \qquad \text{. . . (B9.26)}$$

and

$RIsh_b$ = roughness of the shoulder at end of the analysis year, in m/km IRI
$RIsh_a$ = roughness of the shoulder at start of the analysis year, in m/km IRI
ΔRI = incremental change in shoulder roughness during analysis year, in m/km IRI
a_0 = user specified upper limit of shoulder roughness (default = 20)

B10. ROAD ROUGHNESS

Road roughness draws together the impacts of all other pavement distress forms (cracking, disintegration and deformation) and maintenance. It is the dominant criterion of pavement performance in relation to both economics and quality of service.

B10.1 Measurement of Road Roughness

Road roughness is a measure of the irregularities in the pavement surface and it is the form of pavement distress that gives most concern to road users. Because it is a measure of how road users perceive a road, roughness has long been measured by highway agencies in one form or another. Early measures were subjective and expressed on a scale of, typically, 0 - 10 with 10 being a perfect surface and lower values indicating lower ride qualities. Since subjective ratings vary with the expectations of the observer, many mechanical methods of assessing roughness developed. Most of these methods used their own measurement scale, often relating to the particular type of equipment and/or the vehicle in which the equipment was mounted.

The need for a common internationally recognised scale was addressed in the International Road Roughness Experiment in Brazil in 1982 (Sayers, et al, 1986), where a number of different types of equipment and measurement units for recording roughness were applied to the same test sections which were also accurately profiled. One of the main outcomes from the Experiment was the recommendation of an international index - the International Roughness Index or IRI.

Paterson (1986) defines IRI as:
"The IRI mathematically summarises the longitudinal surface profile of the road in a wheeltrack, representing the vibrations induced in a typical passenger car by road roughness. It is defined by the reference average rectified slope ($RARS_{80}$, the ratio of the accumulated suspension motion to the distance travelled) of a standard quarter-car simulation for a travelling speed of 80 km/h. It is computed from surface elevation data collected by either topographical survey or mechanical profilometer."

Sayers (1995) expanded on this definition:

- IRI is computed from a single longitudinal profile. The sample interval should be no larger than 300 mm for accurate calculations. The required resolution depends on the roughness level, with finer resolution needed for smooth roads.
- The profile is assumed to have a constant slope between sampled elevation points.
- The profile is smoothed with a moving average whose baselength is 250 mm.
- The smoothed profile is filtered using a quarter-car simulation, with specific parameter values (Golden Car), at a simulated speed of 80 km/h.
- The simulated suspension motion is linearly accumulated and divided by the length of the profile to yield IRI. Thus, IRI has units of slope (usually m/km).

The underlying IRI model is a series of differential equations which relate the motions of a simulated quarter-car to the road profile. Figure B10-1 illustrates the quarter-car model used and the parameters adopted (Sayers, 1995).

Figure B10-1
IRI Quarter-car model

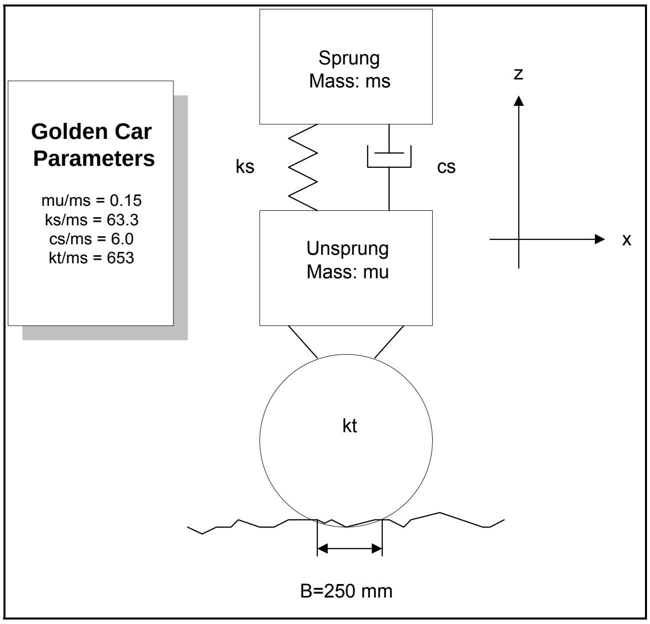

The IRI is the accumulation of the motion between the sprung and unsprung masses in the quarter-car model, normalised by the length of the profile. Mathematically this is expressed as:

$$IRI = \frac{1}{LP}\int_{0}^{LP/S} \left|\dot{z}_s - \dot{z}_u\right| dt \qquad \text{. . . (B10.1)}$$

where

IRI	=	roughness, in m/km IRI
LP	=	length of the profile, in km
S	=	simulated speed (80 km/h)
$\dot{z}_s$	=	time derivative of the height of the sprung mass
$\dot{z}_u$	=	time derivative of the height of the unsprung mass

The algorithm used to calculate the IRI is described in Sayers, et al (1986) and elaborated on in Sayers (1995). Both references provide a computer listing for calculating the IRI; Sayers, et al (1986) in BASIC and Sayers (1995) in FORTRAN.

In order to calculate the IRI the following steps must be taken:

- determine the elevation profile of each wheelpath
- using the profile data, run a quarter-car simulation for the reference vehicle over each wheelpath and calculate the wheelpath IRI
- establish the average IRI for both wheelpaths

Since its introduction the IRI has become increasingly adopted around the world, encouraged by international lending agencies in developing countries and by the FHWA in the USA. In parallel, methods of accurately recording roughness have developed with the application of accelerometers and laser devices replacing the older mechanical instruments in many regions.

Compared with some other types of pavement distress, roughness is relatively easy to measure. A wide range of instruments are commercially available for this purpose ranging from the sophisticated (lasers) to the basic (purely mechanical). The simpler equipment needs calibration against known IRI derived from measured wheelpath profiles. This is done by establishing a relationship between the IRI from the measured wheelpath profiles and the output from the roughness instrument. Many of the systems using lasers or accelerometers claim to be self calibrating in that they measure a continuous profile of the road surface which is then converted to IRI using the quarter-car simulation.

When applying the results of proprietary roughness measuring systems or when calibrating roughness meters the distinction between quarter-car and half-car RARS should be noted. A system that records profile by means of centrally mounted accelerometers is returning a half-car index which will always be less than a quarter-car index (Sayers, et al. 1986). In such cases, a factor of 1.3 can be applied to the results to give IRI (Sayer, et al., 1986). When calibrating roughness meters that are attached to the centre of a rigid axle, both wheelpaths should be profiled and the mean value of IRI used in the regression to obtain a relationship between meter reading and IRI.

B10.2 Modelling Roughness in HDM-III

The basic hypothesis used in developing the HDM-III roughness progression model was that the various mechanisms giving rise to roughness changes should be represented by components within the model (Paterson, 1987). This approach is referred to as the component incremental model. It was considered that these components fell into three broad groups as follows:

Structural Deformation: Deformation in the pavement materials under the shear stresses imposed by traffic loading. This category also includes the effects of environmental factors on material strength and rutting behaviour under loads. However, rut depth alone will not give rise to roughness if the depth is uniform; it is the variation of rut depth which relates to roughness as deviations in the longitudinal profile. Typically, these variations are likely to have medium wavelengths in the range of 2 m to 10 m, but shorter in the case of base deformation.

Surface Distress: Defects such as cracking and potholes are generally associated with shallow-seated distress originating in either the surfacing or base of the pavement. These defects typically range in size from less than 0.3 m to 2 m in diameter, with a corresponding waveband of about 0 to 5 m wavelengths. Cracks are included because of the local or “birdbath” depressions that often develop in cracked areas and also because of the effects of wide or spalled cracks.

Environmental Factors: There are various factors not directly related to traffic or pavement strength which influence roughness. These environmental factors include primarily temperature and moisture fluctuations, and also foundation movements, such as subsidence.

Paterson (1987) developed a model for predicting roughness that consisted of five components: structural deformation, rutting, cracking, potholing and environmental effects.

The HDM-III roughness model is given below:

$$\Delta IRI = K_{gp}\,[134\, e^{m\,t}\,(SNCK + 1)^{-5}\, YE4 + 0.114(RDS_b - RDS_a) + 0.0066\,\Delta CRX + 0.42\,\Delta POT] + m\, IRI_a \quad ...\,(B10.2)$$

where

$$SNCK = \max\,[1.5,\ (SNC - \Delta SNK)] \quad ...\,(B10.3)$$

$\Delta SNK = 0.0000758 [\min (63, CRX_a) HSNEW + (ECR)(HSOLD)]$ . . . (B10.4)

$ECR = \max [\min (CRX_a - PCRX, 40), 0]$ . . . (B10.5)

and

ΔIRI	=	annual incremental increase in roughness, in m/km IRI
IRI_a	=	roughness at the start of the analysis year, in m/km IRI
m	=	environmental coefficient (see Table B10-1) (where $m = 0.023 K_{ge}$)
K_{ge}	=	calibration factor for environmental coefficient
t	=	time since latest overlay or construction (AGE3), in years
SNCK	=	modified structural number for the pavement, reduced for the effect of cracking
YE4	=	annual number of equivalent standard axles, in millions/lane
RDS_b	=	standard deviation of rut depth at end of analysis year, in mm
RDS_a	=	standard deviation of rut depth at start of analysis year, in mm
ΔCRX	=	annual incremental change in area of indexed cracking, in per cent
ΔPOT	=	annual incremental change in area of potholing, in per cent
PCRX	=	area of previous indexed cracking in old layer, in per cent [i.e. 0.62(PCRA) + 0.39(PCRW)]
K_{gp}	=	calibration factor for roughness progression

The pavement strength indicator used in the HDM-III roughness model is SNCK. This variable takes into account the reduction in pavement strength due to cracking in the bituminous layers, both in the surfacing and in the underlying bituminous layer.

The roughness model effectively has two calibration factors, K_{gp} and K_{ge}. K_{gp} is used in a similar manner to the calibration factors in the other distress models; i.e. to adjust the rate of progression. K_{ge} is used to adjust the environmental coefficient, “m”.

The value of “m” was set to 0.023 for the Brazil climate from where the data was collected to develop this roughness model. For use of the model in other climates, K_{ge} is chosen to adjust the value of “m” to that which is appropriate for that climate. The value of K_{ge} is derived as a ratio of the value of “m” for the appropriate climate and 0.023, i.e.

$$K_{ge} = \frac{m}{0.023} \qquad \text{. . . (B10.6)}$$

The values of the environmental coefficient “m” for the climates defined in HDM-III are given in Table B10-1 (Paterson, 1987).

Table B10-1
Environmental coefficient ‘m’ by HDM-III climate zones

Moisture Classification	Thornthwaite Moisture Index	Temperature Classification		
		Tropical Non-freezing	Sub-tropical Non-freezing	Temperate Freezing
Arid	-110 to -61	0.005	0.010	0.025
Semi-arid	-60 to –21	0.010	0.016	0.035
Sub-humid	-20 to +19	0.020	0.030	0.065
Humid, wet	20 to 100	0.025	0.040	0.10 - 0.23

B10.3 Modelling Roughness in HDM-4

The roughness model in HDM-4 is based on the HDM-III model and has the same five components of roughness. The structural, cracking, rutting and environmental components are similar to the HDM-III versions, but the potholing component has been modified. The values of the surface distress variables used in predicting roughness are those that have been adjusted so that the total damaged surface area plus the undamaged area equals 100 per cent. Each component of roughness model is described separately below.

In version 1 of HDM-4, two calibration factors were used for the roughness model,; one for the environmental coefficient 'm' (K_{gm}) and one for roughness progression (K_{gp}). In version 2 of HDM-4 each of the five components of roughness have been assigned their own calibration factor (Morosiuk, 2003a).

B10.3.1 Structural Component

The structural component of roughness in HDM-4 uses the adjusted structural number (SNP) as the pavement strength indicator, rather than the modified structural number (SNC) that was used in HDM-III.

In HDM-III, the calibration factor for the environmental coefficient 'm', K_{ge}, was defined as a ratio of the appropriate 'm' value for the climate and 0.023 (see equation B10.6). In keeping with the default value of all the other calibration factors in both HDM-III and HDM-4, the default value of the calibration factor for 'm' has been set to 1.0 in HDM-4. To distinguish this factor from that used in HDM-III, it has been re-named as K_{gm} in HDM-4. The appropriate values of 'm' are therefore input directly into the HDM-4 structural component of roughness model.

In version 1 of HDM-4, the values of the environmental coefficient 'm' ranged from 0.005 to 0.2 as shown in Table B10-2.

Table B10-2
Environmental coefficient 'm' in version 1 of HDM-4

Moisture Classification	Temperature Classification				
	Tropical	Sub-tropical Hot	Sub-tropical cool	Temperate cool	Temperate Freeze
Arid	0.005	0.010	0.015	0.025	0.040
Semi-arid	0.010	0.015	0.025	0.035	0.060
Sub-humid	0.020	0.025	0.040	0.060	0.100
Humid	0.025	0.030	0.060	0.100	0.200
Per-humid	0.030	0.040	0.070		

A value of 0.2 results in an increase of roughness of 20% per annum due to the environment. This was considered too high (Riley, 2000e), and as a result of communications between the HDM-4 development team, revised 'm' values have been proposed for version 2 of HDM-4 (PIARC, 2004) as shown in Table B10-3.

Table B10-3
Environmental coefficient 'm' in version 2 of HDM-4

Moisture Classification	Temperature Classification				
	Tropical	Sub-tropical Hot	Sub-tropical cool	Temperate cool	Temperate Freeze
Arid	0.005	0.010	0.015	0.020	0.030
Semi-arid	0.010	0.015	0.020	0.030	0.040
Sub-humid	0.020	0.025	0.030	0.040	0.050
Humid	0.025	0.030	0.040	0.050	0.060
Per-humid	0.030	0.040	0.050		

In addition to a calibration factor being assigned to the structural component, a further calibration factor, K_{snpk}, has been introduced into the relationship for predicting the change in structural strength of the pavement due to cracking. This enables the user to alter the influence of cracking on pavement strength based on historical data available to the user.

The HDM-4 structural component of roughness is given by:

$$\Delta RI_s = K_{gs}\, a_0 \exp[K_{gm}\, (m)\, (AGE3)]\, (1 + SNPK_b)^{-5}\, YE4 \qquad \text{. . . (B10.7)}$$

where

$$SNPK_b = \max\,[(SNP_a - dSNPK),\ 1.5] \qquad \text{. . . (B10.8)}$$

$$dSNPK = K_{snpk}\, a_0 \Big[\min(a_1, ACX_a) HSNEW + \max\big(\min(ACX_a - PACX, a_2), 0\big) HSOLD\Big] \qquad \text{. . . (B10.9)}$$

and

ΔRI_s = incremental change in roughness due to structural deterioration during analysis year, in m/km IRI
dSNPK = reduction in adjusted structural number due to cracking
$SNPK_b$ = adjusted structural number due to cracking at end of analysis year
SNP_a = adjusted structural number at start of analysis year
ACX_a = area of indexed cracking at start of analysis year, in per cent
PACX = area of previous indexed cracking in old surfacing, in per cent ie. 0.62 (PCRA) + 0.39 (PCRW)
HSNEW = thickness of the most recent surfacing, in mm
HSOLD = total thickness of previous underlying surfacing layers, in mm
AGE3 = age since last overlay or reconstruction, in years
YE4 = annual number of equivalent standard axles, in millions/lane
m = environmental coefficient (see Table B10-3)
K_{gm} = calibration factor for environmental coefficient
K_{snpk} = calibration factor for SNPK
K_{gs} = calibration factor for the structural component of roughness
the coefficient values for a_0 to a_2 are given in Table B10-5

B10.3.2 Cracking Component

The cracking component of roughness in HDM-4 is the same as in HDM-III, with addition of a calibration factor; i.e. the incremental increase in roughness due to cracking is given by:

$$\Delta RI_c = K_{gc}\, a_0\, \Delta ACRA \qquad \text{. . . (B10.10)}$$

where

ΔRI_c = incremental change in roughness due to cracking during analysis year, in m/km IRI

$\Delta ACRA$ = incremental change in area of total cracking during analysis year, in per cent
K_{gc} = calibration factor for the cracking component of roughness

B10.3.3 Rutting Component

The incremental increase in roughness due to rutting in HDM-4 is a function of the standard deviation of rut depth, as in HDM-III. However, the magnitude of the coefficient a_0 (see Table B10-5) has been adjusted for the changes in definition of rut depths from those measured under a 1.2 m straight-edge in HDM-III to those measured under a 2.0 m straight-edge in HDM-4 (see Section B8.4.1).

The HDM-4 rutting component of roughness is given by:

$$\Delta RI_r = K_{gr} \, a_0 \, (\Delta RDS) \qquad \ldots (B10.11)$$

where

ΔRI_r = incremental change in roughness due to rutting during analysis year, in m/km IRI
ΔRDS = incremental change in standard deviation of rut depth during analysis year, in mm
K_{gr} = calibration factor for the rutting component of roughness

B10.3.4 Potholing Component

Paterson (1987) simulated the effects of different sizes and frequency of potholes on roughness and obtained the highly correlated relationship:

$$\Delta RI_p = 6.0 \, (V_{pot}) \qquad \ldots (B10.12)$$

where

ΔRI_p = incremental change in roughness due to potholing, in m/km IRI
V_{pot} = volume of potholes, in m^3/km

These simulations were based on the vehicle hitting all potholes and the limited field data available suggested that the actual relationship between the volume of potholing and IRI was much lower, since drivers will try to avoid potholes as far as road and traffic conditions allow. The coefficient finally adopted in the HDM-III model was 0.16, a reduction by a factor of about 35 on the computer simulations.

The effect of potholes on a vehicle is complex, being a function of the occurrence and size of potholes and the freedom of manoeuvre of the vehicle to take avoiding action. If all potholes were in the wheelpaths and the vehicle had no freedom of manoeuvre (either because the road width is the same as vehicle width or because of traffic congestion), the vehicle would hit 100 per cent of the potholes in the wheelpaths. At the other extreme, with a few isolated potholes on a two lane road with no other traffic, the vehicle would probably avoid most if not all potholes.

The spatial occurrence of potholes may be considered as random, both longitudinally and laterally. If pothole development continues unchecked, the point will be reached where it is impossible to avoid all potholes even with complete freedom of manoeuvre. However, even when large numbers of potholes are present, a vehicle will still not achieve 100 per cent hits due to the lateral distribution. It is clear that linear relationships do not exist between number of potholes and the effect on vehicles in terms of received impacts. It is postulated that the percentage of potholes hit, and thus the resulting roughness effect, will follow a pattern as shown in Figure B10-2 for different levels of freedom to manoeuvre.

Figure B10-2
Conceptual model of potholing effect on roughness

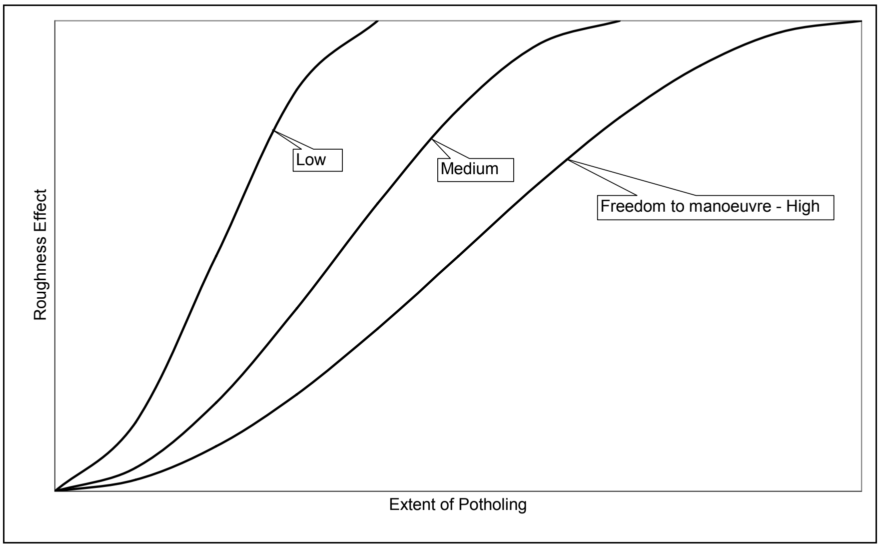

A simple linear model was proposed by the HTRS team in Malaysia (NDLI, 1995) for a freedom to manoeuvre index with a scale of 0 to 1 based on the following premises:

- with a pavement width of 7 m and no traffic, a driver will have complete freedom to avoid potholes
- with a pavement width of 3 m or traffic volume of 5,000 AADT the driver will have no freedom of manoeuvre

From these premises, the following freedom to manoeuvre model was derived:

$$FM = \left(\max\left\{\min\left[0.25\,(CW - 3),\ 1\right],\ 0\right\}\right)\left(\max\left[(1 - AADT/5000),\ 0\right]\right) \qquad ...\ (B10.13)$$

where

FM = freedom to manoeuvre index
CW = carriageway width, in m
AADT = two-way traffic flow, in veh/day

This relationship is illustrated in Figure B10-3.

The FM index can then be applied to the potholing component of roughness model in the following form (NDLI, 1995).

$$RI_p = \min\left[a_0\,(a_1 - FM)\,NPT^{a2},\ a_3\right] \qquad ...\ (B10.14)$$

where

RI_p = roughness due to potholing
NPT = number of pothole units per km
a_0 to a_3 = model coefficients

Figure B10-3
Freedom to manoeuvre index

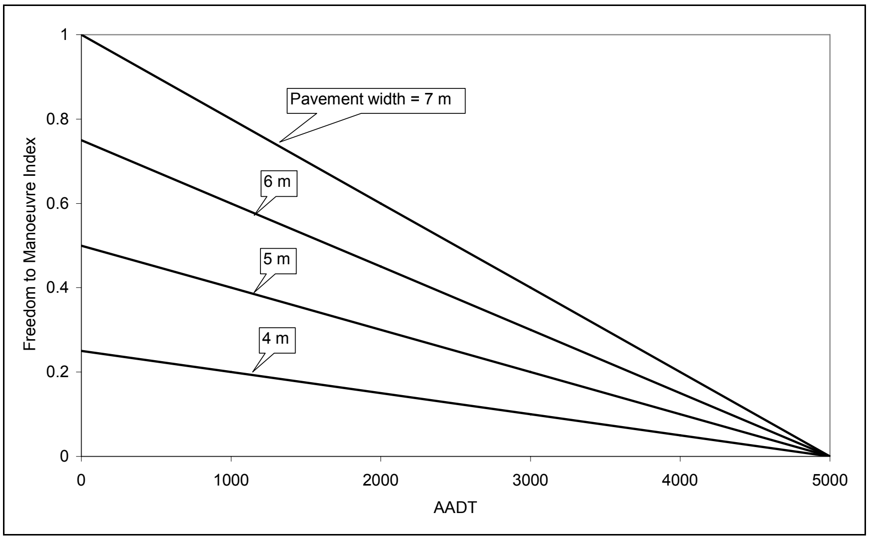

If the HDM-III relationship is converted from per cent area to the number of pothole units per km, it implies that the roughness effect of 1,000 pothole units per lane-km would be approximately 0.84 IRI. This seems patently low. The HTRS team postulated that at this level of potholing the incremental roughness would be 10 IRI if there were total freedom of manoeuvre and 20 IRI if there were no freedom of manoeuvre. Based on this, the coefficient values for the above model are as given in Table B10-4 and the model is illustrated in Figure B10-4.

Table B10-4
Coefficient values for original potholing component of roughness model

a_0	a_1	a_2	a_3
0.0000125	2	1.5	20

Figure B10-4
Original HTRS proposed model for potholing component of roughness

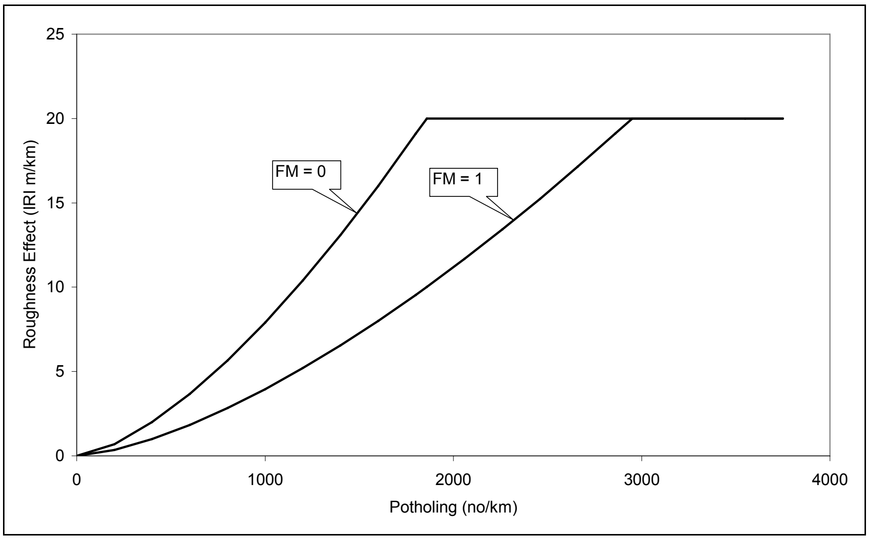

However, in HDM-4, the patching of potholes is modelled to occur at regular intervals throughout the year (using the TLF or PEFF variable – see Section B5.4.2), unlike the other routine maintenance activities, whose effects are modelled only at the end of each analysis year. If potholes are patched more frequently, the user is exposed to their effects for a shorter period of time. Therefore the frequency of patching (Fpat) and the percentage of potholes patched (Ppt) during each patching campaign needs to be incorporated into the potholing component of roughness.

There will also be a difference in the effects of potholes existing at the start of the year (NPT_a) if no patching was applied in the previous year and new potholes occurring during the year (ΔNPT). If, for example, patching frequency is one month, the initial potholes will all be patched after one month and will have no effect for the remaining 11 months of the year. By comparison, new potholes will occur at regular intervals and be patched at regular intervals. Thus the two terms NPT_a and ΔNPT need a different application of the term TLF.

A model for predicting the incremental change in roughness due to potholing, which incorporated the maintenance frequency of pothole patching, was devised by Riley (1998). This model used the original HTRS relationship (equation B10.14) and incorporated the TLF variable in the manner outlined above and has been incorporated into HDM-4 version 1.

The version 1 HDM-4 potholing component of roughness model was as follows:

$$\Delta RI_p = a_0 (a_1 - FM)\left\{\left[(NPT_a)(TLF) + (\Delta NPT)(TLF/2)\right]^{a2} - (NPT_a)^{a2}\right\} \qquad \text{. . . (B10.15)}$$

where

ΔRI_p = incremental change in roughness due to potholing during analysis year, in m/km IRI

ΔNPT = incremental change in pothole units during analysis year, in no/km

NPT_a = number of pothole units per km at start of the analysis year

FM = freedom to manoeuvre index (see equation B10.13)

TLF = time lapse factor (see Table B5-3)

A revised model for the potholing component of roughness has been incorporated in version 2 of HDM-4 (PIARC, 2004) as follows:

$$\Delta RI_p = K_{gp}\, a_0 (a_1 - FM)\left[(NPT_{bu})^{a2} - (NPT_a)^{a2}\right] \qquad \text{. . . (B10.16)}$$

where

$$NPT_{bu} = NPT_b * \left[1 - \left(\frac{Ppt}{100}\right)\left(1 - \frac{Fpat}{365}\right)\right] \qquad \text{. . . (B10.17)}$$

and

ΔRI_p = incremental change in roughness due to potholing during analysis year, in m/km IRI

NPT_a = number of pothole units per km at start of the analysis year

NPT_b = number of potholes per km at end of the analysis year

NPT_{bu} = number of potholes per km at end of the analysis year, as perceived by the road user

FM = freedom to manoeuvre index

Ppt = percentage of potholes patched

Fpat = frequency of pothole patching, in days

K_{gp} = calibration factor for the potholing component of roughness

coefficient values a_0 to a_2 are given in Table B10-5

B10.3.5 Environmental Component

The environmental component of roughness in HDM-4 is similar to that in HDM-III. However, the definition and symbol of the calibration factor K_{gm} have been changed as described in the section on the structural component (Section B10.3.1), resulting in the value of the environmental coefficient, 'm', being input directly into the model.

The environmental component of roughness in HDM-4 is given by:

$$\Delta RI_e = K_{gm}\, m\, RI_a \qquad \text{. . . (B10.18)}$$

where

ΔRI_e = incremental change in roughness due to the environment during analysis year, in m/km IRI

RI_a = roughness at the start of the analysis year, in m/km IRI

m = environmental coefficient (see Table B10-3)

K_{gm} = calibration factor for the environmental component (default = 1.0)

B10.3.6 Total Change in Roughness

The total annual incremental change in roughness is the sum of the various components described above.

The total incremental change in roughness in HDM-4 is given by:

$$\Delta RI = \Delta RI_s + \Delta RI_c + \Delta RI_r + \Delta RI_p + \Delta RI_e \qquad \text{. . . (B10.19)}$$

where

ΔRI = total incremental change in roughness during analysis year, in m/km IRI

The coefficient values for the various roughness components are given in Table B10-5.

Table B10-5
Coefficient values for roughness components

Pavement Type	Roughness Component	Equation	a_0	a_1	a_2
All pavement types	Structural	B10.7	134		
	dSNPK	B10.9	0.0000758	63	40
	Cracking	B10.10	0.0066		
	Rutting	B10.11	0.088		
	Potholing	B10.16	0.00019	2	1.5

The value of a_0 in the potholing component has been altered to 0.00019 from the original value of 0.000125 proposed by the HTRS team, to accommodate the change to the standard size of a pothole unit.

The rates of roughness progression have been plotted in Figure B10-5 for a relatively weak pavement carrying low traffic volumes and in Figure B10-6 for a strong pavement carrying high traffic volumes. Both figures illustrate the contribution from each component of roughness. At low traffic levels the environmental component is by far the highest contributor to roughness. At high traffic flows the rutting component tends to be the highest contributor.

Figure B10-5
HDM-4 predicted rates of roughness progression – low traffic

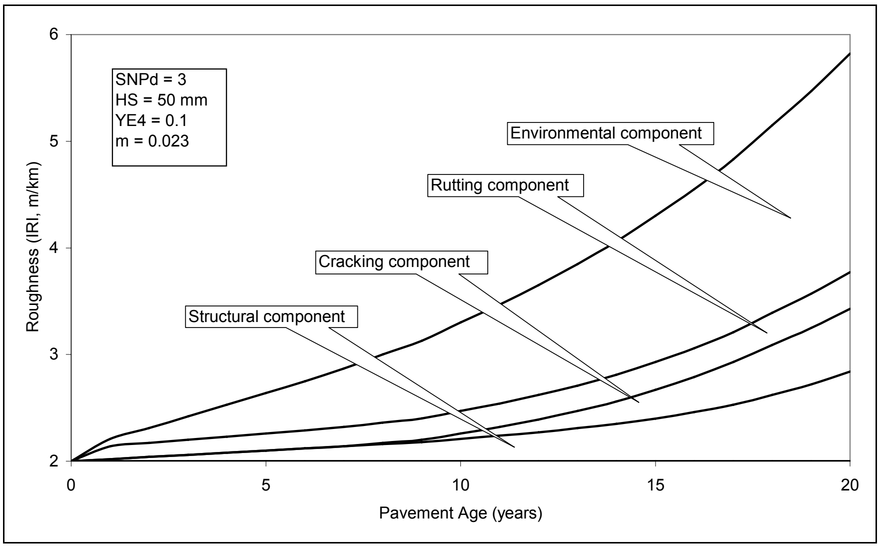

Figure B10-6
HDM-4 predicted rates of roughness progression – high traffic

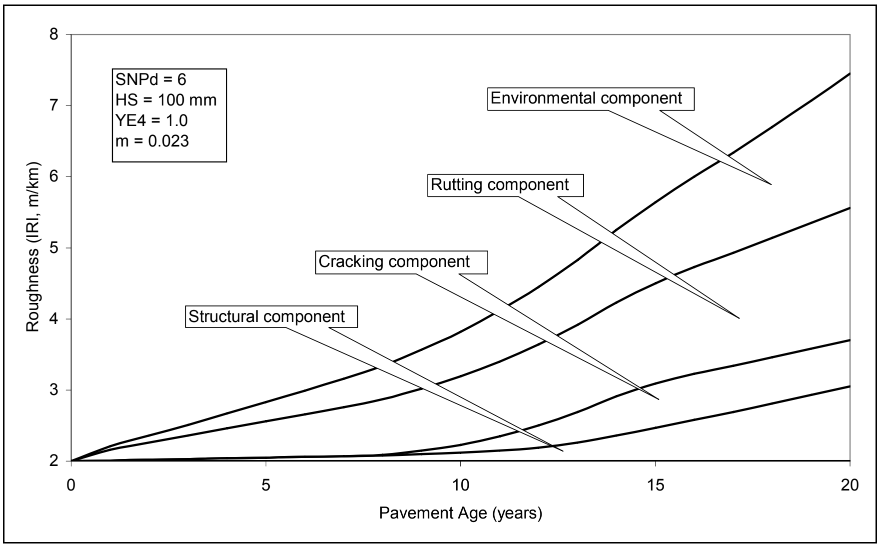

B10.4 Proposed Modifications to the HDM-4 Roughness Model

The roughness of a pavement at the end of a year in relation to what roadworks need to be triggered may be different from the effective roughness of the pavement as perceived by road users. Therefore it is proposed (Riley, 2000a) that two roughness values are derived.

1) The roughness of the pavement representing its longitudinal profile, excluding effects of potholes or partial shoulder use. Used as the roughness of the pavement for triggering works effects.

2) The average roughness experienced by road users during the year which includes the transient effects of potholes and partial shoulder use. Used as the roughness of the pavement in the road user effects relationships – referred to as the effective roughness of the pavement.

The reasons suggested for including the effects of potholes in effective roughness, but not in the roughness used for triggering works effects, are as follows:

- The RD modelling will be simplified as the absolute rather than the incremental model form can be used. There is no need to carry forward the term ΔNPT from the previous year.
- The WE modelling will be simplified as patching effects will only include the residual roughness of the patches and there is no need to reset the pothole effects.
- Pothole effects will not influence roughness interventions for periodic works.

B10.4.1.1 Pavement Roughness for Works Effects

The roughness of the pavement at the end of an analysis year, proposed for use as a trigger level for Works Effects, excludes the potholing component and is derived as follows:

$$RI_b = \min [(RI_a + \Delta RI),\ a_0] \qquad \text{. . . (B10.20)}$$

where

$$\Delta RI = \Delta RI_s + \Delta RI_c + \Delta RI_r + \Delta RI_e \qquad \text{. . . (B10.21)}$$

and

RI_b = roughness of the pavement at end of the analysis year, in m/km IRI
RI_a = roughness of the pavement at start of the analysis year, in m/km IRI
ΔRI = incremental change in roughness during analysis year, in m/km IRI
a_0 = user specified upper limit of pavement roughness (default = 16)
and the other variables are as defined previously

The upper limit of roughness has been currently set in HDM-4 to 16 IRI, as indicated by the default value of a_0 in the above relationship. However, for some bituminous pavement types, such as penetration macadam, the user may wish to set a higher upper limit for RI_b.

B10.4.1.2 Effective Roughness for Road User Effects

On narrow roads vehicles may be forced to make partial use of the shoulders when meeting oncoming traffic or when overtaking. When vehicles are obliged to use the shoulder, they will normally experience a higher roughness than that predicted by the model for the pavement roughness, particularly if the shoulders are unsealed. This effective roughness can be attributed to three causes:

- roughness of the shoulder and proportion of time vehicles spend using the shoulder
- crossing the edge step between pavement and shoulder
- crossing ragged pavement edges characteristic of edge break

These proposed modifications require changes to be made to the potholing component of roughness and the incorporation of the effects of edge break and shoulder deterioration in the effective roughness model.

The model proposed for effective roughness is as follows:

$$RI_{eff} = 0.5(RI_a + RI_b) + RI_p + 0.5(RIsh_b - RI_b)\delta t_{sh} + a_0\ ERATE(a_1 ESTEP + a_2 VEB) \qquad \text{. . . (B10.22)}$$

where

$$RI_p = a_0(a_1 - FM)\left[NPT_a(TLF) + \frac{\Delta NPT}{2}(TLF)\right]^{a2} \qquad \text{. . . (B10.23)}$$

$$\delta t_{sh} = 58(PSH)\ (AADT)\ 10^{-6} \qquad \text{. . . (B10.24)}$$

$$ERATE = 3\left(\frac{(PSH)(AADT)^2}{S}\right)10^{-3} \qquad \text{. . . (B10.25)}$$

and

RI_{eff}	=	effective roughness from use of shoulder, in m/km IRI
RI_a	=	roughness of the pavement at start of the analysis year, in m/km IRI
RI_b	=	roughness of the pavement at end of the analysis year, in m/km IRI
RI_p	=	roughness of the pavement due to potholes, in m/km IRI
$RIsh_b$	=	roughness of the shoulder at end of the analysis year, in m/km IRI
NPT_a	=	number of pothole units per km at start of the analysis year
ΔNPT	=	incremental change in number of pothole units during analysis year, in no/km
FM	=	freedom to manoeuvre index
TLF	=	time lapse factor
δt_{sh}	=	proportion of time vehicles use the shoulder due to road width and traffic volume
ESTEP	=	elevation difference from pavement to shoulder, in mm
ERATE	=	edge crossings per km per hour
VEB	=	volume of lost edge material, in m^3/km
PSH	=	proportion of time vehicles use the shoulder due to road width (see equation B6.8 in the edge break model – Section B6.3)
AADT	=	average annual daily two way traffic, in veh/day
S	=	average traffic speed, in km/h

The effective roughness as specified in equation B10.22 is the roughness value used in the Road User Effects sub-model at the end of each analysis period. The effect on roughness of vehicles having to use the shoulder is illustrated in Figure B10-7.

It should be noted that if the recorded initial roughness of a pavement specified by the user includes the effect of potholes, i.e. in the first year of analysis $NPT_a > 0$, then the input value of roughness should be reduced by the pothole component.

Figure B10-7
Roughness progression from shoulder use

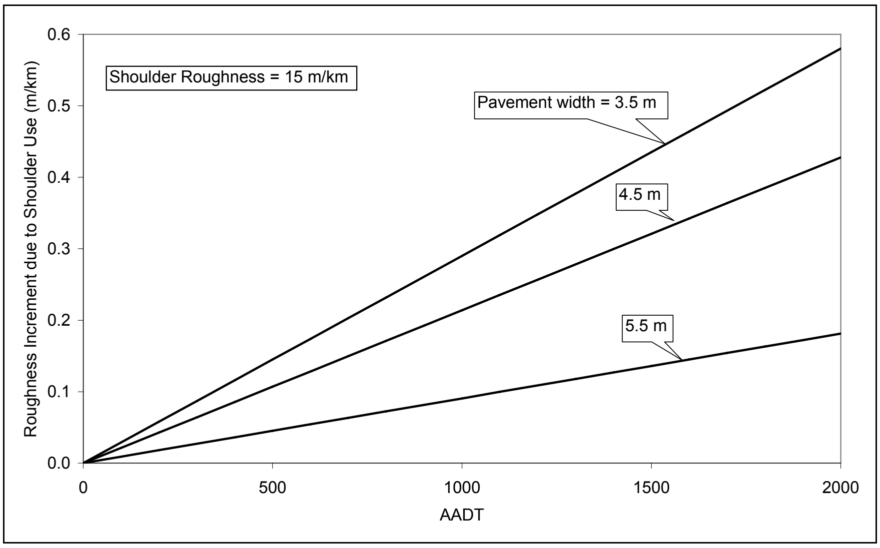

B11. PAVEMENT TEXTURE

In this section, texture depth and skid resistance are discussed, neither of which were modelled in HDM-III. Relationships for modelling the incremental change in texture depth and skid resistance are described for inclusion in HDM-4.

B11.1 Properties of Pavement Texture

Perhaps the most important single variable which determines the magnitude of longitudinal and lateral forces at the tyre-road interface is pavement texture. A road surface exhibits two types of texture classified as **macrotexture** and **microtexture**.

In general, microtexture determines the maximum skid resistance afforded by a dry pavement, while macrotexture determines the drainage ability and therefore how effective the microtexture will be when the pavement is wet. Most skidding related accidents occur on wet pavements. The changes in macrotexture due to wear and compaction resulting from traffic have important safety as well as economic consequences since rolling resistance is a function of texture.

The aggregate particles, generally ranging in size from 6 to 20 mm, in a road surface constitute the macrotexture. Macrotexture is therefore associated with the coarseness of the road surface that affects water drainage from the tyre print, tyre tread rubber deformations and skid resistance at high speed, and the friction-speed gradient. Coarser textures have a flatter friction-speed gradient. Macrotexture is considered optimal for skid resistance purposes if its height is within the range 0.7-1.2 mm and the average distance between the aggregate particle peaks ranges within 6.5 and 12 mm (Babkov, 1985).

Microtexture is the degree of roughness of the surface of individual aggregate particles exposed at the road surface, and has an amplitude ranging typically from 10 to 100 microns. It is known to be a function of aggregate particle mineralogy and petrology and is affected by climate/weather effects and traffic action. Also under this classification must be included the texture of bituminous and cement mortars, which may occupy major portions of the surface of asphalt mix and cement concrete surfacings between any exposed coarse aggregate particles.

The presence of hard gritty grains such as silica, sand or quartzite on road surfaces ensures a continuous gouging and abrasive action under the squirming action of tread rubber in rolling, and this is most effective in preserving a satisfactory microtexture.

The microtexture of the road surface affects the level of skid resistance at all speeds for dry and wet conditions. Surfaces with sharp microtexture projections have a high wet road skid resistance at low speeds but, without macrotexture, show a steep decline in friction as speed rises. Sharp microtexture projections are, however, associated with a high rate of tyre wear, and consequently the action of traffic polishes the surface, reducing its microtexture.

An indication of the values of texture depth (TD) and skid resistance, denoted by the sideway force coefficient (SFC), are shown in Figure B11-1. In this figure surfacings A and B are ST pavement types (SBSD or DBSD) while C and D are AM pavement types (AC or SL) (see Table A2-2 for pavement classification).

Figure B11-1
Surface texture illustration

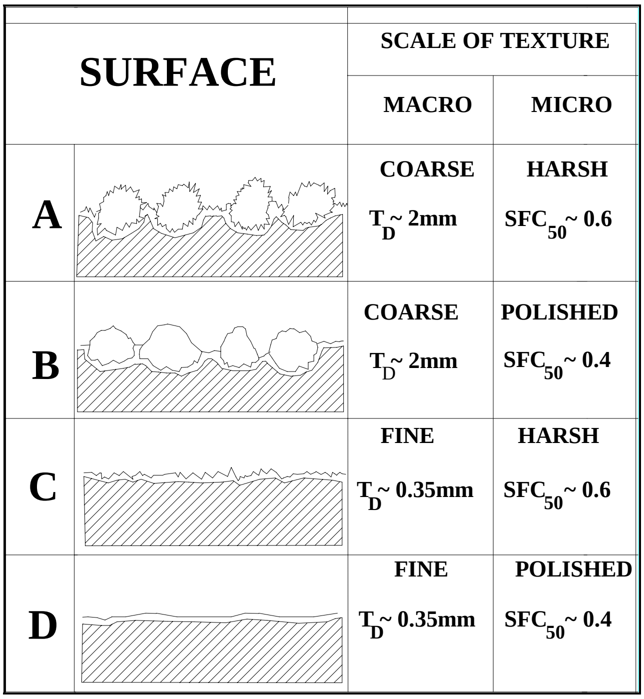

B11.2 Macrotexture

B11.2.1 Deterioration Mechanisms

The macrotexture of a road surface wears as a result of seasonal effects and the overall exposure to traffic. Since wear is the product of tyre pressure, coefficient of sliding friction and scuffing velocity, it is clear that it exhibits a maximum at regions of greatest pressure on a given aggregate particle. There is therefore a tendency to flatten rounded or pointed protrusions, so that a distinct reduction in mean void spacing between tread and texture occurs due to traffic. On the other hand, initially flat aggregate experiences edge wear because of the tendency of tread rubber to drape about the flattened edges, and the higher edge pressures produce a gradual rounding effect. In this case there is a small increase in mean void spacing with progressive wear. A gradual change from centre to edge wear occurs over prolonged periods of time, and the cycle of events repeats continuously.

Superimposed on the centre/edge wear mechanism are seasonal variations due to temperature, rainfall and debris or dust deposits. Lower temperatures prevalent in winter, increase the coefficient of sliding friction so that additional wear can be anticipated. In severe winter climates, frost and brittleness increase the mean texture depth of a road surface by a localised fracture mechanism. The presence of surface grit during the dry summer months produces a polishing action under traffic conditions, and this perhaps inhibits the overall rate of wear while destroying microtexture.

The ability of an aggregate to withstand wear or abrasion can be determined in the laboratory using the Aggregate Abrasion Value (AAV) test (BS 812, 1990). An aggregate with a poor abrasion resistance (indicated by a high AAV) under traffic will be quickly worn with consequent loss of macrotexture. Recommended levels of AAV of aggregate that are necessary to achieve adequate abrasion resistance under different levels of heavy commercial traffic are given in Table B11-1 (Salt, 1977).

Table B11-1
Recommended AAV levels

Traffic (commercial vehicles/lane/day)	Under 250	Up to 1000	Up to 1750	Up to 2500	Up to 3250	Over 3250
Maximum AAV for chippings	14	12	12	10	10	10
Maximum AAV for aggregate in coated macadam wearing courses	16	16	14	14	12	12

Source: After Salt (1977)

In addition to wear, the macrotexture of bituminous surfacings reduces under the action of traffic due to penetration of the aggregate into the substrate and, in the case of single and two coat surface dressings, reorientation of the aggregate particles.

B11.2.2 Modelling Macrotexture Progression

Analysis of limited macrotexture progression data from single surface treatment pavements in New Zealand (Major and Tuohey, 1976) showed mean texture depth, as measured by the volumetric sand patch method, to be strongly correlated to cumulative traffic, yielding the following expression:

$$TD = ALD\,(a_0 - a_1 \log_{10} NELV) \qquad \text{. . . (B11.1)}$$

where

TD = sand patch derived texture depth, in mm
ALD = average least dimension of aggregate particle, in mm
NELV = number of equivalent light vehicle passes since sealing date, where one heavy commercial vehicle is equivalent to 10 light vehicles
a_0, a_1 = regression coefficients

Equation B11.1 shows the rate of change of macrotexture to be a function of aggregate size. The relationship between common aggregate sizes and ALD is given in Table B11-2.

Table B11-2
ALD of typical one size pavement aggregate sizes

Aggregate Size (mm)	Nominal ALD (mm)
20	11
16	9
14	7
10	5.5
7	4

Equation B11.1 can be generalised to apply to all bituminous surfacing types as follows (NDLI, 1995):

$$TD = ITD\,(1 - \Delta TDT \log_{10} NELV) \qquad \text{. . . (B11.2)}$$

where

ITD = initial texture depth which is related to aggregate size or mix type, in mm
ΔTDT = rate of change of texture with traffic and should be constant for similar surfacing types

Representative values of ITD and ΔTDT for different types of bituminous surfacings are given in Table B11-3 and are based on the assumption that the aggregate being used has adequate abrasion resistance for the anticipated heavy commercial vehicle traffic. Based on the available data, the tabulated values appear to be universally applicable.

Table B11-3
Suggested macrotexture model coefficients for different bituminous mixes

Surfacing Type	ITD	ΔTDT
Asphaltic Concrete	0.7	0.005
Slurry Seal	0.7	0.006
Single and Double Bituminous Surface Dressings	1.5 (fine) 3.5 (coarse)	0.120

The figures in Table B11-3 indicate that the macrotexture of surface treatments, whether single or two coat, decreases at a significantly faster rate than for other bituminous surfacings. Another important aspect of surface treatments is that irrespective of the size of the aggregate, the relative rate of change of macrotexture, ΔTDT, remains the same.

In summary, the rate of change of texture for bituminous mixes will be a function of the mix design. For surface treatments, the rate of change of texture will depend on the viscosity of the bitumen, the temperature conditions, and the hardness of the substrate. The constants given in Table B11-3 relate to conditions where the substrate is a sound, hard surface treatment. If the substrate is soft then the rate of change of texture will be significantly greater than the ΔTDT constant given in Table B11-3.

With porous asphalt courses, the deep continuous voids do not allow a realistic measure of macrotexture to be made by methods such as the sand patch or the laser texture meter. However, as the voids fill with detritus, significant macrotexture is still present. For the purposes for calculating texture dependent user costs such as rolling resistance, worn friction course surfaces can be approximated by ITD = 1.5 and ΔTDT = 0.08, i.e. they display characteristics similar to a fine to moderate surface treatment.

B11.2.3 Modelling Macrotexture in HDM-4

Cenek and Griffith-Jones, 1997 proposed an incremental macrotexture model which has been incorporated into HDM-4 as follows:

$$\Delta TD = K_{td} \left\{ ITD - TD_a - a_0\, ITD \log_{10}\left(10^{[(ITD - TDa) / (a0\ ITD)]} + \Delta NELV\right)\right\} \qquad \ldots (B11.3)$$

where

ΔTD	=	incremental change in sand patch derived texture depth during analysis year, in mm
ITD	=	initial texture depth at construction of surfacing, in mm
TD_a	=	texture depth at the beginning of the analysis year, in mm
$\Delta NELV$	=	number of equivalent light vehicle passes during analysis year (one heavy truck or heavy bus is equal to 10 NELV; light vehicles equal 1)
K_{td}	=	calibration factor for texture depth

The coefficient values for a_0 for the texture depth model are given in Table B11-4. This table also includes values for the initial texture depth (ITD) which are used as defaults when resetting pavement surface type. These can be replaced by user definable values.

Table B11-4
Coefficient values for texture depth model

Surface Type	Surface Material	Texture Depth	
		ITD	a_0
AM	AC	0.7	0.005
AM	HRA	0.7	0.005
AM	PMA	0.7	0.005
AM	RAC	0.7	0.005
AM	CM	0.7	0.005
AM	SMA	0.7	0.005
AM	PA	1.5	0.008
ST	SBSD	2.5	0.120
ST	DBSD	2.5	0.120
ST	CAPE	0.7	0.006
ST	SL	0.7	0.006
ST	PM	1.5	0.008

The texture depth at the end of the analysis year is given by the following relationship:

$$TD_b = \max [(TD_a + \Delta TD),\ 0.1] \qquad \text{. . . (B11.4)}$$

where

TD_b = texture depth at the end of the analysis year, in mm
TD_a = texture depth at the beginning of the analysis year, in mm
ΔTD = incremental change in texture depth during analysis year, in mm

The annual average texture depth for a given analysis year will be calculated as follows:

$$TD_{av} = 0.5\ (TD_a + TD_b) \qquad \text{. . . (B11.5)}$$

where

TD_{av} = annual average texture depth for the analysis year, in mm

B11.3 Microtexture

Microtexture is a measure of the degree of polishing of a pavement surface or of the aggregate and the surface. The tendency for an aggregate to polish may be assessed in the laboratory by the Polish Stone Value (PSV) test (BS 812, 1984), in which particles of aggregate are subjected to simulated trafficking in an accelerated polishing machine. A high PSV indicates good resistance to polishing.

Skid resistance of a pavement at low speed (less than 50 km/h) depends primarily on microtexture. Not unexpectedly, measures of low slip friction testers such as the British Pendulum Tester, which measures the skid resistance value (SRV), and the Sideway-Force Coefficient Routine Investigation Machine (SCRIM), which measures SFC, have been shown to correlate well with microtexture (Sandberg, 1990).

B11.3.1 Modelling Skid Resistance

Research performed in the UK by the Transport and Road Research Laboratory (Salt, 1977) established that for bituminous surfacings the three variables SFC, PSV and traffic were inter-related, resulting in the following relationship which applies only to straight road sections:

$$SFC_{50} = 0.024 - 0.663 \times 10^{-4}\ QCV + 1 \times 10^{-2}\ PSV \qquad \text{. . . (B11.6)}$$

where

SFC_{50} = sideway force coefficient measured at 50 km/h
QCV = number of commercial vehicles/lane/day
PSV = polished stone value

The relationship was found to have a highly significant coefficient of determination, i.e. $R^2 = 0.83$ from 139 sets of observations.

Important points arising from equation (B11.6) are:

- a change of 1 unit of PSV corresponds to a change of 0.01 units of SFC at 50 km/h
- for a given commercial vehicle traffic flow, the skid resistance of a pavement reduces to a steady state in around 1-2 years, referred to as the ultimate state of polish. After that time, apart from seasonal variation, it maintains that value until the surfacing deteriorates or the commercial traffic density changes. The effect of traffic on SFC is therefore not cumulative from year to year, and thus the concepts used, for example, in fatigue studies do not apply to skid resistance
- skid resistance varies immensely with the commercial traffic density and, other conditions being equal, a road with the highest commercial traffic flow will have the lowest skid resistance.

The derivation of equation (B11.6) has been regarded as a major advancement in the field of skid resistance as it provides a method of nominating, at the design stage, the properties of the aggregate required to provide a given ultimate skidding resistance, provided that the commercial traffic flow can be estimated.

Equation (B11.6) was modified by Catt (1983) to take into account factors which directly affect skid resistance, with the exception of aggregate type. The derived equation was:

$$SFC_{50} = 0.024 - 0.663 \times 10^{-4}\, QCV + 0.01\,(PSV + SFA - SFB) \qquad \ldots (B11.7)$$

where

SFA = factor depending on the nominal size of the aggregate and type of surfacing (see Table B11-5)
SFB = factor taking braking and turning into account (see Table B11-6)
and the other variables are as defined earlier

Table B11-5
Aggregate factor - SFA

Nominal Size of Aggregate (mm)	SFA	
	Surface Treatment Surfaces	Other Bituminous Surfaces
40	–8	–3
28	–4	–1
20	0	0
14	4	1
10	8	4
6	14	5
3	22	8

Table B11-6
Braking and turning factor - SFB

Traffic Manoeuvre	SFB
Areas where turning and braking occur together	6
Braking only	4
Turning only (bends less than 250 m radius)	3
Pedestrian crossings well clear of bends and junctions	1
Normal sites	0

Equation (B11.7) indicates that:

- aggregate size is a significant factor; the smaller the aggregate size for a nominal PSV the greater the skid resistance
- the degree of braking and turning affects the amount of polishing given to the road surface

The SFC at any speed between 50 and 130 km/h is given by:

$$SFC_s = SFC_{50} \{400 - [2 - \min(TD, 2)] [\max(50, S) - 50]\} / 400 \qquad \text{. . . (B11.8)}$$

where

SFC_s = sideway force coefficient measured at a speed of S km/h
S = traffic speed, in km/h (not less than 50 km/h)
TD = texture depth, in mm

Equation (B11.8) shows that the reduction in skid resistance with traffic speed is nil when the sand patch texture depth is 2 mm, and at 130 km/h reduces linearly to a value of 60 per cent of SFC_{50} at zero texture depth. Therefore on heavily trafficked, high speed roads, the provision of high texture depth may be the most economical way of providing the necessary skid resistance.

Seasonal and Weather Effects

The skid resistance of road surfaces changes significantly due to the short and long term variations of weather conditions (Kennedy, et al, 1990). During periods of dry weather, skid resistance decreases because the aggregate particles are covered by a traffic film of debris containing rubber products and lubricants. However, roads fully or partially recover their frictional characteristics after prolonged periods of rainfall.

The SFC_{50} values derived from Equation (B11.7) pertain to "the mean summer skid resistance coefficient" (MSSC) where skid resistance is at its lowest. Normalisation procedures, such as detailed in Kulakowski, et al (1990), are available for accounting for the effects of seasonal and weather factors. However, the use of MSSC values should ensure conservative estimates of skid resistance, apart from ice and snow conditions.

The magnitude of seasonal variation of skid resistance depends primarily on how much the weather changes between seasons at a particular location, and can vary by as much as 50 per cent. Although temperature has an influence, the proportion of time during which the road is wet appears to be the most significant factor for these observed variations.

B11.3.2 Modelling Skid Resistance in HDM-4

The skid resistance model in HDM-4 predicts the annual incremental change in skid resistance as follows:

$$\Delta SFC_{50} = K_{sfc} \max(0, \Delta QCV) (-0.663 \times 10^{-4}) \qquad \text{. . . (B11.9)}$$

where

ΔSFC_{50} = incremental change in sideway force coefficient during analysis year, measured at 50 km/h

ΔQCV = annual incremental increase in the flow of commercial vehicles, in veh/lane/day

K_{sfc} = calibration factor for skid resistance

The skid resistance measured at 50 km/h at the end of the analysis year is given by the following expression:

$$SFC_{50b} = \max\left[(SFC_{50a} + \Delta SFC_{50}),\ 0.35\right] \qquad \text{. . . (B11.10)}$$

where

SFC_{50b} = sideway force coefficient measured at 50 km/h at end of analysis year

SFC_{50a} = sideway force coefficient measured at 50 km/h at start of analysis year

ΔSFC_{50} = incremental change in sideway force coefficient measured at 50 km/h during analysis year

The annual skid resistance value for a given analysis year is calculated as follows:

$$SFC_{50av} = 0.5\,(SFC_{50a} + SFC_{50b}) \qquad \text{. . . (B11.11)}$$

where

SFC_{50av} = annual average side force coefficient measured at 50 km/h for the analysis year

The average skid resistance value at a given annual average traffic speed is calculated as follows:

$$SFC_s = K_{sfcs}\left\{\frac{SFC_{50av}\left[400-\left(2-\min(TD_{av},2)\right)\left(\max(50,S)-50\right)\right]}{400}\right\} \qquad \text{. . . (B11.12)}$$

where

SFC_s = sideway force coefficient measured at a speed of S km/h

S = traffic speed, in km/h

K_{sfcs} = calibration factor for skid resistance speed effects

and the other variables are as previously defined

The user needs to define a value of SFC_{50} in order for skid resistance modelling to be performed. This also needs to be supplied after maintenance treatments.

B12. ROAD DETERIORATION CALIBRATION FACTORS

The road deterioration models described in the earlier sections of Part B contain calibration factors to facilitate local calibration. Volume 5 of the HDM-4 Series – A Guide to Calibration and Adaptation (Bennett and Paterson, 2000) describes in detail how to calibrate the individual relationships.

All the calibration factors have default values of 1.0 and are summarised in Table B12-1.

Table B12-1
Calibration factors used in the deterioration models

Calibration Factor	Deterioration Model
K_f	Wet/Dry Season SNP Ratio
K_{ddf}	Drainage Factor
K_{cia}	All Structural Cracking – Initiation
K_{ciw}	Wide Structural Cracking - Initiation
K_{cpa}	All Structural Cracking – Progression
K_{cpw}	Wide Structural Cracking – Progression
K_{cit}	Transverse Thermal Cracking - Initiation
K_{cpt}	Transverse Thermal Cracking - Progression
K_{rid}	Rutting - Initial Densification
K_{rst}	Rutting - Structural Deterioration
K_{rpd}	Rutting - Plastic Deformation
K_{rsw}	Rutting - Surface Wear
K_{rds}	Rut Depth Standard Deviation
K_{vi}	Ravelling – Initiation
K_{vp}	Ravelling – Progression
K_{pi}	Pothole – Initiation
K_{pp}	Pothole – Progression
K_{eb}	Edge Break
K_{gs}	Roughness – Structural Component
K_{gc}	Roughness – Cracking Component
K_{gr}	Roughness – Rutting Component
K_{gp}	Roughness – Potholing Component
K_{gm}	Roughness - Environmental Coefficient
K_{snpk}	Roughness – SNPK
K_{td}	Texture Depth – Progression
K_{sfc}	Skid Resistance
K_{sfcs}	Skid Resistance – Speed Effects

B13. ROAD WORKS EFFECTS

Part A3 described the general philosophy of modelling the effects of roadworks, in particular the difference between the immediate effects (reset of model parameters) and long term effects which are simulated by the road deterioration models.

This section describes the immediate effects of different types of roadworks operations on the parameters used to describe the performance of bituminous pavements and, in the case of routine maintenance, illustrates some of the longer term effects on pavement performance.

The works classes for bituminous pavements discussed below are:

- Routine Maintenance (Section B13.2)
- Periodic Maintenance (Section B13.3)
- Improvement Works (Section B13.4)
- Construction (Section B13.5)

B13.1 Modelling Logic

B13.1.1 Ranking of Works

A works activity (or operation) is triggered when any one or a combination of user-specified criteria has been met. When more than one works activity meets the criteria for being applied in a given analysis year, the highest ranking operation for the particular road feature is selected.

Table B13-1 shows the ranking of works activities that are applicable to the carriageway. The operation 'dualisation of an existing road section' is ranked number 1, and takes priority over all the other operations, while routine pavement works (i.e. patching, edge-repair, and crack sealing) is given the lowest priority.

An improvement, or construction works, of a fixed specification is applied to a given road section only once during the analysis period.

Routine pavement works, defined by the user, can be applied as separate operations in each year, or used to repair some distresses before applying the higher-ranking works (e.g. resealing or overlays). Routine pavement works are performed every year in which no periodic maintenance works are applied. When periodic maintenance works are carried out, routine pavement works are considered to be an integral part of the works, and are referred to as **preparatory works**. Although preparatory works are automatically triggered and performed together with the periodic maintenance works, the amount and cost of each of the operations involved are modelled and reported separately.

Drainage works are applied in any given analysis year, if specified by the user, regardless of the hierarchy for carriageway works activities given in Table B13-1. Improvement of side drains takes priority over routine drainage maintenance should both works be applicable in an analysis year.

Table B13-1
Ranking of carriageway road works

Works type	Works activity / operation	Ranking	Unit cost
New section	Dualisation of an existing section	1	per km
Upgrading	Upgrading to a new surface class	2	per km
Realignment	Geometric realignment	3	per km
Widening	Lane addition	4	per m^2 or per km
	Partial widening	5	per m^2 or per km
Reconstruction	Pavement reconstruction	6	per m^2 or per km
Rehabilitation	Mill and replace	7	per m^2
	Overlay rubberised asphalt	8	per m^2
	Overlay dense-graded asphalt	9	per m^2
	Overlay open-graded asphalt	10	per m^2
	Inlay	11	per m^2
	Thin overlay	12	per m^2
Resurfacing (Resealing)	Cape seal with shape correction	13	per m^2
	Cape seal	14	per m^2
	Double surface dressing with shape correction	15	per m^2
	Double surface dressing	16	per m^2
	Single surface dressing with shape correction	17	per m^2
	Single surface dressing	18	per m^2
	Slurry seal	19	per m^2
Preventive Treatment	Fog sealing	20	per m^2
	Rejuvenation	21	per m^2
Routine Pavement	Edge-repair[1]	22	per m^2
	Patching[1]	22	per m^2
	Crack sealing[1]	22	per m^2

Note 1: Routine pavement works (i.e. crack sealing, patching, edge-repair) have the same ranking, and all of them can be performed in the same analysis year

Operations that apply to shoulders and non-motorised transport (NMT) lanes are also performed in any analysis year, if specified by the user, regardless of the works hierarchy described above. Shoulder or NMT lane improvement works takes priority over shoulders repair or NMT lane repair, respectively.

For all road feature types, if more than one works activity of the same operation type (for example, different specifications of overlay) are applicable in an analysis year, the one with the highest cost takes priority over the others.

Works activities whose effects on pavement performance are not modelled endogenously (for example, emergency works, winter maintenance, and routine - miscellaneous works) are applied in a given analysis year, if specified by the user, regardless of any works hierarchy.

B13.1.2 Pavement Types Reset

Maintenance works reset the pavement types in accordance with the pavement classification (see Section A2.3) as shown in Table B13-2.

Table B13-2
Pavement type resets after maintenance works

Works activity	Existing pavement type							
	AMGB	**AMSB**	**AMAB**	**AMAP**	**STGB**	**STSB**	**STAB**	**STAP**
Routine works	AMGB	AMSB	AMAB	AMAP	STGB	STSB	STAB	STAP
Preventive Treatment	AMGB	AMSB	AMAB	AMAP	STGB	STSB	STAB	STAP
Reseal	STAP	STAP / STSB[1]	STAP	STAP	STGB	STSB	STAB	STAP
Overlay	AMAP	AMAP / AMSB[1]	AMAP	AMAP	AMGB	AMSB	AMAB	AMAP
Inlay	AMGB	AMSB	AMAB	AMAP	STGB	STSB	STAB	STAP
Mill & replace part of bituminous layer(s)	**AP	**AP	**AP	**AP	N/A	**SB	**AB	**AP
Mill & replace to base	**GB	**SB	**AB	**AP	**GB	**SB	**AB	**AP

Notes: 1. Pavemnet type depends on the critical thickness (Hmin) of the existing bituminous surfacing that is definable in the HDM-4 Configuration

** Indicates that these two caharcters are dependent on the specific works activity (i.e. AM or ST re-surfacing)

B13.2 Routine Maintenance

Routine maintenance activities comprises works that may need to be undertaken each year or at intervals during the course of a year. Two types of routine works are commonly defined (e.g. Robinson, et al, 1998):

- Cyclic: scheduled works whose needs are dependent on environmental effects rather than traffic, such as vegetation control and cleaning drainage systems;
- Reactive: works responding to minor defects caused by a combination of traffic and environmental effects, such as crack sealing, patching and edge repair.

In HDM-III the only reactive routine maintenance operation modelled was pothole patching. Other routine maintenance operations were deemed to be included in the deterioration models which assumed adequate levels of routine maintenance. Thus HDM-III did not allow the evaluation of the beneficial effects of other routine maintenance works.

In HDM-4, more explicit modelling of pavement strength allows the effects of several routine works to be evaluated. Reactive routine maintenance works which are user-specified are:

- Patching
- Crack Sealing
- Edge Repair
- Drainage maintenance and rehabilitation

B13.2.1 Patching

In version 1 of HDM-4, patching is used to repair the following surface distresses:

- Potholing
- Wide structural cracking
- Ravelling

B13.2.1.1 Patching Potholes

Unlike most works operations which are modelled in HDM-4 as occurring at the end of an analysis year, pothole patching is an operation that can be specified at intervals within a year (see Section B5.4.2). For this reason it is not possible to neatly separate deterioration and works effects as with major treatments. Section B10.3.4 describes the model for the transient effect of potholing on roughness when patching is carried out at intervals varying from 2 weeks to 1 year; the effect is a function of the patching frequency, percentage of potholes to be patched, annual increment in potholing, traffic volume and pavement width.

The result of patching potholes reduces the number of potholes as follows:

$$NPT_{aw} = NPT_{bw}\left(1 - \frac{Ppt}{100}\right) \qquad \text{. . . (B13.1)}$$

where

- NPT_{aw} = number of potholes per km after patching
- NPT_{bw} = number of potholes per km before patching
- Ppt = percentage of potholes to be patched

Although roughness is reduced as a result of patching potholes, roughness is incremented to allow for the residual roughness of the patches.

B13.2.1.2 Patching Wide Structural Cracking

The result of patching wide structural cracking reduces the area of wide structural cracking as follows:

$$ACW_{aw} = ACW_{bw}\left(1 - \frac{Pcw}{100}\right) \qquad \text{. . . (B13.2)}$$

where

- ACW_{aw} = area of wide structural cracking after patching, in per cent of total carriageway area
- ACW_{bw} = area of wide structural cracking before patching, in per cent of total carriageway area
- Pcw = percentage of wide structural cracking to be patched

The effects of wide crack patching on future deterioration are:

- Structural strength of the cracked area is restored, affecting the parameter SNPK in the structural component of the roughness progression model
- The area of cracking that allows ingress of water is reduced in the model for seasonal variation of SNP
- Patched cracks do not develop into potholes

Due to the first effect listed above, crack patching provides an improvement in pavement performance relative to crack sealing. This is illustrated in Figure B13-1 – in both cases the drainage system being maintained in good condition.

Figure B13-1
Pavement performance with crack sealing and patching

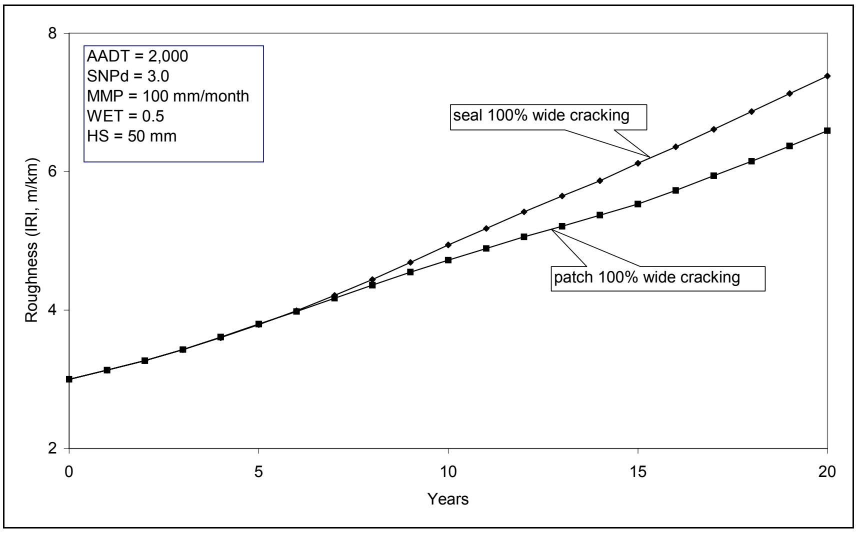

B13.2.1.3 Patching Ravelled Areas

Surface patching of ravelled areas is the replacement of lost surfacing material. The result of patching ravelled areas reduces the area of ravelling as follows:

$$ARV_{aw} = ARV_{bw}\left(1 - \frac{Prv}{100}\right) \qquad \text{. . . (B13.3)}$$

where

ARV_{aw} = area of ravelling after patching, in per cent of total carriageway area
ARV_{bw} = area of ravelling before patching, in per cent of total carriageway area
Prv = percentage of ravelled area to be patched

Patching of ravelled areas prevents the formation of potholes from those areas but otherwise has no effect on future pavement deterioration.

B13.2.2 Crack Sealing

B13.2.2.1 Modelling Crack Sealing in HDM-4

In version 1 of HDM-4, crack sealing was applicable to transverse thermal cracking and wide structural cracking. If the area of wide structural cracking exceeds 20% (i.e. ACW_b>20), then crack sealing cannot be applied to treat wide structural cracking.

The carriageway area sealed is computed as follows:

$$ACSL = \text{Min}(ACSL_{lim}, ASEAL) \qquad \text{. . . (B13.4)}$$

where

$$ASEAL = [(Pcrt)(ACT_{bw}) + (Pcrw)(ACW_{bw})]\,(CW/10) \qquad \text{. . . (B13.5)}$$

and

ACSL = area of crack sealing, in m^2/km
$ACSL_{lim}$ = user specified maximum annual quantity of crack sealing, in m^2/km
ACT_{bw} = area of transverse thermal cracking before crack sealing, in per cent of total carriageway area

ACW_{bw} = area of wide structural cracking before crack sealing, in per cent of total carriageway area
Pcrt = user specified percentage of tranverse thermal cracking to be sealed
Pcrw = user specified percentage of wide structural cracking to be sealed

If both crack sealing and patching are specified to be performed in a given analysis year, it is assumed that patching takes priority over crack sealing in reducing the area of wide structural cracking.

When crack sealing is performed, it is assumed that the treatment of transverse thermal cracking takes priority over that of wide structural cracking, and no crack sealing is performed to fix wide structural cracking until transverse thermal cracking is completely repaired.

The areas of cracking are reduced by the amount of sealing as follows:

$$ACT_{aw} = ACT_{bw} - Min\left[\frac{(Pcrt)(ACT_{bw})}{100},\ \frac{ACSL}{10(CW)}\right] \quad \text{. . . (B13.6)}$$

$$\Delta ACW_{w} = Max\left[0,\ \frac{ACSL}{10(CW)} - (ACT_{bw} - ACT_{aw})\right] \quad \text{. . . (B13.7)}$$

$$ACW_{aw} = ACW_{bw} - \Delta ACW_{w} \quad \text{. . . (B13.8)}$$

$$ACA_{aw} = ACA_{bw} - \Delta ACW_{w} \quad \text{. . . (B13.9)}$$

where:

ACT_{aw} = area of transverse thermal cracking after crack sealing, in per cent of total carriageway area
ACT_{bw} = area of transverse thermal cracking before crack sealing, in per cent of total carriageway area
ΔACW_{w} = reduction in area of wide structural cracking due to crack sealing, in per cent of total carriageway area
ACW_{aw} = area of wide structural cracking after crack sealing, in per cent of total carriageway area
ACW_{bw} = area of wide structural cracking before crack sealing, in per cent of total carriageway area
ACA_{bw} = adjusted area of all structural cracking before crack sealing, in per cent of total carriageway area

B13.2.2.2 Proposed Modifications to Crack Sealing in HDM-4

Cracks that have been sealed will invariably reappear as cracks. Therefore it is proposed that a crack seal life variable is introduced to reflect the expected life of crack sealing.

Sealing Wide Structural and Reflection Cracking

The expected life of crack sealing – crack seal life (CSL_{w} in years) - is a function of the method of crack sealing, the materials used, climate and other factors which may be specific to a particular road network and cannot be expressed as a generalised model parameter.

The annual area of crack sealing is given by:

$$\Delta ACWTs[N] = \frac{P_{csw}}{100} ACWTu \quad \text{. . . (B13.10)}$$

where

$$ACWTu = ACWT_a + \Delta ACW + \Delta ACF - \sum_{y=N-CSLw}^{y=N-1} \Delta ACWTs[y] - ACWTp_a \qquad \text{. . . (B13.11)}$$

and

$\Delta ACWTs[y]$	=	area of sealing of wide structural and reflection cracking in year y, in per cent
P_{csw}	=	annual amount of wide crack sealing (user specified), in per cent
ACWTu	=	area of untreated wide structural and reflection cracking before maintenance, in per cent
$ACWT_a$	=	area of wide structural and reflection cracking at start of analysis year, in per cent
ΔACW	=	increase in wide structural cracking during analysis year, in per cent
ΔACF	=	increase in reflection cracking during analysis year, in per cent
$ACWTp_a$	=	cumulative area of wide structural and reflection cracking that has been patched at start of analysis year, in per cent
N	=	current analysis year
CSL_w	=	crack seal life of wide structural and reflection crack seals, in years

Crack sealing has several effects on future deterioration modelling:

- potholing does not develop from wide cracks that have been sealed
- water ingress is inhibited by sealed cracks with consequent effects on the wet season value of SNP and models that use SNP

In the model for moisture effects on pavement strength, the effects of unsealed cracks and drainage condition are multiplicative (see equation B2.12 in Section B2.3). Thus the benefits of crack sealing are augmented if drainage is maintained in good condition. Figure B13-2 illustrates this for a typical road and climatic zone.

Figure B13-2
Effect of crack sealing and drainage on pavement performance

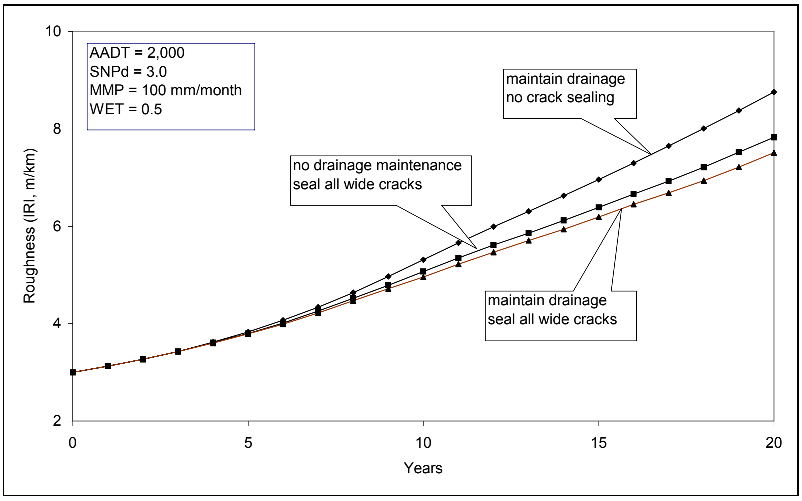

Because of the limited life of crack sealing, the need for sealing will continue after new structural and reflection cracks have stopped developing. Once ACWT has reached 100%, a steady state condition will apply in which the annual need for crack sealing is related to CSL_w. Figure B13-3 shows the annual amounts of crack sealing for different specified percentages when CSL_w is 5 years. Figure B13-4 shows the same with CSL_w of 10 years.

Figure B13-5 compares annual crack sealing when 100% sealing is specified for three values of CSL_w.

These figures illustrate that when a low crack sealing percentage is specified there is a saving in the amount of work in the early years, but later diminishing returns as old cracks re-open and need resealing. When CSL_w is 10 years, the annual steady-state area of sealing is around 10% regardless of the specified policy.

Figure B13-3
Annual areas of crack sealing – CSL_w = 5 years

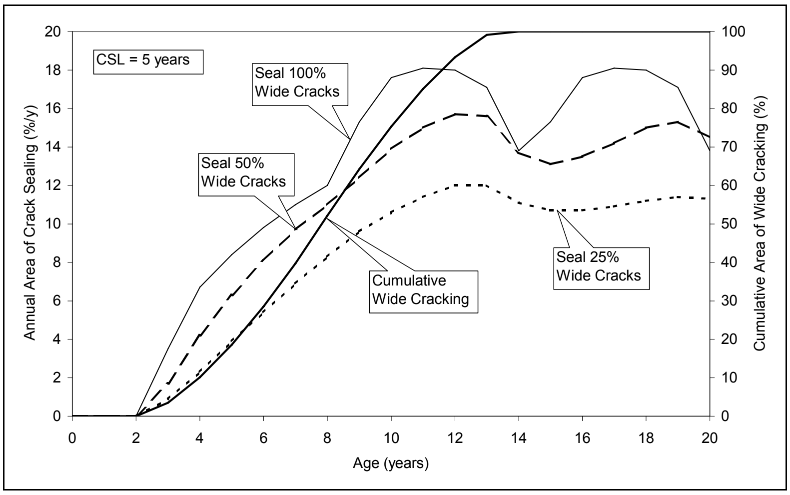

Figure B13-4
Annual areas of crack sealing – CSL_w = 10 years

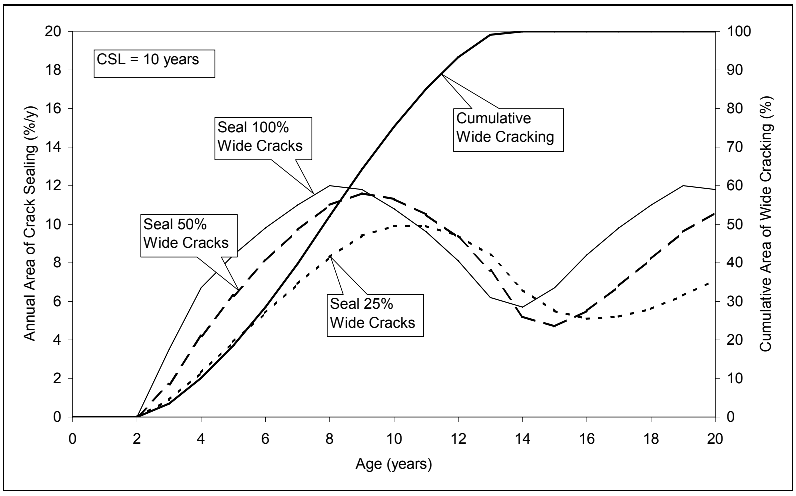

Figure B13-5
Annual areas of crack sealing – P_{crt} = 100

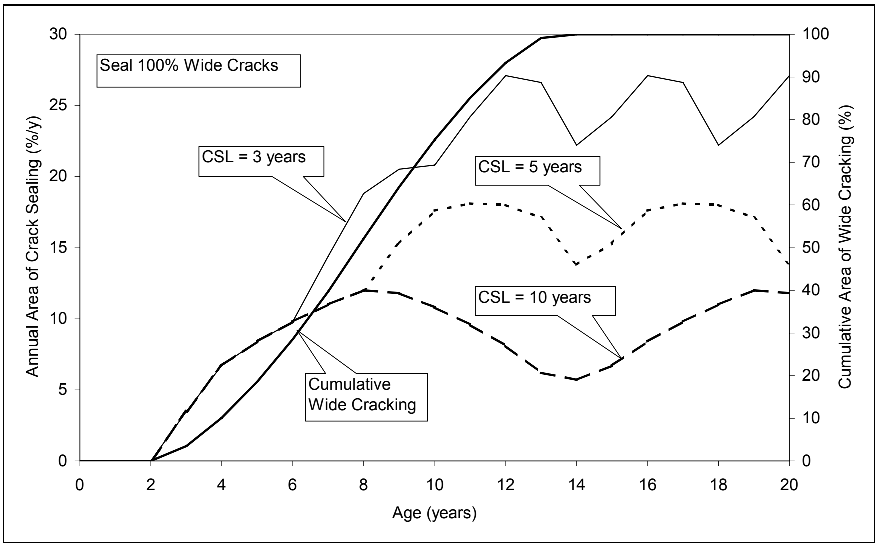

Although the agency cost is similar with both policies there is a not insignificant difference in pavement performance as shown in Figure B13-6. The delay in sealing cracks inherent in the 25% sealing policy allows deterioration of the pavement structure.

Figure B13-6
Pavement deterioration under different crack sealing policies

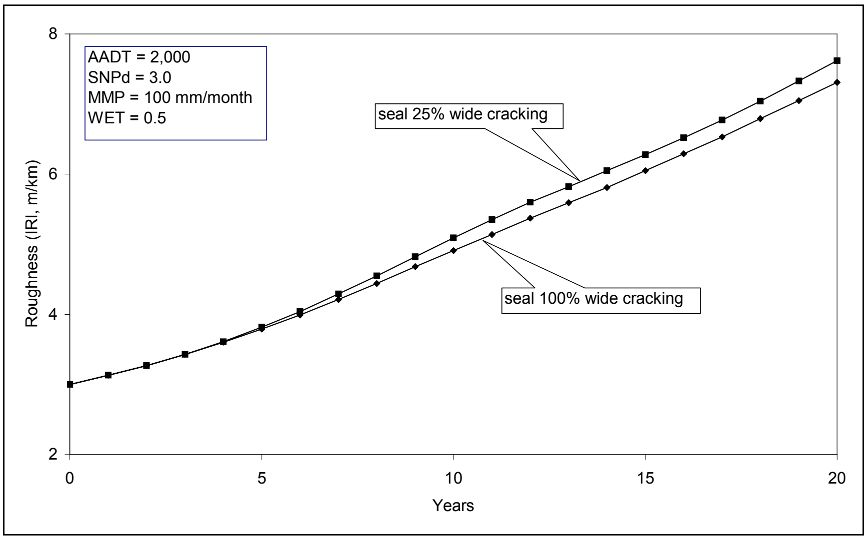

Sealing Transverse Thermal Cracking

Sealing of transverse thermal cracks is a user-specified activity similar to sealing of wide structural and reflection cracks, with the difference that the quantity of sealing is expressed in linear metres rather than area. The amount of cracks to be sealed in any one year can be defined either as a percentage of existing unsealed cracks and/or an upper limit in metres. The life of the seal is also user-specified.

The annual amount of transverse crack sealing is given by:

i) if specified as a percentage

$$\Delta NCTs[N] = \frac{P_{cst}}{100} NCTu \qquad \text{. . . (B13.12)}$$

ii) if specified in linear metres

$$\Delta NCTs[N] = \min\left[NCTu, \frac{LCS_{lim}}{(NCTu)(CW)}\right] \qquad \text{. . . (B13.13)}$$

where

$$NCTu = NCT_a + \Delta NCT - \sum_{y=N-CSLt}^{y=N-1} \Delta NCTs[y] \qquad \text{. . . (B13.14)}$$

and

$\Delta NCTs[y]$	=	sealing of transverse cracks in year y, in no/km
P_{cst}	=	annual amount of transverse crack sealing (user specified), in per cent
LCS_{lim}	=	annual limit of sealing, in m
NCTu	=	area of untreated transverse cracking before maintenance, in no/km
NCT_a	=	transverse cracking at start of analysis year, in no/km
ΔNCT	=	increase in transverse cracking during the year, in no/km
N	=	current analysis year
CSL_t	=	crack seal life of transverse crack seals, in years

Sealing of transverse cracking has two effects on future deterioration modelling:

- potholes does not develop from transverse cracks that have been sealed
- water ingress is inhibited by sealed cracks with consequent effects on the wet season value of SNP and models that use SNP

Compared with the sealing of wide structural and reflection cracking, the effects of sealing transverse cracking are relatively small. The models for pothole progression and SNP use area of cracking; the (default) equilibrium extent of transverse cracking equates to only 1% of the pavement area for freeze climates, where this treatment is most likely to be applied.

B13.2.3 Edge Repair

The immediate effect of repairing edge break is to reduce the volume of the distress:

$$VEB_{aw} = VEB_{bw}\left[1 - \frac{P_{ebr}}{100}\right] \qquad \text{. . . (B13.15)}$$

where

VEB_{aw}	=	volume of edge break after works in m^3/km
VEB_{bw}	=	volume of edge break before works in m^3/km
P_{ebr}	=	user specified percentage of edge break to be repaired

The longer term effect of edge repair is to reduce the effective roughness experienced by vehicles during partial shoulder use on narrow pavements.

B13.2.4 Drainage Works

Drainage condition is represented by a drainage factor (DF) which has a range from 1 - 2 (excellent) to 3 - 5 (very poor), dependent on the type of drain (see Table B2-5 in Section B2.3).

Without maintenance the drainage factor will reduce each year by an amount related to the type of drain, climatic zone and the vertical alignment of the road (see equation B2.13 in Section B2.3). Maintenance operations can be of two types:

- recurrent operations that increments DF each year by a given amount and thus counteracts the annual deterioration
- rehabilitation of drainage which is in poor condition, for example, reducing DF from 5 to 2 in the case of an open earth drain

The immediate effect of these operations, in modelling terms, is simply to reset the drainage factor, DF, to a new value. When drainage works is performed, the drainage factor after works (DF_{aw}) is reset as follows:

$$DF_{aw} = \max\left[DF_{dmin}, \left(DF_{bw} - \Delta DF_{w}\right)\right] \quad \text{. . . (B13.16)}$$

where

$$\Delta DF_{w} = \left(DF_{dmax} - DF_{dmin}\right) DMCF \quad \text{. . . (B13.17)}$$

and

DF_{aw} = drainage factor after maintenance works
DF_{bw} = drainage factor before maintenance works
DF_{dmax} = maximum drainage factor, denoting very poor drainage condition for drain
DF_{dmin} = minimum drainage factor, denoting excellent drainage condition for drain
ΔDF_{w} = change in DF due to the drainage works performed
DMCF = drainage maintenance cost factor, defined as the ratio of the annual cost of drainage works performed to the annual cost required to maintain the drainage system in excellent condition

The drainage factor after works is used in the computation of the adjusted structural number of the pavement (SNP). The future effect on pavement performance is modelled via the ratio between dry and wet season values of SNP, which is in turn used in the deterioration models for cracking, rutting, potholing and roughness. Figure B13-7 illustrates the effect of drainage maintenance and rehabilitation on roughness for a typical road with no roadworks being applied except the patching of potholes.

Figure B13-7
Effect of drainage maintenance on pavement performance

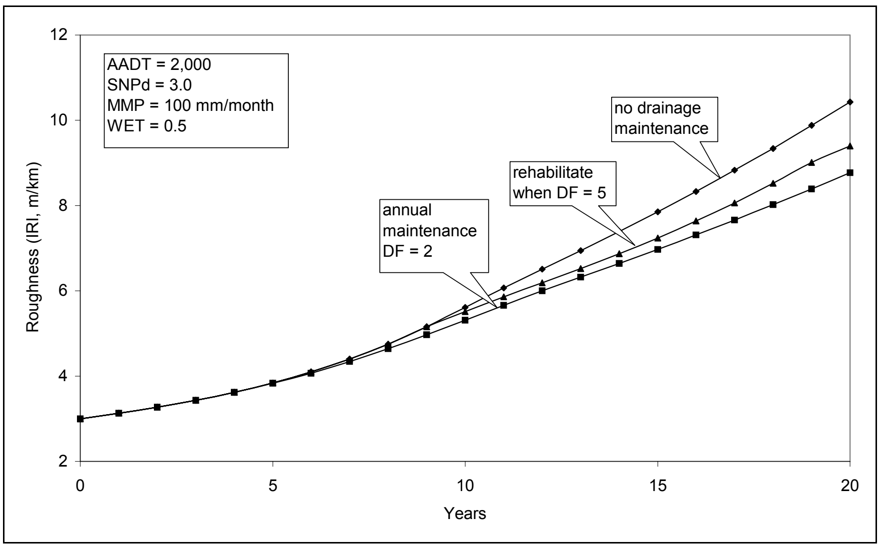

B13.3 Periodic Maintenance

Periodic maintenance of road pavements are commonly defined as works that are planned to be undertaken at intervals of several years and are usually classified as preventive, resurfacing, overlay and reconstruction (Robinson, et al, 1998).

Preventive treatments are proactive; they are applied before significant deterioration is apparent in the pavement surface and are intended to delay the onset of such deterioration. Such treatments include:

- Rejuvenation, a light application of solvents, oils or plasticisers sprayed onto the pavement surface. The effect is to soften an oxidised binder and restore its original viscosity and thus inhibit cracking and ravelling.
- Fog seal, a light sprayed application of bitumen which covers an oxidised binder with a fresh, less viscous material and binds loose surface aggregate.

Resurfacing can similarly be a proactive treatment or may be reactive to relatively low levels of surface distress such as cracking and ravelling or roughness. Resurfacing operations include surface treatments, slurry seals and thin pre-mixed overlays.

Overlays, which increase the structural capacity of the pavement, are normally reactive to high levels of surface distress or deformation. This class of treatment, in addition to thick pre-mix overlays, includes mill and replace operations.

Reconstruction which involves replacement of one or more pavement layers is normally a response to high levels of surface distress in the pavement or severe deformation.

All four types of periodic maintenance were modelled in HDM-III, and the types of treatment and their effects models have been augmented for HDM-4. The following sections detail the models used to describe the effects of periodic maintenance on the different pavement modelling parameters used in HDM-4.

B13.3.1 Pavement Structure

B13.3.1.1 Preventive Treatments

Preventive treatments have no direct effect on the pavement strength parameters.

B13.3.1.2 Resurfacings and Overlays

Resurfacings and overlays increment the dry season value of adjusted structural number (SNP_d) by an amount related to the thickness and materials properties of the new surfacing:

$$SNP_{daw} = \max(1.5,\ SNP_{dbw} + 0.0394\ a_w\ HSNEW_{aw} - dSNPK) \quad \text{. . . (B13.18)}$$

where

SNP_{daw} = adjusted structural number for the dry season after works

SNP_{dbw} = adjusted structural number for the dry season before works

a_w = layer strength coefficient of the new surfacing layer

$HSNEW_{aw}$ = thickness of the new surfacing layer, in mm

$dSNPK$ = reduction in strength due to cracking in the bound layers before works as given in equation B2.18

After resurfacing or overlay, the thickness of the new surfacing layer (HSNEW) is reset to the value specified for the operation. The thickness of old surfacing layers is given by:

$$HSOLD_{aw} = HSOLD_{bw} + HSNEW_{bw} \qquad \text{. . . (B13.19)}$$

where

$HSOLD_{aw}$ = thickness of old surfacing layers after works, in mm
$HSOLD_{bw}$ = thickness of old surfacing layers before works, in mm
$HSNEW_{bw}$ = thickness of new surfacing layers before works, in mm

B13.3.1.3 Mill and Replace

The reset of dry season adjusted structural number after a mill and replace operation is dependent on the depth of milling relative to the depth of old and new surfacings before treatment and the thickness of the replacement surfacing layers.

$$SNP_{daw} = SNP_{dbw} - SN_{mill} + SN_{sw} \qquad \text{. . . (B13.20)}$$

where

SN_{mill} = strength contribution of layers removed by milling
SN_{sw} = strength contribution of new surfacing layer
and the other variables are as defined previously

and

$$SN_{mill} = 0.0394 \{\min (MILLD, HSNEW_{bw})a_n + \min [\min (MILLD - HSNEW_{bw}, 0), HSOLD_{bw}]a_0 + \min (MILLD - HSNEW_{bw} - HSOLD_{bw}, 0)a_b\} \qquad \text{. . . (B13.21)}$$

$$SN = 0.0394\, HSNEW_{aw}\, a_{sw} \qquad \text{. . . (B13.22)}$$

where

MILLD = specified depth of milling, in mm
a_n = strength coefficient of new surfacing layers before works
a_o = strength coefficient of old surfacing layers before works
a_b = strength coefficient of base layer
a_{sw} = specified strength coefficient of new surfacing layer
and the other variables are as defined previously

If the strength coefficients for the layers in the old pavement were not user-specified, default values are adopted as shown in Table B13-3.

Table B13-3
Default strength coefficients for pavement layers

Layer	Type	Strength coefficient
New or Old Surfacing	AM	0.35
	ST	0.20
Base	GB	0.15
	AB	0.30
	SB	0.50
	AP	0.35

B13.3.1.4 Reconstruction

Pavement reconstruction involves replacing or reworking surfacing and base layers and the specification of the work includes all parameters related to pavement structure except the subgrade which is assumed to remain unchanged. The dry season adjusted structural number is reset by:

$$SNP_{daw} = SN_{new} + SNSG \qquad \text{. . . (B13.23)}$$

where

SNP_{daw} = dry season adjusted structural number after works
SN_{new} = specified structural number of new pavement
SNSG = subgrade structural number contribution

B13.3.2 Pavement Ages

HDM-4 uses four pavement age parameters to define the number of years since preventive treatment (AGE1), since resurfacing (AGE2), since structural overlay or (re)construction (AGE3) and (re)construction including base (AGE4) (see Section A2.5.3). The reset of pavement ages is shown in Table B13-4.

Table B13-4
Reset of pavement ages

Works Type	AGE1	AGE2	AGE3	AGE4
Preventive	0	N	N	N
Resurfacing	0	0	N	N
Overlay	0	0	0	N
Mill and Replace	0	0	0	N
Reconstruction	0	0	0	0

Note: 0 – reset to zero N – no reset

B13.3.3 Cracking and Ravelling

B13.3.3.1 Preventive Treatments

Preventive treatments modelled in HDM-4 are rejuvenation and fog seals. The objective of these treatments is to delay the initiation and/or progression or structural cracking and ravelling and they are applied either before the initiation of these distresses or when only a small area of the pavement has been affected (less than 5% cracking or 10% ravelling).

The effect of preventive treatments is modelled through the parameters CRT (cracking retardation time) and RRF (ravelling retardation factor). The reset of these parameters follows the models used in HDM-III.

The change in cracking retardation time due to a preventive treatment is given by:

$$CRT_{aw} = \min\left[CRT_{bw} + \frac{CRM}{YXK},\ \frac{CRTMAX}{YXK},\ 8\right] \qquad \text{. . . (B13.24)}$$

where

YXK = max (YAX, 0.1)

and

CRT_{aw} = cracking retardation time after works, in years
CRT_{bw} = cracking retardation time before works, in years
CRM = change in CRT due to preventive treatment
CRTMAX = maximum limit of CRT
YAX = annual number of axles, in millions per lane

The default values of CRM and CRTMAX are related to pavement and materials characteristics as shown in Table B13-5. The values in Table B13-5 indicate that rejuvenation treatments are more effective in delaying cracking than fog seals.

Table B13-5
Cracking retardation time after preventive treatments

Pavement Type	Surfacing Material	HSOLD	Rejuvenation		Fog Seal	
			CRM	CRTMAX	CRM	CRTMAX
AMGB	All	0	1.5	3.0	0.8	1.6
	All except CM	> 0	1.5	3.0	0.8	0.4
	CM	> 0	0.75	1.5	0.4	1.6
AMAB			1.5	3.0	0.8	1.6
AMAP			1.5	3.0	0.8	1.6
AMSB			1.5	3.0	0.8	1.6
STGB	All	0	3.0	6.0	1.6	3.2
		> 0	1.5	3.0	0.8	1.6
STAB			1.5	3.0	0.8	1.6
STAP			1.5	3.0	0.8	1.6
STSB			1.5	3.0	0.8	1.6

The change in ravelling retardation factor after preventive treatments is given by:

$$RRF_{aw} = \min[(RRF_{bw})(RRM), RRFMAX] \qquad \text{. . . (B13.25)}$$

where

RRF_{aw} = ravelling retardation factor after works
RRF_{bw} = ravelling retardation factor before works
RRM = change in RRF due to preventive treatment
RRFMAX = maximum limit of RRF

The default values for RRM and RRFMAX are shown in Table B13-6, which indicate that fog seals are slightly more effective in inhibiting ravelling than rejuvenation treatments.

Table B13-6
Ravelling retardation factor after preventive treatments

Pavement Type	Surfacing Material	Rejuvenation		Fog Seal	
		RRM	RRFMAX	RRM	RRFMAX
All	All	1.15	2.0	1.3	3.0

B13.3.3.2 Other Operations

Resurfacing, overlay and reconstruction will reset all cracking and ravelling values in the new surfacing layer to zero.

In the case of **resurfacing and overlay**, values of previous cracking are reset as follows:

If $ACAT_{bw} \geq PACA_{bw}$

$$PACA_{aw} = ACAT_{bw} \qquad \text{. . . (B13.26)}$$

else

$$PACA_{aw} = w(PACA_{bw}) + (1 - w)PACA_{bw} \qquad \text{. . . (B13.27)}$$

If $ACWT_{bw} \geq PACW_{bw}$

$$PACW_{aw} = ACWT_{bw} \qquad \text{. . . (B13.28)}$$

else

$$PACW_{aw} = w(PACW_{bw}) + (1 - w)PACW_{bw} \qquad \text{. . . (B13.29)}$$

where

$ACAT_{bw}$ = all structural and reflection cracking before works, in per cent
$PACA_{bw}$ = previous all structural and reflection cracking before works, in per cent
$PACA_{aw}$ = previous all structural and reflection cracking after works, in per cent
$ACWT_{bw}$ = wide structural and reflection cracking before works, in per cent
$PACW_{bw}$ = previous wide structural and reflection cracking before works, in per cent
$PACW_{aw}$ = previous wide structural and reflection cracking after works, in per cent
w = weighting factor

The model for the weighting factor, w, is related to type of works:

Surface treatment and thin overlay

$$w = \min\left[0.70 + 0.1(HSNEW_{aw}),\ 1\right] \qquad \text{. . . (B13.30)}$$

Thick overlay, stabilised base

$$w = \max\left[\frac{HSNEW_{bw}}{HSOLD_{aw} + HBASE},\ 0.6\right] \qquad \text{. . . (B13.31)}$$

Thick overlay, all other base types

$$w = \max\left[\frac{HSNEW_{bw}}{HSOLD_{aw}},\ 0.6\right] \qquad \text{. . . (B13.32)}$$

where

$HSNEW_{aw}$ = thickness of new surfacing layer after works, in mm
$HSNEW_{bw}$ = thickness of new surfacing layer before works, in mm
$HSOLD_{aw}$ = thickness of old surfacing layers after works, in mm
HBASE = thickness of the base layer, in mm

For **mill and replace** operations, reset of previous cracking is given by:

if $MILLD < HSNEW_{bw}$

if $ACAT_{bw} \geq PACA_{bw}$

$$PACA_{aw} = wf(ACAT_{bw}) \qquad \text{. . . (B13.33)}$$

else

$$PACA_{aw} = wf(PACA_{bw}) + (1 - w)PACA_{bw} \qquad \text{. . . (B13.34)}$$

if $ACWT_{bw} \geq PACW_{bw}$

$$PACW_{aw} = wf(ACWT_{bw}) \qquad \text{. . . (B13.35)}$$

else

$$PACW_{aw} = wf(PACW_{bw}) + (1 - w)PACW_{bw} \qquad \text{. . . (B13.36)}$$

else

$$PACA_{aw} = wg(PACA_{bw}) \qquad \text{. . . (B13.37)}$$

and

$$PACW_{aw} = wg(PACW_{bw}) \qquad \text{. . . (B13.38)}$$

where

MILLD = specified depth of milling
w = weighting factor as defined previously for overlays
wf, wg = weighting factors as defined below

$$wf = w\left[1 - \frac{MILLD}{HSNEW_{bw}}\right] \qquad \text{. . . (B13.39)}$$

$$wg = \max\left[0, \frac{HSNEW_{bw} + HSOLD_{bw} - MILLD}{HSOLD_{bw}}\right] \quad \text{. . . (B13.40)}$$

For all the above operations, previous indexed structural cracking is given by:

$$PACX_{aw} = 0.62(PACA_{aw}) + 0.39(PACW_{aw}) \quad \text{. . . (B13.41)}$$

For all the above operations, previous transverse thermal cracking is given by:

if $MILLD < HSNEW_{bw} + HSOLD_{bw}$

$$PNCT_{aw} = NCT_{bw} \quad \text{. . . (B13.42)}$$

else

$$PNCT_{aw} = 0 \quad \text{. . . (B13.43)}$$

where

NCT_{bw} = transverse thermal cracking before works, in no/km
$PNCT_{aw}$ = previous transverse thermal cracking after works, in no/km

In the case of **pavement reconstruction**, all previous cracking is set to zero.

B13.3.4 Rutting

B13.3.4.1 Preventive Treatments and Seals without Shape Correction

Preventive treatments, surface treatments and slurries without shape correction have no effect on rut depth.

B13.3.4.2 Seals with Shape Correction and Overlays

Seals with shape correction and overlays reset mean rut depth as:

$$RDM_{aw} = a_0(RDM_{bw}) \quad \text{. . . (B13.44)}$$

where

RDM_{aw} = mean rut depth after works, in mm
RDM_{bw} = mean rut depth before works, in mm
a_0 = user definable coefficient (default = 0.15)

B13.3.4.3 Other Operations

In all other works operations, the mean rut depth after treatment is zero, unless specified otherwise by the user.

B13.3.5 Roughness

B13.3.5.1 Seals and Thin Surfacings

HDM-III provided three models for roughness reduction after the application of thin surfacings: surface treatment, slurry seal and reseal with shape correction. All three models first reduce the roughness component for potholes before applying the following relationships:

Single or Double Surface Treatment

$$RI_a = RI_b + \min\{0, \max[0.3(5.4 - RI_b), \ -0.5]\} - 0.0066(ACX) \quad \text{. . . (B13.45)}$$

Slurry Seals and Cape Seals

$$RI_a = RI_b + \min\{0, \max[0.3(4.6 - RI_b), \ -0.09(Hsl)]\} - 0.0066(ACX) \quad \text{. . . (B13.46)}$$

Reseal with Shape Correction

$$RI_a = RI_b + \min\{0, \max[-0.0075(Hsc)(RI_b), \ -0.0225(Hsc)\max(RI_b - 4, \ 0)]\} - 0.0066(ACX) \quad \text{. . . (B13.47)}$$

where

RI_a	=	roughness after seal, in m/km IRI
RI_b	=	roughness after pothole patching and before seal, in m/km IRI
Hsl	=	thickness of slurry seal, in mm
Hsc	=	thickness of reseal including shape correction layer, in mm
	=	min(Hsc, 50)
ACX	=	area of indexed cracking, in per cent

The HDM-III models for the effects of thin surfacings on roughness are illustrated in Figure B13-8 and Figure B13-9.

The HDM-III model shows a very small reduction in roughness for surface treatments - about 0.5 IRI when the pre-seal roughness is more than 5 IRI. A 5 mm slurry seal gives roughly the same effect while a 10 mm slurry is predicted to give a reduction of about 1.0 IRI when pre-seal roughness is more than 7 IRI. At lower levels of roughness, as would be found on a well developed highway network, seals are modelled as having no effect on roughness.

The HDM-III model for reseal with shape correction gives higher roughness reductions if the thickness is 20 mm or more. Figure B13-9 shows that for a thickness of 50 mm the model is somewhat anomalous, with the line having a downward slope between pre-treatment roughness of 4 and 6 IRI. Watanatada, et al, (1987) do not explain what is meant by a reseal with shape correction: if the total thickness of such a treatment were 50 mm it should surely be considered and modelled as an overlay.

Figure B13-8
Effects of surface treatments and slurry seals on roughness in HDM-III

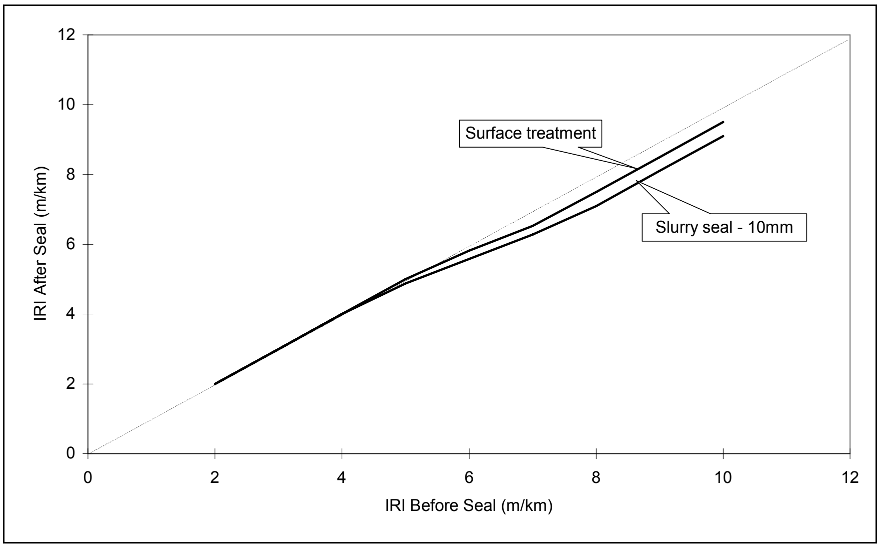

Figure B13-9
Effects of reseal with shape correction on roughness in HDM-III

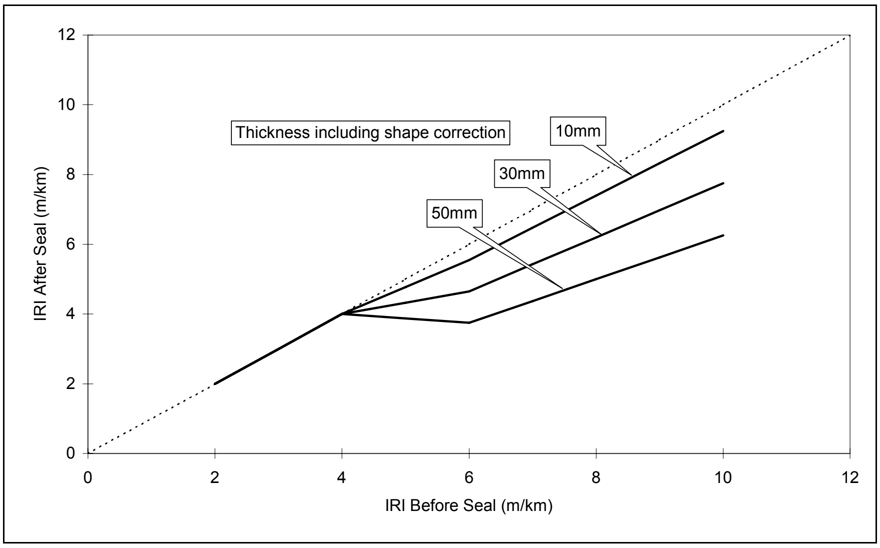

Djarf (1995) presented data from Sweden for the effects on roughness of a single surface treatment on asphalt surfacing with pre-treatment roughness in a range from 1 to 2.5 IRI. The regression showed a slight increase in roughness (possibly because of the coarser texture of the surface treatment) and Djarf (1995) concluded that surface treatments had no effect on roughness.

When evaluating the effects of surface treatments on higher roughness pavements it is normal that some preparatory patching is carried out; it is this pre-treatment repair, rather than the seal itself, that often gives the reduction in roughness. It is concluded that seals give little or no immediate reduction in roughness and the HDM-III models for surface treatment and slurries should be retained in HDM-4. For reseal with shape correction, it is recommended that an upper limit of 20 mm be placed on the thickness for modelling purposes: thicker treatments should be considered as overlays.

B13.3.5.2 Overlays

HDM-III models the reduction in roughness after overlay as a function of pre-overlay roughness and overlay thickness: two models are provided, one for a "regular" paver and one for an automatic-levelling long-base paver. These models were derived partly from field observations and partly by means of computer simulations. The two models are expressed as follows:

Regular Paver

$$RI_a = 3.85 - \frac{\min(H, 80) + \min(H, 40)}{52} + \frac{28\max(RI_b - 3.85)}{\max(H, 28)} \qquad \text{. . . (B13.48)}$$

Automatic-Levelling Long-Base Paver

$$RI_a = \max\{(1.5 + 0.22\ RI_b - 0.00523\ H),\ [RI_b\ (1 - 0.008\ \max(H - 20.0) - 1.5]\} \qquad \text{. . . (B13.49)}$$

where

RI_a = roughness after overlay, in m/km IRI
RI_b = roughness after patching and before overlay, in m/km IRI
H = thickness of overlay, in mm

The effects of these models are shown in Figure B13-10 and Figure B13-11. When considering the roughness reduction effects of overlays, it has been found that the nature of the roughness of the old surface must be taken into account. If the surface contains a large amount of short baselength roughness, for example as found in hand-laid surfacings or due to extensive patching of utility cuts, thin overlays will give a greater reduction in roughness than predicted by the HDM-III models, which were predicated on longer wavelength deformation of asphalt pavements.

Figure B13-10
Roughness reduction after overlay with regular paver

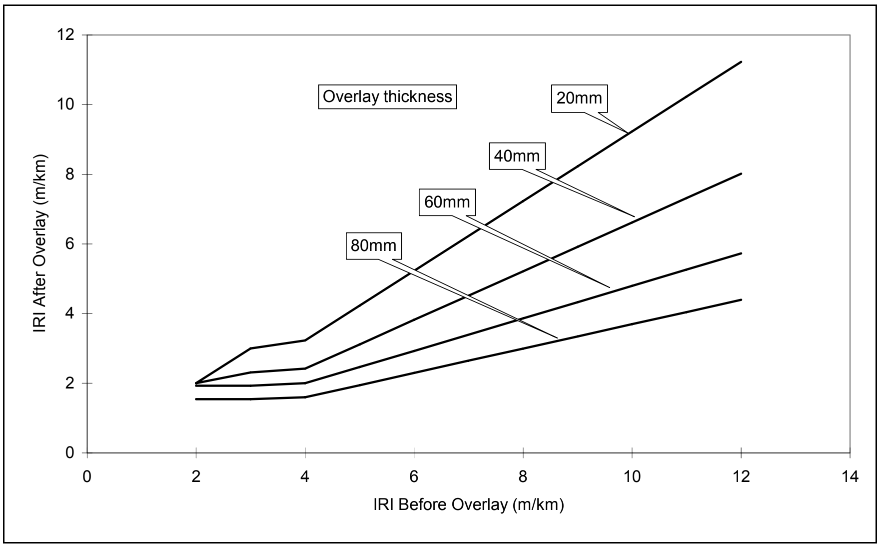

Figure B13-11
Roughness reduction after overlay with automatic-levelling long-base paver

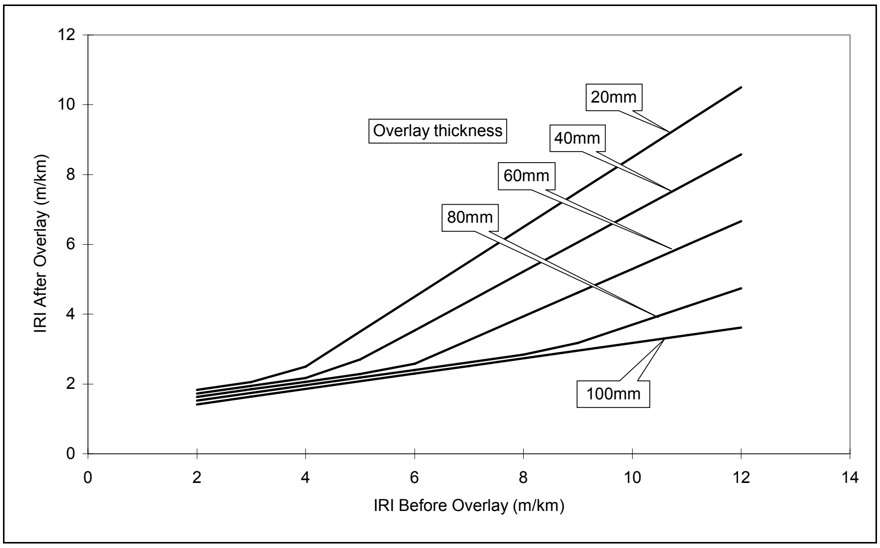

A study in Indonesia (Corne, 1989) measured roughness before and after thin (average 35 mm) machine-laid asphalt was applied to penetration macadam surfaces. The same study found that for multi-layer treatments with a thickness of 80 mm or more the mean roughness was 2.0 m/km. By interpolation, the following relationship was developed:

$$RI_a = 2.0 + 0.0071 \max(80 - H, 0) \max(RI_b - 2.0, 0) \quad \text{. . . (B13.50)}$$

Subsequent studies in Nepal (NDLI, 1993) and Barbados (NDLI, 1994a) showed the relationship from Corne (1989) to be valid for thin overlays on hand-laid surfaces if the constant was changed to 2.5.

A study in Thailand (NDLI, 1991) examined the effect of 50 mm overlays on existing asphalt or surface treated surfaces and found the following relationship:

$$RI_a = 1.87 + 0.25\, RI_b \quad \text{. . . (B13.51)}$$

Data from Djarf (1995) gave the following relationship for change in IRI for overlays in Sweden in the thickness range from 25 to 60 mm:

$$RI_a = 0.55 + 0.29\, RI_b \quad \text{. . . (B13.52)}$$

A study in Trinidad (NDLI, 1994b) of the effects of 40 mm overlays showed an almost completely flat regression line (IRI_a = 2.5) with no effects from pre-overlay roughness. It was postulated that the reason for this was that the high values for the previous roughness derived mainly from badly patched utility cuts. These contribute to very short wavelength roughness, which is easily removed with a thin overlay as shown in Indonesia, Nepal and Barbados.

Figure B13-12 compares the models from HDM-III (regular paver), Thailand, Indonesia and Sweden for an overlay thickness of 50 mm. When considering Figure B13-12 it should be borne in mind that the models from HDM-III, Thailand and Sweden were derived from pre-overlay roughness values up to about 6 m/km IRI: only in Indonesia did observed pre-overlay roughness reach 12 m/km IRI. Comparing the HDM, Thailand and Sweden models in the range 2 - 6 m/km IRI, the HDM model seems to lie in between the other two. It is apparent that asphalt finish is much better in Sweden than in Thailand, with most of the post-overlay values being below 2 m/km IRI. Obviously, standards of workmanship are an important variable in any model of this nature and thus local calibration must be made to reflect this.

Figure B13-12
Comparison of different models for the effect on roughness of a 50 mm overlay

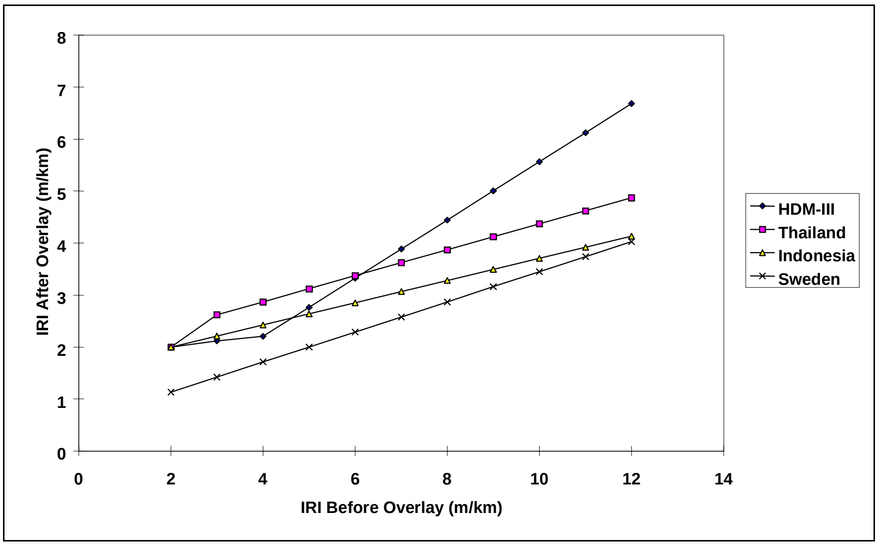

Given the effect on roughness reduction of the pre-overlay roughness and local standards of workmanship, the HDM-III models seem unnecessarily complex and it is considered that a simpler model form will prove easier to calibrate. The following model form is therefore used in HDM-4:

$$RI_a = a_0 + a_1 \max(RI_b - a_0, 0) \max(a_2 - H, 0) \qquad \text{. . . (B13.53)}$$

In this model, the constant a_0 represents the general standard of workmanship that is achieved in the country or region on either new construction or after thick overlays; this value can easily be obtained from roughness surveys of recently completed projects. It will range between 1, for areas with high standards of asphalt paving (such as Sweden), to 2.5 where paving standards are average to poor. The constant a_2 is the thickness, in mm, at or above which the value a_0 is achieved independently of existing roughness: this was found to be about 80 mm in Indonesia, which is in line with the HDM-III model for regular pavers. The coefficient a_1 represents the sensitivity of the roughness reduction to overlay thickness in the range from, say, 20 mm up to 80 mm; it can be varied for different types of pre-overlay surface. Field measurements of pre and post overlay roughness with different thicknesses are needed to calibrate this coefficient. An HDM-4 default value of 0.01, a little higher than Indonesia, is proposed. Figure B13-13 shows the effects of this model with the default parameters given in Table B13-7.

Table B13-7
Default model coefficients for effects of overlay on roughness

Coefficient	Value
a_0	2.0
a_1	0.01
a_2	80

Figure B13-13
Effects of overlay on roughness in HDM-4

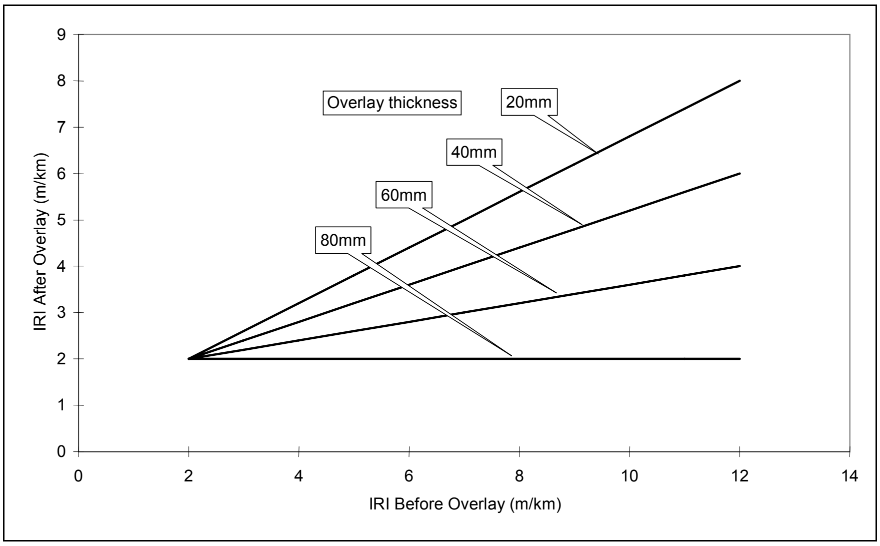

B13.3.5.3 Proposed Modifications to the Overlay Model

It has been suggested that the simplified linear relationship currently in HDM-4 does not adequately take into account the dual effects of overlay; that is, the short wavelength / high frequency roughness corrected by thin overlays, and the medium wavelength / medium frequency roughness corrected by thick overlays. Therefore two new models have been proposed that address these issues (Odoki, 2001).

Method 1

The overlay-roughness relationship for a specified overlay thickness, overlay execution technique and pavement type can be represented diagrammatically as shown in Figure B13-14.

Figure B13-14
Effects of overlay on roughness – Method 1

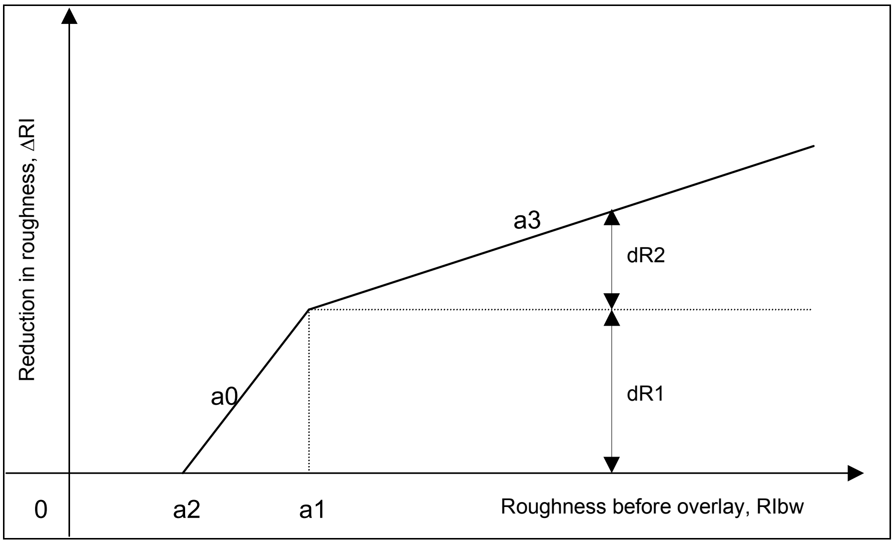

The reduction in roughness after overlay, ΔRI, is given by the sum of dR1 and dR2, and this is expressed as follows:

$$\Delta RI = \max\{0,\ a_0[\min(a_1,\ RI_{bw}) - a_2] + a_3\max[0,\ (RI_{bw} - a_1)]\} \quad ...\ (\text{B13.54})$$

and

$$RI_{bw} = \max(1.0,\ RI_{ap}) \quad ...\ (\text{B13.55})$$

$$RI_{aw} = RI_{bw} - \Delta RI \quad ...\ (\text{B13.56})$$

where

ΔRI = reduction in roughness after overlay, in m/km IRI
RI_{bw} = roughness before overlay, in m/km IRI
RI_{aw} = roughness after overlay, in m/km IRI
RI_{ap} = adjusted roughness after preparatory patching works, in m/km IRI

and the user-definable coefficients a_0 to a_3 are:

a_0 = slope of the first line, default = 0.9
a_1 = roughness before overlay at which the two lines meet, in m/km IRI
a_2 = minimum roughness after overlay, m/km IRI
a_3 = slope of the second line

The user-definable coefficients a_1 to a_3 can be computed as a function of the thickness of overlay as follows:

$$a_1 = \max\{4.0\ \ 2.1\exp[0.019(HSNEW_{aw})[\} \quad ...\ (\text{B13.57})$$

$$a_2 = 1 + 0.018\max[0,\ (100 - HSNEW_{aw})] \quad ...\ (\text{B13.58})$$

$$a_3 = \min\{a_0,\ \max[0,\ (0.01(HSNEW_{aw}) - 0.15)]\} \quad ...\ (\text{B13.59})$$

where

$HSNEW_{aw}$ = thickness of overlay, in mm

The reduction in roughness after overlay as computed by equation B13.54 is illustrated in Figure B13-15, for various overlay thickness.

Figure B13-15
Reduction in overlay – Method 1

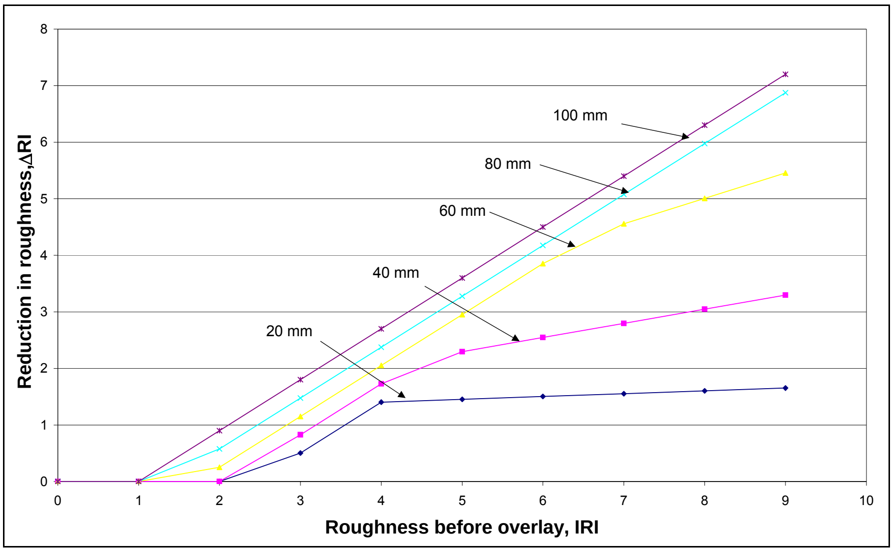

Method 2

The overlay-roughness relationship for a specified overlay thickness, overlay execution technique, and pavement type can be represented diagrammatically as shown in Figure B13-16.

Figure B13-16
Effects of overlay on roughness – Method 2

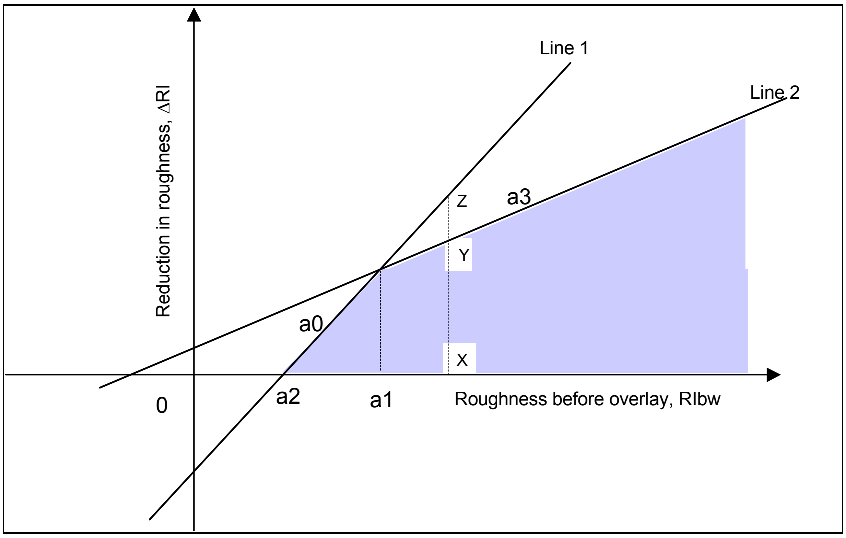

The reduction in roughness after overlay is given by the smaller of the ordinates from the x-axis to Line 1 (XZ) and Line 2 (XY). This is expressed as follows:

$$\Delta RI = \max\{0,\ \min[a_0(RI_{bw} - a_2),\ a_0(a_1 - a_2) + a_3 \max[0,\ (RI_{bw} - a_1)]]\} \quad \ldots (B13.60)$$

where

ΔRI = reduction in roughness after overlay, in m/km IRI

RI_{bw} = roughness before overlay, in m/km IRI

The user-definable coefficients a_0 to a_3 are shown in Figure B13-16 and defined as described in Method 1 above. The coefficients a_1 to a_3 can be computed as a function of overlay thickness using equations B13.57, B13.58, B13.59. Equation B13.60 computes the same reduction in roughness after overlays as does equation B13.54.

B13.3.5.4 Reconstruction

If a pavement is reconstructed the roughness after the operation will normally be independent of the previous roughness. There is inherent roughness in any pavement surfacing: even the highest quality asphalt will not normally have a roughness below 1 IRI. While in many countries the average roughness for new construction is in the range between 1 and 2 IRI, it may be as high as 2.5 IRI for asphalt mixes or more for surface treatments. Hand laid surfacings, such as those used in many parts of Asia, may have a much higher roughness immediately after construction. Surveys of local roads in Indonesia have shown an average roughness for new penetration macadam surfacings to be 8 IRI and in India the roughness of hand laid premix asphalt is typically around 6 IRI.

In HDM-4, roughness after reconstruction is therefore specified by the user as an absolute value that depends on the type of surfacing material and construction quality.

B13.3.6 Surface Texture

After any periodic operation, apart from preventive treatments, texture depth (TD) and skid resistance (SFC) are reset to user specified values.

B13.4 Improvement Works

Improvement works for bituminous pavements comprises the following:

- Widening
- Realignment

B13.4.1 Widening

The operations included under widening are lane addition and partial widening. The difference between the two is that partial widening does not increase the number of lanes. It is considered that both widening operations do not alter the road alignment. After widening, the required modelling parameters are reset as described below.

B13.4.1.1 Carriageway Width

The new carriageway width after widening is given as follows:

$$CW_{aw} = CW_{bw} + \Delta CW \qquad \text{. . . (B13.61)}$$

where

CW_{aw} = carriageway after works, in m
CW_{bw} = carriageway before works, in m
ΔCW = increase in carriageway width, in m

For partial widening, the increase in carriageway width (ΔCW) is specified directly by the user. For lane addition works, the increase in carriageway width is either user-specified, or if this is not specified the increase is given by:

$$\Delta CW = \frac{(ADDLN)(CW_{bw})}{NLANES_{bw}} \qquad \text{. . . (B13.62)}$$

where

ADDLN = additional number of lanes, user specified

$NLANES_{bw}$ = number of lanes before works

For lane addition works, the number of lanes after widening works ($NLANES_{aw}$) is equal to the number of lanes before works ($NLANES_{bw}$) plus the user-specified additional number of lanes (ADDLN).

B13.4.1.2 Thickness of Surfacing Layers

i) Existing carriageway is to be re-surfaced

If the existing carriageway is to be re-surfaced, the thickness of the new surfacing after widening works is obtained as follows:

$$HSNEW_{aw} = \frac{[(CW_{bw})(HRESF) + (\Delta CW)(HSNEW_{ww})]}{CW_{aw}} \qquad \text{. . . (B13.63)}$$

where

$HSNEW_{aw}$ = new surfacing thickness after works, in mm

$HSNEW_{ww}$ = surfacing thickness of the widened part of the carriageway, in mm

HRESF = user-specified thickness of the re-surfaced layer on the existing carriageway, in mm

The thickness of old surfacing after widening is given as:

$$HSOLD_{aw} = \frac{[(CW_{bw})(HS_{bw})]}{CW_{aw}} \qquad \text{. . . (B13.64)}$$

where

$HSOLD_{aw}$ = thickness of old surfacing after works, in mm

HS_{bw} = total surfacing thickness of the existing carriageway before works, in mm

ii) Existing carriageway is not to be re-surfaced

If the existing carriageway is not to be re-surfaced, the thickness of new surfacing after widening works is obtained as follows:

$$HSNEW_{aw} = \frac{[(CW_{bw})(HSNEW_{bw}) + (\Delta CW)(HSNEW_{ww})]}{CW_{aw}} \qquad \text{. . . (B13.65)}$$

where

$HSNEW_{aw}$ = new surfacing thickness after works, in mm

$HSNEW_{bw}$ = new surfacing thickness before works, in mm

$HSNEW_{ww}$ = surfacing thickness of the widened part of the carriageway, in mm

The thickness of old surfacing after widening is given by:

$$HSOLD_{aw} = \frac{(CW_{bw})(HSOLD_{bw})}{CW_{aw}} \qquad \text{. . . (B13.66)}$$

where

$HSOLD_{aw}$ = thickness of old surfacing after works, in mm

$HSOLD_{bw}$ = thickness of old surfacing before works, in mm

B13.4.1.3 Pavement Strength

The dry season adjusted structural number of the pavement is reset to the weighted average of that of the existing carriageway and that of the widened part of carriageway, as follows:

$$SNP_{daw} = (SNP_{dexcw})(SNP_{dww})\left[\frac{(CW_{bw} + \Delta CW)}{(CW_{bw}[SNP_{dww}]^5 + \Delta CW[SNP_{dexcw}]^5)}\right]^{0.2} \qquad \text{. . . (B13.67)}$$

where

SNP_{daw} = dry season adjusted structural number of the pavement after works

SNP_{dexcw} = dry season adjusted structural number of the pavement of the existing carriageway after works

SNP_{dww} = dry season adjusted structural number of the widened part of the carriageway

The Benkelman beam deflection after widening works is given by:

$$DEF_{aw} = DEF_{bw}\left[\frac{SNP_{aw}}{SNP_{bw}}\right]^{-1.6} \qquad \text{. . . (B13.68)}$$

where

DEF_{aw} = Benkelman beam deflection after works, in mm

DEF_{bw} = Benkelman beam deflection before works, in mm

SNP_{aw} = adjusted structural number of the pavement after works

SNP_{bw} = adjusted structural number of the pavement before works

B13.4.1.4 Surface Material

i) Existing carriageway is to be re-surfaced

If the existing carriageway is to be re-surfaced, the surface material after works is reset to that specified for the widening works. This is based on the assumption that the same surfacing material is used for the re-surfacing.

ii) Existing carriageway is not to be re-surfaced

If the existing carriageway is not to be re-surfaced, the surface material after works is reset as follows:

a) If CW_{bw} is greater than ΔCW, the surface material after widening works is reset to that of the existing carriageway.

b) Otherwise the surface material after widening works is reset to that of the widened part of the carriageway.

B13.4.1.5 Construction Quality

The construction defects indicator for bituminous surfacings (CDS) and the construction defects indicator for the roadbase (CDB) are reset to a weighted average as follows:

$$CDi_{aw} = \left[\frac{(CDi_{bw})(CW_{bw}) + (CDi_{ww} + \Delta CW)}{CW_{aw}}\right] \qquad \text{. . . (B13.69)}$$

where

CDi_{aw} = construction defects indicator i after works (i = CDS or CDB)

CDi_{bw} = construction defects indicator i before works (i = CDS or CDB)

CDi_{ww} = construction defects indicator i specified for the works (i = CDS or CDB)

B13.4.1.6 Pavement Surface Distress

i) Existing carriageway is to be re-surfaced

If the existing carriageway is to be re-surfaced, the amounts of all surface distresses after widening works are reset to zero.

ii) Existing carriageway is not to be re-surfaced

If the existing carriageway is not to be re-surfaced, the areas of edge-break, potholing, transverse thermal cracking, wide structural cracking, reflection cracking and ravelling after widening works are all reset to zero.

The area of all structural cracking and the total area of cracking are calculated as follows:

$$ACA_{aw} = \left[\frac{(ACA_{bw} - ACW_{bw})CW_{bw}}{CW_{aw}}\right] \qquad \text{. . . (B13.70)}$$

$$ACRA_{aw} = ACA_{aw} \qquad \text{. . . (B13.71)}$$

where

ACA_{aw} = area of all structural cracking after works, in per cent of carriageway area

ACA_{bw} = area of all structural cracking before works, in per cent of carriageway area

ACW_{bw} = area of wide structural cracking before works, in per cent of carriageway area

$ACRA_{aw}$ = total area of carriageway cracked after works, in per cent

B13.4.1.7 Rutting

The mean rut depth is reset to a user-specified value. If this is not specified, the mean rut depth is calculated as follows:

$$RDM_{aw} = \left[\frac{a_0(CW_{bw})(RDM_{bw})}{CW_{aw}}\right] \qquad \text{. . . (B13.72)}$$

where

RDM_{aw} = mean rut depth after works, in mm

RDM_{bw} = mean rut depth before works, in mm

a_0 = user-specified coefficient (0.15 if existing carriageway is to be re-surfaced; 1.0 otherwise)

B13.4.1.8 Roughness

After widening works, roughness is reset to a user-specified value. If this is not specified, the value of roughness is obtained as follows:

i) Existing carriageway is to be re-surfaced

If the existing carriageway is to be re-surfaced the following default values are used:

a) AM surface type: RI_{aw} = 2.0 (m/km IRI)

b) ST surface type: RI_{aw} = 2.8 (m/km IRI)

ii) Existing carriageway is not to be re-surfaced

If the existing carriageway is not to be re-surfaced, it is assumed that patching and crack sealing that may be performed on the existing carriageway would affect the roughness after widening works as follows:

$$RI_{aw} = \left[\frac{\left[(RI_n)(\Delta CW) + (CW_{bw})(RI_{ap}) \right]}{CW_{aw}} \right] \quad \text{. . . (B13.73)}$$

where

RI_{aw} = roughness after works, in m/km IRI

RI_n = user-specified roughness for new construction, in m/km IRI (default = 2.0 for AM and 2.8 for ST)

RI_{ap} = roughness after patching and crack sealing, in m/km IRI

B13.4.1.9 Texture Depth and Skid Resistance

After widening, texture depth and skid resistance are reset to user-specified values. If these are not specified, texture depth and skid resistance after works are estimated as follows:

i) Existing carriageway is to be re-surfaced

If the existing carriageway is to be re-surfaced the following values are used as defaults:

a) AM surface type:
SFC_{aw} = 0.5
TD_{aw} is reset to the default value of ITD given in Table B11-4

b) ST surface type:
SFC_{aw} = 0.6
TD_{aw} is reset to the default value of ITD given in Table B11-4

ii) Existing carriageway is not to be re-surfaced

If the existing carriageway is not to be re-surfaced, the values of texture depth and skid resistance after works are computed as a weighted average of the values before and after widening.

B13.4.1.10 Previous Cracking

i) Existing carriageway is to be re-surfaced

The amounts of previous cracking (PCRA, PCRW, and PNCT) are reset as follows:

if $CRAi_b \geq PCRi_{bw}$

$$PCRi_{aw} = \left[\frac{(CW_{bw})(CRAi_{bw})}{CW_{aw}} \right] \quad \text{. . . (B13.74)}$$

if $CRAi_b < PCRi_{bw}$

$$PCRi_{aw} = \left\{ \frac{CW_{bw} \left[w(CRAi_b) + (1-w)(PCRi_{bw}) \right]}{CW_{aw}} \right\} \quad \text{. . . (B13.75)}$$

The weighting factor, w, is obtained in the following manner:

a) If the re-surfacing is an overlay (i.e. surface type AM):
for roadbase types AB, AP, GB:

$$w = \max\left\{\left[\frac{HSNEW_{bw}}{HSOLD_{aw}}\right], 0.6\right\} \quad \text{. . . (B13.76)}$$

for roadbase type SB:

$$w = \max\left\{\left[\frac{HSNEW_{bw}}{(HSOLD_{aw} + HSBASE)}\right], 0.6\right\} \quad \text{. . . (B13.77)}$$

b) If the re-surfacing is a reseal (i.e. surface type ST)

$$w = \min(0.70 + 0.1(HSNEW_{aw}),\ 1) \quad \text{. . . (B13.78)}$$

where

$PCRi_{aw}$ = amount of previous cracking type i (i = all structural, wide structural, reflection or transverse thermal cracking) after works
$PCRi_{bw}$ = amount of previous cracking type i before works
$CRAi_b$ = amount of cracking type i at the end of the year
w = weighting for averaging the cracking in the old and new surfacing layers
HBASE = thickness of the roadbase layer in the original pavement, in mm (required for the roadbase type SB only)
all other variables as previously defined

ii) Existing carriageway is not to be re-surfaced

If the existing carriageway is not to be re-surfaced, the areas of previous cracking (PCRA, PCRW, and PNCT) are reset as follows:

$$PCRi_{aw} = \left[\frac{(CW_{bw})(PCRi_{bw})}{CW_{aw}}\right] \quad \text{. . . (B13.79)}$$

B13.4.1.11 Pavement Age

The pavement ages after widening are reset as follows:

i) Existing carriageway is to be re-surfaced

a) If the existing carriageway is to be re-surfaced by an overlay, AGE1, AGE2 and AGE3 are reset to zero. AGE4 is calculated from the expression:

$$AGE4_{aw} = \left[\frac{(CW_{bw})(AGE4_{bw})}{CW_{aw}}\right] \quad \text{. . . (B13.80)}$$

b) If the existing carriageway is to be resurfaced by resealing, AGE1 and AGE2 are reset to zero. AGE3 and AGE4 are given as:

$$AGEi_{aw} = \left[\frac{(CW_{bw})(AGEi_{bw})}{CW_{aw}}\right] \quad (\textit{for } i = 3 \textit{ or } 4) \quad \text{. . . (B13.81)}$$

ii) Existing carriageway is not to be re-surfaced

If the existing carriageway is not to be re-surfaced, the pavement ages are calculated as follows:

$$AGEi_{aw} = \left[\frac{(CW_{bw})(AGEi_{bw})}{CW_{aw}}\right] \quad \text{. . . (B13.82)}$$

where

$AGEi_{aw}$ = AGE type i (i = 1, 2. 3 or 4) after works, in years
$AGEi_{bw}$ = AGE type i (i = 1, 2. 3 or 4) before works, in years

Other required parameters, that are user-specified, include calibration factors, traffic flow patterns and speed factors.

B13.4.2 Realignment

In HDM-4, realignment refers to local geometric improvements of an existing road. This may also result in a reduction of the road length. However, it is assumed that the carriageway width remains unaltered.

After realignment, the required modelling parameters are reset as described below:

B13.4.2.1 Thickness of Surfacing Layer

i) Re-surfacing non-realigned segments

If the non-realigned parts of the existing carriageway are to be re-surfaced, the thickness of the new surfacing after realignment works is obtained as follows:

$$HSNEW_{aw} = (1 - Pconew)(HRESF) + (Pconew)(HSNEW_{rw}) \qquad \text{. . . (B13.83)}$$

where

$HSNEW_{aw}$ = new surfacing thickness after works, in mm
$HSNEW_{rw}$ = surfacing thickness of the new construction parts of the carriageway, in mm
HRESF = user-specified thickness of the re-surfacing layer on the existing carriageway, in mm
Pconew = proportion of new construction (0 < Pconew < 1)

The thickness of the old surfacing after realignment works is given by:

$$HSOLD_{aw} = (1 - Pconew)HS_{bw} \qquad \text{. . . (B13.84)}$$

where

$HSOLD_{aw}$ = thickness of old surfacing after works, in mm
HS_{bw} = total surfacing thickness of the existing carriageway before works, in mm

ii) No re-surfacing of non-realigned segments

If the non-realigned parts of the existing carriageway are not to be re-surfaced, the thickness of new surfacing after realignment works is obtained as follows:

$$HSNEW_{aw} = (1 - Pconew)(HSNEW_{bw}) + (Pconew)(HSNEW_{rw}) \qquad \text{. . . (B13.85)}$$

where

$HSNEW_{bw}$ = new surfacing thickness before works, in mm
and the other variables are as defined previously

The thickness of old surfacing after realignment works is given by:

$$HSOLD_{aw} = (1 - Pconew)HSOLD_{bw} \qquad \text{. . . (B13.86)}$$

where

$HSOLD_{bw}$ = thickness of old surfacing before works, in mm
and the other variables are as defined previously

B13.4.2.2 Pavement Strength

The dry season adjusted structural number of the pavement is reset to the weighted average of the structural number of the non-realigned parts of the existing carriageway and that of the newly constructed segments, as follows:

$$SNP_{daw} = (1 - Pconew)SNP_{dexcw} + (Pconew)SNP_{drw} \qquad \text{. . . (B13.87)}$$

where

SNP_{daw} = dry season adjusted structural number of the pavement after works

SNP_{dexcw} = dry season adjusted structural number of the existing carriageway before works

SNP_{drw} = dry season adjusted structural number of the pavement of the newly constructed parts of the carriageway

The Benkelman beam deflection after realignment works is given by:

$$DEF_{aw} = DEF_{bw}\left(\frac{SNP_{aw}}{SNP_{bw}}\right)^{-1.6} \qquad \text{. . . (B13.88)}$$

where

DEF_{aw} = Benkelman beam deflection after works, in mm

DEF_{bw} = Benkelman beam deflection before works, in mm

SNP_{aw} = adjusted structural number of the pavement after works

SNP_{bw} = adjusted structural number of the pavement before works

B13.4.2.3 Surface Material

i) Existing carriageway is to be re-surfaced

If the existing carriageway is to be re-surfaced, the surface material after works is reset to that specified for the realignment works. This is based on the assumption that the same surfacing material is used for the re-surfacing.

ii) Existing carriageway is not to be re-surfaced

If the existing carriageway is not to be re-surfaced, the surface material after works is reset as follows:

if Pconew < 0.5

the surface material after works is reset to that of the existing carriageway;

otherwise

the surface material after works is reset to that of the realigned parts of the carriageway.

B13.4.2.4 Construction Quality

The construction defects indicator for bituminous surfacing (CDS) and the construction defects indicator for the roadbase (CDB) are reset to a weighted average as follows:

$$CDi_{aw} = (1 - Pconew)CDi_{bw} + (Pconew)CDi_{rw} \qquad \text{. . . (B13.89)}$$

where

CDi_{aw} = construction defects indicator i (i = CDS or CDB) after works

CDi_{bw} = construction defects indicator i before works

CDi_{rw} = construction defects indicator i specified for the realignment works

B13.4.2.5 Pavement Surface Distresses

i) Re-surfacing non-realigned segments

If the non-realigned parts of the existing carriageway are to be re-surfaced the surface distresses (i.e. edge-break, potholing, cracking and ravelling) are all reset to zero.

ii) No re-surfacing of non-realigned segments

If the non-realigned parts of the existing carriageway are not to be re-surfaced, the area of edge-break, potholing, transverse thermal cracking, wide structural cracking, reflection cracking and ravelling are reset to zero. The area of all structural cracking after realignment works is reset as follows:

$$ACA_{aw} = \frac{[(1 - Pconew)(ACA_{bw} - ACW_{bw})]}{LF} \qquad \text{. . . (B13.90)}$$

where

ACA_{aw} = area of all structural cracking after works, in per cent of carriageway area
ACA_{bw} = area of all structural cracking before works, in per cent of carriageway area
ACW_{bw} = area of wide structural cracking before works, in per cent of carriageway area
LF = length adjustment factor

The length adjustment factor, LF, is defined as the ratio of the lengths of the carriageway after (L_{aw}) and before (L_{bw}) works as follows:

$$LF = L_{aw} / L_{bw} \qquad \text{. . . (B13.91)}$$

B13.4.2.6 Rutting

The mean rut depth is reset to a user-specified value. If this is not specified, the mean rut depth is calculated as follows:

$$RDM_{aw} = a_0(1 - Pconew)RDM_{bw} \qquad \text{. . . (B13.92)}$$

where

RDM_{aw} = mean rut depth after works, in mm
RDM_{bw} = mean rut depth before works, in mm
a_0 = user-definable coefficient (default = 0.15 if the non-realigned parts of the carriageway are to be re-surfaced, otherwise 1.0)

B13.4.2.7 Roughness

After realignment works, roughness is reset to a user-specified value. If this is not specified, the value of roughness is obtained as follows:

i) Re-surfacing non-realigned segments

If the non-realigned parts of the existing carriageway are to be re-surfaced the following values are used as defaults:

AM surface type: RI_{aw} = 2.0 (m/km IRI)
ST surface type: RI_{aw} = 2.8 (m/km IRI)

ii) No re-surfacing of non-realigned segments

If the non-realigned parts of the existing carriageway are not to be re-surfaced, roughness after realignment works is reset as follows:

$$RI_{aw} = (Pconew)(RI_n) + (1 - Pconew)RI_{ap} \qquad \text{. . . (B13.93)}$$

where

RI_{aw} = roughness after works, in m/km IRI
RI_n = user-specified roughness for realigned parts of carriageway, in m/km IRI
RI_{aw} = roughness after patching and crack sealing, in m/km IRI

B13.4.2.8 Texture Depth and Skid Resistance

After realignment, texture depth and skid resistance are reset to user-specified values. If these are not specified, texture depth and skid resistance after works are obtained in the following ways:

i) Re-surfacing non-realigned segments

If the non-realigned parts of the existing carriageway are to be re-surfaced:

a) AM surface type:

$SFC_{aw} = 0.5$

TD_{aw} is reset to the default value of ITD given in Table B11-4

b) ST surface type:

$SFC_{aw} = 0.6$

TD_{aw} is reset to the default value of ITD given in Table B11-4

ii) No re-surfacing of non-realigned segments

If the non-realigned parts of the existing carriageway are not to be re-surfaced, then the values of texture depth and skid resistance after works are computed as a weighted average of the values before and after realignment.

B13.4.2.9 Previous Cracking

i) Re-surfacing non-realigned segments

If the non-realigned parts of the existing carriageway are to be re-surfaced, the amounts of previous cracking (PCRA, PCRW, and PNCT) are reset as follows:

if $CRAi_b \geq PCRi_{bw}$

$$PCRi_{aw} = \left[\frac{(1-Pconew)(CRAi_{bw})}{LF}\right] \qquad \text{. . . (B13.94)}$$

if $CRAi_b < PCRi_{bw}$

$$PCRi_{aw} = \left\{\frac{(1-Pconew)\left[w(CRAi_b) + (1-w)(PCRi_{bw})\right]}{LF}\right\} \qquad \text{. . . (B13.95)}$$

The weighting factor, w, is obtained in the following manner:

a) If the re-surfacing is an overlay (i.e. surface type AM):

for roadbase types AB, AP, GB:

$$w = \max\left\{\left[\frac{HSNEW_{bw}}{HSOLD_{aw}}\right], 0.6\right\} \qquad \text{. . . (B13.96)}$$

for roadbase type SB:

$$w = \max\left\{\left[\frac{HSNEW_{bw}}{(HSOLD_{aw} + HSBASE)}\right],\ 0.6\right\} \quad \text{. . . (B13.97)}$$

b) If the re-surfacing is a reseal (i.e. surface type ST)

$$w = \min\left(0.70 + 0.1(HSNEW_{aw}),\ 1\right) \quad \text{. . . (B13.98)}$$

where

$PCRi_{aw}$ = amount of previous cracking type i (i = all structural, wide structural, reflection or transverse thermal cracking) after works

$PCRi_{bw}$ = amount of previous cracking type i before works

$CRAi_b$ = amount of cracking type i at the end of the year

LF = length adjustment factor (see Equation B13.91)

w = weighting used for averaging the cracking in the old and new surfacing layers

HBASE = thickness of the roadbase layer in the original pavement, in mm (required for the roadbase type SB only)

all other variables as previously defined

ii) No re-surfacing of non-realigned segments

If the existing carriageway is not to be re-surfaced, the areas of previous cracking (PCRA, PCRW, and PNCT) are reset as follows:

$$PCRi_{aw} = \left[\frac{(1 - Pconew)(PCRi_{bw})}{LF}\right] \quad \text{. . . (B13.99)}$$

B13.4.2.10 Pavement Age

The pavement ages after realignment are reset as follows:

i) Re-surfacing non-realigned segments

a) If the non-realigned parts of the existing carriageway are to be re-surfaced by an overlay, AGE1, AGE2 and AGE3 are reset to zero. AGE4 is calculated from the expression:

$$AGE4_{aw} = (1 - Pconew)\ AGE4_{bw} \quad \text{. . . (B13.100)}$$

b) If the non-realigned parts of the existing carriageway are to be resurfaced by resealing, AGE1 and AGE2 are reset to zero. AGE3 and AGE4 are given as:

$$AGEi_{aw} = (1 - Pconew)\ AGE4_{bw} \quad \text{(for i = 3 or 4)} \quad \text{. . . (B13.101)}$$

ii) No re-surfacing of non-realigned segments

If the non-realigned parts of the existing carriageway are not to be re-surfaced, the pavement ages are calculated as follows:

$$AGEi_{aw} = (1 - Pconew)AGEi_{bw} \quad \text{. . . (B13.102)}$$

where

$AGEi_{aw}$ = AGE type i (i = 1, 2. 3 or 4) after works, in years

$AGEi_{bw}$ = AGE type i (i = 1, 2. 3 or 4) before works, in years

Other required parameters, that are user-specified, include calibration factors, traffic flow patterns and speed factors.

B13.5 Construction

Construction works comprises the following:

- Upgrading
- Construction of a new section or link

B13.5.1 Upgrading

A bituminous pavement road may be upgraded to a rigid concrete pavement road or to a bituminous pavement of a higher-grade.

After upgrading, the pavement type is reset to the new type specified by the user. Depending on the new pavement type, the required modelling parameters are obtained in the following ways:

- Pavement structure, strength, layer material properties and construction quality are set to user-specified values
- Pavement condition after works is reset to as new
- Pavement history data is reset to reflect new construction
- The new carriageway width after upgrading is calculated using equation B13.61. The increase in carriageway width is either specified directly by the user, or calculated using equation B13.62. The number of lanes after upgrading works, $NLANES_{aw}$, is equal to the number of lanes before works, $NLANES_{bw}$, plus the user-specified additional number of lanes, ADDLN.

Other required parameters that are user-specified include calibration factors, traffic flow patterns and speed factors.

B13.5.2 New Section

The required components of the new section to be constructed are defined using the following information:

- Road section data (i.e. all the data items that are required to define a road section in HDM-4).
- Traffic data. This includes i) diverted traffic (i.e. traffic that is diverted from the nearby routes and other transport modes); ii) generated traffic (i.e. additional traffic that occurs in response to the new investment).

Other information required includes construction costs and duration, exogenous benefits and costs, and maintenance and improvement standards.

PART C. CONCRETE PAVEMENTS

The prediction models for the deterioration and works effects of concrete pavements included in the first release of the HDM-4 software were based on the work of the Latin American Study Team (LAST) and reported in LAST (1996). This study drew largely on research in the USA which used data from the LTPP databank and the models are mostly taken from a report to FHWA by ERES Consultants (ERES, 1995). With the exception of the model for transverse cracking of JP pavements, the models are wholly empirical and all were reported in imperial units.

Subsequently, ERES Consultants produced a final report on their study (ERES, 1999) which gave different models for pavement deterioration. The new models are mostly of the mechanistic empirical form and were reported in metric units. The models provided by both LAST (1996) and ERES (1999) are absolute models rather than of the incremental form used in HDM-4 for bituminous pavements.

In producing this document, the ERES (1999) models were examined and an attempt was made to compare them with the LAST models for inclusion in this document. However, numerous errors or anomalies were identified in the ERES (1999) models, most of which to date have not been corrected or clarified. Therefore neither the models nor the comparison have been included in the current version of this document.

C1. STRUCTURAL CHARACTERISATION

Concrete pavements differ from bituminous pavements in two major respects:

- In a concrete pavement the top pavement layer (the concrete slab) provides most of the structural strength of the pavement as well as, in most cases, the wearing surface.
- Apart from CRCP, transverse joints are constructed to allow for contraction and expansion of the slabs.

Consequently, the structural characterisation of concrete pavements is entirely different to bituminous pavements.

C1.1 Classification

A classification of concrete pavements according to the type of concrete slab and transverse joints is presented below.

C1.1.1 Jointed Plain Concrete Pavements (JPCP) without Dowels

This pavement is formed of short slabs without reinforcement steel as shown in Figure C1-1. Spacing between transverse joints (slab length) must be such that the induced stresses, either due to temperature changes and/or moisture content, do not produce intermediate cracking between the joints. The spacing between joints must be such as to minimise movement and maximise load transfer between slabs at the joints. Typical values of slab length vary between 3 and 6 m. In this type of pavement, load transfer between slabs is accomplished by the mechanical interlock of the aggregates.

Figure C1-1
Jointed plain concrete pavement without dowels

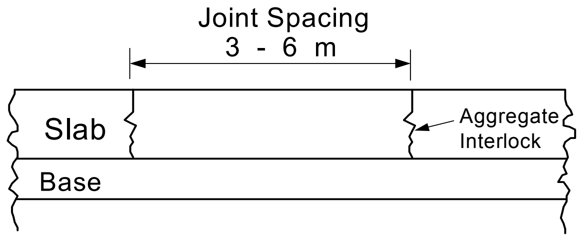

C1.1.2 Jointed Plain Concrete Pavements (JPCP) with Dowels

This type of pavement is similar to JPCP without dowels, with the only difference being that the transverse joints have dowel bars to assist load transfer between slabs. This is shown in Figure C1-2.

Figure C1-2
Jointed plain concrete pavement with dowels

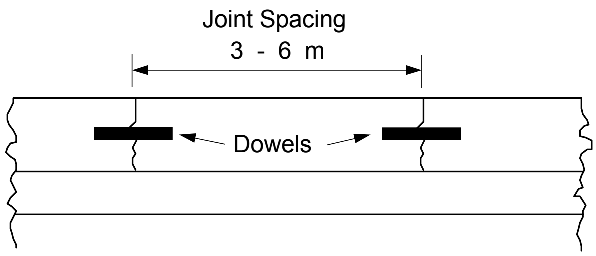

C1.1.3 Jointed Reinforced Concrete Pavements (JRCP)

These pavements have longitudinal reinforcement steel which permits longer slab lengths, typically between 10 and 20 m, as shown in Figure C1-3. Reinforcement steel controls transverse cracking that can occur due to movements of the foundation and/or stresses produced by temperature or humidity changes. Load transfer in transverse joints in this type of pavement normally uses dowels.

Figure C1-3
Jointed reinforced concrete pavement

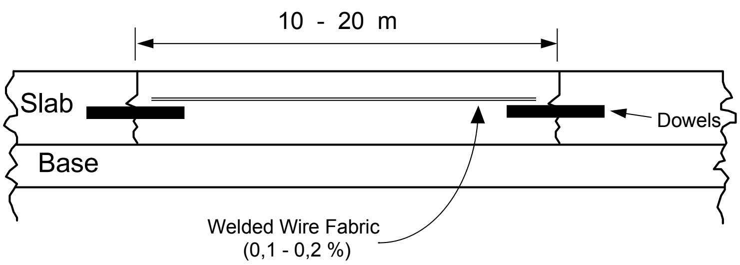

C1.1.4 Continuously Reinforced Concrete Pavements (CRCP)

This type of pavement has longitudinal reinforcement along the whole length and has no transverse joints, as shown in Figure C1-4. The objective of the longitudinal steel is to control the cracks that are produced in the pavement due to shrinkage and thermal effects.

Figure C1-4
Continuously reinforced concrete pavement

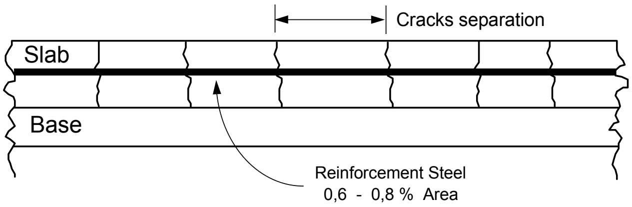

C1.2 Concrete Pavements Included in HDM-4

All four types of concrete pavements described above are included in the HDM-4 modelling. In addition to the type of slab, alternative types of base and subgrade can also be specified. These are given in Table C1-1.

Table C1-1
Base and subgrade types in HDM-4

Base	Subgrade
Asphalt treated	Granular
Cement treated	Fine
Granular	
Fine	

C1.3 Properties of Concrete Slabs

C1.3.1 Modulus of Rupture

A means of characterising the strength of concrete is through the Modulus of Rupture (MR) or Flexural Resistance. MR is determined by testing beams to destruction at 28 days, applying loads at the third points as illustrated in Figure C1-5 (ASTM C78 or AASHTO T97).

Figure C1-5
Test for Modulus of Rupture

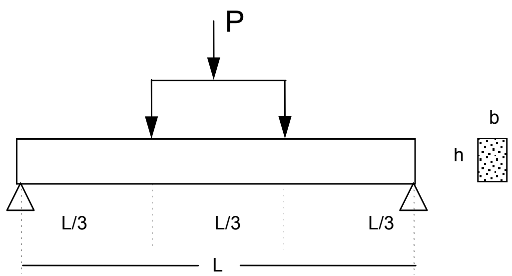

The Modulus of Rupture is derived as follows:

$$MR = \frac{(P_{ult})(L)}{b(h^2)} \qquad \ldots (C1.1)$$

where

MR = modulus of rupture, in MPa
P_{ult} = load at failure, in N
h = height of the beam, in mm

b = width of the beam, in mm
L = length of the beam between supports, in mm

The modulus of rupture can be estimated from the compressive strength (AASHTO T22, T140 or ASTM C39) as:

$$MR = 0.67\,(f'_c)^{0.5} \qquad \text{. . . (C1.2)}$$

where

f'_c = compressive strength, in MPa

As an alternative to laboratory results, the Modulus of Rupture can be estimated from the Modulus of Elasticity (E_c), obtained from FWD (Falling Weight Deflectometer) back analysis. One of the empirical equations for this estimate was proposed by Foxworthy (1985):

$$MR = 43.5\left(\frac{E_c}{10^6}\right) + 3.369 \qquad \text{. . . (C1.3)}$$

where

MR = modulus of rupture, in MPa
E_c = modulus of elasticity, in MPa

The development of performance models considered the modulus of rupture in the long term rather than at 28 days. An 11% increase in MR from the 28 day value was assumed for the long term.

C1.3.2 Elastic Modulus

The Elastic Modulus of concrete (E_c) can be obtained by analysis of deflection measurements or from laboratory testing (ASTM C469). Also it can be estimated from compressive strength by:

$$E_c = 4744\,(f'_c)^{0.5} \qquad \text{. . . (C1.4)}$$

The typical value of Elasticity Modulus of the concrete used in the development of the models was 35,000 MPa.

C1.3.3 Poisson's Ratio

Poisson's ratio (μ) is defined as the ratio between the lateral strain (ε_1) and the axial strain (ε_a) caused by an axial load, as indicated in Figure C1-6.

Figure C1-6
Poisson's ratio

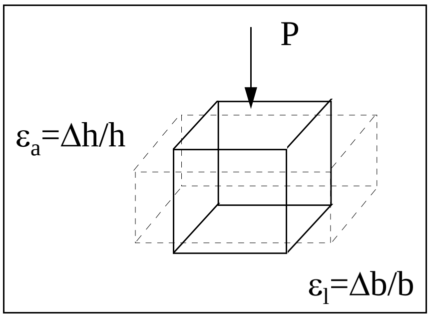

For cemented materials, Poisson's ratio can range between 0.10 and 0.25 but for PCC, a value of 0.15 is normally adopted.

C1.3.4 Coefficient of Thermal Expansion

This coefficient is used to determine the stress experienced by a slab when it is submitted to a difference of mean temperature. The stress in the edge of the slab is given by:

$$\sigma Temp = 0.5\ c\ (E_c)\ \alpha\ Tdiff \qquad \text{. . . (C1.5)}$$

where

$\sigma Temp$ = stress due to temperature difference, in MPa
E_c = modulus of elasticity, in MPa
c = warping coefficient
Tdiff = temperature difference, in ^oC
α = coefficient of thermal expansion, in $^oC^{-1}$

Table C1-2 shows values of α given in AASHTO (1993) converted to Celsius.

Table C1-2
Recommended values for coefficient of thermal expansion

Type of Aggregate	α ($10^{-6}/^oC$)
quartz	11.86
sandstone	11.70
gravel	10.79
granite	9.53
basalt	8.62
limestone	6.84

C1.3.5 Temperature Difference

A difference of temperature between the upper part (T_{sup}) and lower (T_{inf}) of the slab will affect the concavity or convexity of the slab. This will have the effect of increasing or reducing the stresses that are sustained when it is submitted to traffic loads. It is said to have a positive gradient when this difference by thickness unit is positive, and a negative gradient otherwise, as illustrated in Figure C1-7.

Figure C1-7
Thermal gradient in a concrete slab

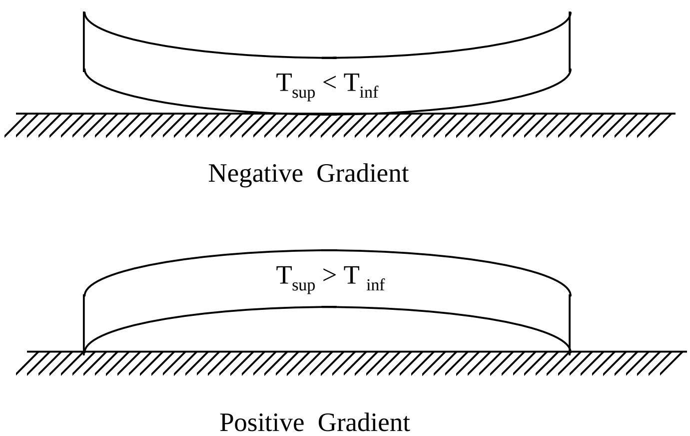

The model for estimation of transverse cracking in plain concrete slabs requires a histogram of temperature gradients representing different time periods. An example of such a histogram is shown in Table C1-3.

Table C1-3
Histogram of temperature gradient

ΔT (ºF)	Frequency	ΔT (ºF)	Frequency
-20	0.024	8	0.029
-18	0.040	10	0.032
-16	0.054	12	0.022
-14	0.057	14	0.029
-12	0.079	16	0.042
-10	0.073	18	0.022
-8	0.076	20	0.036
-6	0.064	22	0.026
-4	0.069	24	0.033
-2	0.042	26	0.032
0	0.038	28	0.012
2	0.026	30	0.000
4	0.024	32	0.000
6	0.019	34	0.000

C1.3.6 Hydraulic Shrinkage Coefficient

Hydraulic shrinkage in concrete is due to loss of water during the curing process and is affected by cement content, chemical additives, climate and the method of curing. The hydraulic shrinkage coefficient (e) and strength are inter-related as a higher water/cement ratio will reduce strength and increase shrinkage. A relationship can be derived from AASHTO (1993):

$$e = 0.00128 - 0.00024(ITS) \qquad \text{. . . (C1.6)}$$

where

e = hydraulic shrinkage coefficient (dimensionless)
ITS = indirect tensile strength, in MPa

The slabs of a concrete pavement are subjected to daily changes of temperature and unrestricted movement would not result in induced stresses. However, under site conditions, there exists a resistance between the slab and the base. The hydraulic shrinkage coefficient is used in the estimation of the opening of the joints caused by the mean temperature variation that is experienced by the slab.

$$OPENING = 1000(CON)(L)[\alpha(TRANGE / 2) + e] \qquad \text{. . . (C1.7)}$$

where

OPENING = transverse joint opening, in mm
CON = base type coefficient
= 0.80 for non stabilised base
= 0.65 for stabilised base
L = mean joint spacing, in m
α = coefficient of thermal expansion, in $^{o}C^{-1}$
TRANGE = temperature range, in ºC
e = hydraulic shrinkage coefficient

C1.4 Properties of Other Pavement Materials

C1.4.1 Bases

The type of base can influence the behaviour of a concrete slab, mainly as a result of the support and the drainage conditions. A more rigid base will generally provide better support to the slab and reduce the occurrence of faulting in the transverse joints. However, a more rigid base can also increase the warping effect caused by temperature or humidity and that, as a consequence, will increase the transverse crack occurrence. Table C1-4 indicates typical values of elastic modulus for different types of base.

Table C1-4
Elastic modulus for different base types

Base Type	Elastic Modulus (MPa)
Granular	150 – 200
Asphalt treated	4,000
Cement treated	3,000
Lean concrete	7,000

C1.4.2 Steel

Steel is used in concrete pavements as reinforcement in the concrete slab and as dowel bars at transverse joints. The amount of reinforcing steel is expressed as percentage of the cross sectional area (PSTEEL). Most of the sections used in the formulation of the cracking model for JRCP pavements had a percentage of reinforcement steel within range 0.04 to 0.29%. Where this information is not available, a default value of 0.1% is recommended.

The elastic modulus of dowel bars (E_s) is used to estimate the amount of load transfer. A characteristic value is 2.0×10^5 MPa. The diameter of the dowel bars (DOWEL) is used in several models.

C1.4.3 Modulus of Subgrade Reaction

The modulus of subgrade reaction is a measure of the stiffness of the subgrade and its resistance to deformation. It can be determined by the plate bearing test and is given by:

$$k = \frac{P}{d} \qquad \text{. . . (C1.8)}$$

where

k = modulus of subgrade reaction, in MPa/mm
P = loading pressure, in MPa
d = deflection, in mm

k can also be obtained by back analysis of FWD measurements.

C1.5 Load Transfer in Transverse Joints

C1.5.1 Load Transfer Efficiency

The load transfer in the transverse boards is the mechanism through which the traffic loads are transferred from one slab to the next. The effective transfer of the traffic loads between slabs will reduce the tensions and deformations of the slab at the joints. This in turn reduces deterioration such as pumping, loss of support and corner breaks.

The efficiency of load transfer (LTE) is determined by the ratio between the deflection of the pavement on the unloaded side and loaded side:

$$LTE = \frac{D_{unloaded}}{D_{loaded}} \qquad \text{. . . (C1.9)}$$

where

- LTE = efficiency of load transfer
- $D_{unloaded}$ = deflection on the unloaded slab, in mm
- D_{loaded} = deflection on the loaded slab, in mm

The load transfer in the joints can be evaluated with equipment such as the FWD (Falling Weight Deflectometer), registering the deformations to both sides of the joint. Typically, load transfer efficiency is 0.45.

Theoretically, if a dowel bar is one hundred per cent efficient, it will be capable of assigning half of the applied load on a slab to the other. However, the lack of bond that is developed, during the life of the pavement, in the zone where the transfer bar is inlaid in the slab, tends to reduce the load transfer. This reduction is due mainly to the magnitude and to the repeated action of the traffic loads. The reduction in the load transfer can be assumed to be around 5 – 10%.

C1.5.2 Modulus of Dowel Support

The modulus of bar support (K_d) is used to calculate the relative inflexibility (β) of the system between the load transfer bars and the concrete slab. This is given by:

$$\beta = \left(\frac{16\ K_d}{\pi\ (E_S)(DOWEL)^3} \right)^{0.25} \qquad \text{. . . (C1.10)}$$

where

- β = relative inflexibility of the bar- concrete system, in mm^{-1}
- K_d = modulus of bar support, in MPa/mm
- DOWEL = dowel bar diameter, in mm
- E_S = elastic modulus of bars, in MPa

The support modulus of the bars (K_d) varies between 80 and 400. Due to the fact that β varies with the fourth root of the modulus, large variations in this parameter do significantly affect the estimation of β. Therefore a default value of 400 is recommended.

C1.5.3 Dowel/Concrete Bearing Stress

To calculate the concrete-dowel maximum bearing stress (BSTRESS), the analysis of Heinrichs, et al, (1989) was modified:

$$BSTRESS = f_d(P)(LTE)(K_d)\frac{(2+\beta\ OPENING)}{4\ \beta^3\ (E_s)(I)}10^3 \qquad \text{. . . (C1.11)}$$

where

$$f_d = 610/(\ell + 305) \qquad \text{. . . (C1.12)}$$

$$\ell = \left[\frac{E_c \, (H_p)^3}{12\,(k)\left(1-\mu^2\right)} \right]^{0.25} \qquad \text{. . . (C1.13)}$$

and

BSTRESS	=	maximum dowel/concrete bearing stress, in MPa
f_d	=	distribution factor, dimensionless
ℓ	=	radius of relative stiffness slab-subgrade, in mm
H_p	=	slab thickness, in mm
K_d	=	modulus of bar support, in MPa/mm
E_c	=	elastic modulus of concrete, in MPa
μ	=	Poisson's ratio for concrete
β	=	modulus of dowel support, in mm^{-1}
k	=	modulus of subgrade reaction, in MPa/mm
P	=	applied wheel load (40 kN)
LTE	=	efficiency of load transfer across joints (0.45)
I	=	moment of inertia of the dowel bar, in mm^4
	=	Π $(DOWEL)^4$ / 64

C1.6 Lane Widening and Shoulder Effects

Lane widening is the increase in the width of the slab greater than that necessary to serve traffic, as shown in Figure C1-8. Its existence will permit stress reduction at the edge of the slab, since the traffic loads will be applied further from the edge. Other effects are the reduction of possible water infiltration between the shoulder slab border and a better safety sensation perceived by the road user. Nevertheless, there exists the possibility of the formation of longitudinal cracks from the transverse joint if the widening is not an integral part of the original slab construction.

Figure C1-8
Lane Widening

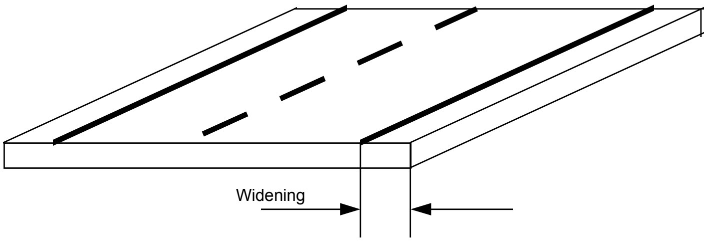

In the prediction of faulting, the existence or not of lane widening is considered through the use of the variable WIDENED. This variable has a value 0 or 1 depending on the presence, or not, of lane widening. In order to consider the effect of concrete shoulders in the faulting model, the same variable is used but divided by two as an indicator of the presence of concrete shoulders.

An adequate maintenance and design of the shoulders is important in concrete pavements. Inadequate maintenance can cause excessive infiltration of the surface water in the edge of the pavement bringing, as consequence, loss of support in the subgrade, and in some instances "pumping". The use of paved or stabilised shoulders is an economic question. Stabilised or paved shoulders are always recommended in terms of the stability of the pavement and also by a way of providing an area for the parking of vehicles in the event of an emergency.

Concrete shoulders contribute to a decrease in deformation and stress due to the effect of traffic loads. A concrete shoulder can be of lesser thickness than the pavement slab provided it is tied to the slab. Generally, shoulders have a width of 3 m.

The effect of concrete shoulders on slab cracking uses the term:

$$LTE_{stress} = \frac{Stress_{unloaded}}{Stress_{loaded}} 100\% \qquad \text{. . . (C1.14)}$$

If concrete shoulders are provided as part of the original construction, LTE_{stress} is given a value of 20%. If concrete shoulders are constructed later it becomes 10%.

C2. TRANSVERSE JOINT FAULTING

C2.1 Definition of Faulting

Faulting represents the elevation difference between the edges of a transverse joint or crack, as illustrated in Figure C2-1.

Figure C2-1
Faulting of transverse joints

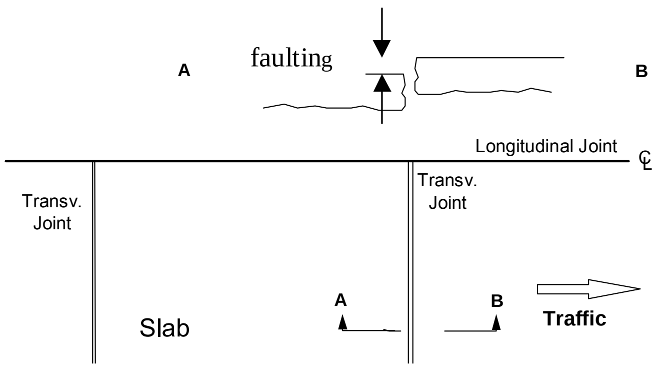

Faulting is caused by the loss of fine material under the edge of a leading slab with an increase in fine material under the adjoining trailing slab. This flow of fines is called pumping and occurs due to the presence of high levels of free moisture under the slab when it is subjected to traffic loading. Thermal and moisture-induced slab curling, as well as poor load transfer, increase the likelihood that pumping will occur.

C2.2 LAST (1996) Models for Joint Faulting

LAST gave independent empirical models for faulting of joints with and without dowels. These models, taken from ERES (1995), apply to both JPCP and JRCP pavement types.

C2.2.1 Faulting in Transverse Joints without Dowels

Load transfer in concrete pavements without load transfer dowels is achieved only by the mechanical interlock between the irregular faces of the slabs. The degree of load transfer by mechanical interlock is affected by the size of the joint opening; greater opening gives less interlock and hence greater faulting. Other factors are the number of loading repetitions, slab thickness, climatic variables and the drainage properties of the base.

The model is as follows:

$$FAULT = 25.4(NE4)^{0.25} \max\{0, 0.2347 - 0.1516(C_d) - 2.88\times10^{-7} [(H_p)^2/(L)^{0.25}] - 0.0115(BASE) + 6.45\times10^{-8} (FI)^{1.5}(MMP)^{0.25} - 0.002478(DAYS90)^{0.5} - 0.0415(WIDENED)\} \quad \ldots (C2.1)$$

where

FAULT	=	average transverse joint faulting, in mm
NE4	=	cumluative axle loading, in million ESAL
C_d	=	AASHTO drainage coefficient
H_p	=	slab thickness, in mm
L	=	mean transverse joint spacing, in m
BASE	=	base type (0 if not stabilised; 1 if stabilised)

FI = Freezing Index (see equation A2.10)
MMP = mean monthly precipitation, in mm/month
DAYS90 = number of days with temperature > 32ºC
WIDENED = widened lane (0 if not widened; 1 if widened)

The distribution and characteristics of the pavement sections used in the development of this model are presented in Table C2-1. The figures in Table C2-1 indicate that the sections with stabilised bases are quite well distributed in all climatic regions except for dry frost zones. The sections without stabilised bases are located mainly in wet regions with frost.

Table C2-1
Distribution of pavement sections used in the faulting without dowels model

Climatic Region	Non-Stabilised Base Joint Spacing (m)		Stabilised Base Joint Spacing (m)	
	$\leq$ 6	> 6	$\leq$ 6	> 6
Wet - with frost	17	7	19	4
Wet - without frost	0	4	22	11
Dry - with frost	2	2	0	0
Dry - without frost	6	0	37	0

Table C2-2 shows the range of variables used in deriving the model.

Table C2-2
Range of variables used in the faulting without dowels model

Variable	Range
NE4	0 – 15 million
Hp	200 - 300 mm
L	4.5 - 6.0 m
BASE	stabilised & non-stabilised
FI	0 – 1000
MMP	20 - 125 mm/month
DAYS90	0 - 90 days
Cd	0.8 - 1.2
WIDENED	with & without widening

The sensitivity of this model to the independent variables is shown in Table C2-3.

Table C2-3
Sensitivity of the variables in the faulting without dowels model

Variable	Sensitivity
NE4	High
Cd	High
Hp	Medium
L	Low
BASE	Medium
FI	Low
MMP	Low
DAYS90	High
WIDENED	High

Figure C2-2 shows the sensitivity of the model to the drainage coefficient (C_d), while Figure C2-3 shows sensitivity to the climatic parameter DAYS90.

Figure C2-2
Sensitivity of the faulting without dowels model to drainage coefficient

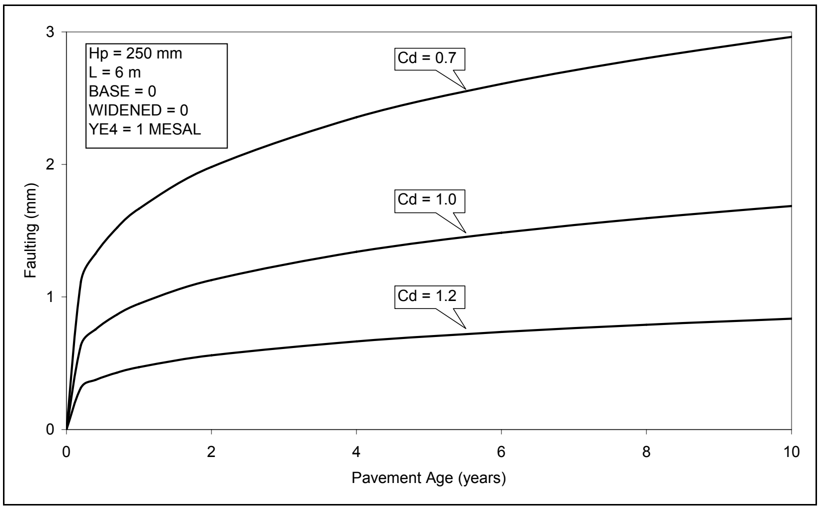

Figure C2-3
Sensitivity of the faulting without dowels model to DAYS90

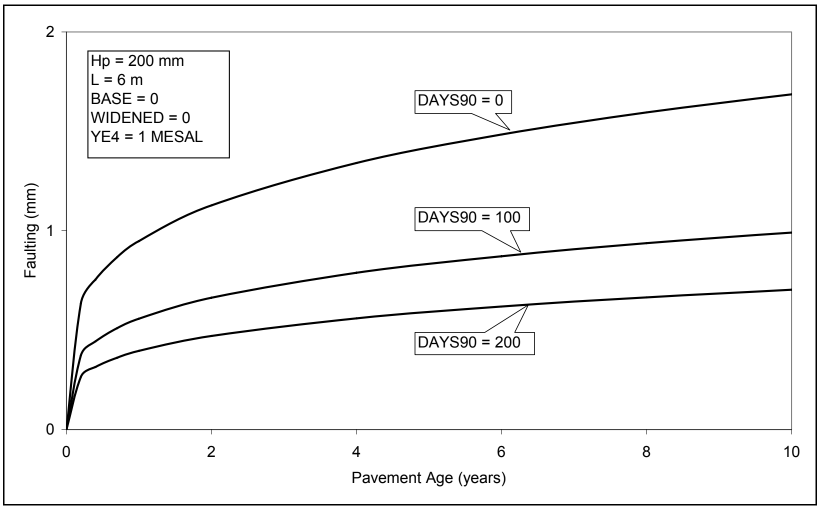

C2.2.2 Faulting in Transverse Joints with Dowels

Load transfer dowels can reduce the extent of transverse joint faulting. The model uses the parameter BSTRESS (described in Section C1.5.3) to represent the effect of the dowels.

$$\begin{aligned} FAULT = 25.4(NE4)^{0.25} \max\{0,\ & 0.0628(1 - C_d) + 7.721\text{x}10^{-5}(BSTRESS)^2 \\ & + 4.431\text{x}10^{-5}(L^2) + 5.13\text{x}10^{-10}(FI)^2(MMP)^{0.5} - 0.009503(BASE) \\ & - 0.01917(WIDENED) + 0.0009217(AGE3)\} \end{aligned} \quad \text{. . . (C2.2)}$$

where

FAULT = average transverse joint faulting, in mm
BSTRESS = maximum dowel/concrete bearing stress, in MPa
AGE3 = age since pavement construction, in years
and the other variables are as defined for the faulting without dowels model

The distribution by climatic region of the pavement sections used in the model development is shown in Table C2-4. The figures in Table C2-4 indicate that most of the pavement sections were located in wet climatic region with frost. Also it is observed that most of the pavement sections had non-stablised bases.

Table C2-4
Distribution of pavement sections used in the faulting with dowels model

Climatic Region	JPCP		JRCP	
	Non-Stabilised	Stabilised	Non-Stabilised	Stabilised
Wet – with frost	21	2	48	26
Wet – without frost	4	7	2	0
Dry – with frost	6	0	14	14
Dry – without frost	0	2	0	0

Table C2-5 shows the range of variables used in deriving the model.

Table C2-5
Range of variables used in the faulting with dowels model

Variable	Range
NE4	0 - 15 million
AGE3	0 - 25 years
BSTRESS	10 – 20 MPa
DOWEL	25 - 38 mm
L	3.0 – 21 m
FI	0 – 1500
MMP	40 – 106 mm/month
BASE	stabilised & non-stabilised
WIDENED	with & without widening
Cd	0.7 – 1.1
Hp	200 – 300 mm

Table C2-6 shows the sensitivity of this model to the independent variables.

Table C2-6
Sensitivity of the variables in the faulting with dowels model

Variable	Sensitivity
NE4	High
Cd	High (1)
BSTRESS	High (2)
L	Low
BASE	High
FI	Low
MMP	Low
WIDENED	High
AGE3	Low

(1) if Cd > 1
(2) depends on dowel diameter

The parameter BSTRESS is highly sensitive to dowel diameter. Using typical values for other parameters in the model for BSTRESS, its value changes from 9 MPa with a bar diameter of 38 mm to 19 MPa with a bar diameter of 25 mm. Figure C2-4 shows the effect of dowel diameter and drainage on the progression of faulting using this model.

Figure C2-4
Sensitivity of the faulting with dowels model to drainage factor and dowel diameter

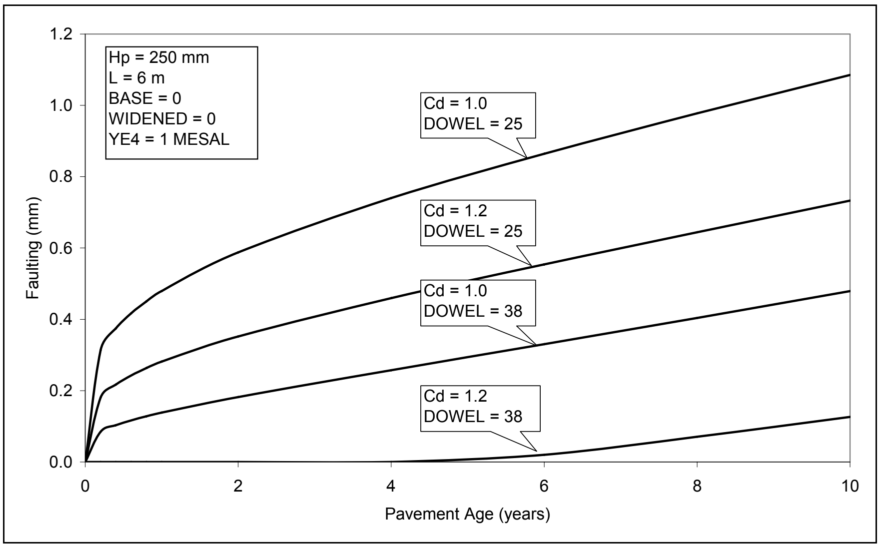

C3. TRANSVERSE JOINT SPALLING

C3.1 Definition of Spalling

Spalling of transverse joints is defined as breaks or cracks up to a distance of 600 mm from the joint as illustrated in Figure C3-1. The SHRP handbook (SHRP, 1993) defines three levels of severity:

- Low – spalling less than 75 mm from joint centre with or without material loss
- Medium – spalling between 75 mm and 150 mm from joint centre with loss of material
- High – spalling more than 150 mm from joint centre with loss of material

Figure C3-1
Spalling of transverse joints

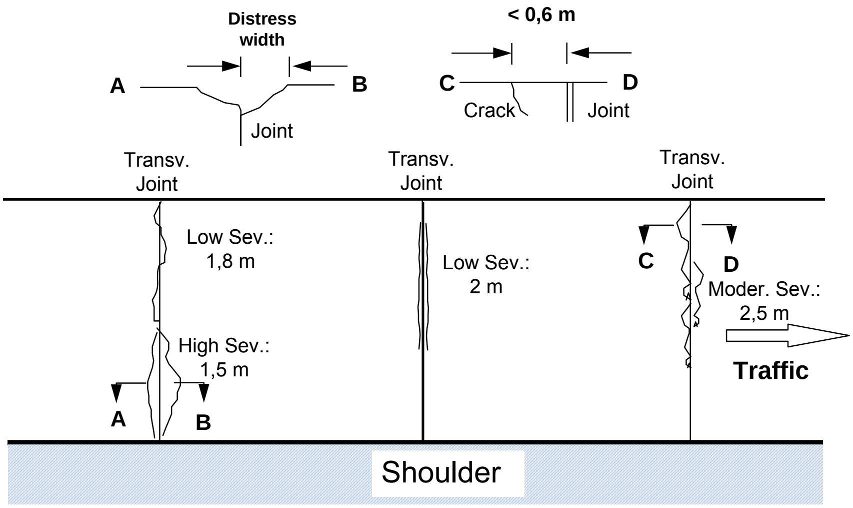

The mechanism of joint spalling is believed to be a concentration of stress close to a joint caused by a combination of:

- traffic loading
- environmental stress due to temperature variations and shrinkage
- stiffness of material in the joint which may range from moderately soft joint sealants or preformed seals to incompressible materials that enter the joint in the absence of a sealant.

C3.2 LAST (1996) Models for Joint Spalling

C3.2.1 Transverse Joint Spalling (JPCP)

The model for transverse joint spalling for JPCP is as follows:

$$\begin{aligned}SPALL = {} & 3.281\times10^{-6}(AGE3)^2(L)\{549.9 - 895.7(LIQSEAL + PREFSEAL) \\ & + 1.11\times10^{-3}(DAYS90)^3 + 375(DOWLCOR) \\ & + FI\,[29.01 - 27.6(LIQSEAL) - 28.59(PREFSEAL) - 27.09(SILSEAL)]\}\end{aligned} \quad \ldots (C3.1)$$

where

SPALL = per cent of medium and high severity spalled joints

AGE3	=	age since construction in years
DOWELCOR	=	dowel corrosion
	=	0 if no dowels exist, or are protected from corrosion
	=	1 if dowels are not protected from corrosion
L	=	mean transverse joint spacing in m
FI	=	Freezing Index in ºF-days
DAYS90	=	number of days with T > 32ºC
LIQSEAL	=	presence of liquid sealant in joint (1 if present; 0 otherwise)
SILSEAL	=	presence of silicone sealant in joint (1 if present; 0 otherwise)
PREFSEAL	=	presence of preformed sealant in joint (1 if present; 0 otherwise)

The distribution and characteristics of the pavement sections used in the development of this model are presented in Table C3-1.

Table C3-1
Distribution of pavement sections used in the spalling model for JPCP

Climatic Region	Seal type	Age (years)		
		0 - 10	11- 20	21 - 35
Cold FI > 200	Preformed	12	3	4
	Liquid	8	2	8
	Silicon	8	2	0
	Without seal	16	0	0
Temperate FI < 200 DAYS90 < 100	Preformed	0	18	0
	Liquid	1	11	17
	Silicon	4	0	0
	Without seal	6	21	10
Warm FI < 200 DAYS90 > 100	Preformed	0	0	0
	Liquid	5	8	0
	Silicon	0	0	0
	Without seal	0	0	0
Total		60	65	39

Table C3-2 shows the range of variables used in deriving the model.

Table C3-2
Range of variables used in the spalling model for JPCP

Variable	Range
AGE3	0 - 25 years
DAYS90	0 - 100 days
FI	0 – 1600
L	4.5 - 6.0 m
DOWELCOR	with & without protection

C3.2.2 Transverse Joint Spalling (JRCP)

The model for transverse joint spalling for JRCP is as follows:

$$SPALL = 3.281x10^{-5}(AGE3)^{3}(L)\{1.94(DOWELCOR) + 8.819(BASE)(1 - PREFSEAL) + 0.0071(FI)\} \quad \text{. . . (C3.2)}$$

where

SPALL = per cent of medium and high severity spalled joints

BASE = base type (1 if stabilised; 0 otherwise)
and the other variables are as defined previously

The distribution and characteristics of the pavement sections used in the development of this model are presented in Table C3-3.

Table C3-3
Distribution of pavement sections used in the spalling model for JRCP

Climatic Region	Seal Type	Age (years)			
		0 – 10		11 – 25	
		Stabilised Base		Stabilised Base	
		No	Yes	No	Yes
FI < 111	Preformed	0	4	10	4
	Liquid	1	1	3	1
	Silicon	0	0	0	0
	Without seal	0	0	0	0
FI > 111	Preformed	6	5	0	0
	Liquid	3	3	30	32
	Silicon	2	0	2	0
	Without seal	0	0	2	0

Table C3-4 shows the range of variables used in deriving the model.

Table C3-4
Range of variables used in the spalling model for JRCP

Variable	Range
AGE3	0 - 25 years
L	8 - 18 m
FI	0 – 2200
DOWELCOR	with & without protection

The above models are sensitive to all the variables used. Figure C3-2 shows the sensitivity to freeze index and Figure C3-3 to the presence of a preformed seal at the joint.

Figure C3-2
Joint spalling model (1996) – sensitivity to freeze index

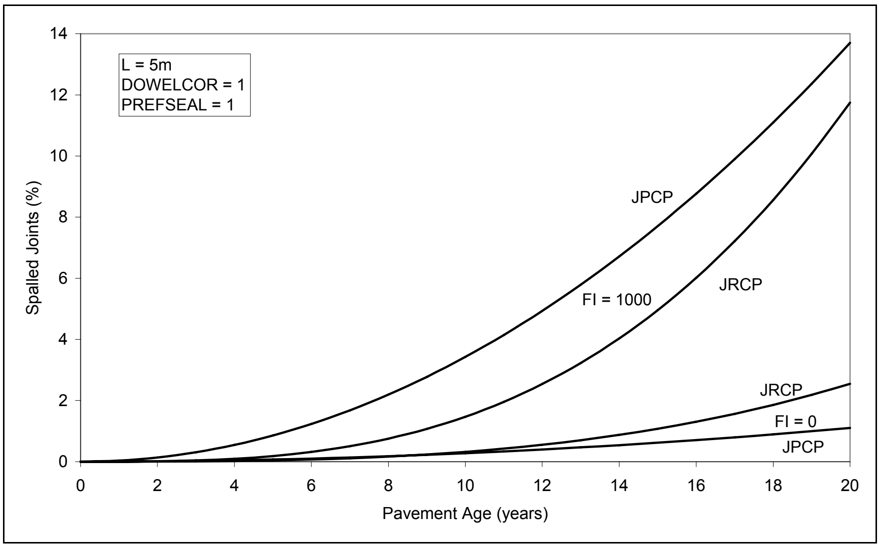

Figure C3-3
Joint spalling model (1996) – sensitivity to joint seal

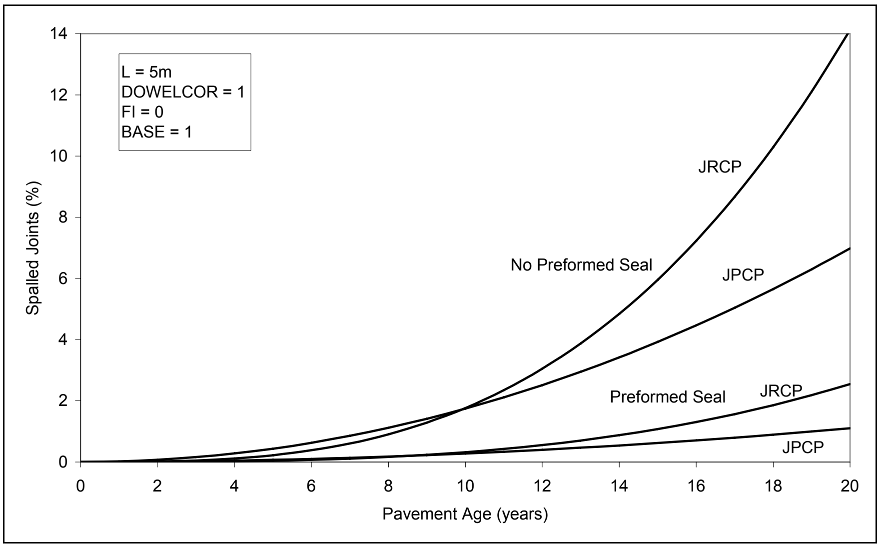

C4. TRANSVERSE CRACKING

C4.1 Definition of Cracking

Transverse cracking of unreinforced concrete slabs normally occurs over the entire width of the slab as shown in Figure C4-1. SHRP (1993) defines three levels of severity:

- Low - width of cracks less than 3 mm, without visible spalling or faulting; or well sealed, with a non-determinable width
- Medium - width of cracks between 3 and 6 mm, or with spalling less than 75 mm, or faulting less than 6 mm
- High - width of cracks greater than 6 mm, or spalling more than 75 mm, or faulting more than 6 mm

Figure C4-1
Transverse cracking

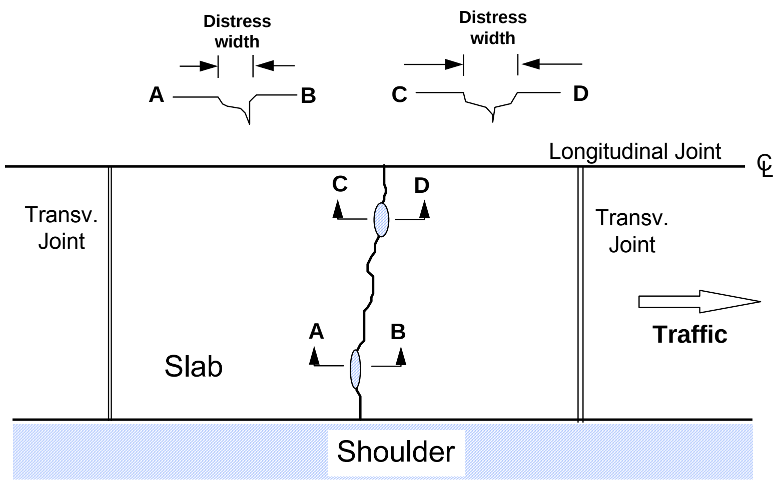

Transverse cracking is normally due to fatigue and is related to traffic loading and the properties of the slab, its supporting structure and the type of joints. Cracking at mid slab starts at the bottom of the slab at the outer edge and spreads vertically and transversely until the slab is split into two halves. The resulting joint is then subject to faulting and spalling as for construction joints.

C4.2 LAST (1996) Models for Transverse Cracking

C4.2.1 Transverse Cracking in Plain Concrete Slabs

The model presented in LAST (1996) is of the mechanistic empirical form and has two major components:

1. estimation of cumulative fatigue effects following a mechanistic procedure based upon the properties of the pavement, climatic variables and traffic loading;
2. estimation of the number of cracked slabs using the results of 1. above and an empirical relationship derived from LTPP data.

The structure of this model is shown in Figure C4-2.

Figure C4-2
Structure of transverse cracking model

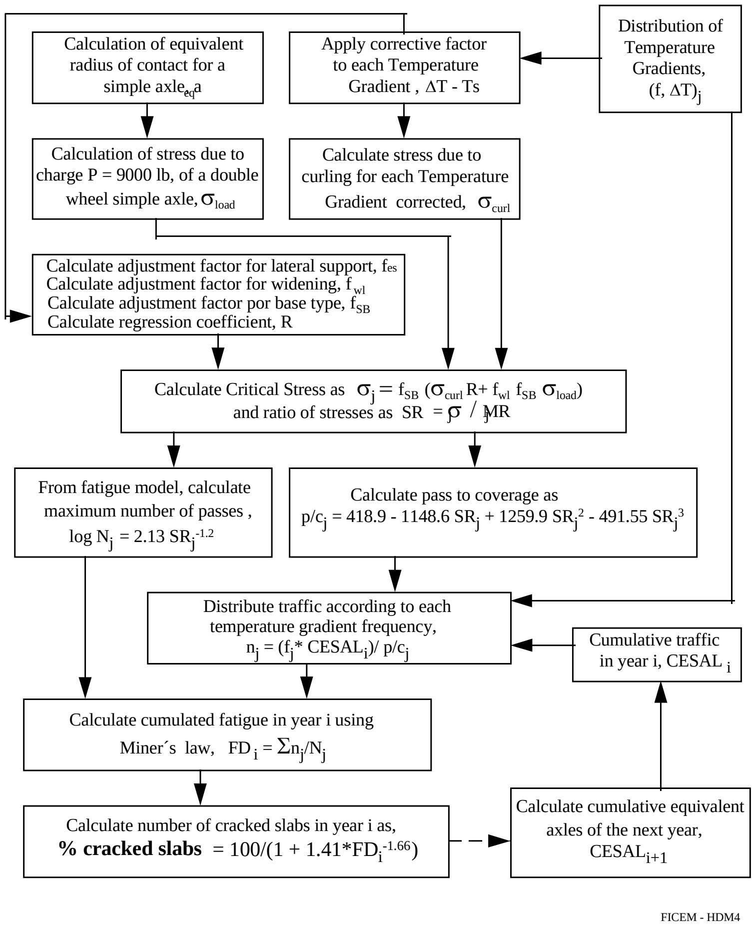

C4.2.2 Cumulative Fatigue Model

The computational stages of this model are as follows:

Calculation of load induced stress

The stress in the slab edge produced by traffic loads has the following form:

$$\sigma_{load} = f_{ES}\ f_{WL}\ \sigma_e \qquad \text{. . . (C4.1)}$$

where

σ_{load} = stress due to load application, in psi

f_{ES} = adjustment factor by shoulder type

f_{WL} = adjustment factor for widened lanes

σ_{ε} = stress obtained from Westergaard equation for an edge load in a circular plate, in psi

Calculation of edge stress

Edge stress in the slab is calculated using the Westergaard (1948) equation for a circular load:

$$\sigma_e = \frac{3(1+\mu)P}{\pi(3+\mu)thick_{slab}^2}\left[\ln\left(\frac{E_{pcc} * thick_{slab}^3}{100ka^4}\right) + 1.84 - \frac{4\mu}{3} + \frac{1-\mu}{2} + 1.18(1+2\mu)\frac{a}{\ell}\right] \qquad \text{. . . (C4.2)}$$

where

- P = total load applied by each wheel, in lbf
- μ = Poisson ratio
- E_{pcc} = elastic modulus of concrete, in psi
- $thick_{slab}$ = slab thickness, in ins
- k = modulus of subgrade reaction, in psi/in
- p = tyre pressure, in psi
- ℓ = radius of relative stiffness, in ins
- $\ell = \sqrt[4]{\dfrac{E_{pcc}\left(thick_{slab}\right)^3}{12\left(1-\mu^2\right)k}}$
- a = load application radius, in in
- $a = \sqrt{\dfrac{P}{\pi(p)}}$

To obtain edge stress in the slab for a double wheel, it is necessary to calculate the equivalent radius, a_{eq}, and to replace it in the stress equation. Equivalent ratio is calculated according to the following equation:

$$a_{eq} = a\left[0.909 + 0.339485\left(\frac{S}{a}\right) + 0.103946\left(\frac{a}{\ell}\right) - 0.017881\left(\frac{S}{a}\right)^2 - 0.045229\left(\frac{S}{a}\right)^2\left(\frac{a}{\ell}\right) + 0.000436\left(\frac{S}{a}\right)^3 - 0.301805\left(\frac{S}{a}\right)\left(\frac{a}{\ell}\right)^3 + 0.034664\left(\frac{S}{\ell}\right)^2 + 0.001\left(\frac{S}{a}\right)^3\left(\frac{a}{\ell}\right)\right] \quad \text{. . . (C4.3)}$$

Limits: $0 \leq S/a \leq 20$
$0 \leq a/\ell \leq 0.5$

where

- a_{eq} = equivalent radius for a single axle with double wheels, in ins
- a = radius of load application for a single axle, in ins
- S = spacing between wheel centres, in ins
- ℓ = radius of relative stiffness, in ins

Replacing the load application radius by the equivalent radius for a single axle, and P by 2P (i.e. dual wheel load rather than single wheel load), the edge stress is

$$\sigma_e = \frac{3(1+\mu)(2P)}{\pi(3+\mu)thick_{slab}^2}\left[\ln\left(\frac{E_{pcc} * thick_{slab}^3}{100\,k\,a_{eq}{}^4}\right) + 1.84 - \frac{4\mu}{3} + \frac{1-\mu}{2} + 1.18(1+2\mu)\frac{a_{eq}}{\ell}\right] \quad \text{. . . (C4.4)}$$

Calculation of the adjustment factor by shoulder type, f_{ES}

To calculate the effect of tied concrete shoulders, the efficiency in load transfer in stress (LTE) was determined from load transfer in deflection, using the following equation:

$$\log_{10}(LTE_\sigma) = \left[0.064787 + 0.0047221(LTE_\Delta) + 0.00089586(LTE_\Delta)^2 - 1.6478x10^{-5}(LTE_\Delta)^3 + 8.9222x10^{-8}(LTE_\Delta)^4\right] \quad \text{. . . (C4.5)}$$

where

- LTE_σ = load transfer efficiency in stress, in per cent
- LTE_Δ = load transfer efficiency in deflection, in per cent

In pavement sections with concrete shoulders or other forms of edge support (such as adjacent lanes, or curb and gutter), load stress should be multiplied by the following factor to quantify the effect of the edge support:

$$f_{ES} = \frac{100}{100 + LTE_{\sigma}} \qquad \text{. . . (C4.6)}$$

where

f_{ES} = adjustment factor for the edge support

Calculation for adjustment factor by widened lane, f_{WL}

In sections with lane widening, the critical location for fatigue damage is in the bottom of the slab, directly under the wheels. Studies have demonstrated that widened slabs will not be overloaded in the outside edge (Benekohal, et al, 1990). To obtain the maximum stress directly under loaded wheels, the following adjustment factor should be used:

$$f_{WL} = 0.454147 + \frac{0.013211}{D/\ell} + 0.386201\left(\frac{a_{eq}}{D}\right) - 0.24565\left(\frac{a_{eq}}{D}\right)^2 + 0.053891\left(\frac{a_{eq}}{D}\right)^3 \qquad \text{. . . (C4.7)}$$

where

f_{WL} = adjustment factor for widened lanes
a_{eq} = equivalent radius for a single axle with double wheels, in ins
D = distance of wheel from slab edge, in ins
ℓ = radius of relative stiffness, in ins

Calculation of stresses produced by curling, σ_{curl}

Curling stress is determined using the following equation:

$$\sigma_{curl} = \frac{C(E_{pcc})\alpha_T(\Delta T)}{2} \qquad \text{. . . (C4.8)}$$

where

σ_{curl} = curling stress, in psi
C = curling stress coefficient
E_{pcc} = elastic modulus of concrete, in psi
α_T = concrete thermal expansion coefficient, (default = 5.5x10^{-6})
ΔT = temperature difference between edge and bottom of the slab, in ºF obtained from the temperature frequency histogram

For the equation for σ_{curl}, Westergaard (1926) and Bradbury (1938) developed coefficients to solve it. For the maximum stress in the longitudinal edge, coefficient C for curling stress is obtained from the following equation:

$$C = 1 - \frac{2\cos(\lambda)\cosh(\lambda)}{(\sin(2\lambda) + 2\sinh(\lambda)\cosh(\lambda))} * \left(\tan(\lambda) + \frac{\sinh(\lambda)}{\cosh(\lambda)}\right) \qquad \text{. . . (C4.9)}$$

where

λ = $\frac{Jtspace}{\ell\sqrt{8}}$, in sexadecimal degrees
Jtspace = slab length, in ins
ℓ = radius of relative stiffness, in ins

Curling stress must be determined for each difference of temperature in the histogram.

Combined edge stress, σ_{comb}

The combined stress due to curling and loads is obtained from the following equation:

$$\sigma_{comb} = f_{SB}\,[\sigma_{load} + R(\sigma_{curl})] \qquad \text{. . . (C4.10)}$$

where

σ_{comb} = combined stress in the slab edge, in psi
σ_{load} = stress in slab edge in psi, in psi
σ_{curl} = curling stress, in psi
f_{SB} = adjustment factor for stabilised bases (1.0 if $thick_e$ = thick)
$thick_e$ = effective slab thickness, in ins
R = regression coefficient

Calculation of the adjustment factor for stabilised bases, f_{SB}

The effect of stabilised bases was considered using directly effective slab thickness determined by results of measurements with FWD. This effective slab thickness represents the equivalent thickness of a plain concrete slab that would give the same structural response as the total pavement, (slab plus sub-base).

The effective thickness, determined below, quantifies the structural contribution of all the pavement layers and any interaction between layers, and is used to determine the maximum tensile stress at the bottom of the slab.

$$f_{SB} = \frac{2(thick_{slab} - x)}{thick_e} \qquad \text{. . . (C4.11)}$$

where

f_{SB} = adjustment factor for stabilised bases (1.0 if $thick_e$ = thick)
$thick_{slab}$ = thickness of the existing slab, in ins
$thick_e$ = effective slab thickness, in ins
x = location of the neutral axle

and

$$x = \left[\frac{\dfrac{(thick_{slab})^2}{2} + \left(\dfrac{E_{base}}{E_{pcc}}\right) thick_{base}\left(thick_{slab} + \dfrac{thick_{base}}{2}\right)}{thick_{slab} + \left(\dfrac{E_{base}}{E_{pcc}}\right) thick_{base}}\right] \qquad \text{. . . (C4.12)}$$

$$thick_e = \left[(thick_{slab})^2 + (thick_{base})^2\,\frac{(E_{base})thick_{base}}{(E_{slab})thick_{slab}}\right]^{0.5} \qquad \text{. . . (C4.13)}$$

where

$thick_{slab}$ = slab thickness, in ins
$thick_{base}$ = thickness of the stabilised base, in ins
E_{pcc} = elastic modulus of concrete, in psi
E_{base} = elastic modulus of base, in psi

Unlike other adjustment factors, f_{SB}, is applied to combined stress, because this factor is an adjustment of the slab thickness.

Calculation of the regression coefficient, R

The R coefficient is necessary because the stresses due to load and curling cannot be added directly. Curling produces an unbonding of the slab with the base which negates the permanent contact supposition used in the calculation of stresses produced by traffic loads. The regression coefficient R gives the necessary adjustment so that the curling stress gives the correct combination of edge stresses in the slab.

The regression coefficient R is given by:

$$R = \Bigg[1.062 - 0.015757dT - 0.0000876k - 1.068\left(0.01\frac{Jt_{space}}{\ell}\right) + 0.387317(dT)\left(0.01\frac{Jt_{space}}{\ell}\right)$$

$$+1.17x10^{-11}(E_{pcc})(dT)(k) - 1.81x10^{-12}(E_{pcc})(dT)^2(k) - 1.051x10^{-9}(E_{pcc})\left(0.01\frac{Jt_{space}}{\ell}\right)^2(dT)(k)$$

$$+1.84x10^{-11}(E_{pcc})(dT)^2\left(0.01\frac{Jt_{space}}{\ell}\right)(k) - 1.7487\left(0.01\frac{Jt_{space}}{\ell}\right)^2 dT + 0.000034351(dT)^3$$

$$+86.97\left(0.01\frac{Jt_{space}}{\ell}\right)^3 - 0.00816396(dT)^2\left(0.01\frac{Jt_{space}}{\ell}\right)\Bigg] \quad \text{. . . (C4.14)}$$

where

dT	=	$\alpha \Delta T \ 10^{-5}$
α	=	concrete thermal expansion coefficient, in /ºF
T	=	temperature difference in slab, in ºF
k	=	modulus of subgrade reaction, in psi
Jt_{space}	=	slab length, in ins
ℓ	=	radius of relative stiffness, in ins
E_{pcc}	=	elastic modulus of concrete, in psi

Fatigue damage determination

Accumulated fatigue damage is determined using Miner's law, by the following equation:

$$FD = \sum \frac{n}{N} \quad \text{. . . (C4.15)}$$

where

FD	=	accumulated fatigue damage
n	=	number of load applications, in ESA
N	=	number of load applications until failure

According to Miner's law (Miner, 1945), failure or cracks would be produced when the cumulated fatigue consumption, FD is 1.0, and the number of repetitions to the failure, N, depends on the applied stress level. The number of load repetitions until failure is a basic fatigue concept, and is calculated through a law of fatigue.

Law of Fatigue

In this model the law of fatigue developed by the US Corps of Engineers, using data from 51 full-scale pavement sections, was used. Edge stress was calculated using H-51 program (Pickett and Ray graphics), and multiplied by 0.75 to quantify the edge support or shoulder type of sections (Darter, 1988).

$$\log N = 2.13\ (SR)^{-1.2} \quad \text{. . . (C4.16)}$$

where

SR = ratio between total stress in slab and the modulus of rupture
= σ_{comb} / MR

σ_{comb} = combined edge stress due to loads (σ_{load}) and curling (σ_{curl}), in psi

MR = modulus of rupture of concrete, in psi

This fatigue law was initially developed for airport pavements, but it has shown good results in many other applications.

Determination of the coverage passes (p/c)

Assuming that the lateral wander of traffic is normally distributed, the probable lateral distribution of the traffic wheels is determined. Then, considering the contribution of the fatigue damage at the critical location (longitudinal edge for all normal - width sections) by the traffic passing through any point and the probability that the traffic will pass through that point, the pass to coverage (p/c) ratio is determined.

The p/c ratio is simply the ratio that gives the number of traffic passes needed to produce the same amount of fatigue damage at the critical location as one pass that would cause the critical loading condition (i.e. edge loading condition). The number of fatigue loading cycles (or coverage) that the applied traffic causes is the number traffic passes to cause the same amount of damage as one load placed directly at the edge.

For fatigue analysis of JPCP pavements, the most relevant location of interest is the longitudinal edge midway between transverse joints.

The definition of p/c involves a considerable quantity of analysis. However, since it is a measure of the relative damage caused by loads located at several points, it is not very sensitive to the pavement structure. The p/c ratio is affected by many factors, some of which are emphasised:

- average loading location
- standard deviation of the expected traffic
- stress level

The value of p/c is low (this means greater damage) for high stress levels, since stress due to loads located at greater distances from the edge of the slab begin to be meaningful. To be used in this analysis, and considering that the average wheel location is 22 in from the edge of the slab, with a standard deviation of 8.4 in, the following regression equation for p/c was developed:

$$p/c = 418.9 - 1148.6(SR) + 1259.9(SR)^2 - 491.55(SR)^3 \qquad \text{. . . (C4.17)}$$

where

SR = ratio between total stress in slab and modulus of rupture

Distribution of traffic according to temperature gradient frequency

Total traffic during the design period is separated according to the distribution of temperature gradients and its respective occurrence frequency. Furthermore, the p/c ratio that is produced for each temperature range should be considered. In this way, the number of traffic passes (n) is obtained for each slab thermal condition or temperature gradient, according to the following equation:

$$n = \frac{\text{Total Traffic}}{p/c}\text{Freqq} \qquad \text{. . . (C4.18)}$$

where

n = number of traffic passes expected for each temperature gradient.

Total Traffic = total traffic in the design period.
Freqq = frequency of each temperature gradient.
p/c = coverage ratio

Considerations of residual and by humidity temperature gradients

As was presented previously, curling by temperature or humidity has a significant effect on the critical stresses produced in a pavement slab. Many factors exist that can cause concave curling of the slabs. Curling effects by additional factors are added directly to the curling effects of temperature; therefore, a major error can be made if only curling due to temperature is considered.

In the development of this model, cumulative curling effects due to factors apart from temperature have been considered with a correction to temperature gradients determined for each pavement section. The current magnitude of the effective residual curling is unknown. However, considering the procedure proposed by Eisenmann and Leykauf (1990), the following equations have been developed to correct the difference of temperature measured in the slab as a function of the climatic zone.

Dry Climate with Frosts (DF)

$$T_s = \Delta T - \left[6.29 + 436.36(\mathrm{thick}_{slab} - 2)/(\mathrm{thick}_{slab})^3\right] \qquad \text{. . . (C4.19)}$$

Dry Climate without Frosts (DNF)

$$T_s = \Delta T - \left[7.68 + 436.36(\mathrm{thick}_{slab} - 2)/(\mathrm{thick}_{slab})^3\right] \qquad \text{. . . (C4.20)}$$

Wet Climate with Frosts (WF)

$$T_s = \Delta T - \left[5.03 + 327.27(\mathrm{thick}_{slab} - 2)/(\mathrm{thick}_{slab})^3\right] \qquad \text{. . . (C4.21)}$$

Wet Climate without Frosts (WNF)

$$T_s = \Delta T - \left[6.66 + 218.18(\mathrm{thick}_{slab} - 2)/(\mathrm{thick}_{slab})^3\right] \qquad \text{. . . (C4.22)}$$

where

T_s = adjusted temperature, in ºF
T = temperature difference between top and bottom of slab, in ºF
thick_{slab} = slab thickness, in ins

It is important to emphasise that the temperature correction is applied to each ΔT obtained from the temperature histogram. It is not enough to apply this correction to a value of average slab temperature. In Table C4-1 the histogram of a 10 in thickness concrete slab located in Carolina State is presented, dry climate without frosts (DNF), with and without the shift of temperature correction. For this case, the shift of temperature is 11.17 ºF.

Table C4-1
Example of temperature correction histogram

ΔT (ºF)	ΔT - Shift (ºF)	Frequency
-20	-31.17	0.024
-18	-29.17	0.040
-16	-27.17	0.054
-14	-25.17	0.057
-12	-23.17	0.079
-10	-21.17	0.073
-8	-19.17	0.076
-6	-17.17	0.064
-4	-15.17	0.069
-2	-13.17	0.042
0	-11.17	0.038
2	-9.17	0.026
4	-7.17	0.024
6	-5.17	0.019

ΔT (ºF)	ΔT - Shift (ºF)	Frequency
8	-3.17	0.029
10	-1.17	0.032
12	0.83	0.022
14	2.83	0.029
16	4.83	0.042
18	6.83	0.022
20	8.83	0.036
22	10.83	0.026
24	12.83	0.033
26	14.83	0.032
28	16.83	0.012
30	18.83	0.000
32	20.83	0.000
34	22.83	0.000

C4.2.3 Percentage of Cracked Slabs Model

The percentage of slabs cracked in a JCPC pavement is obtained from:

$$Pcrack = \frac{100}{1 + 1.41\,(FD)^{-1.66}} \qquad \text{. . . (C4.23)}$$

where

Pcrack = percentage of cracked slabs
FD = cumulative fatigue damage

The distribution and characteristics of the pavement sections used in the development of this model are presented in Table C4-2.

Table C4-2
Distribution of pavement sections used in the cracked slabs model

Climatic Region	Base Type	Slab Thickness (mm)					
		< 230		= 230		> 230	
		Joint Spacing (m)		Joint Spacing (m)		Joint Spacing (m)	
		≤ 4.6	> 4.6	≤ 4.6	> 4.6	≤ 4.6	> 4.6
Humid With Frost	Stabilised	14	14	40	48	0	12
	Non- Stabilised	4	4	30	44	25	31
Humid No Frost	Stabilised	0	0	30	54	0	8
	Non- Stabilised	0	0	0	6	4	4
Dry With Frost	Stabilised	0	0	0	0	0	0
	Non- Stabilised	8	8	8	8	0	0
Dry No Frost	Stabilised	40	28	32	22	22	12
	Non- Stabilised	0	0	0	0	12	6
Total		66	54	140	182	63	73

C4.2.4 Transverse Cracks for JRCP

Low severity cracks normally occur in JRCP pavements and are caused by shrinkage, curling and contraction due to variations in mean temperature. Reinforcement in a JRCP pavement is intended to mitigate such cracking but traffic loading, environmental effects and an insufficiency of reinforcement can lead to fracture of the reinforcement and subsequent crack deterioration. Transverse medium and high severity cracks are considered, since they increase roughness.

The crack deterioration model from ERES (1995) is as follows:

$$\mathrm{NCRACKS} = (\mathrm{AGE3})^{2.5}\left[\frac{6.88\mathrm{x}10^{-5}(\mathrm{FI})}{\mathrm{THICK}} + \mathrm{NE4}(0.116 - 0.073(\mathrm{BASE}))(1-\exp(-0.032\mathrm{MI}))\right.$$
$$\left.\exp(7.5518 - E_c - 66.5(\mathrm{PSTEEL}) + 5(\mathrm{PSTEEL})(E_c))\right] \quad \text{. . . (C4.24)}$$

where

NCRACKS	=	number of medium and high severity cracks per mile
NE4	=	cumulative axle loading, in million ESA
AGE3	=	age since pavement construction, in years
FI	=	Freezing Index, in ºF-days
THICK	=	slab thickness, in ins
BASE	=	base type (0 if non stabilised; 1 if stabilised)
MI	=	Thornthwaite moisture index
E_c	=	elastic modulus of concrete in Mpsi
PSTEEL	=	percentage of steel (longitudinal reinforcement)

The distribution of pavement sections used in the development of this transverse crack model for JRCP pavements is given in Table C4-3.

Table C4-3
Distribution of pavement sections used in the transverse crack model for JRCP

Climatic Region	PSTEEL Reinforcement ratio (%)	Age (years) 0 – 10		Age (years) 11 – 25	
		Stabilised Base		Stabilised Base	
		No	Yes	No	Yes
FI < 111	0.04 - 0.10	0	0	9	4
	0.11 - 0.29	1	4	3	1
FI > 111	0.04 - 0.10	7	4	29	30
	0.11 - 0.29	2	4	8	5
Total		**10**	**12**	**49**	**40**

Table C4-4 shows the range of variables used in the transverse model for JRCP.

Table C4-4
Range of variables used in the transverse cracking model for JRCP

Variable	Range
ESA	0 - 15 millions
AGE3	0 - 25 years
FI	0 – 2200
THICK	20 - 25 cm
MI	0 – 50
Ec	27.6 - 41.4 MPa
PSTEEL	0.06 - 0.15 %
BASE	Stabilised and not stabilised

C5. ROUGHNESS

C5.1 Measures of Pavement Functional Condition

Roughness in HDM-4 is defined in terms of the International Roughness Index (IRI) with units of m/km IRI. Some of the models expressed ride quality in terms of Present Serviceability Rating (PSR) shown in Table C5-1.

Table C5-1
Present Serviceability Rating

PSR	Condition
0 – 1	Very Poor
1 - 2	Poor
2 - 3	Fair
3 - 4	Good
4 - 5	Very Good

A relationship between PSR and IRI has been taken from Al-Omari and Darter (1994):

$$IRI = -3.67 \log_e(0.2\ PSR) \qquad \text{. . . (C5.1)}$$

where

IRI = International Roughness Index, in m/km IRI
PSR = Present Serviceability Rating

This relationship is shown in Figure C5-1.

Figure C5-1
IRI v PSR

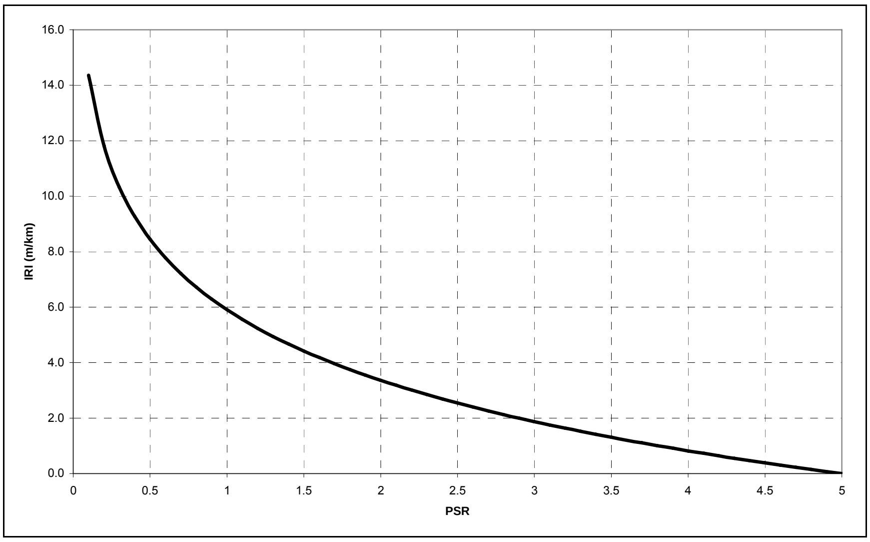

C5.2 LAST (1996) Models for Roughness and PSR

C5.2.1 Roughness Model for JPCP

The roughness model for JPCP is taken from ERES (1995):

$$IRI = IRI_o + 0.00265(TFAULT) + 0.0291(SPALL) + 0.15x10^{-6}(TCRACK)^3 \quad \text{. . . (C5.2)}$$

where

IRI	=	International Roughness Index, in m/km IRI
IRI_0	=	initial roughness at construction, in m/km IRI
TFAULT	=	transverse joint faulting, in mm/km
	=	1000 FAULT / L
SPALL	=	spalled joints, in per cent
TCRACK	=	transverse cracks, in no/km
	=	10 CRACKING / L
CRACKING	=	percentage of cracked slabs
L	=	mean transverse joint spacing, in m

The range of variables used in the roughness model for JPCP are given in Table C5-2.

Table C5-2
Range of variables used in the roughness model for JPCP

Variable	Range
TFAULT	0 – 789 mm/km
TCRACK	0 – 186 cracks/km
SPALL	0 - 40%

This model can be expressed in an incremental form as:

$$\Delta IRI = 0.00265(\Delta TFAULT) + 0.0291(\Delta SPALL) + 4.51x10^{-7}(TCRACK)^2 (\Delta TCRACK) \quad \text{. . . (C5.3)}$$

where

ΔIRI	=	incremental increase in roughness, in m/km IRI
$\Delta TFAULT$	=	incremental increase in transverse joint faulting, in mm/km
$\Delta SPALL$	=	incremental increase in spalled joints, in per cent
$\Delta TCRACK$	=	incremental increase in transverse cracks, in no/km

C5.2.2 Roughness Model for JRCP

The roughness model for JRCP is given below:

$$PSR = 4.165 - 0.0169(TFAULT)^{0.5} - 0.1447(SPALL)^{0.25} – 8.367x10^{-5}(TCRACK)^2 \quad \text{. . . (C5.4)}$$

where the variables are as defined previously.

The distribution of the pavement sections used in the development of the model is given in Table C5-3.

Table C5-3
Distribution of pavement sections used in the roughness model for JRCP

Climatic Region	Number
Wet - with frost	52
Wet – without frost	8
Dry - with frost	22
Dry – without frost	8

The range of variables used in the roughness model for JRCP are given in Table C5-4.

Table C5-4
Range of variables used in the roughness model for JRCP

Variable	Range
TFAULT	0 - 473 mm/km
NCRACKS	0 - 62 cracks/km
SPALL	0 - 60 %

This model can be expressed in incremental form as:

$$\Delta PSR = -0.00845(TFAULT)^{-0.5}(\Delta TFAULT) - 0.112(SPALL)^{-0.75}(\Delta SPALL) -16.734x10^{-5}(TCRACK)(\Delta TCRACK) \quad ...(C5.5)$$

where

ΔPSR = incremental increase in PSR
$\Delta TFAULT$ = incremental increase in transverse joint faulting, in mm/km
$\Delta SPALL$ = incremental increase in spalled joints, in per cent
$\Delta TCRACK$ = incremental increase in transverse cracks, in no/km

The effect of faulting, joint spalling and transverse cracking on roughness are illustrated in Figure C5-2, Figure C5-3 and Figure C5-4 respectively.

Figure C5-2
Effect of faulting on roughness

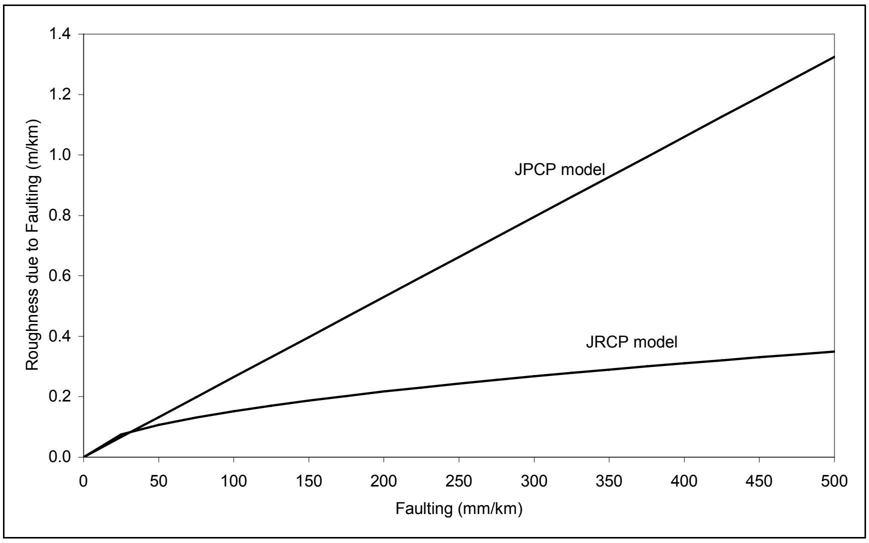

Figure C5-3
Effect of joint spalling on roughness

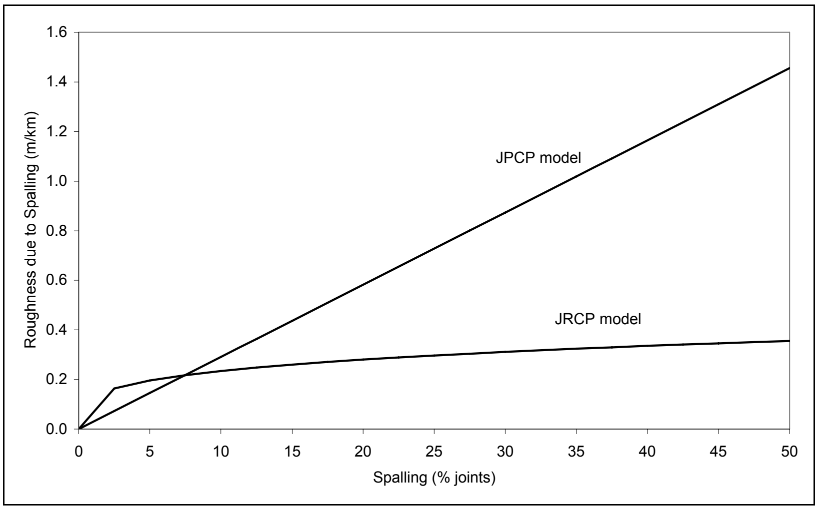

Figure C5-4
Effect of transverse cracking on roughness

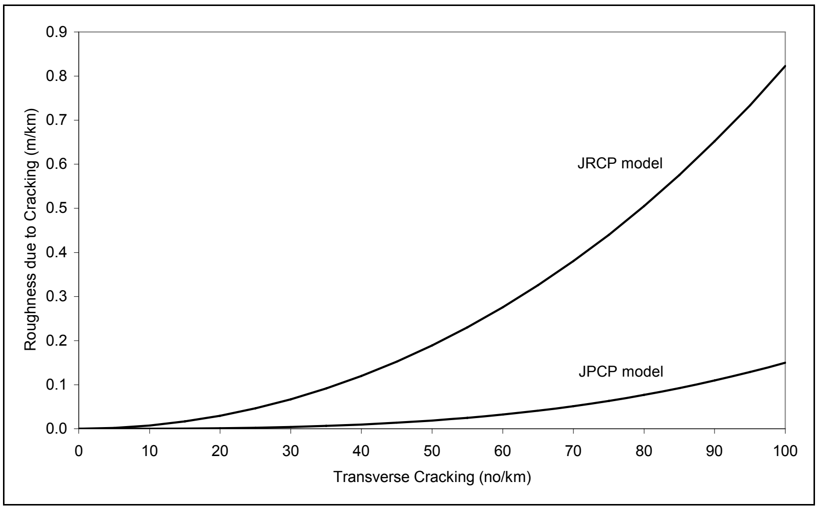

One would not expect such a large difference between pavement types in the contribution of faulting to roughness when faulting is expressed in cumulative terms and is independent of joint spacing. The difference in the spalling component can probably be explained by the difference in typical slab length – 3 to 6 m for JPCP as against 10 to 20 m for JRCP.

C5.2.3 Roughness Model for CRCP

The model for CRCP is taken from Lee, et al (1991):

$$PSR = PSR_0 - 430(AGE3)^{0.1849}\,(NE4)^{0.2634}\,(H_p)^{-1.3121} \qquad \text{. . . (C5.6)}$$

where

PSR_0 = initial construction PSR, (in the analysis 4.5 was used)
H_p = slab thickness, in mm
AGE3 = age since pavement construction, in years
NE4 = cumulative axle loading since construction, in million ESA

An incremental form of this model has been derived:

$$\Delta PSR = -193(H_p)^{-1.3121} (AGE3)^{-0.5517} (YE4)^{0.2634} \quad \ldots (C5.7)$$

where

ΔPSR = incremental increase in PSR
YE4 = annual axle loading, in million ESA

The roughness progression for CRCP is illustrated in Figure C5-5. With traffic growth rates below 5% the incremental form of the model gives very close agreement with the absolute form. If high growth rates are prevalent, some modification of this model may be needed to incorporate the growth rate for heavy vehicles.

Figure C5-5
Roughness progression for CRCP

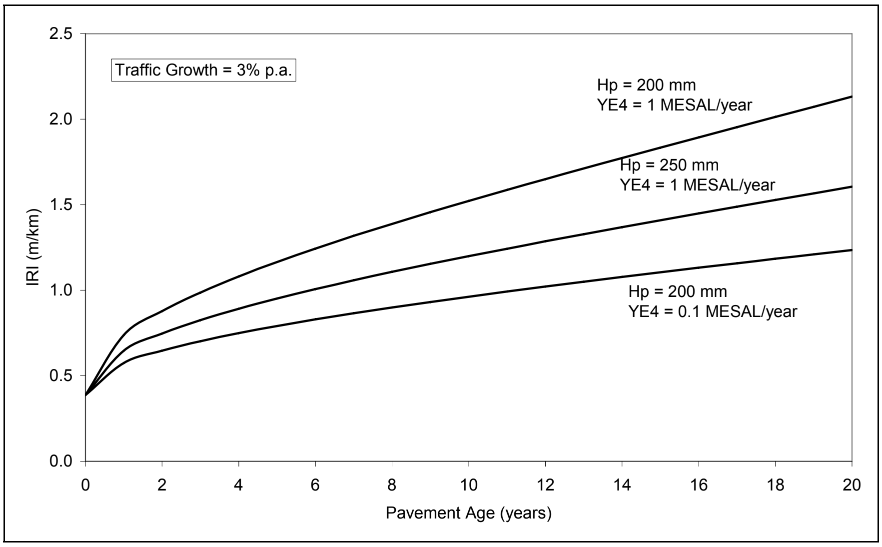

C6. OTHER DISTRESS MODES

C6.1 Failures on CRCP

Deterioration in CRCP pavements includes loosening and breaking of reinforcement steel, spalling of transverse cracks and D cracking. The model given by LAST (1996) for failures in CRCP is:

$$\log_e(FAIL) = 6.8004 - 0.0334(H_p)^2 - 6.5858(PSTEEL) + 1.2875\log_e(NE4) - 1.1408(BAM) - 0.9367(CAM) - 0.8908(GRAN) - 0.1258(CHAIRS) \quad \text{. . . (C6.1)}$$

where

FAIL	=	total number of fails per mile in the more trafficked lane
H_p	=	CRCP pavement slab thickness, in ins
PSTEEL	=	longitudinal reinforcement, percentage
NE4	=	cumulative axle loading, in million ESA
BAM	=	1, if base type material has asphalt mixed with aggregate 0, otherwise
CAM	=	1, if base material is aggregate with cement 0, otherwise
GRAN	=	1, if base material is granular 0, otherwise
CHAIRS	=	1, if chairs are used for installation of the reinforcement 0, if tubes are used

The range and sensitivity of the variables used in the development of the failure model for CRCP are given in Table C6-1.

Table C6-1
Range and sensitivity of variables used in the CRCP failure model

Variable	Range	Sensitivity
NE4	0 - 25 millions	0 - 80 millions
Hp	18 - 25 cm.	15 - 35 cm
PSTEEL	0.3 - 1.0 %	0.2 - 1.0 %
BAM	Base –Treated with Asphalt	Base -Treated with Asphalt
CAM	Base –Treated with Cement	Base -Treated with Cement
GRAN	Granular Base	Granular Base
CHAIRS	Tubes and Chairs	Tubes and Chairs

The types of distress represented by this model are not included in the roughness progression model presented earlier. By applying maintenance works to rectify these defects during life-cycle modelling, agency costs will be incurred without any corresponding benefits. Thus the inclusion of this model in HDM-4 is questionable.

C6.2 Rutting

Concrete pavements are not subject to rutting due to deformation in the same way as bituminous pavements. The only form of rutting which may occur is surface abrasion due to the use of studded tyres. The model given in Part B was derived from data in Sweden for bituminous pavements and its applicability to concrete surfacings cannot be verified.

C6.3 Surface Texture

C6.3.1 Skid Resistance

NDLI (1995) gives the following model for predicting skid resistance of cement concrete pavements:

$$SFC_{50} = 0.45 + 0.002(PSVF) - 0.01(AAVF) + 0.0032(AAVC) - 0.00191(UCS) + 0.0008(PCTFINES) \quad \text{. . . (C6.2)}$$

where

SFC50	=	sideway force coefficient measured at 50 km/h
PSVF	=	Polished Stone Value for the fine aggregate
AAVF	=	Aggregate Abrasion Value for the fine aggregate
AAVC	=	Aggregate Abrasion Value for the coarse aggregate
UCS	=	28 day compressive strength of concrete, in MPa
PCTFINES	=	aggregate passing a 4.76 mm sieve, in per cent

C6.3.2 Texture Depth

A variety of methods are used to apply macrotexture to concrete pavements at the time of construction. These range from simple brooming of the surface to plastic grooving and removal of laitance by wire-brushing or grit blasting. No models have been presented to the ISOHDM study that predict the loss of texture depth due to traffic and environment.

C7. ABSOLUTE and INCREMENTAL MODEL FORMS

Most of the models presented above are of the absolute form. In general they are non-linear, with the rate of deterioration changing with time, whether expressed as years since construction or as cumulative axle loading. The use of absolute models presents few problems if predicting the performance of a new pavement, but if the pavement being modelled is not new, certain difficulties are found. It is unlikely that the past performance of an existing pavement will have exactly followed the prediction models and some adjustment is needed to avoid apparent jumps in the amounts of distress in the first analysis year. This can be done by back-calculating the apparent age of the pavement using the recorded distress and the prediction model; this apparent age rather than the real age is then incremented in the predictions of future deterioration. This process is sometimes known as “curve shifting”.

It is generally more satisfactory to use incremental prediction models, the approach used in the HDM models for bituminous pavements. This model form not only eliminates the need for back-calculation of apparent ages for each distress mode, but also makes it easier to model the effects of maintenance operations which are applied to only a percentage of the pavement elements (a subject discussed under works effects – Section C8).

Given the form of most of the models given by LAST (1996) and ERES (1999) a satisfactory incremental model can be derived from the absolute form. Consider an absolute model of the form:

$$D_b = a\,(AGE)^b \qquad \text{. . . (C7.1)}$$

where

D_b = extent of distress at the end of the year
AGE = pavement age at the end of the year
a, b = model coefficients

The extent of distress at the start of the year is given by:

$$D_a = a\,(AGE - 1)^b \qquad \text{. . . (C7.2)}$$

The first differential of the model gives the annual increment as:

$$\Delta D = a\,b\,(AGE - 0.5)^{b-1} \qquad \text{. . . (C7.3)}$$

From this one can derive the relationship:

$$\Delta D = \frac{b\,(AGE - 0.5)^{b-1}}{(AGE - 1)^b} D_a \qquad \text{. . . (C7.4)}$$

In this expression the term a is eliminated and the increment becomes a function of the distress at the start of the year, the age and the age exponent. If predicting the progression of the distress for an existing pavement, the initial value of D_a is the observed value rather than that predicted by the model for the pavement age. If the observed value at a certain age is higher than the value which would have been predicted by the model, it is not unreasonable to expect that progression will also be higher than the prediction of the absolute model. Conversely, if the observed value is lower than the predicted value one would expect the future progression to be lower. Figure C7-1 illustrates this for a hypothetical model where the age exponent is 0.3.

Figure C7-1
Absolute and incremental model forms

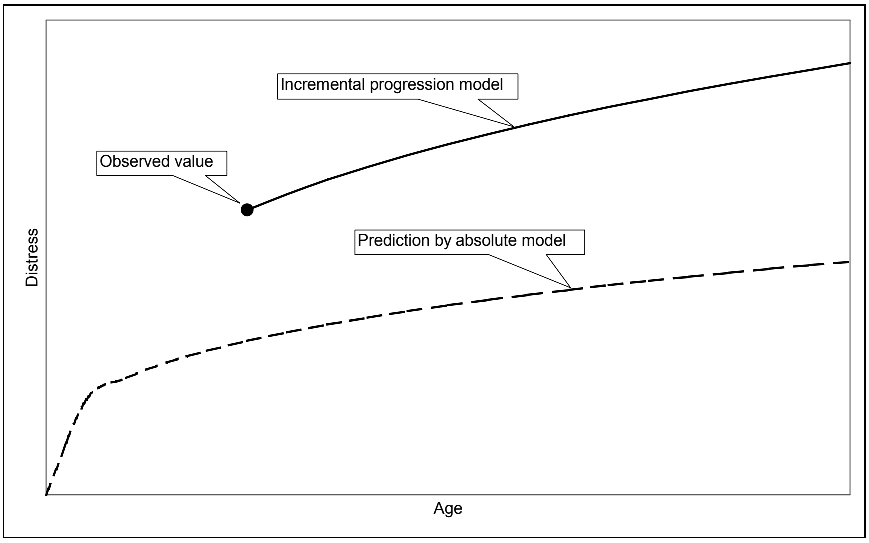

When using an incremental model of this form it is necessary to use the absolute model form for the first year if analysing a new pavement. This type of derived incremental model was used for the deformation component of rut depth for bituminous pavements.

It is noted that this incremental model form eliminates the coefficient a in the absolute model. This coefficient normally represents the scaling factor in the regression model which may contain a combination of parameters some of which are invariate (e.g. climatic parameters) and others which may be modified by works activities (e.g. drainage factor, joint sealants). To allow for a change in the scaling factor, the model form requires a modifier when the scaling factor is changed:

$$\Delta D = \frac{b\,(AGE - 0.5)^{b-1}}{(AGE - 1)^{b}} D_a \, \frac{a'}{a} \qquad \text{. . . (C7.5)}$$

where

a = scaling factor before works

a' = scaling factor after works

If the age term is expressed in cumulative axle loading, a similar incremental form of expression can be derived. The basic model is:

$$D_b = a\,(NE4)^b \qquad \text{. . . (C7.6)}$$

where

NE4 = cumulative axle loading to the end of the year

This can be expressed as:

$$D_b = a\,[(AGE)(YE4)]^b \qquad \text{. . . (C7.7)}$$

where

YE4 = annual axle loading

Taking the first differential and substituting as above, the YE4 term cancels out and one is left with the same expression as for the age related model (equation C7.4). This of course assumes that there is no traffic growth, but with growth rates typically in developed countries between 2 and 4% p.a. the error is quite small, especially for low values of AGE.

One problem that can be experienced with this incremental model form is if there is no observed defect on an existing pavement. That might well be the case with, say, joint spalling in a relatively young pavement. The proposed incremental model will then predict no progression of the distress in the future which may not be the reality. In such cases one must fall back on the absolute model to predict a notional initial value for the actual age of the pavement.

C8. WORKS EFFECTS

C8.1 Works Activities for Concrete Pavements

LAST (1996) proposed 11 types of works activities appropriate to concrete pavement modelling. Table C8-1 lists the applicability of these activities to the different types of concrete pavement and Table C8-2 lists the distresses that are affected by the activities.

Table C8-1
Works activities applicability by pavement type

Works Activity	Pavmement Type		
	JPCP	JRCP	CRCP
Load transfer dowels retrofit	4		
Tied concrete shoulders retrofit	4	4	
Longitudinal edge drains retrofit	4	4	
Joint sealing	4	4	
Slab replacement	4		
Full depth repair		4	4
Partial depth repair	4		
Diamond grinding	4	4	
Bonded concrete overlay	4	4	4
Unbonded concrete overlay	4	4	4
Pavement reconstruction	4	4	4

Table C8-2
Effect of works activities on modelled distress types

Works	Faulting	Spalling	Cracking
Load transfer dowels retrofit	4		
Tied concrete shoulders retrofit	4		4
Longitudinal edge drains retrofit	4		?
Joint sealing		4	
Slab replacement	4	4	4
Full depth repair	4	4	4
Partial depth repair		4	
Diamond grinding	4	4	
Bonded concrete overlay	4		4
Unbonded concrete overlay	4	4	4

C8.2 General Concepts

A number of the works activities defined above are applied only partially; for example, repair of spalled joints applies only to the percentage of joints that are spalled. Most of the deterioration relationships are non-linear with time and this complicates the modelling of the effects of partial works activities. The problem can be generalised as follows:

$$D = f(Y) \quad \ldots (C8.1)$$

where

D = extent of distress, in per cent

Y = time, either in years or cumulative axle loading since construction

If the distress is periodically repaired, there will be an age spectrum of the elements receiving repair, from zero (those which have just been repaired), to pavement age (those which have never been repaired). Using an absolute model form, the extent of distress after repair will be:

$$D = f\left[Y\left(1 - \sum \frac{Pct_i}{100}\right)\right] + \sum\left[f(Y - T_i)\frac{Pct_i}{100}\right] - \sum Pct_i \qquad \text{. . . (C8.2)}$$

where

D = extent of distress at time Y

Pct_i = per cent of distress repaired at time T_i

If the deterioration relationship is incremental of the form $\Delta D = f(Y)$, the annual increment in distress after partial repairs will be:

$$\Delta D = f\left[Y\left(1 - \sum \frac{Pct_i}{100}\right)\right] + \sum\left[f(Y - T_i)\frac{Pct_i}{100}\right] \qquad \text{. . . (C8.3)}$$

Figure C8-1 illustrates this concept.

Figure C8-1
Illustration of the effects of partial repair

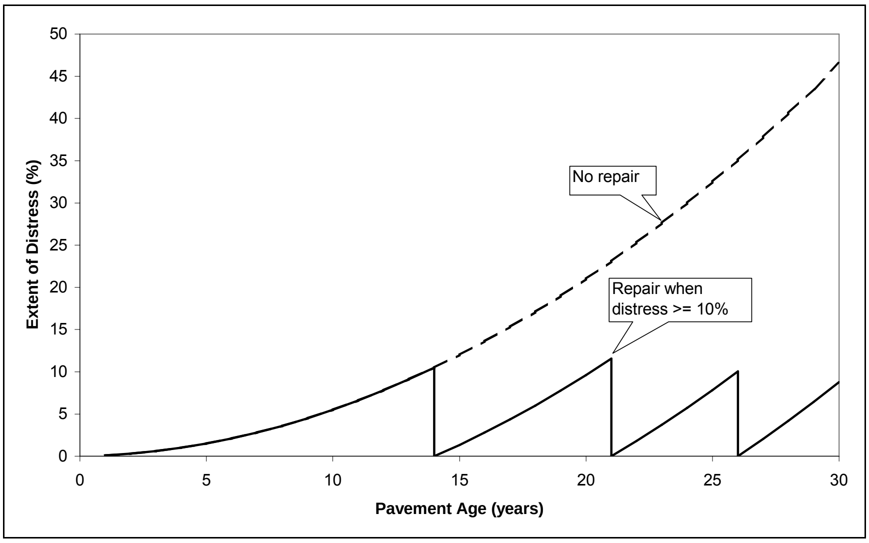

The partial repair has two effects; the immediate reduction of the extent to zero and a secondary effect of reducing the average age of the elements subject to the particular distress and hence changing the future rate of occurrence of the distress. In the example shown, typical of joint spalling, the age reduction reduces the rate of distress. In the case of faulting, the age exponent is less than unity and a works activity, such as slab replacement, will increase the rate of distress.

This conceptual formulation of works effects from partial repair may seem pedantic, but in the context of concrete pavements is important. Typically concrete pavements are designed for a “life” of 30 years or more and, unlike a bituminous pavements which receives periodic resurfacing, a concrete pavement may only receive partial repairs until it reaches the point of needing total replacement (the design “life”).

This approach of course increases the complexity of the deterioration modelling. It is necessary to maintain a record of both extent and timing of each partial repair.

C8.3 Routine Maintenance

The HDM-4 software allows the user to specify routine maintenance as a works activity with a related cost. However, this activity does not reset any model parameters and thus has no effect on future pavement deterioration.

There are routine activities which could be incorporated into the modelling of concrete pavements in a similar way to those applied to bituminous pavements. These are activities that have no immediate effect on the distress parameters but which reduce the rate of future deterioration. Examples are:

- Cleaning of unsealed transverse joints. The presence of incompressible material in the joints increases spalling and the effect of joint cleaning could be modelled by changing, for example, the modulus of joint “sealant”.
- Drainage maintenance. The drainage factor (C_d) is a significant parameter in the faulting models where it is considered as a constant over the life of the pavement. In practice some deterioration in drainage conditions might be expected unless the drainage system is maintained. A deterioration model which reduces C_d with time might be applied, similar to that adopted for the factor DF in bituminous pavement modelling. With routine maintenance this deterioration would be attenuated.

C8.4 Load Transfer Dowels Retrofit

Fitting load transfer dowels at transverse joints post construction will reduce the progression of faulting. However, most faulting takes place early in the life of the pavement; the LAST model predicts that faulting in the first year after construction is about 50% of the long term amount. Thus, to have a significant effect, this treatment should be applied very soon after construction. It seems esoteric that one might construct a JPCP pavement without dowel bars and then, a year or so later, retrofit them given the high cost both in terms of the work itself and associated lane closures. It is questionable whether this is a sensible works activity to include in HDM-4.

C8.5 Tied Concrete Shoulders Retrofit

The LAST models for joint faulting and cracking of unreinforced slabs include a parameter to account for the effect of lane widening or concrete shoulders that are tied to the main pavement structure.

C8.6 Longitudinal Edge Drains Retrofit

Provision or rehabilitation of the drainage system will affect the drainage coefficient C_d, which in turn will affect the progression of distress models that include this parameter, i.e. the LAST model for joint faulting.

C8.7 Joint Sealing

The type (or absence) of joint sealant is a significant parameter in the LAST model for joint spalling. The model assumes that, once fitted, a joint seal will retain its properties indefinitely. By comparison, the model for crack sealing of bituminous pavements assumes a finite life from the seal. When this life is exceeded the crack is deemed to be open and this affects the pavement performance via models such as wet-season strength and potholing.

It is improbable that joint seals will last the life of a well constructed concrete pavement (often 30 years or more). It is therefore suggested that the models for joint spalling allow for this either by setting a “life” for different types of sealant or by modelling a gradual reduction in the effectiveness of the seal. The LAST regression models undoubtedly include the effects of sealant deterioration in the age term so the addition of a seal deterioration component may be double counting. Nonetheless, if true life cycle costs are to be estimated the replacement of seals as a periodic activity should be allowed for in some way.

The effect of replacing joint seals, as described by LAST, is to effectively reset the age of the joint to zero ignoring cumulative fatigue effects that have occurred before replacing the seal. If using the LAST spalling models it would be more correct to leave the age unchanged and reset the scaling factor to reflect the change in sealant as described in Section C7.

C8.8 Slab Replacement

The complete replacement of cracked JPCP slabs results in a proportion of the pavement having an age reset to zero while the remainder of the pavement retains its previous age. Given that slab replacement may be a recurring operation (slabs are replaced as they crack), the effect on future deterioration must be modelled using the form of equations given in Section C8.2 to take account of the age spectrum. This applies to the progression models for faulting, spalling and cracking.

In the HDM-4 software, the user is not allowed to specify the properties of the replacement slabs which are assumed to be the same as the old. Thus it is not necessary to recalculate the allowable loading cycles for each distress type.

C8.9 Full Depth Repair

LAST (1996) describes full depth repair as a treatment that is responsive to:

- cracking and spalling at transverse joints in JRCP pavements
- deteriorated cracks in JRCP pavements
- localised failures in CRCP pavements

As the locality of deteriorated cracking in JRCP may not be at or near the joints, the effects of the activity should be related to the condition and locality to which is applied. If applied to transverse joints it will reset the extent of spalling and faulting, but not deteriorated cracking in mid slab. If performed in response to deteriorated cracking it will reset the extent of this distress but have no effect on joint spalling and faulting. The HDM-4 software allows the user to specify to which distress the activity is applied in the form of a percentage of distress to be treated.

Again, this may be a recurring activity implying an age spectrum if full depth repair is applied to spalled joints. The model given by LAST implies that the age of repaired joints is reset in the faulting model but it is thought that this may be incorrect. Faulting is caused by pumping of fines which is at its most intense early in the life of the pavement and diminishes with time. If a joint is repaired after the transfer of fines has mainly taken place, it will not necessarily trigger a recurrence of this phenomenon.

In respect of joint spalling, it seems to be correct to reset the age; the repaired joint should not retain any accumulated fatigue damage. In this case the age spectrum model should be applied to future spalling progression.

If full depth repair is applied to spalled joints then the joint seal, if any, would need replacement. This would be modelled in the same way as for joint sealing discussed above.

C8.10 Partial Depth Repair

Partial depth repair is only applied to spalled joints in JPCP. In the last model, the effect of this treatment is to reset the percentage of spalled joints but not the age of the repaired joints. As with full depth joint repair, it is considered that age should be reset and the age spectrum model should be applied to future spalling progression.

C8.11 Diamond Grinding

LAST (1996) presents diamond grinding as a corrective treatment for the following defects:

- joint faulting
- slab warping
- surface deformations caused by studded tyres
- inadequate crossfall
- inadequate surface texture
- roughness (longitudinal profile)

Of these defects, only faulting, studded tyre wear and roughness are explicitly modelled and only faulting and roughness are available in HDM-4 as intervention criteria. LAST (1996) only gives faulting as a parameter to be reset after diamond grinding.

Diamond grinding is not necessarily applied to the whole pavement area. If used in response to faulting it would only be carried out over localised areas adjacent to the transverse joints. Rectification of such defects as crossfall deficiency, texture depth and roughness implies treatment of most or all of the pavement area. Thus two different activities need to be considered:

C8.11.1 Local Grinding to Remove Joint Faulting

As a partial treatment, the area or volume of grinding needs to be defined. This will be a function of the amount of faulting and the number of joints. If one assumes that the amount of grinding is a prism at the edge of the slab on one side of the joint only, an expression of the following form could be applied:

$$VDG = a_0 \frac{(FAULT)^2 \ (CW)}{L} \qquad \text{. . . (C8.4)}$$

where

VDG = volume of diamond grinding, in m^3/km
FAULT = mean joint faulting, in mm
L = mean joint spacing, in m
CW = pavement width, in m
a_0 = model coefficient

It is thought that an appropriate default value for a_0 will lie in the range of 20 to 50.

If the volume of grinding is user specified, the expression can be inverted to give the reduction in mean faulting:

$$\Delta FAULT = \left[\frac{(VDG)(L)}{a_0\ (CW)} \right]^{0.5} \qquad \text{. . . (C8.5)}$$

where

ΔFAULT = reduction in mean faulting, in mm

The LAST model for diamond grinding appears to reset the age of joints to zero. This is incorrect; surface grinding will not affect the transfer of fines under the slab and future progression of faulting should be modelled using the original pavement age.

C8.11.2 Total Area of Grinding

In this case, the depth of grinding should be user specified and the volume will be a function of this and the pavement area.

If a works activity is responsive to a certain condition it would be expected that it would have some effect on this condition, e.g. roughness. This activity is in some ways analogous to placing a thin asphaltic overlay; there the roughness reduction is a function of the roughness before overlay and the overlay thickness. In the case of diamond grinding the reduction would be a function of the grinding depth. Adapting the overlay model, one has:

$$RI_a = a_0 + a_1 \max[RI_b - a_0,\ 0] \max[a_2 - GD,\ 0] \qquad \text{. . . (C8.6)}$$

where

RI_a = roughness after grinding, in m/km IRI
RI_b = roughness before grinding, in m/km IRI
GD = grinding depth, in mm

No default values for the model coefficients are postulated.

If grinding is in response to rutting caused by studded tyres, the reduction in mean rut depth would be given by:

$$RDM_a = RDM_b - GD \qquad \text{. . . (C8.7)}$$

where

RDM_a = mean rut depth after works in mm
RDM_b = mean rut depth before works in mm

If total area grinding is performed it should be assumed that faulting will be reset to zero.

C8.12 Bonded Concrete Overlay

A bonded concrete overlay creates a thicker monolithic slab, but some of the defects in the old slab may be retained depending on the amount of preparatory works (for example, replacing cracked slabs in the case of JPCP). The future performance of the overlaid pavement is discussed below by type of distress.

C8.12.1 Cracking

If existing cracked JPCP slabs are not replaced before overlaying the new layer will be subject to reflection of the underlying cracks. The model provided by LAST (1996) does not reset transverse cracking after a bonded overlay if the previous cracked slabs are not replaced. This implies that reflection cracking will be almost instantaneous. Thereafter, LAST models the overlaid pavement using the same crack progression model as for new pavements but retaining the cumulative fatigue in the old slab.

In the case of bonded overlays on JRCP pavements, LAST adjusts the slab thickness to account for the presence of deteriorated transverse cracks that have not been repaired prior to overlay. This adjusted thickness is then applied in the JRCP model for progression of deteriorated cracks. This model does not reset cracking to zero if the cracks are not repaired which again suggests some sort of immediate crack reflection through the overlay. This is questionable; even if the cracks did reflect quickly, the parameter being modelled is *deteriorated* cracks. There should be some time lag between the reflection of an underlying crack at the new pavement surface and spalling to the stage where it reaches the deteriorated classification.

C8.12.2 Faulting

LAST (1996) resets faulting to zero after a bonded overlay and also apparently resets the age to zero. As discussed previously, this seems to be incorrect as the overlay should not affect the conditions under the edges of the old underlying slab and the progression of faulting should be based on the original pavement age.

C8.12.3 Spalling

LAST (1996) resets both joint spalling and age to zero after the overlay. This is reasonable; the overlay presents new joint faces which are not subject to any accumulated traffic or environmental fatigue effects.

C8.13 Unbonded Concrete Overlay

LAST (1996) models the performance of an unbonded overlay as a new pavement on a rigid base (the old pavement). The model assumes that there is an interface between the old and new concrete layers which will prevent crack propagation of cracks in the old pavement. This works activity is not included in release 1.0 of HDM-4.

PART D. BLOCK PAVEMENTS

Block pavement modelling was introduced in the original ISOHDM report (NDLI, 1995). Currently insufficient performance data exist to verify the models proposed in the report for inclusion in the current version of HDM-4. However, the chapter from the NDLI report on block pavement modelling has been used as the basis of this Section, with a view that these models should be reviewed, and if necessary amended, in order that models for block pavements can be included in future versions of HDM-4.

D1. INTRODUCTION

The term block (also known as segmental) paving is used to describe the small-element surfacing mostly used to pave urban areas. The use of this type of surfacing dates back to medieval times and up to the end of the 19th century surfaces dressed with stone or hardwood were common for urban streets (Shackel, 1990). The advent of the motor vehicle - combined with the ease of construction, durability and cost of bituminous surfacing - resulted in the less frequent use of block paving. With developments in concrete technology and improved plant for concrete block manufacturing in the last 30 years, the use of block pavements in the form of concrete blocks has become acceptable again throughout the world (CCANZ, 1988).

This increased usage of block paving combined with the aim of extending the global applicability of the HDM-4 pavement performance models, in particular for the urban environment, has necessitated that performance models for block paving should be considered for inclusion in HDM-4.

In this section the modelling of the life cycle performance of block paving in HDM-4 is introduced. Firstly the various factors influencing block pavement performance and how the influence of these factors has been modelled is examined. This is followed by a discussion of the models that are proposed for inclusion in HDM-4.

D2. OVERVIEW OF AVAILABLE BLOCK PAVING MODELS

D2.1 Block Paving History and Terminology

Historically the following four types of block paving have been used to pave mostly urban areas (Shackel, 1990):

Stone-sett: Initially, cobblestones were used, typically 100 to 150 mm in diameter and collected from riverbeds, laid in a layer of coarse sand. The very rough uneven surface resulted in cobblestones being replaced by stone setts quarried from granite, sandstone, basalt, and even limestone. Typical thickness of the setts ranged between 90 and 180 mm.

The requirement for carefully dressed stones to maintain narrow joint spacing, which is crucial for the performance of block pavements (as discussed later), resulted in the stones being very expensive and time consuming to produce. This resulted in the use of alternative materials which were cheaper and faster to produce. Today stone setts are primarily used for architectural purposes.

Wood-blocks: From the early nineteenth century wooden blocks were often used as an alternative to stone setts, especially where it was desired to reduce the noise from steel wheels and horses' hooves. Generally the blocks were 125 to 250 mm long and 75 to 100 mm square, laid on end with the grain running vertically, and often bedded on a 3 mm thick layer of bituminous mastic. These wood-blocks could be constructed for about 65 per cent of the cost of a stone-sett.

Although they reduced traffic noise, the pavements absorbed horse ordure and became noisy when wet. Moreover, they proved to be slippery under pneumatic tyres and, with the advent of motor vehicles, their use was largely abandoned.

Brick-blocks: Because of the lack of local stone in some areas, pavements were surfaced with bricks. The durability of brick-blocks under traffic, however, was very low, resulting in frequent overlays with new bricks being required. The widespread application of brick paving was not achieved until the advent of vitrified bricks fired at high temperatures. Initially, the use of brick-blocks tended to be restricted to pedestrian areas whilst stone setts were used to carry the steel-wheeled vehicles common up to the end of the 19th century. With the advent of rubber tyres the use of brick-blocks for trafficked areas increased because a brick-block surfacing could be constructed for 50 to 60 per cent of the cost of a stone-sett surfacing. The principal problem associated with these brick pavements was their propensity to surface damage, manifested as cracking and cobbling of the pavers (blocks). To overcome this problem, high quality paving bricks were made from clay with a high lime content which was moulded in steel forms under high pressure and fired at high temperatures. These bricks are still used today, although mostly for architectural purposes.

Concrete blocks: The first concrete blocks were manufactured at the end of the 19th century and it was soon realised that these blocks provided better uniformity than stone setts. It was only after World War II, when the need for reconstruction led to a shortage in bricks, that concrete blocks were reluctantly accepted as a substitute for bricks. As the industry and equipment developed, manufacturers were able to manufacture concrete blocks at 40 per cent of the cost of bricks.

Today most block pavements are constructed with concrete blocks of various shapes and sizes, some of which have little resemblance to the original forms of block paving used. The various components of a typical concrete block pavement structure are illustrated in Figure D2-1.

Figure D2-1
Typical concrete block pavement structure

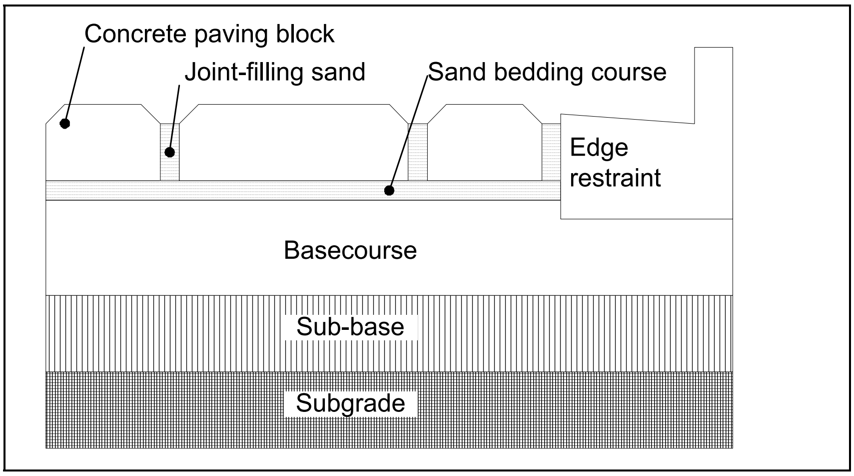

D2.2 Factors Influencing the Performance of Block Pavements

The factors influencing the performance of concrete block pavements under traffic are summarised in Table D2-1. The influence of each of these factors are discussed below, based on the findings of laboratory and field observations of limited experiments over the years.

Table D2-1
Factors affecting performance of block pavements

Pavement Component	Factors affecting performance
Paving Blocks	Shape Size Thickness Laying Pattern
Bedding Sand	Thickness Grading Angularity Moisture Content
Base and sub-base	Material type Thickness
Subgrade	Material type Strength (Bearing Capacity)

Source: Shackel (1990)

D2.2.1 Paving Blocks

The factors that influence the performance of concrete block pavers are:

Block shape: Figure D2-2 illustrates some of the different block shapes commonly available.

Figure D2-2
Classification of common block shapes

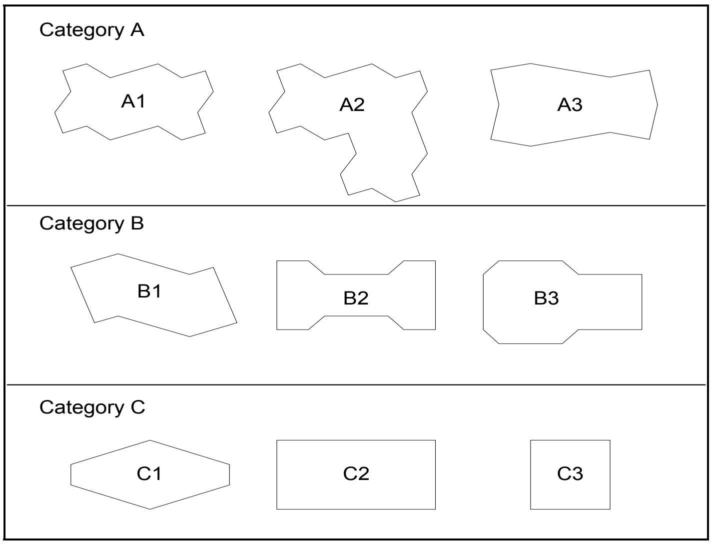

Source: Shackel (1990)

At present there seems to be somewhat divergent views on the relevance of block shape when joint sand is complete, dense and the joints between blocks are uniform in the range 2 to 4 mm. In New Zealand and England, for example, all shapes are considered equal for designing road pavements as long as they can satisfy the required laying pattern. In South Africa and Australia research results indicate that block shape influences the performance of the pavement as follows:

- the horizontal creep under traffic of blocks with indented faces has been observed to be much less than the traditional rectangular blocks. The difference in performance is illustrated in Figure D2-3.
- the development of rutting seems to be less for shaped blocks compared to rectangular blocks, as illustrated in Figure D2-4.

Figure D2-3
Effect of block shape on horizontal creep

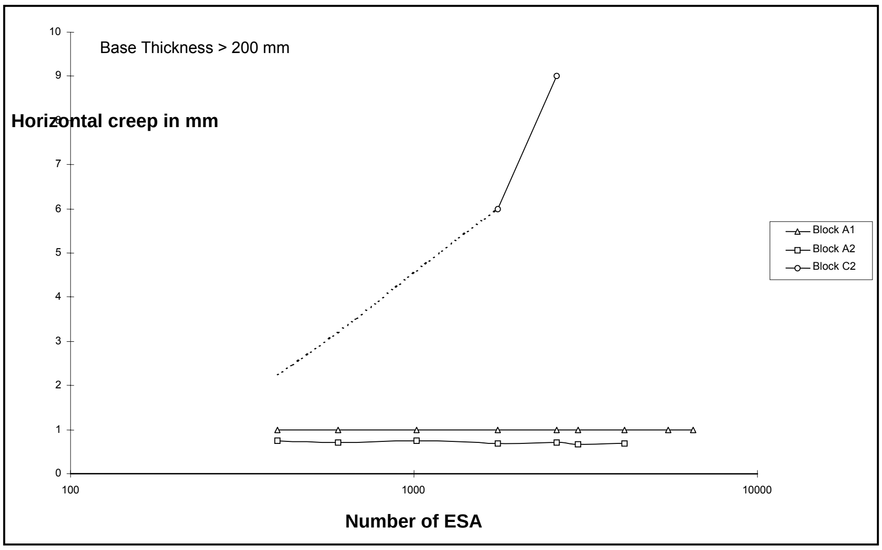

Source: Shackel (1990)

Figure D2-4
Effect of block shape on mean rut depth

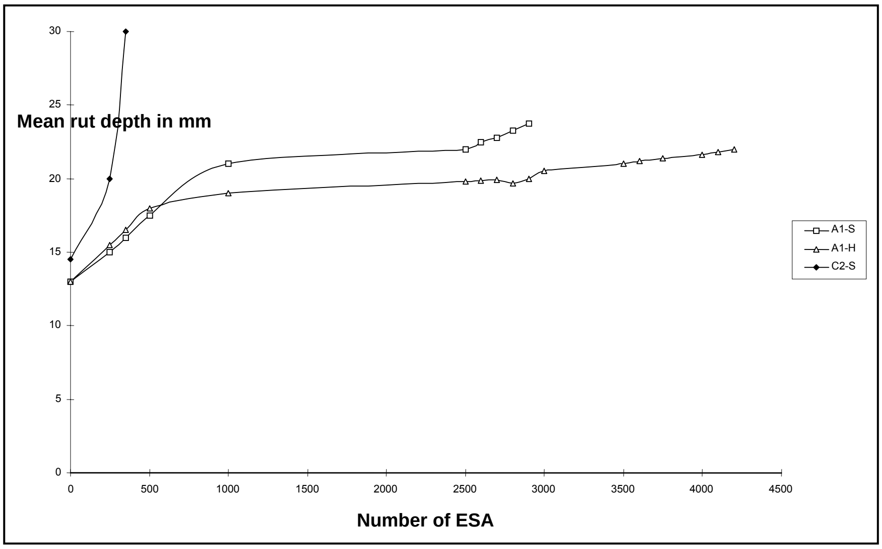

Source: Shackel (1979)

Based on these observations, the Cement and Concrete Association of Australia and the Concrete Masonry Association of South Africa have devised the following general classification to distinguish between the performance of the various block shapes available:

Category A: Comprises indented units which key into one another on all four faces and which, by their plan geometry when keyed together, resist the spread of joints parallel to both the longitudinal and transverse axes of the joints.

Category B: Comprises indented units which key into one another on two faces only and which, when keyed together, resist the spread of joints parallel to the longitudinal axes of the units but rely on their dimensional accuracy of laying to interlock on the other faces.

Category C: Comprises non-indented units which do not key together and which rely on their dimensional and laying accuracy to develop interlock.

Examples of some of the block shapes available today, following the above classification, were illustrated in Figure D2-2. In the Australian design method it is assumed that only Category A blocks are suitable for moderate to heavy traffic intensities in excess of 150 heavy vehicles per day.

Block size: Some evidence exists to indicate that block size has limited influence on performance. The unit size should be such that it fits comfortably into a person's hand: experience has shown that larger units are not suited for hand laying and may crack in service.

Block thickness: Accelerated pavement testing in Australia, South Africa, USA and Japan has shown that an increase in block thickness is beneficial to pavement performance. Typical results are shown in Figure D2-5. Experience has shown that it is possible to standardise block thickness to 80 mm for road pavements and then to vary base type and thickness to accommodate the design requirements.

Figure D2-5
Influence of block thickness on mean rut depth

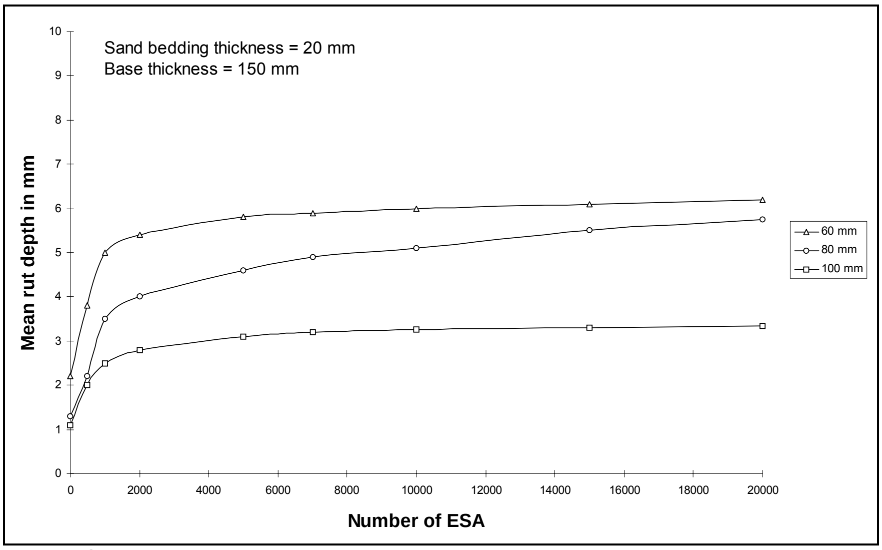

Source: Shackel (1982)

Laying pattern: Of the various block shapes, some can only be laid in a stretcher bond. Some of the shapes can, however, be installed in any of the three patterns illustrated in Figure D2-6.

Figure D2-6
Common block laying patterns

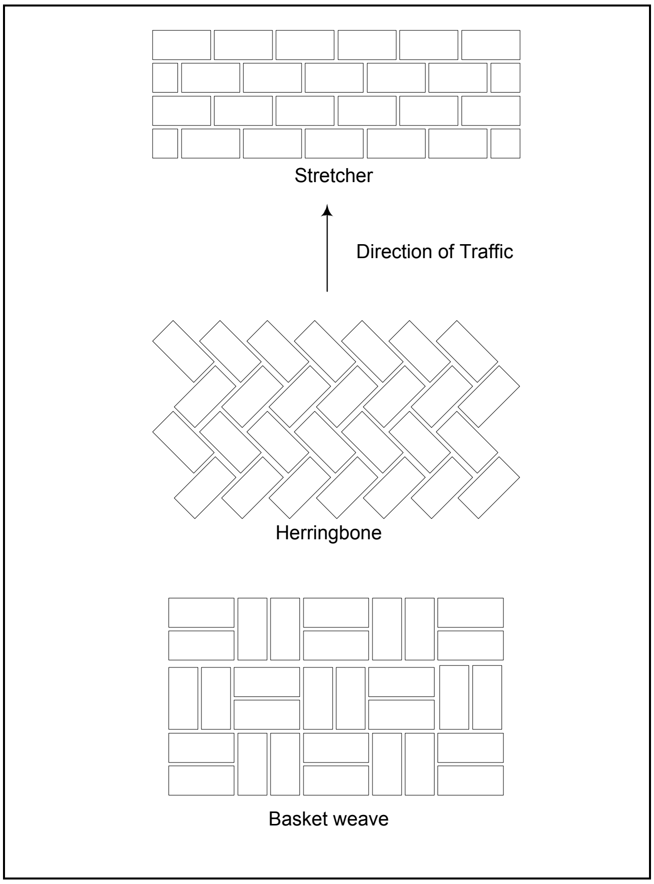

The best performance (smallest deformations) under traffic were found in pavements laid in herringbone bond, and the worst (largest deformations) were found in pavements with stretcher bond, particularly when the bond lies along rather than across the direction of travel. The differences in performance are illustrated in Figure D2-7.

Figure D2-7
Influence of laying pattern on mean rut depth

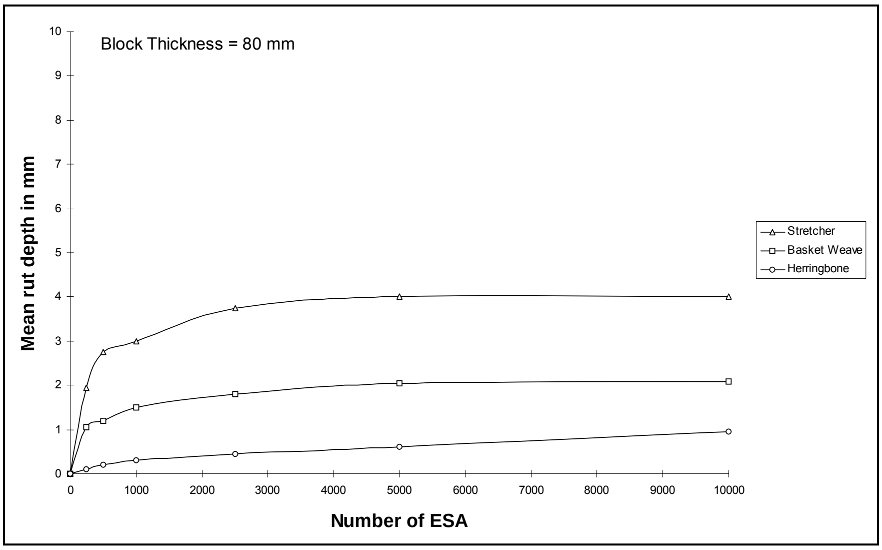

Source: Shackel (1980)

D2.2.2 Bedding and Joint Filling Sand

Bedding sand acts both as a barrier against the propagation of cracks from the base to the pavement surface and as a construction expedient providing a smooth surface on which to lay and bed the blocks. It is also the source of sand to fill the lower portions of the joints. The following properties of this sand layer have been identified as crucial to the performance of block pavements under traffic:

Thickness of bedding sand: Traditionally, a thickness of 50 mm after compaction was used, based on European practice. However, accelerated testing in South Africa, Australia and Japan showed that early traffic-associated deformations decrease with a decrease in sand layer thickness. This finding, illustrated Figure D2-8, was subsequently confirmed in field trials. This resulted in recommendations that the bedding sand layer should be between 20 to 40 mm after compaction, as included in the design manuals of South Africa, Australia and New Zealand. It was also recommended that the thickness of this sand layer should be uniform, since tests had shown that if this layer was allowed to vary, the density after compaction would also vary, resulting in an uneven deformation under traffic and thus increased roughness.

Grading of the sand: If the grading of the bedding sand conforms to the limits specified in CCANZ (1988), the deformations associated with the bedding sand layer tend to be very small (typically less than 3 mm). However, should an unsuitable sand be used the performance of the pavement may be adversely affected and, in some cases, a complete failure may occur under traffic (Shackel, 1980). In particular, the use of sands containing plastic fines should be avoided. Accelerated trafficking data suggest that the grading of the jointing sand is not crucial to the performance of a block pavement (Shackel, 1980).

Figure D2-8
Influence of bedding sand thickness on mean rut depth

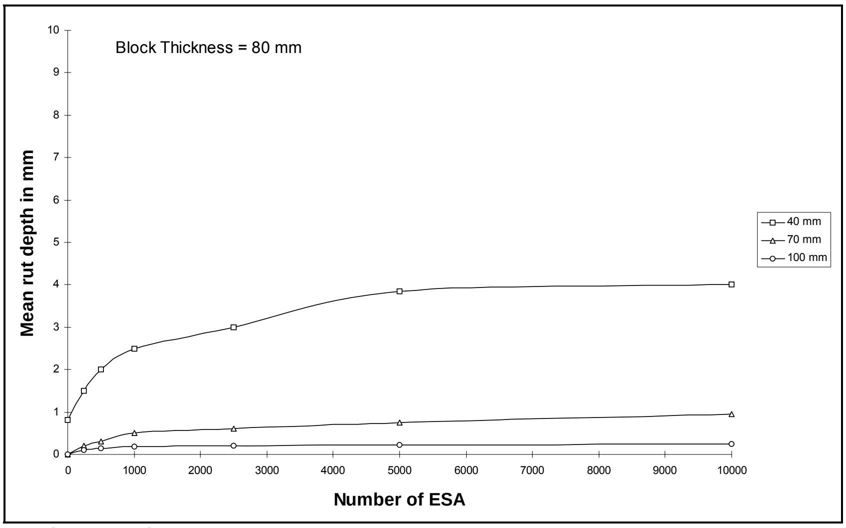

Source: Shackel (1980)

Angularity of the sand: It has been found that for similar sand gradings, block pavements laid on angular sands performed better than pavements laid on rounded sands (Shackel, 1980). The sand exhibiting the highest angle of shearing resistance should normally be used as bedding sand. The sands also should be selected such that they will not degrade under traffic. In contrast the joint filling sand should be rounded to ensure the complete filling of block pavement joints, a crucial factor in the performance of block pavements.

Moisture content of bedding sand: The moisture content of the bedding sand is of special importance during construction. A moisture content of 4 to 8 per cent has been found to be suitable (CCANZ, 1988). The variations in moisture content should be kept as low as possible, since large variations may result in different behaviour under compaction which could affect the final roughness. The sand used for joint filling should be as dry as possible to ensure complete joint filling, otherwise bridging within the joints can occur which will prevent complete filling. This will adversely affect the performance of the pavement.

D2.2.3 Base and Sub-base

Most of the base and sub-base types used for flexible pavements have also been used successfully for block pavements. As with flexible pavements, the following factors regarding the base and sub-base influence the performance under traffic:

Material type: An important factor to be considered, especially during the selection of the base material, is the probability of water ingress through the block surface layer. This has resulted in the more frequent use of non-water susceptible bases such as soil-cements and even asphalt concrete layers in humid areas. The effect of base-course type on the performance of block pavements is illustrated in Figure D2-9. From this illustration it is evident that the performance of block pavements tends to be similar to that of flexible pavements; cement-treated bases seem to perform better than crushed rock bases which, in turn, perform better than natural gravels.

Thickness: The selection of base or sub-base thickness has been identified as the prime requirement of block pavement design. The effect of base-course thickness on the performance of block pavements is illustrated in Figure D2-10. Although a change in block thickness has a more significant effect on pavement performance than a corresponding change in base thickness, the difference in cost/unit depth for base and sub-base are normally far less than that of the block layer, making it more economical to use a thicker base-course than thicker pavers.

Figure D2-9
Influence of base type on mean rut depth

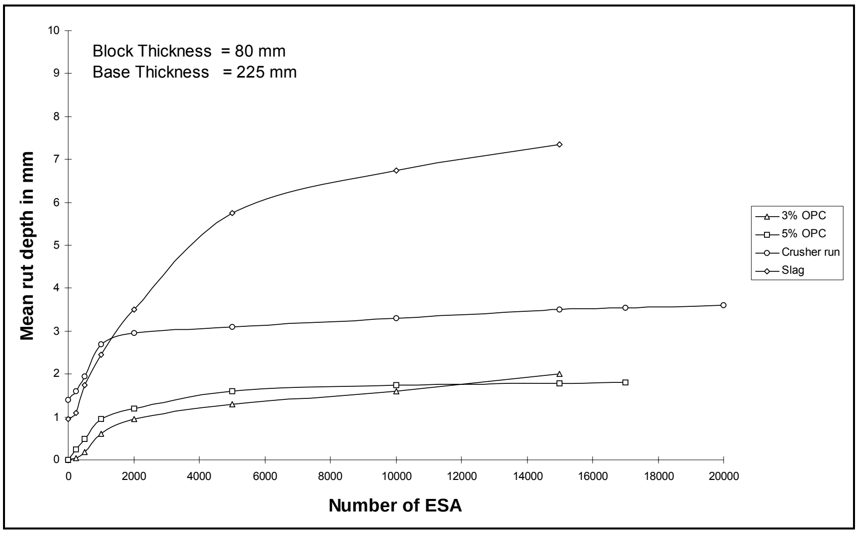

Source: Shackel (1990)

Figure D2-10
Effects of base thickness on mean rut depth

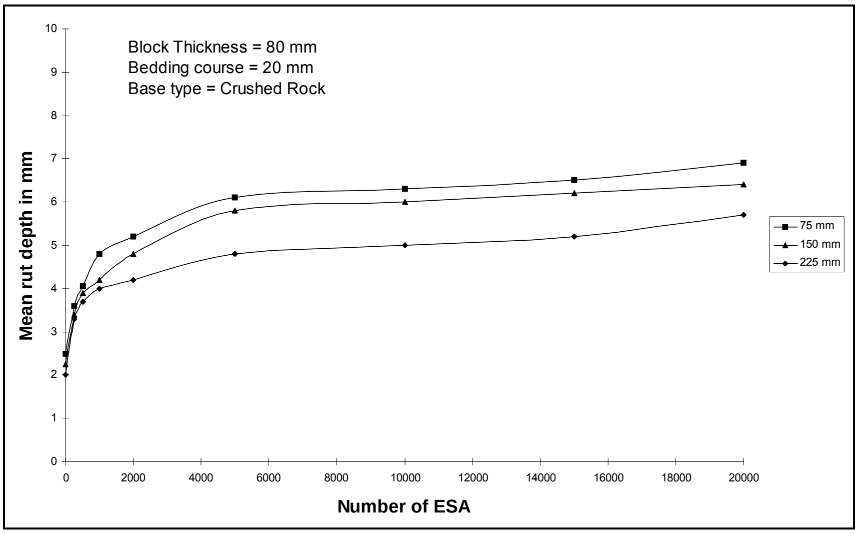

Source: Shackel (1990)

D2.2.4 Subgrade

As expected, the subgrade treatment appropriate for a block pavement is little different to that needed for a conventional flexible pavement. However, block pavements tend to be constructed on poorer subgrades, especially in Europe where 80 per cent of block pavements are constructed on subgrades with CBR below 3 per cent. This is possible because of the result of better load spreading capabilities of the block layer.

D2.2.5 Lock-up

Lock-up is a term used to refer to the progressive stiffening of a block pavement layer under traffic, resulting from the progressive wedging action between the blocks (Shackel, 1979) and the blocks being locked together by the friction of the joint sand between the blocks (CCANZ, 1988). With an increase in the amount of lock-up, the structural behaviour of the concrete blocks changes from truly flexible to semi-rigid, allowing the block layer to act as a solid mat in spreading applied loads. This allows the concrete blocks to transfer shear through the joints and to provide a degree of interlock resulting in smaller deflections, and thus a reduction in the rate of accumulation of permanent deformation. This behaviour is highly dependent on the joints being just wide enough to let sand in, but narrow enough to allow the joint sand to lock the blocks together during construction vibration and subsequent trafficking (CCANZ, 1988). It is also dependent on the degree of base support. The following three base support conditions can be identified (Kuipers, 1992):

Unyielding: This refers to the typical support provided by a high quality crushed stone and/or heavily stabilised pavement structure. In this instance, the paving blocks merely act as a wearing course and the deflections under the wheels range from very small to zero with the block pavement layer not called upon to spread the load.

Very Weak to Zero: This refers to the situation where virtually no support is provided by the base and it is the block pavement layer that is required to distribute a heavy load over a large area. This may well exceed the capacity of the blocks to sustain the subsequent stresses, shears and rotations. The block pavement layer then fails in the joints, resulting in deformation and, in severe instances, chipping of the paving blocks.

Balanced: This refers to the situation where the support provided by the base is approximately matched by the load spreading capability of the block pavement layer, resulting in the maximum utilisation of the structural capabilities of the block layer.

The above three base support conditions are illustrated in Figure D2-11. It is believed that a balanced condition will seldom be attained. In general the block pavement layer will be under utilised, with a few instances in which balance will be exceeded, resulting in the failure of the pavement. The influence on deformation of the development of lock-up within a block pavement is illustrated in Figure D2-12. As shown, once the pavement has accumulated sufficient deformation to cause the wedging of the blocks, the loads on the pavement can be considerably increased without causing any significant further deformation. This type of behaviour seems to be unique to block pavements.

D2.2.6 Water Ingress

Block pavements, particularly in their early life, are not entirely waterproof. Work in the Netherlands has demonstrated that the infiltration of water through joints in a pavement can amount to about 45 per cent of the annual rainfall. If suitable preventive measures (for example, the use of moisture resistant materials to seal the base) are not used, this infiltration can lead to a significant loss in performance. This water mostly penetrates through the joints since the blocks themselves can be regarded as being impermeable. With time, the joints become clogged with detritus, rubber and oil, resulting in such a decrease in their permeability that the pavement can be considered as substantially waterproof, provided there is no ponding of water on the surface (Clifford, 1981). To avoid ponding it is recommended that a crossfall of at least 3 per cent be provided (CCANZ, 1989).

Figure D2-11
Illustration of base support conditions

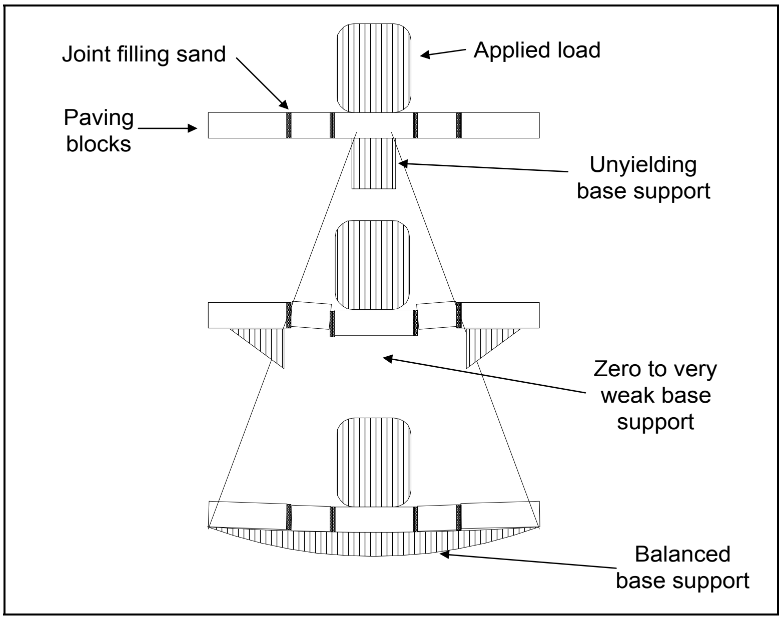

Source: Kuipers (1992)

Figure D2-12
Influence of lock-up on block pavement deformation

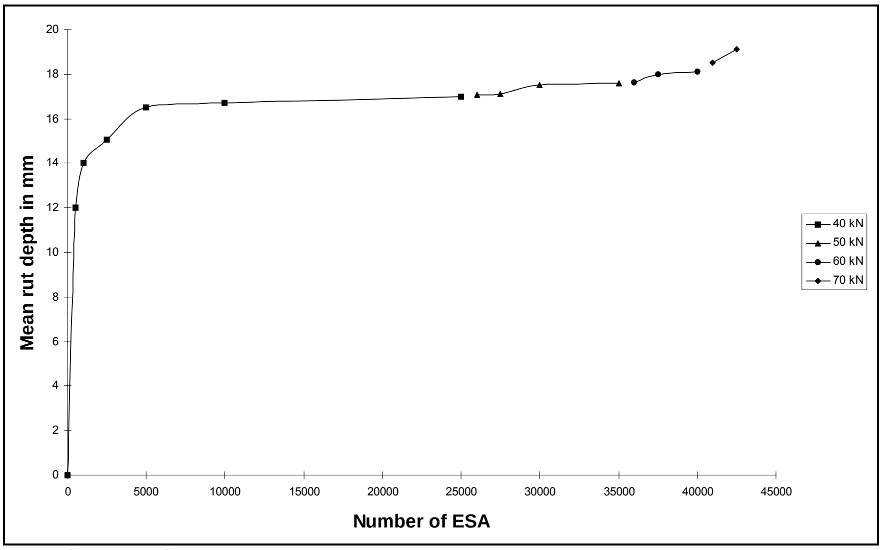

Source: Shackel (1979)

D2.2.7 Compaction

As with flexible pavements, the selection and application of compaction standards is vital to the subsequent performance of a block pavement. Effective compaction improves subgrade, sub-base, base course and bedding sand bearing capacity and stability, decreases permeability and reduces long term settlement and rutting. Inadequate compaction is a common cause of block pavement failures (Shackel, 1990). In all instances the material used and compaction standards required should comply with the requirements for flexible pavements in similar conditions.

D2.3 Methods of Predicting Block Pavement Performance

The amount of research conducted into the performance of concrete block pavements is far less than for asphalt and concrete pavements. Many models developed from pavement research are failure limit models used for design and these are inappropriate for life cycle predictions of pavement performance. A further limitation in the case of block paving is that most of the research has concentrated on deformation (rutting) with little study of roughness or surface texture. Some of the available studies are described below.

D2.3.1 Dutch Design Method

This design method is based on the analysis of Falling Weight Deflectometer (FWD) deflections and rutting measurements on various pavement sections within the Netherlands. According to the research, the development of rutting within the pavement sections could be described by the following method (Houben, et al, 1992):

$$Rd_c = a_0\, NE3^{\,a1} \qquad \text{. . . (D2.1)}$$

where

Rd_c = characteristic rut depth, being the value used for end of life condition, equal to 15 mm with a 30 per cent probability of exceeding

NE3 = cumulative number of equivalent 80 kN standard axle load repetitions (equivalency exponent of 3) per lane in the wheel track (channelised traffic)

a_0 and a_1 are coefficients that describe the pavement structure

The pavement coefficients were derived from the base and sub-base type and thickness, and the subgrade modulus. The modulus of elasticity (E_{sg}) of the subgrade was calculated from FWD measurements by means of the following equation:

$$\log_{10} E_{sg} = 3.869 - 1.009 \log d_2 \qquad \text{. . . (D2.2)}$$

where

E_{sg} = subgrade modulus of elasticity, in N/mm^2

d_2 = deflection at a distance of 2 m from centre of a 50 kN load, in microns

From the analysis of the pavement sections monitored over a period of 4 to 9 years the coefficients in Table D2-2 were obtained.

Table D2-2
Coefficients for pavement sections

Pavement section	Base Thick/Type (mm)	Sub-base Thick/Type (mm)	Subgrade modulus (N/mm^2)	NE3 per year	a0	a1
A2	250/CC	450/SA	30	5730	2.867	0.156
R1+R2	-	900/SA	69	110520	0.176	0.358
R3+R4	300/CC	600/SA	72	110520	0.140	0.314
R5+R6	300/CB	580/SA	75	110520	0.132	0.314
E1 (i-s)	-	870/SA	103	324820	1.376	0.181
E1(s-i)	-	870/SA	103	138580	0..913	0.196
E2(i-s)	150/CC	720/SA	120	324820	2.646	0.054
E2(s-i)	150/CC	720/SA	120	138580	0.195	0.205
E3(i-s)	300/CC	570/SA	139	324820	1.162	0.142
E3(s-i)	300/CC	570/SA	139	138580	1.913	0.069
E01(i-s)	300/CB	570/SA	155	324820	1.762	0.052
E01(s-i)	300/CB	570/SA	155	138580	1.805	0.037

Notes: CC - Crushed Concrete Base, CB - Crushed Concrete / Crushed Clay Brick Base
SA - Sand Sub-base

This research is the most comprehensive identified on in-service pavements. Typical predictions for some of the pavement types over their valid traffic range are illustrated in Figure D2-13. The influence of base support, as previously discussed, is obvious and also the lock-up of the balanced pavements.

Figure D2-13
Illustration of model predictions over their valid range

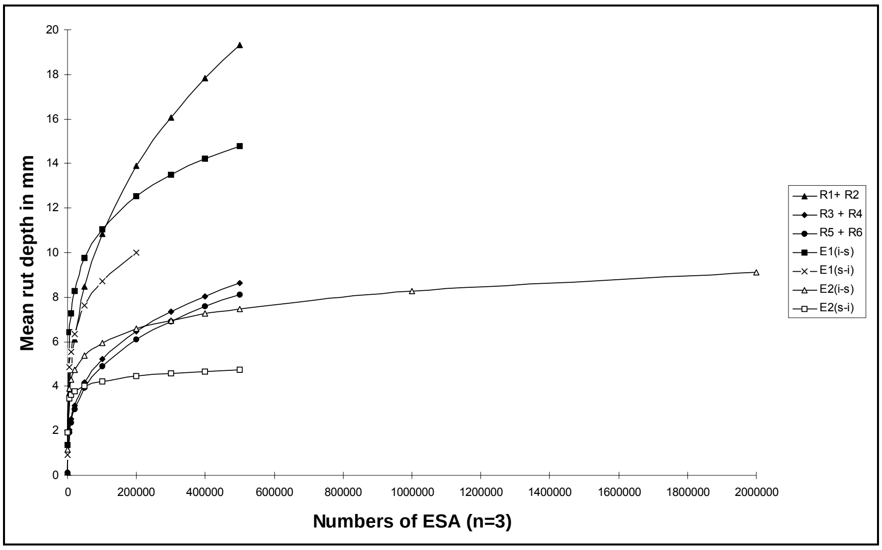

D2.3.2 Research in Denmark

Research in Denmark comprised a series of three annual measurements of skid resistance and two of roughness on a 1.3 km long climbing lane in which vehicles travelled up to 90 km/h (Lekso, 1982). The only conclusions made from the results were that the standards, in terms of roughness, normally expected for speeds of 90 km/h were not met, and that sections which were uneven after construction tended to even out under traffic. For the skid measurements, recorded with a stradograph, there was a major fall in the first year but the levels still remained satisfactory.

D2.3.3 Other Studies

At this stage no other life cycle performance models have been identified, except for one-off experiments consisting of one or two measurements of roughness, skid resistance or rutting. Unfortunately, for most of these measurements, no other data were collected, for example on traffic levels or rainfall.

D3. Proposed Block Pavement Models for HDM-4

From the evaluation of available literature during the original ISOHDM study, only a single attempt at predicting the life cycle performance of a block pavement could be identified; the Dutch rut depth model described above. After discussions with various leading experts in the field of block pavement performance, the ISOHDM project team concluded that block pavement models for HDM-4 should include the following essential components:

- a method of structural characterisation
- prediction of rut depth
- prediction of roughness
- prediction of skid resistance

Models to predict surface abrasion and chipping would be desirable, but were not considered essential in the context of HDM-4 modelling.

The lack of existing models meant that new generic models need to be developed since only the single attempt in developing a rut model was identified. The generic models developed should contain the various individual parameters influencing the life cycle performance of block pavements. The proposed generic models for the three distress modes considered essential – rutting, roughness and skid resistance – are described below.

D3.1 Structural Characterisation of Block Pavements

In HDM-4, the adjusted structural number (SNP) has been used to provide an indicator of total pavement strength of bituminous surfaced pavements, as described in Section B2.2. Apart from the top layer, the structure of a block pavement is generally similar to that of a bituminous pavement and it is considered that SNP is the most appropriate way to characterise the strength of such pavements.

The estimation of SNP for block pavement is given by:

$$SNP = SN_{PL} + SN_{BL} \qquad \text{. . . (D3.1)}$$

where

SNP = adjusted structural number of the pavement

SN_{PL} = structural number based on the contribution of the pavement layers including subgrade, but excluding the block layer

SN_{BL} = contribution to the structural strength of the pavement by the block layer

The base and lower layers of a block pavement are normally constructed using the same materials types as bituminous surfaced pavements. Thus the methodology for deriving structural number for these layers, presented in Section B2.2, is equally applicable in this context.

When considering the contribution of the block layer to the structural number it is important to consider the factors identified earlier as influencing the performance of the paving block layer (thus affecting the structural contribution of paving block layer). These were:

- block shape
- block thickness
- block laying pattern

It is proposed that the influence of these factors be incorporated within the structural contribution term of the paving block layer (SN_{BL}) as follows:

$SN_{BL} = a_0\, a_1\, (BTHICK)\, \min(NE4, 0.01)$ . . . (D3.2)

where

BTHICK = thickness of the paving block, in mm
NE4 = cumulative number of equivalent standard axle loads, in million ESA. It is assumed that lock-up occurs after the first 0.01 million ESA
a_0 = coefficient for the influence of block shape (see Table D3-1)
a_1 = coefficient for the influence of the laying pattern (see Table D3-2)

Table D3-1
Coefficient for influence of block shape on SN_{BL}

Paving block shape	a_0
Indented	2.29
Rectangular	1.76

Note: These coefficients are based on assumptions that relative strength contribution of indented and rectangular paving blocks are 1.3 and 1.0 times respectively that of an asphalt layer with a strength coefficient of 0.44

Table D3-2
Coefficient for influence of laying pattern on SN_{BL}

Paving block laying pattern	a_1
Herringbone	1.0
Basket weave	0.75
Stretcher bond	0.25

Source: Based on results obtained by Shackel (1980)

D3.2 Rut Depth Prediction

The rutting model for block pavements should, as far as is consistent with observed performance, follow the broad mechanisms and use the model parameters already described for bituminous surfacings. Therefore, a model consisting of the following three phases is proposed:

- an initial densification phase (bedding in phase) of the new pavement layers under traffic until lock-up of the blocks occur
- a stable phase during which there is a relatively small increase in deformation over time or traffic
- a final phase of accelerated deformation: from the current state of knowledge there seems to be no certainty about the exact mechanisms during this final phase

The following component model, similar to that for flexible pavements is proposed:

$RDM = RDO + RDST$ . . . (D3.3)

where

RDM = mean rut depth, under a 2 m straight-edge, in mm
RDO = initial densification, in mm
RDST = structural deformation under traffic, in mm

D3.2.1 Initial Densification

Only the single model developed in the Netherlands (Houben, et al, 1992) is currently available. Although this model predicts the deterioration observed for the specific test pavement sections, its applicability to other pavements will be limited by the fact that the variables influencing the difference in rutting from one location to another (i.e. environment) are not separately quantified within the model.

To overcome this problem it is proposed that the generic model should incorporate network level obtainable parameters. Based on the earlier discussions in this section and the models and parameters described elsewhere in this document, it is recommended that the following parameters be included:

- the applied traffic load (although there is an indication that an equivalency exponent of 3 should be used, for consistency within the HDM-4 model the fourth power ESA should also be applied in the models for block paving)
- structural strength of the pavement expressed as the adjusted structural number (SNP)
- relative compaction of the layers achieved during construction (COMP)
- environmental parameters (i.e. rainfall) (MMP)
- various block pavement parameters quantifying the difference in performance

The mechanism of early densification of the lower pavement layers is thought to be basically the same for any flexible surfacing, whether asphalt or block. Therefore the form of model already presented for bituminous pavements can be applied.

One difference between the application of this model to bituminous and to block surfacings is the permeability of the surface during the first year after construction. With bituminous pavements, cracking of the surface at this stage is an abnormal event. By comparison, block pavements are at their most porous at this stage, as discussed earlier. With age, the joints become clogged with fine materials and the porosity of the surfacing reduces.

The relationship for initial densification, RDO, of bituminous pavements used in HDM-4 (equation B8.12) is based on the HDM-III model (equation B8.5) with the cracking term removed. For block pavements the cracking term needs to be retained. It is tentatively suggested that the term ACX can be quantified as 50 per cent to represent the permeability of the block pavement during its early life.

The proposed relationship for initial densification of block pavements is:

$$RDO = K_{rid}\,[a_0\,(YE4\;10^6)^{(a1 + a2\,DEF + a3\,MMP)}\;SNP^{a4}\;COMP^{a5}] \qquad \text{. . . (D3.4)}$$

where

RDO = rutting due to initial densification, in mm
YE4 = annual number of equivalent standard axles, in millions/lane
DEF = average annual Benkelman beam deflection, in mm
SNP = average annual adjusted structural number of the pavement
COMP = relative compaction, in per cent (see Section B2.5)
MMP = mean monthly precipitation, in mm/month
K_{rid} = calibration factor for initial densification

In the absence of any field validation on this model, the default values for the coefficients have been derived from those for bituminous surfaced pavements, as shown in Table D3-3.

Table D3-3
Coefficient values for initial densification of block pavements

a_0	a_1	a_2	a_3	a_4	a_5
51740	0.09	0.0384	0.00008	-0.502	-2.30

D3.2.2 Structural Deformation

Shackel (1990) suggests that once lock-up occurs within a block pavement, subsequent performance is independent of traffic, thus allowing the use of similar principles to those used in the modelling of flexible pavements. The same view is, however, not shared by other block pavement model experts (Sharp and Armstrong, 1985). Thus, it was considered that the model should contain terms for non-traffic and traffic related increase in rut depth.

The structural deformation model for bituminous pavements consists of two components; i) without cracking (equation B8.13) and ii) after cracking (equation B8.14). Block pavements need to be considered as porous throughout their life, and therefore only the 'structural deformation after cracking' component would be appropriate for block pavements.

As stated for initial densification, a value of 50 per cent for ACX is suggested. Using this value of ACX in equation B8.14, the proposed relationship for structural deformation of block pavements is as follows:

$$\Delta RDST = K_{rst} [a_0 \; SNP^{a1} \; YE4^{a2} \; MMP^{a3}] \qquad \text{. . . (D3.5)}$$

where

$\Delta RDST$ = incremental increase in structural deformation in analysis year, in mm
SNP = average annual adjusted structural number of the pavement
YE4 = annual number of equivalent standard axles, in millions/lane
MMP = mean monthly precipitation, in mm/month
K_{rst} = calibration factor for structural deformation

The coefficient values a_0 to a_3 for the structural deformation model are given in Table D3-4.

Table D3-4
Coefficient values for structural deformation of block pavements

a_0	a_1	a_2	a_3
0.0019	-0.84	0.14	1.07

D3.2.3 Total Rut Depth

The annual incremental increase in total rut depth, ΔRDM, is derived as follows:

if $AGE4 \leq 1$

$$\Delta RDM = RDO + \Delta RDST \qquad \text{. . . (D3.6)}$$

otherwise

$$\Delta RDM = \Delta RDST \qquad \text{. . . (D3.7)}$$

where

ΔRDM = incremental increase in total mean rut depth in both wheelpaths in analysis year, in mm
RDO = initial densification
$\Delta RDST$ = incremental increase in structural deformation in analysis year, in mm

D3.2.4 Standard Deviation of Rut Depth

The model used for predicting the standard deviation of rut depth for bituminous pavements is proposed as the relationship for predicting RDS of block pavements.

$$\Delta RDS = K_{rds} \max [a_0, \; a_1 - a_2(RDM_b)] \; \Delta RDM \qquad \text{. . . (D3.8)}$$

where

ΔRDS = incremental change in rut depth standard deviation in analysis year, in mm
RDM_b = mean rut depth at end of analysis year, in mm
ΔRDM = change in mean rut depth during analysis year, in mm
K_{rds} = calibration factor for rut depth standard deviation

The coefficient values a_0 to a_2 for the rut depth standard deviation model are given in Table D3-5.

Table D3-5
Coefficient values for rut depth standard deviation model

Pavement Type	a_0	a_1	a_2
All pavement types	0.2	0.65	0.03

The rut depth standard deviation at the end of an analysis year is given by:

$$RDS_b = RDS_a + \Delta RDS \qquad \text{. . . (D3.9)}$$

where

RDS_b = rut depth standard deviation at end of analysis year, in mm
RDS_a = rut depth standard deviation at start of analysis year, in mm
ΔRDS = incremental change in rut depth standard deviation in analysis year, in mm

D3.3 Roughness Progression

No model for predicting roughness on block pavements has been identified. The only information available seems to be occasional measurements indicating that roughness levels on block pavements are higher than on flexible pavements. It is proposed that a similar component incremental roughness model be adopted for block pavements as used for predicting the roughness of bituminous pavements. The higher roughness levels for block pavements can be accommodated in the initial roughness values set by the user.

For block pavements, neither cracking nor potholing is currently modelled. Therefore it is proposed that the roughness model for block pavements includes only the structural, rutting and environmental components used for bituminous pavements.

D3.3.1 Structural Component

The structural component of roughness for bituminous pavements includes a term for the reduction in adjusted structural number due to cracking. For block pavements, a constant level of cracking (50%) has been assumed (see Section D3.2.1). Therefore the reduction in SNP due to cracking term is not required for block pavements.

The structural component of roughness for block pavements is proposed as:

$$\Delta RI_s = K_{gs}\, a_0 \exp(m\, K_{gm}\, AGE3)\, (1 + SNP_a)^{-5}\, YE4 \qquad \text{. . . (D3.10)}$$

where

ΔRI_s = incremental change in roughness due to structural deterioration during analysis year, in m/km IRI
SNP_a = adjusted structural number at start of analysis year
$AGE3$ = age since last reconstruction, in years
$YE4$ = annual number of equivalent standard axles, in millions/lane
m = environmental coefficient (see Table B10-3)

K_{gm} = calibration factor for environmental coefficient
K_{gs} = calibration factor for the structural component of roughness

D3.3.2 Rutting Component

As for bituminous pavements, the proposed incremental increase in roughness due to rutting of block pavements is a function of the standard deviation of rut depth.

The proposed rutting component of roughness is given by:

$$\Delta RI_r = K_{gr} \, a_0 \, (RDS_b - RDS_a) \quad \text{. . . (D3.11)}$$

where

ΔRI_r = incremental change in roughness due to rutting during analysis year, in m/km IRI
RDS_b = standard deviation of rut depth at end of analysis year, in mm
RDS_a = standard deviation of rut depth at start of analysis year, in mm
K_{gr} = calibration factor for the rutting component of roughness

D3.3.3 Environmental Component

The proposed environmental component of roughness for block pavements is given by:

$$\Delta RI_e = K_{gm} \, m \, RI_a \quad \text{. . . (D3.12)}$$

where

ΔRI_e = incremental change in roughness due to environment during analysis year, in m/km IRI
RI_a = roughness at the start of the analysis year, in m/km IRI
m = environmental coefficient (see Table B10-3)
K_{gm} = calibration factor for the environmental component

D3.3.4 Total Change in Roughness

The total annual incremental change in roughness is the sum of the various components described above.

The total incremental change in roughness in HDM-4 is given by:

$$\Delta RI = \Delta RI_s + \Delta RI_r + \Delta RI_e \quad \text{. . . (D3.13)}$$

where

ΔRI = total incremental change in roughness during analysis year, in m/km IRI
and the other variables are as defined previously

The coefficient values for the various roughness components are given in Table D3-6.

Table D3-6
Coefficient values for roughness components

Roughness Component	Equation	a_0
Structural	D3.9	134
Rutting	D3.10	0.088

D3.3.5 End of Year Roughness

Two end-of-year roughness values are derived for bituminous pavements; one is used for triggering works effects and the other is used in the road user effects sub-model. It is proposed that the same principle is adopted for block pavements.

D3.3.5.1 Pavement Roughness for Works Effects

The roughness of the pavement at the end of an analysis year, for use as a trigger level in the Works Effects sub-model, is derived as follows:

$$RI_b = \min [(RI_a + \Delta RI), \ a_0] \qquad \text{. . . (D3.14)}$$

where

RI_b = roughness of the pavement at end of the analysis period, in m/km IRI
RI_a = roughness of the pavement at start of the analysis period, in m/km IRI
ΔRI = total incremental change in roughness during analysis year, in m/km IRI
a_0 = user specified upper limit of pavement roughness (default = 20)

A default value of 20 m/km IRI for the upper limit of roughness for block pavements is proposed, as indicated by the default value of a_0 in the above relationship. It is also proposed that the user should have the option to increase this value.

D3.3.5.2 Effective Roughness for Road User Effects

On narrow roads vehicles may be forced to make partial use of the shoulders when meeting oncoming traffic or when overtaking. If the shoulders are unsealed they will normally have a higher roughness than the pavement itself and therefore the 'effective roughness' experienced by a vehicle will also be higher. Effective roughness is a function of pavement and shoulder roughness and the proportion of time vehicles spend using the shoulder.

The following relationships are proposed, based on those derived for bituminous pavements.

$$RI_{eff} = RI_b + (RI_{sh} - RI_b) \left(\frac{\delta t_{sh}}{2} \right) \qquad \text{. . . (D3.15)}$$

where

$$\delta t_{sh} = 58(PSH)\,(AADT)\,10^{-6} \qquad \text{. . . (D3.16)}$$

and

RI_{eff} = effective roughness from use of shoulder, in m/km IRI
RI_b = roughness of the pavement at end of the analysis period, in m/km IRI
RI_{sh} = roughness of the shoulder at end of the analysis period, in m/km IRI
δt_{sh} = proportion of time vehicles use the shoulder due to road width and traffic volume
PSH = proportion of time vehicles use the shoulder due to road width (see equation B6.8 in the edge break model – Section B6.3)
AADT = average annual daily two way traffic, in veh/day

The effective roughness as specified in equation D3.15 is the roughness value for block pavements proposed for use in the Road User Effects sub-model at the end of each analysis period.

D3.4 Pavement Texture

As described in Section B11, a road surface exhibits two types of texture, classified as macrotexture and microtexture. Macrotexture is normally an interest on high speed roads.

As block paving is, with rare exceptions, used only in areas where traffic is moving relatively slowly, it is proposed that only microtexture needs be modelled for block pavements.

The modelling of sideway force coefficient, SFC, on bituminous roads is described in Section B11.3.2. Although this model may not be directly applicable to block pavements, it is proposed that it is considered for use for block pavements pending further research in this area. The relationships used for modelling SFC on bituminous pavements are re-produced below.

The annual incremental change in skid resistance is modelled as follows:

$$\Delta SFC_{50} = K_{sfc} \max(0, \Delta QCV)(-0.663 \times 10^{-4}) \qquad \text{. . . (D3.17)}$$

where

ΔSFC_{50} = incremental change in sideway force coefficient during analysis year, measured at 50 km/h

ΔQCV = annual incremental increase in the flow of commercial vehicles, in veh/lane/day

K_{sfc} = calibration factor for skid resistance

The skid resistance measured at 50 km/h at the end of the analysis year is given by the following expression:

$$SFC_{50b} = \max[(SFC_{50a} + \Delta SFC_{50}),\ 0.35] \qquad \text{. . . (D3.18)}$$

where

SFC_{50b} = sideway force coefficient measured at 50 km/h at end of analysis year

SFC_{50a} = sideway force coefficient measured at 50 km/h at start of analysis year

ΔSFC_{50} = incremental change in sideway force coefficient measured at 50 km/h during analysis year

The annual skid resistance value for a given analysis year is calculated as follows:

$$SFC_{50av} = 0.5\,(SFC_{50a} + SFC_{50b}) \qquad \text{. . . (D3.19)}$$

where

SFC_{50av} = annual average side force coefficient measured at 50 km/h for the analysis year

The average skid resistance value at a given annual average traffic speed is calculated as follows:

$$SFC_s = K_{sfcs}\left\{\frac{SFC_{50av}\left[400 - \left(2 - \min(TD_{av}, 2)\right)\left(\max(50, S) - 50\right)\right]}{400}\right\} \qquad \text{. . . (D3.20)}$$

where

SFC_s = sideway force coefficient measured at a speed of S km/h

S = traffic speed, in km/h

K_{sfcs} = calibration factor for skid resistance speed effects

and the other variables are as previously defined

The user needs to define a value of SFC_{50} in order for skid resistance modelling to be performed. This also needs to be supplied after maintenance treatments.

D3.5 Summary

This Section introduced the subject of block pavements and examined available research that may form the basis for performance prediction models in HDM-4. The basis for such models is extremely limited, most performance studies of block pavements being limited to deformation. Tentative model forms have been proposed, based primarily on those used for bituminous pavements. By including the relationships in this version of Volume 6, it is hoped that comments will be received from the peer review, with the objective of including the modelling of block pavements in HDM-4.

PART E. UNSEALED ROADS

The focus of the ISOHDM study was to improve the deterioration and maintenance models for bituminous pavements, and introduce new models for concrete pavements. These have been described in Parts B and C respectively. The models for unsealed roads were not examined during the ISOHDM study and therefore the models incorporated in HDM-4 are effectively those in HDM-III. This part of the document describes the modelling of the deterioration and maintenance of unsealed roads, primarily based on the descriptions and specifications used for HDM-III, given in Paterson (1987) and Watanatada, et al (1987).

E1. CLASSIFICATION

Unsealed roads are broadly classified into engineered roads or tracks, with gravel or earth surfacings, since these factors influence both the level of service and the deterioration of the road. Engineered roads have controlled alignment, formation width, cross-section profile and drainage, whereas tracks are essentially ways formed by trafficking along natural contours with or without the removal of topsoil. Unsealed roads classified in a country's network are usually engineered or partly engineered, and tracks are usually not classified.

Generally, unsealed roads carry low volumes of traffic ranging from a few vehicles to several hundred vehicles per day. The deterioration and maintenance effects models for unsealed roads in HDM are designed primarily for engineered roads rather than tracks, because the empirical data used to derive the models were based on a variety of such roads. In some instances, the models may be applicable to tracks as a first estimate, but the user needs to be aware that the environmental effects of drainage and rainfall may be poorly represented for tracks in regions where these factors are important.

A variety of definitions have been used to classify unsealed roads into gravel and earth roads. The term “earth road” is sometimes used to denote a track as opposed to an engineered road. In the Kenya study of road deterioration, “earth road” described all unsealed engineered roads for which the surfacing material was outside the material gradation specification for gravels of the Kenya Ministry of Works (Hodges, et al, 1975). In the Brazil study “earth road” denoted those unsealed roads having a surface of predominantly fine soil materials with more than 35 per cent finer than 0.075 mm particle size (GEIPOT, 1982). In HDM-III, this last definition was adopted because of its simple physical definition and transferability, and because the Brazilian data were used as the primary database.

E2. DETERIORATION AND MAINTENANCE CONCEPTS

E2.1 Deterioration Mechanisms

The deterioration of unsealed roads is governed by the behaviour of the surfacing material and the roadbed under the combined actions of traffic and the environment. The surfacing is typically 100 to 300 mm thick and serves as both the wearing course and the basecourse of the pavement, providing sufficient structural strength and cover thickness to distribute the applied traffic loads to the roadbed material. As the surfacing comprises a natural material, it is usually permeable although in some cases the permeability may be very low, such as in densely-graded plastic gravel or cemented material. Thus material properties, rainfall, and surface drainage influence the behaviour of the surfacing under traffic; likewise, surface water runoff and side drainage usually affect the moisture penetration to the roadbed and thus its bearing capacity.

There are three fundamental mechanisms of deterioration:

- wear and abrasion of the surface material under traffic
- deformation of the surface and roadbed material under the stresses induced by traffic loading and moisture condition
- erosion of the surface by traffic, water and wind

Consequently, the modes of deterioration differ in dry weather and wet weather, and also depend on the strength of the surfacing and roadbed material, which are most critical in wet weather. The modes and the approaches for modelling thus can be placed in four categories as follows (Visser, 1981):

Dry weather deterioration

Under dry weather conditions, the most prominent deterioration mechanisms are:

- Wear and abrasion of the surface, which generates loose material and develops ruts.
- Loss of the surfacing material by whip-off and dust.
- Movement of loose material into corrugations under traffic action.
- Ravelling of the surface, in cases where there is insufficient cohesion in the material to keep the surface intact. This could be caused either by the abrasive action of vehicle tyres, or by injudicious blading of the surface. At points where ravelling occurs, tyre action continues the abrasion process, and loose material is removed from the abraded areas. This results in depressions and increased roughness.

These mechanisms result in roughness and material loss, the rates of deterioration being primarily a function of the properties of the surfacing material.

Wet weather deterioration of adequate pavements

Under wet weather conditions the shear strengths of the materials determine the pattern of deterioration. When the shear strengths of the surfacing and roadbed materials are adequate for the stresses induced by traffic, deterioration occurs only at the surface. This is prevalent in regions where either road drainage Is good, or good quality materials are found. The major modes of deterioration under these conditions are:

- Environmental and traffic Influences on surface erosion.
- Wear and abrasion of the surface by traffic causing rutting and loss of the surfacing material.
- Formation of potholes under traffic action. Free water on the surface accumulates in the depressions, and the passage of a vehicle tyre stirs up the water causing fine material to pass into suspension. Water, with the suspended fine material, is also forced out of the depression. Under the action of many wheel passages and sufficient water, this is a rapidly accelerating phenomenon.

Wet weather deterioration with weak surfacing layer

When the surfacing layer has inadequate shear strength under the operative drainage conditions to sustain the stresses applied by traffic loadings, shear failure and deformation occur. The road surface will be soft and slushy under wet conditions so that, while it may be possible for a few light vehicles to pass, the road will become impassable after a relatively small number of vehicle passages. Traditionally, a simple shear strength test such as the California Bearing Ratio (CBR) has been used to identify materials that resist shear failures, but other material properties such as plasticity and fineness also influence the behaviour under these conditions.

Empirical studies by Visser (1981) showed that the soaked CBR of the surfacing material was the most reliable indicator of passability, and preferable to the plasticity index or percentage of fines. The proposed criteria for ensuring that a road remains passable during a wet season (given there is no flooding) was as follows:

$$SFCBR > 8.25 + 3.75 \log_{10}(ADT) \qquad \text{. . . (E2.1)}$$

where

SFCBR = soaked California Bearing Ratio at standard AASHTO compaction, in per cent, which is the minimum for ensuring passability

ADT = average daily traffic in both directions, in vehicles per day.

Wet weather deterioration with weak roadbed material

Where the in situ roadbed soil is weak, a pavement needs to be placed to protect the roadbed and limit the deformation developing under traffic to acceptable levels. When the pavement is inadequate and the subgrade or roadbed is over stressed, deterioration takes the form of rutting, or permanent deformation in the wheelpaths. This type of deterioration is prevalent in areas of poor surface and subsurface drainage, or during spring thaw conditions in freezing climates when the roadbed reaches relatively high moisture contents, or in areas of weak soils when design standards are inadequate.

The thickness and stiffness of the pavement layer(s) (typically only one layer, the surfacing, is required for unsealed roads) need to be sufficient to distribute the applied loads so that the stresses and strains induced within the roadbed have been reduced to levels at which the permanent deformation of the roadbed material is acceptable. These stress levels depend to a large extent on the volume and loading of traffic, and the shear strength of the roadbed material in situ, which in turn, depends on the compacted density and moisture content associated with the climate and drainage conditions.

The thickness and material strength required have been determined by empirical methods. For example, the criteria developed by the United States Corps of Engineers for the thickness of cover required depending on the strengths of the roadbed and surfacings materials can be expressed as follows (based on Hammitt, 1970 and Barber, et al, 1978):

$$\log_{10}HG = 1.4 + 12.3\ C1^{-0.466}\ C2^{-0.142}\ NE^{0.124}\ RD^{-0.5} \qquad \text{. . . (E2.2)}$$

where

HG	=	thickness of gravel surfacing, in mm
C1	=	soaked CBR of surfacing material, in per cent
C2	=	soaked CBR of roadbed soil, in per cent
NE	=	design number of cumulative equivalent 40 kN single wheel loads at 550 kPa tyre pressure
RD	=	maximum allowable mean rut depth, in mm

In the more general case, the coefficient 12.3 was replaced by:

$$0.856\ P^{0.235}\ Q^{0.285}$$

where

P	=	equivalent single wheel load, in kN
Q	=	tyre pressure, in kPa

and NE is replaced by N, the number of coverages of load (P, Q)

E2.2 Modes of Distress

For unsealed roads with generally adequate material specifications and pavement thickness, the principal modes of distress are:

- **Roughness**, which increases over time under the actions of traffic and environment, and is defined in units of a standard roughness scale such as m/km IRI.
- **Material loss** from the surfacing, which occurs under the actions of traffic (through whip-off of stones and dust loss) and of erosion by water and wind, and is defined by the change in average thickness of the surfacing material over time.

These two modes of distress are the ones which are corrected by regular maintenance activities, such as grading/blading by motorised or towed grader, spot regravelling, dust palliatives, and full-width regravelling (although this last is usually classified as a rehabilitation activity).

The other modes of distress are ones which need to be addressed at the "design" or material selection stage of the construction or rehabilitation of unsealed roads, namely:

- **Rutting,** which develops under traffic when the surface or roadbed materials have inadequate shear strength under the traffic loading and moisture conditions prevailing, and which is measured, for example, as the average rut depth in the wheelpaths.
- **Surface looseness**, which affects the tracking, skidding and safety of vehicles and is measured by depth of loose material (see Hodges, et al, 1975).
- **Impassability,** which occurs when the surfacing material has inadequate strength (usually through saturation or inundation) to allow a vehicle to pass over the surface.

These modes of distress are controlled through the material strength and thickness design criteria discussed in the previous section.

E2.3 Maintenance Activities

The maintenance activities on unsealed roads can be generally categorised as routine maintenance, resurfacing, rehabilitation and betterment, as summarised in Table E2-1 (Paterson, 1987).

Table E2-1
Maintenance categories and activities for unsealed roads

Mode	Activity	Effect
Routine Maintenance	Spot regravelling	Fill potholes and small depressions; reduce roughness, exclude surface water
	Drainage and verge maintenance	Control runoff of surface water, reduce erosion and material loss, improve surfacing and subgrade strengths by lowering moisture contents
	Dragging	Re-distribute surface gravel, fill minor depressions, improve safety
	Shallow grading/blading	Re-distribute surface material, fill minor depressions, reduce roughness
	Dust control	Controls depth of loose fine material and dust loss
Resurfacing	Full regravelling	Restore required thickness of surfacing
	Deep grading/blading with re-profiling and/or recompaction	Reshape road profile, reduce roughness and rate of deterioration, improve crown and drainage
Rehabilitation	Major regravelling after ripping, recompaction and drainage rehabilitation	Improve strength shape, drainage and performance
Betterment	Rehabilitation and geometric improvement, drainage rehabilitation	Improve the geometric and structural standards
	Upgrading earth road to gravel road	Improve structural standards, performance and all-weather passability

after Paterson, 1987

Generally, spot regravelling, drainage and verge maintenance, dragging, dust control, and "shallow" grading/blading, are all regular or routine maintenance activities normally carried out under annual financing and requiring only operational programming at the local level. In some instances, however, where equipment resources are scarce and require special financing, dragging and shallow grading/blading are only undertaken when specifically programmed and funded in the same way as periodic maintenance.

Resurfacing, comprising regravelling, or deep grading/blading with re-profiling and (preferably) recompaction, is a less frequent, periodic maintenance activity which restores and maintains the existing road standards. Rehabilitation is typically a major resurfacing exercise, combined with reformation of the existing pavement and overhaul or renewal of the drainage facilities, designed to fully restore the road standards and enhance them to meet current structural needs. Betterment works include rehabilitation with the enhancement of geometric standards, and the upgrading of earth roads by the provision of all-weather gravel surfacing.

E2.4 Life Cycle of Deterioration and Maintenance

The life cycle of deterioration and maintenance of unsealed roads is often graphically referred to as the “saw-tooth” trend.

The trend for roughness is one of generally frequent phases of increasing roughness followed by a reduction due to grading/blading maintenance. Roughness tends to increase substantially and often rapidly under traffic, and grading/blading maintenance may be applied at intervals ranging from one week to one year, depending on the traffic and other conditions. When the roughness reaches a high level, grading/blading maintenance using a towed or motor grader is usually undertaken to reduce the roughness, though with variable effectiveness. Usually the operation comprises minor reshaping and a redistribution of the surface gravel, filling the wheelpath ruts and any potholes without major reshaping or re-profiling. The frequency of grading/blading operations in practice is related either to keeping the roughness down at an acceptable level ("condition-responsive"), or to the season ("scheduled"), e.g., at the beginning and end of the rainy season.

On gravel roads, over a number of such grading/blading cycles, there is a net loss of surfacing gravel. Regravelling, with the import of additional material, is undertaken at infrequent intervals to restore the protection of the subgrade.

When deep grading/blading, or ripping and grading/blading, or resurfacing, are supplemented with controlled or heavy compaction, there appears to be a substantial effect of reducing the rate of roughness In the early stages of the cycle, according to Butler, et al, (1985). Resurfacing and rehabilitation effectively mark the commencement of a new life cycle.

The trend of condition thus shows a strong cyclic character under a regular maintenance policy, whether as "scheduled maintenance" undertaken at regular time-intervals, or a "condition-responsive maintenance" undertaken whenever the condition reaches a specified threshold. Maintenance policies thus tend to be cited in terms of a fixed frequency; for example, the number of gradings/bladings per year (or the average interval in days between gradings/bladings, or the number of vehicles between successive gradings/bladings), and the years between resurfacings of a specified thickness.

E3. MODELLING DETERIORATION AND GRADING

In HDM-III, the roughness units were specified in terms of Quarter car index, QI, whereas in HDM-4 roughness is specified as m/km IRI. Therefore the HDM-III relationships given in this section have been amended from those stated by Paterson (1987) and Watanatada, et al (1987) to reflect roughness in IRI units.

E3.1 Roughness Progression

The roughness of unsealed roads increases through the shear, mechanical disintegration, and erosion of the surfacing material caused by traffic and surface water runoff. Roughness levels are generally between 4 and 15 m/km IRI although lower levels sometimes occur with fine materials.

The roughness modelled for economic evaluation is the profile in the wheelpaths of the traffic, since this generates the vehicle operating costs. The location of the wheelpaths tends to vary when roughness reaches high levels as vehicles seek to minimise the dynamic impact. On account of the high variability of material properties, drainage, surface erosion and the high roughness levels of unsealed roads, prediction errors tend to be large, in the order of 1.5 to 2.5 m/km IRI standard error, or equivalent to 95 percentile confidence intervals of 20 to 40 per cent.

E3.1.1 Roughness Progression in HDM-III

The model form adopted in HDM-III constrains the roughness to a high upper limit, or maximum roughness (RI_{max}), by a convex function in which the rate of progression decreases linearly with roughness to zero at RI_{max}. From the Brazil-UNDP study, the maximum roughness was found to be a function of material properties and road geometry, and the rate of roughness progression to be a function of the roughness, maximum roughness, time, light and heavy vehicle passes and material properties (Paterson, 1987).

The HDM-III roughness progression relationship is given by:

$$RI_{TG2} = RI_{max} - b\,[RI_{max} - RI_{TG1}] \qquad \text{. . . (E3.1)}$$

where

$$RI_{max} = \max\{[21.5 - 32.4(0.5 - MGD)^2 + 0.017(HC) - 0.764(RF)(MMP/1000)],\ 11.5\} \qquad \text{. . . (E3.2)}$$

$$b = \exp\,[c(TG_2 - TG_1)] \qquad \text{where } 0 < b < 1 \qquad \text{. . . (E3.3)}$$

$$c = \{-0.001[0.461 + 0.0174(ADL) + 0.0114(ADH) - 0.0287(ADT)(MMP/1000)]\} \qquad \text{. . . (E3.4)}$$

and

RI_{TG1}	=	roughness at time TG1, in m/km IRI
RI_{TG2}	=	roughness at time TG2, in m/km IRI
RI_{max}	=	maximum allowable roughness for specified material, in m/km IRI
TG1, TG2	=	time elapsed since latest grading, in days
ADL	=	average daily light traffic (GVW < 3500kg) in both directions, in veh/day
ADH	=	average daily heavy traffic (GVW $\geq$ 3500kg) in both directions, in veh/day
ADT	=	average daily vehicular traffic in both directions, in veh/day
MMP	=	mean monthly precipitation, in mm/month
HC	=	average horizontal curvature of the road, in deg/km

RF = average rise plus fall of the road, in m/km
MGD = material gradation dust ratio
= P075 / P425 if P425 > 0
= 1 if P425 = 0
P425 = amount of material passing the 0.425 mm sieve, in per cent by mass
P075 = amount of material passing the 0.075 mm sieve, in per cent by mass

This roughness progression model is illustrated in Figure E3-1 for a range of traffic levels with a rainfall of 100 mm/month. An initial roughness of 5 IRI has been assumed and a maximum roughness of 20 IRI. The plots in Figure E3-1 show that at high traffic levels of 500 veh/day, the rate of roughness progression is high, the maximum roughness being reached after approximately one year of no maintenance. At low traffic levels, the rates of roughness progression are significantly lower.

Figure E3-1
Roughness progressions on unsealed roads with no maintenance

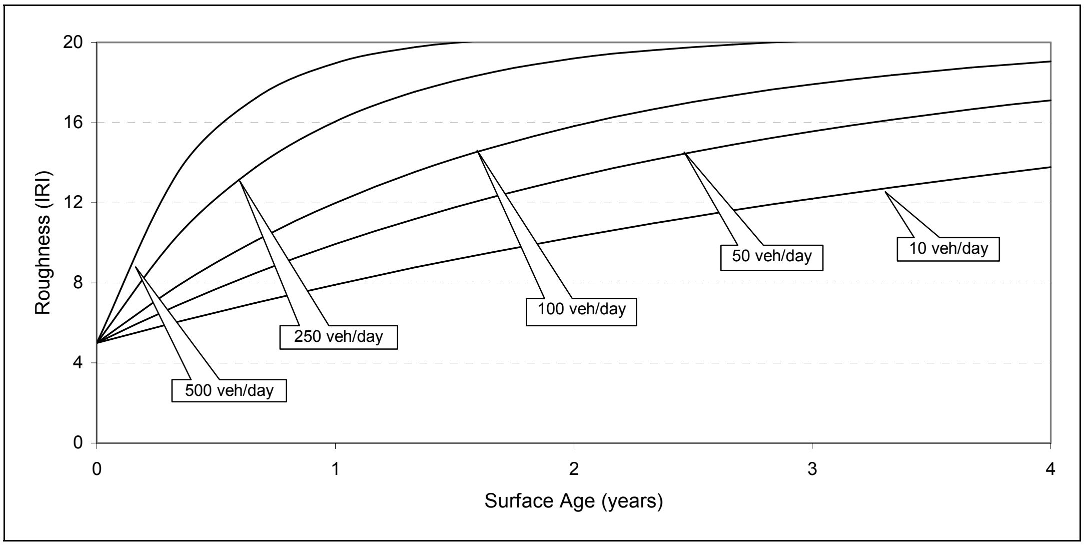

The HDM-III roughness progression relationship was derived using observations from roads with no special compaction. Paterson (1987) observed that rates of roughness progression after construction or rehabilitation with full mechanical shaping and compaction were much slower than given by the model.

Thus if "mechanical compaction" is specified in the model inputs, the coefficient c is reduced, initially to one quarter of its predicted value and rising to the full predicted value after a few grading cycles, but in a period not exceeding 4 years, as follows:

$$c' = c\left\{\min\left[1,\ 0.25(t)\max\left(1,\ n^{0.33}\right)\right]\right\} \qquad \text{. . . (E3.5)}$$

where
t = time since regravelling or construction with mechanical compaction, in years
n = frequency of grading, in cycles/year
and

$$b' = \exp\left[365\left(\frac{c'}{n}\right)\right] \qquad \text{. . . (E3.6)}$$

When mechanical compaction is specified, then b’ and c’ are used in place of b (equation E3.3) and c (equation E3.4) respectively in the roughness progression relationship.

The effect of mechanical compaction on roughness progression is illustrated in Figure E3-2. In this example the roughness progression over a year with no maintenance is shown for roads constructed with and without mechanical compaction, for traffic levels of 50 and 250 veh/day, with a rainfall of 100 mm/month. These plots show that the rates of roughness progression are significantly lower when roads are constructed with mechanical compaction.

Figure E3-2
Effect of mechanical compaction on roughness progression

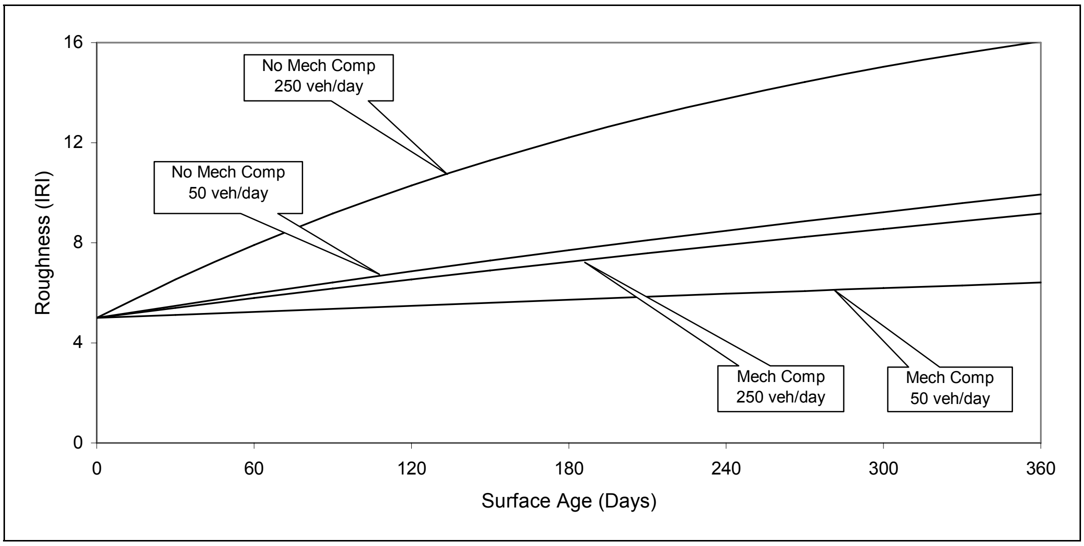

E3.1.2 Roughness Progression in HDM-4

In version 1 of HDM-4, the HDM-III roughness progression relationship was used. In version 2 the relationship has been amended primarily with the addition of a calibration factor to enable the user to adjust the rate of roughness progression (Morosiuk, 200b).

The HDM-4 roughness progression relationship is given by:

$$RI_{TG2} = RI_{max} - b\,[RI_{max} - RI_{TG1}] \qquad \text{. . . (E3.7)}$$

where

$$RI_{max} = \max\{[21.5 - 32.4(0.5 - MGD)^2 + 0.017(HC) - 0.764(RF)(MMP/1000)],\ 11.5\} \qquad \text{. . . (E3.8)}$$

$$b = \exp\,[c(TG_2 - TG_1)] \qquad \text{where } 0 < b < 1 \qquad \text{. . . (E3.9)}$$

$$c = K_c \min[1, COMPGR\ (t) \max(1, n^{0.33})]\ \{-0.001[0.461 + 0.0174(ADL) + 0.0114(ADH) - 0.0287(ADT)(MMP/1000)]\} \qquad \text{. . . (E3.10)}$$

and

COMPGR = type of compaction used during construction or regravelling
= 1.0 (no mechanical compaction during construction or regravelling)
= 0.25 (mechanical compaction during construction or regravelling)

K_c = calibration factor for roughness progression (default = 1.0)

and the other variables are as defined previously

E3.2 Effect of Grading

Maintenance, in the form of grading, on unsealed roads is generally carried out several times a year, each grading tending to reduce the level of roughness. The magnitude of this reduction in roughness was found to depend on the roughness before grading, the material properties and the minimum roughness (RI_{min}) (Paterson, 1987). The minimum roughness, below which grading cannot reduce roughness, increases as the maximum particle size increases and the gradation of the surfacing material worsens.

E3.2.1 Effect of Grading in HDM-III

The HDM-III relationship for predicting the roughness after grading is expressed as a linear function of the roughness before grading, dust ratio and the minimum roughness, as follows:

$$RI_{ag} = RI_{min} + a\,[RI_{bg} - RI_{min}] \qquad \text{. . . (E3.11)}$$

where

$$a = 0.553 + 0.23(MGD) \qquad \text{. . . (E3.12)}$$

$$RI_{min} = \max\{0.8,\ \min[7.7,\ 0.36(D95)(1 - 2.78MG)]\} \qquad \text{. . . (E3.13)}$$

and

RI_{ag} = roughness after grading, in m/km IRI
RI_{bg} = roughness before grading, in m/km IRI
RI_{min} = minimum allowable roughness after grading, in m/km IRI
D95 = maximum particle size of the material, defined as the equivalent sieve size through which 95 per cent of the material passes, in mm
MG = slope of mean material gradation
MGD = material gradation dust ratio

The slope of mean material gradation is calculated as follows:

$$MG = \min[MGM,\ (1 - MGM),\ 0.36] \qquad \text{. . . (E3.14)}$$

where

$$MGM = \frac{MG075 + MG425 + MG02}{3} \qquad \text{. . . (E3.15)}$$

$$MG075 = \frac{\log_e\left(P075/95\right)}{\log_e\left(0.075/D95\right)} \quad \text{if D95 > 0.4} \qquad \text{. . . (E3.16)}$$

$$= 0.3 \quad \text{otherwise}$$

$$MG425 = \frac{\log_e\left(P425/95\right)}{\log_e\left(0.425/D95\right)} \quad \text{if D95 > 1.0} \qquad \text{. . . (E3.17)}$$

$$= 0.3 \quad \text{otherwise}$$

$$MG02 = \frac{\log_e\left(P02/95\right)}{\log_e\left(2.0/D95\right)} \quad \text{if D95 > 4.0} \qquad \text{. . . (E3.18)}$$

$$= MG425 \quad \text{otherwise}$$

E3.2.2 Effect of Grading in HDM-4

In version 1 of HDM-4, the HDM-III relationship for the effect of grading was used. In version 2 the relationship has been amended to enable the user to specify the type of grading employed and adjust the effect of the selected grading (Morosiuk, 2003b).

The HDM-4 relationship for predicting the effect of grading is as follows:

$$RI_{ag} = \min[RI_{min} + a\,(RI_{bg} - RI_{min}),\ RI_{bg}] \qquad \text{. . . (E3.19)}$$

where

$$a = K_a \max\left\{0.5,\ \min\left[GRAD\,[0.553 + 0.23(MGD)],\ 1\right]\right\} \qquad \text{. . . (E3.20)}$$

$$RI_{min} = \max\left\{0.8,\ \min\left[7.7,\ 0.36(D95)(1 - 2.78MG)\right]\right\} \qquad \text{. . . (E3.21)}$$

and

GRAD = dependent on type of grading (GRAD values are given in Table E3-1)
K_a = calibration factor for effect of grading
and the other variables are as defined previously

Descriptions of the types of grading (GRAD) are given in Table E3-1 and their effects on roughness are illustrated in Figure E3-3.

Table E3-1
Default GRAD values for various types of grading

Type of Grading	GRAD
Non-motorised grading, bush or tyre dragging	1.4
Light motorised grading, little or no water, no mechanical compaction	1.0
Heavy motorised grading with water and mechanical compaction	0.75
Full re-processing of wearing course with water and heavy roller compaction	0.2

NB Full re-processing of the wearing course has been observed to produce GRAD values of 0.2. However, as this type of grading is unusual, it has not been included in the default options. Users can obtain lower values of ‘a’ than the minimum value of 0.5 through the calibration factor K_a.

Figure E3-3
Effect of grading on roughness

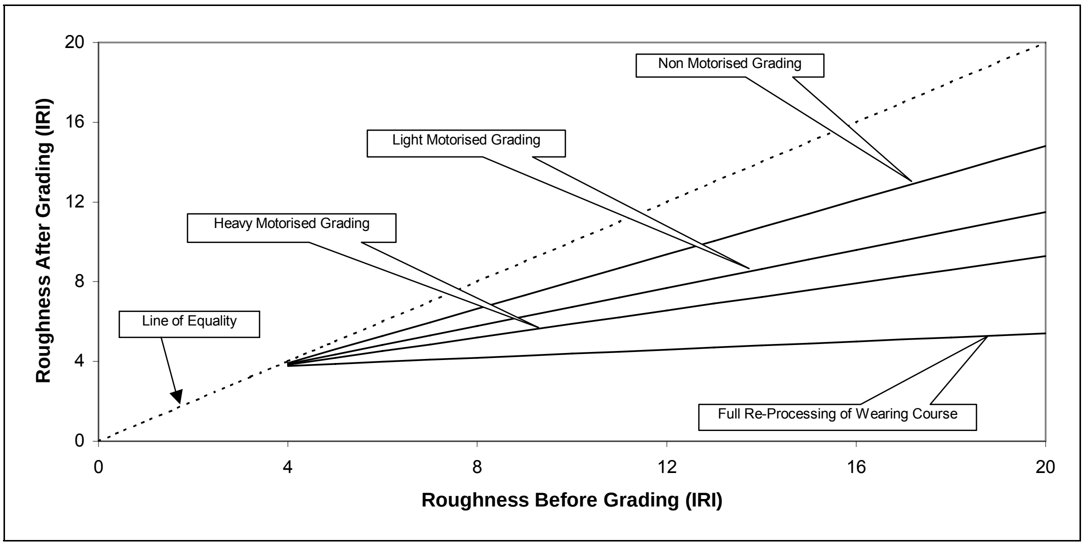

E3.3 Average Roughness During Analysis Year

The above models predict the rate of roughness progression between grading cycles and the reduction in roughness due to grading. Therefore during an analysis period of one year, there will generally be several increases and decreases in roughness. As HDM uses the average roughness during an analysis year as an input of the roughness of a road in, for example the road user effects sub-model, it is necessary to derive this value of roughness.

The average roughness during an analysis year is computed by combining the progression and grading-effect relationships and integrating (Paterson, 1987). The year's average is expressed as follows:

i) if $t*n \geq 1$
The average roughness during year t, RI_{avg}, is given by:

$$RI_{avg} = (1 - y)\, RI_{max} + S_N\, (y/n) \qquad \text{. . . (E3.22)}$$

where

$$y = (b-1)\left(\frac{n}{365c}\right) \qquad \text{. . . (E3.23)}$$

$$S_N = \frac{nk + [1-(ab)^n]RI_a - k\dfrac{[1-(ab)^n]}{(1-ab)}}{(1-ab)} \qquad \text{. . . (E3.24)}$$

$$k = (1 - a)\, RI_{min} + a(1 - b)\, RI_{max} \qquad \text{. . . (E3.25)}$$

and

RI_{avg}	=	average roughness during year t, in m/km IRI
RI_a	=	roughness at beginning of year t, in m/km IRI
RI_{min}	=	minimum roughness for specified material, in m/km IRI (see equation E3.13)
RI_{max}	=	maximum roughness for specified material, in m/km IRI (see equation E3.2)
t	=	time since regravelling or construction with mechanical compaction, in years
n	=	frequency of grading, in cycles/year
a	=	as defined in equation E3.20
b	=	as defined in equation E3.9
c	=	as defined in equation E3.10

The roughness at the beginning of the year, RI_a, is obtained as follows:

- For the first year of analysis after regravelling (t = 1), RI_a is as specified by the user.
- For subsequent analysis years, RI_a is the roughness at the end of the previous year t-1, as given below:

In any given analysis year t, the roughness at the end of the year, RI_b is derived as follows:

$$RI_b = (ab)^n RI_a + \frac{k[1-(ab)^n]}{(1-ab)} \qquad \text{. . . (E3.26)}$$

ii) if $t*n < 1$
The average roughness during the year, RI_{avg}, is given by:

$$RI_{avg} = RI_{max} - (RI_{max} - RI_a)\left(\frac{\exp(365c)-1}{365c}\right) \qquad \text{. . . (E3.27)}$$

The roughness at the end of the year, RI_b, is given by:

$$RI_b = RI_{max} - (RI_{max} - RI_a)\exp(365c) \qquad \text{. . . (E3.28)}$$

E3.4 Steady State Roughness Cycle

When grading is performed regularly at constant time intervals, or a fixed roughness level, or fixed traffic intervals, the process of roughness change described by these relationships without restriction eventually leads to a steady state, as shown in Paterson (1987). This steady state is characterised by a saw-toothed pattern of roughness-time profile, in which the highs and lows represent the roughness immediately before and after grading, respectively.

These highs and lows, denoted by RI_H and RI_L, are given by:

$$RI_H = \frac{(1-b)RI_{max} + b(1-a)RI_{min}}{(1-ab)} \quad \text{. . . (E3.29)}$$

$$RI_L = \frac{(1-a)RI_{min} + a(1-b)RI_{max}}{(1-ab)} \quad \text{. . . (E3.30)}$$

where

RI_H = roughness immediately before grading, in m/km IRI
RI_L = roughness immediately after grading, in m/km IRI
and the other variables are as defined previously

The saw-toothed patterns of roughness progression illustrated by Paterson (1987) have been reproduced in Figure E3-4 and Figure E3-5. The effects of various traffic volumes under a regular 90-day grading policy are illustrated in Figure E3-4 and the effects of various grading frequencies on roughness progression for a traffic volume of 300 veh/day are shown in Figure E3-5.

Figure E3-4
Effect of traffic volume on roughness progression under regular 90-day grading policy

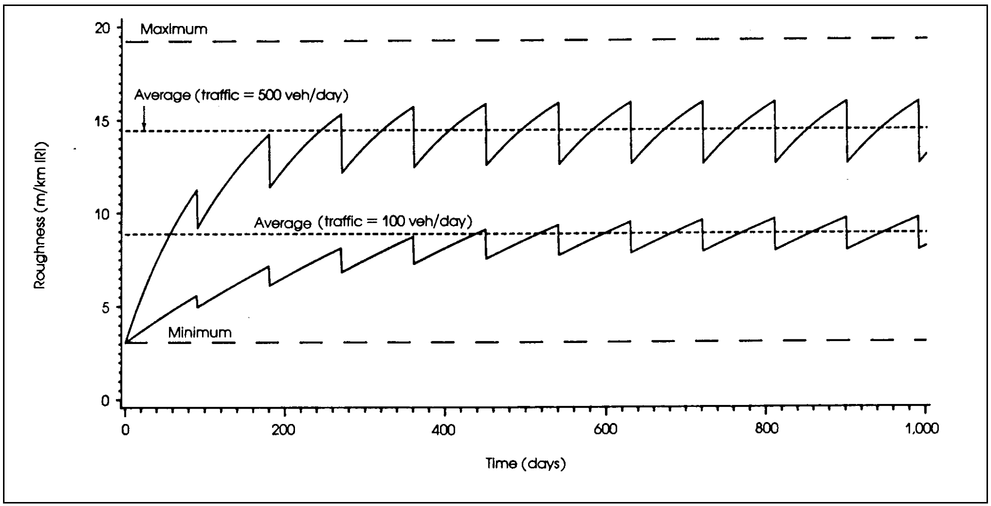

after Paterson, 1987

Figure E3-5
Effect of grading frequency on roughness progression for traffic of 300 veh/day

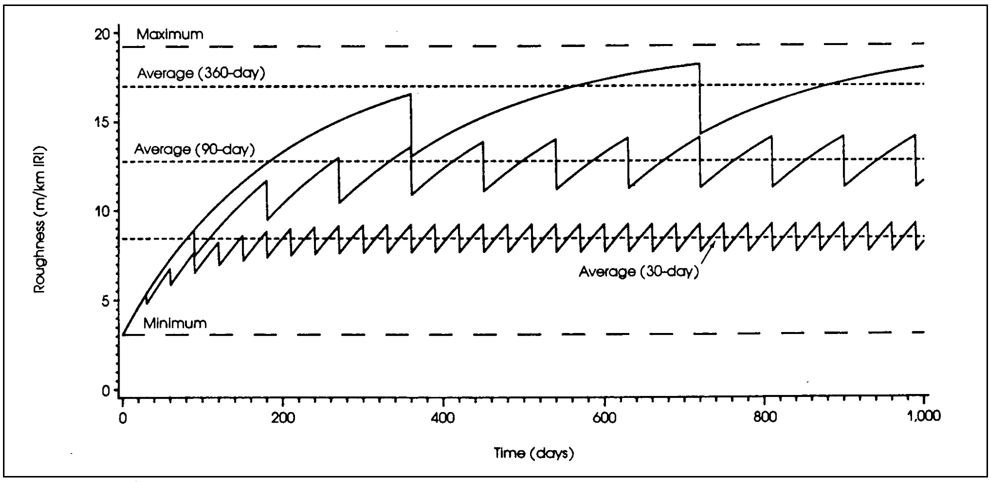

after Paterson, 1987

The long-term average roughness, RI_{lta}, at this steady state is dependent on the grading frequency (embodied in the variable b defined previously) and is derived by integration over the roughness-time profile. Therefore the annual average roughness RI_{avg} tends to the long-term average roughness, RI_{lta}, which is defined as follows:

$$RI_{lta} = RI_{max} + (1-a)(1-b)\left(\frac{(RI_{max} - RI_{min}}{(1-ab)\log_e b}\right) \qquad \text{. . . (E3.31)}$$

where

RI_{lta} = steady state long-term average roughness, in m/km IRI
and the other variables are as defined previously

The long-term average roughness progressions are illustrated in Figure E3-6 for a range of traffic levels and grading frequencies.

Figure E3-6
Long-term average roughness for various grading frequencies

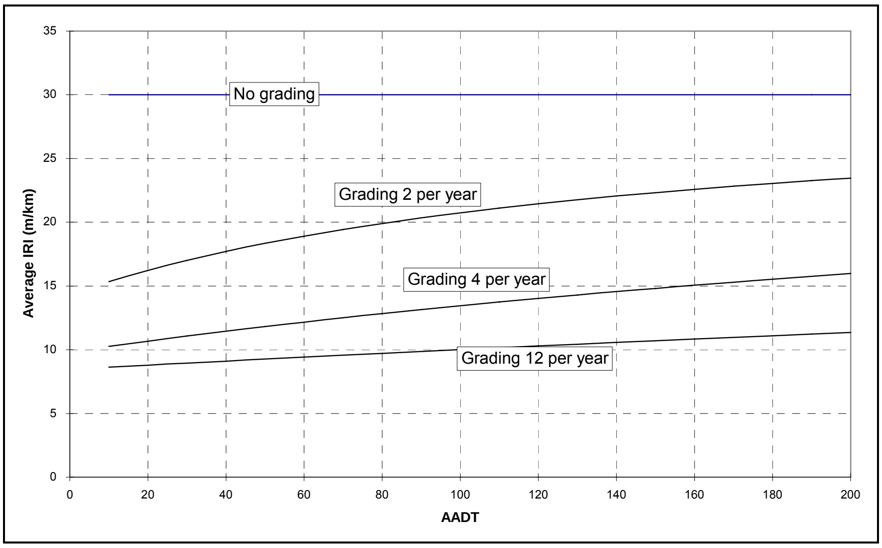

If no maintenance is carried out, the long-term average roughness tends to the maximum roughness for the specified material. At high levels of grading frequencies, the long-term average roughness is predicted to be much lower, tending to the minimum roughness.

E3.5 Material Loss

Regravelling is the major maintenance operation on unsealed roads, analogous in importance to the overlaying of a paved road, so the frequency required is an important planning decision. Gravel loss is defined as the change in gravel thickness over a period of time and is used to estimate when the thickness of the gravel wearing course has decreased to a level where regravelling is necessary.

Paterson (1987) identified three major factors as affecting gravel loss; weathering, traffic, and the influence of grading. Material properties, road alignment and road width influence the gravel loss generated by each of these factors. The following relationship for predicting the annual quantity of material loss as a function of monthly rainfall, traffic volume, road geometry and characteristics of the gravel (if a gravel road) and the subgrade (if an earth road) was derived:

$$MLA = K_{gl}\, 3.65\, [3.46 + 0.246(MMP/1000)(RF) + (KT)(AADT)] \qquad \text{. . . (E3.32)}$$

where

$$KT = K_{kt} \max [0,\ 0.022 + 0.969(HC/57300) + 0.00342(MMP/1000)(P075) - 0.0092(MMP/1000)(PI) - 0.101(MMP/1000)] \qquad \text{. . . (E3.33)}$$

and

MLA	=	annual material loss, in mm/year
KT	=	traffic-induced material whip-off coefficient
AADT	=	annual average daily traffic, in veh/day
MMP	=	mean monthly precipitation, in mm/month
RF	=	average rise plus fall of the road, in m/km
HC	=	average horizontal curvature of the road, in deg/km
PI	=	plasticity index of the material, in per cent
K_{gl}	=	calibration factor for material loss
K_{kt}	=	calibration factor for traffic-induced material whip-off coefficient

The rates of material loss predicted by the above relationship have been plotted in Figure E3-7 for a range of traffic levels and rainfall. The predicted rates of material loss illustrated in Figure E3-7 show the effects of traffic and rainfall for an unsealed road in flat terrain.

Figure E3-7
Material loss related to traffic and rainfall

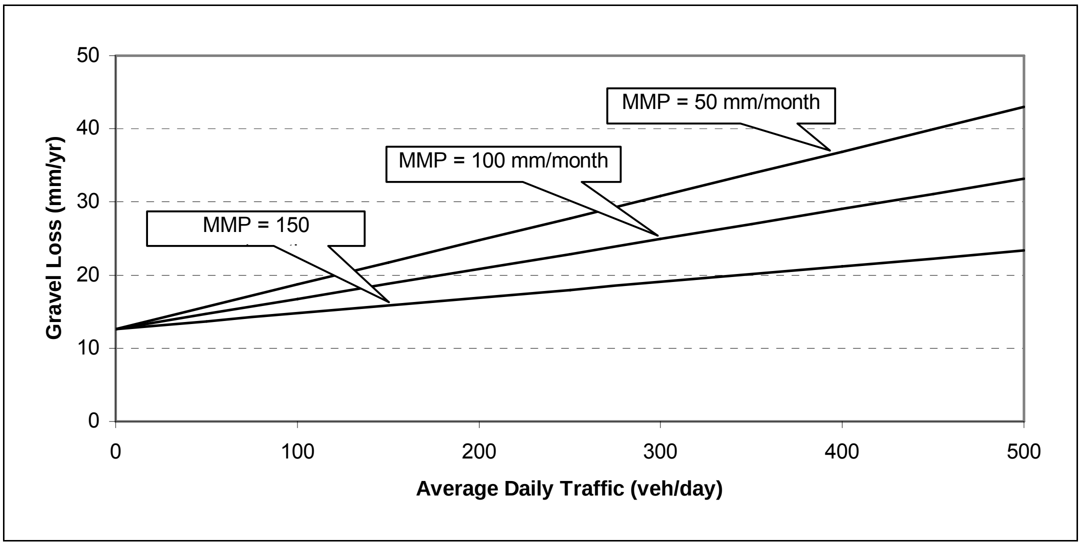

E3.6 Passability

Passability has been defined by Paterson (1987) as the quality of the road surface which ensures the safe passage of vehicles. In the road user effects sub-model, provision has been made to determine the economic impact of a partial reduction in passability through factors augmenting the operating costs of the various vehicle types. This augmentation comes into effect when the gravel surfacing thickness drops below a minimum, and relates to the risk of the subgrade material being impassable.

The user however must determine exogenously whether passability will be a problem in the subgrade material, because no physical estimation of it is made within the model. The following criteria from Visser (1981) are adequate for ensuring passability and surface stability:

- Passability which is a function of the shear strength of saturated material, is satisfactory when:
  $SFCBR \geq 8.25 + 3.75 \log_{10} (ADT)$
- Surfacing stability, which relates to ravelling and looseness, is satisfactory when:
  $P075 \geq 14$

where

SFCBR = the (minimum) soaked California Bearing Ratio at standard Proctor laboratory compaction for ensuring passability

E4. ROAD WORKS EFFECTS

This section of the document describes the modelling of road works effects for unsealed roads. An unsealed road is considered to comprise two layers, **a** gravel wearing course surfacing and a subgrade. A gravel road has both layers, but an earth road has a zero thickness of gravel surfacing and its surface characteristics are those of the subgrade. When a gravel road loses all of its gravel wearing course, then its classification reverts to that of earth road. Upon gravel resurfacing, all unsealed roads become gravel roads by definition of the new surfacing layer.

The works classes for unsealed roads discussed below are:

- Maintenance
- Improvement
- Construction

The methods of defining works activities and intervention criteria, the calculation of physical quantities of works and the costs to road administration for each of these work classes are detailed in Volume 4 of the HDM-4 Series – Analytical Framework and Model Descriptions (Odoki and Kerali, 2000).

E4.1 Maintenance Works

The maintenance of unsealed roads comprises the following operations:

- Periodic grading
- Spot regravelling
- Gravel resurfacing
- Routine-miscellaneous maintenance of drainage and verges

E4.1.1 Periodic Grading

Periodic grading by motorised or towed grader to restore surfacing gravel from the shoulders to the roadway and to reduce roughness is one of the principal routine maintenance for unsealed roads. The periodic grading of unsealed roads is usually undertaken on a more-or-less regular basis for management purposes, either seasonally or frequently enough to keep the roughness within tolerable limits.

The average roughness between successive grading, RI_{avg} is computed as a function of the number of days between grading (DG), as described in Section E3. If the time interval between successive gradings is fixed by the user (i.e. scheduled maintenance), DG is specified directly by the user.

If the time interval between successive gradings is a function of either traffic or roughness (i.e. responsive maintenance), DG is determined as follows:

if $DG_{max} < DG'$	then	$DG = DG_{max}$
if $DG_{min} < DG' \leq DG_{max}$	then	$DG = DG'$
if $DG_{min} \geq DG'$	then	$DG = DG_{min}$

where

DG_{max} = maximum allowable time interval between successive gradings, in days (user specified; default = 10,000)

DG_{min} = minimum applicable time interval between successive gradings, in days (user specified; default = 5)
DG' = time between successive gradings, determined from traffic or roughness levels, in days

The variable DG' is determined as follows:

i) for the traffic-responsive maintenance option

$$DG' = VEHG / AADT \qquad \text{. . . (E4.1)}$$

ii) for the roughness-responsive maintenance option

$$DG' = \left(\frac{1}{c}\right)\log_e\left\{\frac{(RI_{max} - RI_{max\,o})}{[RI_{max} - (1-a)RI_{min} - aRI_{max\,o}]}\right\} \qquad \text{. . . (E4.2)}$$

where
VEHG = traffic interval between successive gradings, user specified, in vehicles
RI_{maxo} = maximum allowable roughness specified by the user, in m/km IRI
RI_{min}, RI_{max}, a and c are as defined in Section E3.

If no grading is specified, the long-term average roughness is equal to the maximum roughness.

E4.1.2 Spot Regravelling

Spot regravelling provides repair to areas of severe depression. It may be specified by the user either as a fixed number of cubic metres per kilometre per year, or as a percentage of gravel or subgrade material loss in the current analysis year to be replaced. When spot regravelling is performed, the added material is assumed to be the same type as the existing.

E4.1.2.1 Gravel Thickness

For gravel roads, the thickness of the gravel layer is increased to reflect the volume of material added, according to the following formula:

$$\Delta THGS = \frac{VGS}{(CW + SW)} \qquad \text{. . . (E4.3)}$$

where
$\Delta THGS$ = increase in gravel thickness due to spot regravelling, in mm
VGS = in-place volume of gravel added due to spot regravelling, in m^3/km
CW = carriageway width, in m
SW = shoulder width, in m

E4.1.2.2 Roughness

Spot regravelling is predicted to reduce the average roughness on the assumption that the gravel is applied in the major depressions and potholes that have appeared in the surface in the upper ranges of roughness. Roughness levels above 15 m/km IRI are invariably associated with the presence of visible birdbath type depressions or potholes, which become larger or more frequent as the roughness level increases, and these can be effectively patched, with high benefits, by spot regravelling.

Over the roughness range of 11 to 15 m/km IRI, such patchable depressions are frequently but not always present so that, in this range, spot regravelling may not always be effective.

For example, spot regravelling is not effective maintenance on corrugations or on runoff-induced surface erosion, which are conditions that commonly induce roughness levels within this range. At roughness levels below 11 m/km IRI spot regravelling is considered to be ineffective on roughness.

This logic is defined in the algorithm given in equation E4.4, by adopting the roughness to volume of depression ratio as equal to 0.15 m/km IRI per m^3/lane/km, allowing for the spot regravelling to be only 60% effective (i.e. 0.09 m/km IRI per m^3/lane/km), and adopting an average effective lane width of 3 m (Watanatada, et al, 1987):

$$RI_{avg(aw)} = \max\left\{11.5,\ \left[RI_{avg(bw)} - \min\left(0.077,\ \frac{RI_{avg(bw)} - 11.5}{3.1}\right)\frac{3.6(VGS)}{CW}\right]\right\} \quad \text{. . . (E4.4)}$$

where

$RI_{avg(aw)}$ = average roughness after works, in m/km IRI

$RI_{avg(bw)}$ = average roughness before works, in m/km IRI

and the other variables are as defined previously

The effects of different amounts of spot regravelling on roughness are illustrated in Figure E4-1. It should be noted that spot regravelling affords only a temporary repair of depressions, and that the most effective means is by grading, or in severe cases by scarifying, grading and recompacting.

Figure E4-1
Effect of spot regravelling on roughness

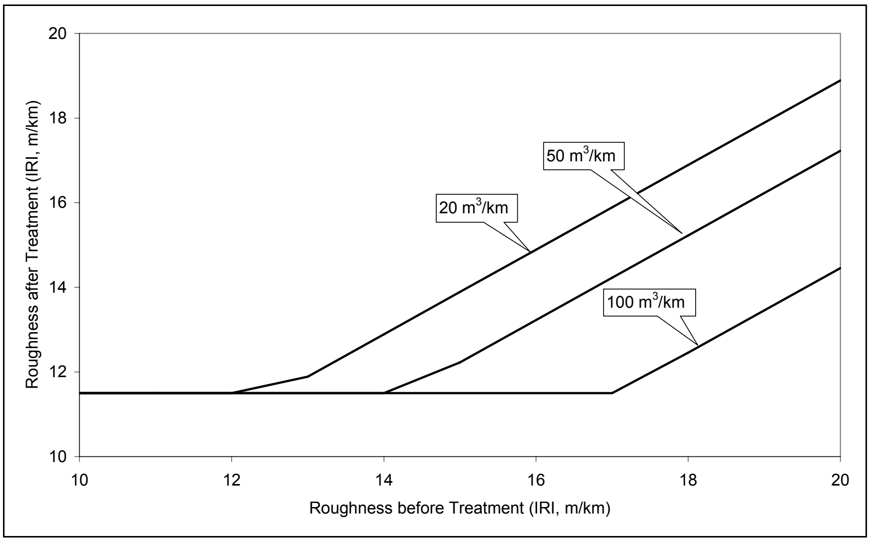

E4.1.3 Gravel Resurfacing

Gravel resurfacing is performed to replace or augment the gravel-surfacing layer in response to material loss. When gravel resurfacing is performed the pavement type is set to gravel regardless of the previous surface type. The existing surface material is changed to the material specified by the user and the surface material attributes (P02, P425, P075, D95, PI, RI_{min} and RI_{max}) are replaced either by the new values provided by the user, or by the default values from the previous gravel attributes.

E4.1.3.1 Gravel Thickness

The thickness of the gravel surfacing is increased according to the formula given below:

i) if the final gravel thickness is specified

$$THG_{aw} = THG_o \quad \text{. . . (E4.5)}$$

ii) if an increase in the gravel thickness is specified

$$THG_{aw} = THG_{bw} + \Delta THG \quad \text{. . . (E4.6)}$$

where

THG_{aw} = gravel thickness after works, in mm

THG_{bw} = gravel thickness before works, in mm

ΔTHG = increase in gravel thickness due to gravel resurfacing, specified by the user, in mm

THG_o = gravel thickness after gravel resurfacing, specified by the user, in mm

E4.1.3.2 Roughness

The roughness after gravel resurfacing is reset to a user specified value. If this is not specified, the roughness after works is reset to the minimum allowable value, RI_{min}.

E4.1.4 Routine-Miscellaneous Maintenance

This includes drainage maintenance, vegetation control, shoulder maintenance, safety installations, and other items that are not modelled as affecting the riding quality of the pavement. A lump sum cost per km per year is used as the basis for costing routine maintenance. Because the unsealed road deterioration relationships employed are based on the assumption of adequate drainage, the cost of drainage maintenance should be included, when it is normally done. Otherwise, some allowance due to the lack of drainage, for example, in the form of frequent road closures, washouts, etc., should be incorporated in the economic analysis.

E4.2 Improvement Works

Improvement works for unsealed roads comprises the following:

- Widening
- Realignment

E4.2.1 Widening

The operations included under widening are lane addition and partial widening. The difference between the two is that partial widening does not increase the number of lanes. It is considered that these operations do not alter the road alignment, hence there is no change in section length.

It is considered that widening works do not alter the road surface class. After widening, the required modelling parameters are reset as described below.

E4.2.1.1 Carriageway Width

The new carriageway width after works is given as follows:

$$CW_{aw} = CW_{bw} + \Delta CW \quad \text{. . . (E4.7)}$$

where

CW_{aw} = carriageway width after works, in m
CW_{bw} = carriageway width before works, in m
ΔCW = increase in carriageway width, in m

For partial widening, the increase in carriageway width, ΔCW, is specified directly by the user. For lane addition works, the increase in carriageway width is given by:

$$\Delta CW = \frac{(ADDLN)(CW_{bw})}{LN_{bw}} \qquad \ldots (E4.8)$$

where
ADDLN = additional number of lanes, specified by the user
LN_{bw} = number of lanes before works

For lane addition works, the number of lanes after widening works, LN_{aw}, is equal to the number of lanes before works, LN_{bw}, plus the user-specified additional number of lanes, ADDLN.

E4.2.1.2 Gravel Thickness

Gravel thickness after widening is calculated as a weighted average as follows:

$$THG_{aw} = \frac{[(CW_{bw})(THG_{excw}) + (\Delta CW)(THG_{ww})]}{CW_{aw}} \qquad \ldots (E4.9)$$

where
THG_{aw} = gravel thickness after works, in mm
THG_{ww} = gravel thickness on the widened part of the carriageway, in mm
THG_{bw} = gravel thickness before works, in mm
THG_{excw} = gravel thickness over the existing carriageway after works, in mm
and the other variables are as defined previously

The gravel thickness over the existing carriageway after widening, THG_{excw}, is obtained as follows:

i) if the existing carriageway is to be regravelled:

$$THG_{excw} = THG_{bw} + \Delta THG_{gr} \qquad \ldots (E4.10)$$

ii) if the existing carriageway is not to be regravelled:

$$THG_{excw} = THG_{bw} + \Delta THGS \qquad \ldots (E4.11)$$

where
ΔTHG_{gr} = increase in gravel thickness over the existing carriageway due to regravelling, in mm
$\Delta THGS$ = increase in gravel thickness over the existing carriageway due to spot regravelling, in mm

The increase in gravel thickness over the existing carriageway due to spot regravelling, $\Delta THGS$, is obtained using equation E4.3.

E4.2.1.3 Surface Material Properties

After widening, the surface material properties, SMPi, are reset as follows:

i) if the existing carriageway is to be regravelled, all the surface material properties are reset to those of the new gravel material.

ii) if the existing carriageway is not to be regravelled:

$$SMPi_{aw} = \left\{ \frac{[(CW_{bw})(SMPi_{bw}) + (\Delta CW)(SMPi_{ww})]}{CW_{aw}} \right\} \qquad \text{. . . (E4.12)}$$

where

$SMPi_{aw}$ = surface material property i after works, (i = P02, P425, P075, D95, PI)
$SMPi_{bw}$ = surface material property i before works, (i = P02, P425, P075, D95, PI)
$SMPi_{ww}$ = surface material property i of the widened part of the carriageway, (i = P02, P425, P075, D95, PI)

and the other variables are as defined previously

E4.2.1.4 Roughness

Roughness after widening works, RI_{aw}, is reset to a user specified value. If this is not specified, RI_{aw} is reset to the minimum allowable roughness RI_{min}.

E4.2.2 Realignment

In HDM-4, realignment refers to local geometric improvements of an existing road. This may result in a reduction of the road length. However, it is assumed that the carriageway width remains unaltered.

E4.2.2.1 Gravel Thickness

The gravel thickness after realignment is calculated as follows:

$$THG_{aw} = (1 - Pconew)THG_{excw} + (Pconew)(THG_{rw}) \qquad \text{. . . (E4.13)}$$

where

THG_{aw} = gravel thickness after works, in mm
THG_{excw} = gravel thickness of the non-realigned parts of the existing carriageway after realignment works, in mm
THG_{rw} = gravel thickness of the realigned parts of the carriageway, in mm
Pconew = proportion of new construction (0 < Pconew < 1)

The gravel thickness over the non-realigned parts of the existing carriageway after realignment works is derived as follows:

i) if the non-realigned parts of the existing carriageway are to be regravelled

$$THG_{excw} = THG_{bw} + \Delta THG_{gr} \qquad \text{. . . (E4.14)}$$

ii) if the non-realigned parts of the existing carriageway are not to be regravelled

$$THG_{excw} = THG_{bw} + \Delta THGS \qquad \text{. . . (E4.15)}$$

where

THG_{bw} = gravel thickness before works, in mm
ΔTHG_{gr} = increase in gravel thickness over the non-realigned parts of the existing carriageway due to regravelling, in mm
$\Delta THGS$ = increase in gravel thickness over the non-realigned parts of the existing carriageway due to spot regravelling, in mm

The increase in gravel thickness over the non-realigned parts of the existing carriageway due to spot regravelling, ΔTHGS, is derived from equation E4.3.

E4.2.2.2 Surface Material Properties

After realignment works, the surface material properties, SMPi, are reset as follows:

i) if the non-realigned parts of the existing carriageway are to be regravelled, all the surface material properties are reset to those of the new gravel material.

ii) if the non-realigned parts of the existing carriageway are not to be regravelled

$$SMPi_{aw} = (1 - Pconew)SMPi_{bw} + (Pconew)(SMPi_{rw}) \qquad \text{. . . (E4.16)}$$

where

$SMPi_{aw}$ = surface material property i after works, (i = P02, P425, P075, D95, PI)
$SMPi_{bw}$ = surface material property i before works, (i = P02, P425, P075, D95, PI)
$SMPi_{rw}$ = surface material property i of the realigned parts of the carriageway, (i = P02, P425, P075, D95, PI)
and the other variables are as defined previously

E4.2.2.3 Roughness

Roughness after realignment works, RI_{aw}, is reset to a user-specified value. If this is not specified, RI_{aw}, is reset to the minimum allowable roughness, RI_{min}.

E4.3 Construction Works

In HDM-4, construction works for unsealed roads currently comprises the following:

- Upgrading
- New section

E4.3.1 Upgrading

An unsealed road can be upgraded to a bituminous or concrete pavement. It is also possible to upgrade an earth road to a gravel road, although both are of the same surface class.

After upgrading, the pavement type is reset to the new type specified by the user. Depending on the new pavement type, the required modelling parameters are obtained in the following ways:

- Pavement structure, strength, layer material properties and construction quality are set to user-specified values
- Pavement condition after works is reset to as new
- Pavement history data is reset to reflect new construction
- The new carriageway width after upgrading is calculated using equation E4.7. The increase in carriageway width is either specified directly by the user, or calculated using equation E4.8. The number of lanes after upgrading works, LN_{aw}, is equal to the number of lanes before works, LN_{bw}, plus the user-specified additional number of lanes, ADDLN.

Other required parameters that are user-specified include calibration factors, traffic flow patterns and speed factors.

E4.3.2 New Section

The required components of the new section to be constructed are defined using the following information:

- Road section data (i.e. all the data items that are required to define a road section in HDM-4).
- Traffic data. This includes i) diverted traffic (i.e. traffic that is diverted from the nearby routes and other transport modes; ii) generated traffic (i.e. additional traffic that occurs in response to the new investment.

Other information required includes construction costs and duration, exogenous benefits and costs, and maintenance and improvement standards.

PART F. REFERENCES

AASHO (1972). AASHO interim guide for design of pavement structures. American Association of State Highway and Transportation Officials, Washington, D.C.

AASHTO (1986). Guide for the Design of Pavement Structures, (Volumes I and II). American Association of State Highway and Transportation Officials, Washington, D.C.

AASHTO (1993). AASHTO Guide for Design of Pavement Structures. American Association of State Highway and Transportation Officials, Washington, D.C.

AASHTO T22 (1992), Standard Method of Test for Compressive Strength of Cylindrical Concrete Specimens. American Association of State Highway and Transportation Officials, Washington, D.C.

AASHTO T97 (1992). Standard Method of Test of Time of Setting of Concrete Mixtures by Penetration Resistance. American Association of State Highway and Transportation Officials, Washington, D.C.

AASHTO T140 (1992). Standard Method of Test for Compressive Strength of Concrete using Portions of Beams Broken in Flexure. American Association of State Highway and Transportation Officials, Washington, D.C.

Al-Omari, B and M I Darter (1994). Relationships Between IRI and PSR. Transportation Research Board, 73rd Annual Meeting, Washington, D.C.

Asgari, M A (1992). Validation of empirical HDM-III models for prediction of asphalt deterioration by means of mechanistic analysis. M.Sc thesis, Delft Technical University, Netherlands.

Asphalt Institute (1989). The Asphalt Handbook. Manual Series N°4.

ASTM C39 (1994). Standard Test Method for Compressive Strength of Cylindrical Concrete Specimens. American Society for Testing Materials.

ASTM C78 (1994). Standard Test Method for Flexural Strength of Concrete (Using Simple Beam with Third-Point Loading). American Soceity for Testing Materials.

ASTM C469 (1994). Standard Test Method for Elasticity and Poisson's Ratio of Concrete in Compression. American Soceity for Testing Materials.

Babkov, V F (1985). Highway Engineering. MIR Publishers, Moscow.

Barber, V C, W N Odom and R W Patrick (1978). The Deterioration and Rehabilitation of Pavements. Technical Report S-78-8. Waterways Experimental Station, Vicksburg, Virginia.

Benekohal, R F, K T Hall and H W Miller (1990). Effects of Lane Widening on Lateral Distribution of Truck Wheels. Transportation Research Record 1286, Transportation Research Board, Washington, D.C.

Bennett, C R and W D O Paterson (2000). Volume 5 – A Guide to Calibration and Adaptation. HDM-4 series of publications, PIARC.

Bradbury, R D (1938). Reinforced Concrete Pavements. Wire Reinforcement Institute.

BSI (1990). Method for determination of aggregate abrasion value. Part 113. British Standards Institution.

Butler, B C, R Harrison and P Flanagan (1985). Setting Maintenance Levels for Aggregate Surface Roads. Transportation Research Record 1035, Transportation Research Board, Washington, D.C.

Catt, C A (1983). An Alternative View of TRRL's Research into Skidding Resistance. Asphalt Technology, No. 33, pp. 7-12.

CCANZ (1988). Interlocking Concrete Block Road Pavements, Cement and Concrete Association of New Zealand, Porirua.

CCANZ (1989). Construction of Concrete Block Pavements. Cement and Concrete Association of New Zealand, Porirua.

Cenek, P D and G Griffith-Jones (1997). Incremental Forms for Modelling Texture Depth and Friction Parameters in HDM-4. Works Central Laboratories, New Zealand. Communication to the ISOHDM, University of Birmingham.

Clifford, J M (1981). Evaluation of Tests to Determine Waterproofing Characteristics of Segmental Block Pavements. Technical Report TP/39/81, National Institute for Transport and Road Research, CSIR, South Africa.

Corne, C P (1989). Roughness Reduction from Overlays. Report to Directorate General of Highways, Indonesia. C.P. Corne and Associates, Indonesia.

Daines, M R (1992). The performance of hot rolled asphalt containing crushed rock fines, A303 Mere. Research Report 298. Transport Research Laboratory, Crowthorne, UK.

Darter, M I (1998). A Comparison Between Corps of Engineers and ERES Consultants, Inc. Rigid Pavement Design Procedures. Technical Report Prepared for the United States Air Force SAC, Urbana, IL.

Djarf, L (1995). Road Deterioration and Maintenance Effects Models in Cold Climates. Swedish Road Research Institute, Sweden.

Eisenmann, J and G Leykauf (1990). Simplified Calculation Method of Slab Curling Caused by Surface Shrinkage. Proceedings, Second International Workshop on Theoretical Design of Concrete Pavements, Madrid, Spain.

ERES (1995). Performance of Concrete Pavements, Volume III: Improving Concrete Pavement Performance. U.S. Department of Transportation and Federal Highway Administration. Champaign, Illinois.

ERES (1999). Design and Construction of PCC Pavements, Volume III: Improved PCC Performance Models. Report RD-98-113, FHWA, Washington D.C.

Foxworthy, P T (1985). Concepts for the Development of a Nondestructive Testing and Evaluation System for Rigid Airfield Pavements, PH.D. thesis, University of Illinois.

Freeme, C R (1983). Evaluation of Pavement Behaviour for Major Rehabilitation of Roads. ITRR Technical Report RP/19/83. CSIR. South Africa.

GEIPOT (1982). Research on the Interrelationships between Costs of Highway Construction, Maintenance and Utilisation (PICR). Final Report, 12 volumes. Empresa Brasileira de Planejamento de Transportes (GEIPOT), Ministry of Transport, Brasilia.

Hammitt, G M (1970). Thickness Requirements for Unsurfaced Roads and Airfields. Technical Report S-70-5. Waterways Experimental Station, Vicksburg, Viginia.

Harun, M H and G Morosiuk (1995). A Study of the Performance of Various Bituminous Surfacings for Use on Climbing Lanes. Proceedings of the 8th REAAA Conference, Taipei.

Heinrichs, K W, et al, (1989). Rigid Pavaments Analysis and Design. Federal Highway Administration, FHWA-RD-88-068.

Hide, H and D Keith (1979). Effect of Simple Road Improvement Measures on Vehicle Operating Costs in the Eastern Caribbean. Transportation Research Record 702, Transportation Research Board, Washington, D.C.

Highway Research Board (1962). The AASHTO Road Test. Special Report Nos. 61A – 61G and 73. Washington, D.C.

Hoban, C J (1987). Evaluating Traffic Capacity and Improvements to Road Geometry. World Bank Technical Paper No. 74, Washington, D.C.

Hodges, J W, J Rolt and T E Jones (1975). The Kenya Road Transport Cost Study: Research on Road Deterioration, TRRL Laboratory Report 673, Transport Research Laboratory, Crowthorne, UK.

Hoff & Overgaard (1994). Kabupaten Road Economic Evaluation Model. Draft Report on Pavement Models. Jakarta, Indonesia.

Hoff & Overgaard (1995). Database from Study of Kabupaten Road Pavements. Jakarta, Indonesia.

Houben, L J M, et al (1992). First Verification of the Dutch Design Method for Concrete Block Pavements. Proceedings of the Fourth International Conference on Concrete Block Paving, Volume II, University of Auckland, New Zealand.

Howard, K (1993) Notes on adaptions to Jameson procedure. Snowy Mountain Engineering Corporation, Cooma.

Jameson, G W (1993). Development of procedures to predict structural number and subgrade strength from falling weight deflections. (Unpublished).

Kennedy, C K, A E Young and I C Butler (1990). Measurement of Skidding Resistance and Surface Texture and the Use of Results in the United Kingdom. Surface Characteristics of Roadways: International Research and Technologies.

Kuipers, G (1992). The Effect of Concrete Block Lock-up on Pavement Performance. Proceedings of the Fourth International Conference on Concrete Block Paving, Volume I, University of Auckland, New Zealand.

Kulakowski, B T, D W Harwood, D R Hiltunen, J M Mason Jr, W E Meyer, S L Simoneau and J C Wambold (1990). Skid Resistance Manual. FHWA Report IP-90-013. The Pennsylvania Transportation Institute.

LAST (1996). Implementation of Road Deterioration Models in HDM-4, Part 2, Concrete Pavements, Report to ISOHDM by Latin American Study Team.

Lee, Y H, A Mohseni and M I Darter (1991). Pavement Model Enhancements For The Higway Performance Monitoring System (HPMS). Final Report, Illinois Department of Transportation and Federal Higway Administration.

Lesko, S (1982). The Use of Concrete Block Pavements for Highways. Proceedings of the First International Conference on Concrete Block Paving, UK.

Lytton, R L, C H Michalak and T Scullion (1982). The Texas Flexible Pavement System. Proceedings, Fifth International Conference on the Structural Design of Flexible Pavements, Volume 1. University of Michigan. Ann Arbor.

Major, N G and G J Tuohey (1976). Surface Treatments for Asphaltic Concrete for High Speed Traffic. Proceedings, 8th ARRB Conference, Vol. 8, p. 21.

Miner, M A (1945). Cumulative Damage in Fatigue. ASME, Transactions, Volume 67.

Morosiuk, G (1998a). Notes on the coefficient values for estimating drain life. Communication to the ISOHDM, University of Birmingham.

Morosiuk, G (1998b). Notes on modifications to the edge break model. Communication to the ISOHDM, University of Birmingham.

Morosiuk, G (1998c). Derivation of a new rut depth model for the structural deformation component in HDM-4. TRL Unpublished Project Report PR/ORC/610/98. Transport Research Laboratory, Crowthorne, UK.

Morosiuk, G (2003a). Revised specifications for modelling the deterioration of bituminous pavements for version 2 of HDM-4. Unpublished report for PIARC HDM-4 development team.

Morosiuk, G (2003b). Revised specifications for modelling the deterioration of unsealed roads for version 2 of HDM-4. Unpublished report for PIARC HDM-4 development team.

NDLI (1991). Thailand Road Maintenance Project, Final Report. Report to Department of Highways, Bangkok. N.D. Lea International, Vancouver.

NDLI (1993). Consultancy Services for Road Maintenance Programme. Report to Ministry of Works and Transport, Department of Roads, Nepal. N.D. Lea International, Vancouver.

NDLI (1994a). Road Network Rationalisation Study — Draft Final Report. Report to Public Works Division, Barbados, N.D. Lea International, Vancouver.

NDLI (1994b). Comprehensive Highway Maintenance Study — Phase 1 Final Report. Report to Ministry of Works and Transport, Trinidad and Tobago, N.D. Lea International, Vancouver.

NDLI (1995). Modelling Road Deterioration and Maintenance Effects in HDM-4. Final Report Asian Development Bank Project RETA 5549. N.D. Lea International, Vancouver.

Odoki, J B (1997). Notes on the effects of patching on the progression of potholing. Communication to the ISOHDM, University of Birmingham.

Odoki, J B and H G R Kerali (2000). Volume 4 – Analytical Framework and Model Descriptions. HDM-4 series of publications, PIARC.

Odoki, J B (2001). Effects of Overlays on Roughness. Communication to the ISOHDM, University of Birmingham.

Paterson, W D O (1986). International Roughness Index: Relationship to Other Measures of Roughness and Riding Quality. Transportation Research Record 1084, Transportation Research Board, Washington, D.C.

Paterson, W D O (1987). Road Deterioration and Maintenance Effects. World Bank Publications, Washington, D.C.

Paterson, W D O (1994). Proposal of Universal Cracking Indicator for Pavements. Transportation Research Record No. 1455. TRB. Washington, D.C.

Paterson, W D O (1998). Notes on modelling the deterioration of drainage. Communication to the ISOHDM, University of Birmingham.

Paterson, W D O (1999). Notes on the inclusion of a traffic component in the structural crack progression model. Communication to the ISOHDM, University of Birmingham.

PIARC (2004). Specificactions for road deterioration and works effects for bituminous pavements for version 2 of HDM-4. Unpublished report for HDM-4 development team.

Riley, M J (1996a & 1999a). Notes on seasonal adjustment of pavement strength. Communication to the ISOHDM, University of Birmingham.

Riley, M J (1996b). Notes on modification of the models for the initiation and progression of potholing. Communication to the ISOHDM, University of Birmingham.

Riley, M J (1997). Notes on proposed models for the initiation and progression of transverse thermal cracking. Communication to the ISOHDM, University of Birmingham.

Riley, M J (1998). Notes on modelling the effect of patching potholes on roughness. Communication to the ISOHDM, University of Birmingham.

Riley, M J (1999b). Notes on inclusion of the effect of traffic on the progression of ravelling. Communication to the ISOHDM, University of Birmingham.

Riley, M J (2000a). Notes on shoulder deterioration, edge break and effective roughness. Communications to the ISOHDM, University of Birmingham.

Riley, M J (2000b). Notes on modifications to the traffic component in the structural crack progression model. Communication to the ISOHDM, University of Birmingham.

Riley, M J (2000c). Notes on modifications to the time lapse factor used in modelling the effect of patching potholes. Communication to the ISOHDM, University of Birmingham.

Riley, M J (2000d). Notes on modifications to the rut depth standard deviation model. Communication to the ISOHDM, University of Birmingham.

Riley, M J (2000e). Notes on environmental component of the roughness progression model. Communication to members of the HDM-4 development team.

Roberts, J (1999). Notes on estimating structural number from FWD deflections. Communications to TRL.

Robinson, R, U Danielson and M Snaith (1998). Road Maintenance Management, Concepts and Systems. MacMillan Press Ltd, Basingstoke, UK.

Rohde, G T (1994). Determining Pavement Structural Number from FWD Testing. Transportation Research Record 1448, Transportation Research Board, Washington DC, USA.

Rohde, G T (1995). The Use of FWD Deflections in HDM-4. Report to the HTRS project in Malaysia.

Rolt, J and C C Parkman (2000). Characteristics of Pavement Strength in HDM-III and Changes Adopted for HDM-4. Proceedings of 10th International Conference of the Road Engineering Association of Asia and Australasia, REAAA, September 2000. Tokyo, Japan.

Rolt, J (2000). Pavement Structural Number from FWD Measurements for Network Analysis. TRL Unpublished Project Report PR\INT\664\00. Transport Research Laboratory, Crowthorne, UK.

Salt, G (1999). Determining the Structural Capacity of Unbound Granular Pavements in New Zealand Using Deflection Testing. Communications to HTC Infrastructure Management Ltd.

Salt, G F (1977). Research on Skid Resistance at the Transport and Road Research Laboratory (1927 to 1977). Transportation Research Record 622, pp. 26-38, Transportation Research Board, Washington, D.C.

Sandberg, U S I (1990). Relation Between Tyre/Road Friction and Road Texture. Swedish Road and Traffic Research Institute, Linkoping, Sweden.

Sayers, M W (1995). On the Calculation of IRI from Longitudinal Road Profile. TRB Paper No. 950842, Transportation Research Board, Washington, D.C.

Sayers, M W, T D Gillespie and W D O Paterson (1986). Guidelines for the Conduct and Calibration of Road Roughness Measurements. World Bank Technical Paper No. 46, The World Bank, Washington, D.C.

Shackel, B (1979). A Pilot Study of the Performance of Block Paving Under Traffic Using a Heavy Vehicle Simulator. Proceedings of Symposium of Precast Concrete Paving Units, Johannesburg, South Africa.

Shackel, B (1980). An Experimental Investigation of the Roles the Bedding and Jointing Sands in the Performance of Interlocking Concrete Block Pavements. Concrete/Beton No. 19. Johannesburg, South Africa.

Shackel, B (1982). An Experimental Investigation of Factors Influencing the Design of Interlocking Concrete Block Pavements for Roads. Proceedings of Australian Road Research Board, Volume II, Australia.

Shackel, B (1990). Design and Construction of Interlocking Concrete Block Pavements. Elsevier Applied Science, England.

Shahin, M Y, M I Darter and S D Kohn (1977). Development of a Pavement Maintenance Management System, Volume I: Airfield Pavement Condition Rating. AFCEC-TR-27 (Air Force Civil Engineering Center).

Sharp, K G and P J Armstrong (1985). Interlocking Concrete Block Pavements. Special Report SR 31, Australian Road Research Board, Victoria.

SHRP (1993). Distress Identification Manual for the Long-Term Pavement Performance Project. Strategic Highway Research Program, SHRP-P-338. National Research Council. Washington, D.C.

Toole, T, G Jameson, N Michel and Z Hoque (2003). Review of Specifications for the Enhancement of Technical Models for HDM-4 Version 2. Project Report RC3568-1, Australian Road Research Board, Melbourne.

TRL (1993). A Guide to the Structural Design of Bitumen-Surfaced Roads in Tropical and Sub-Tropical Countries.Overseas Road Note 31, Transport Research Laboratory, Crowthorne, UK.

Verhaeghe, B M J A, G A Airey, and C P Marais (1993). Stability of Mixes at Intersections. South African Roads Board, RDAC RR 91/153, Pretoria.

Visser, A T (1981). An Evaluation of Unpaved Road Performance and Maintenance. Ph.D thesis. Department of Civil Engineering, University of Texas, Austin, USA.

Watanatada, T, C G Harral, W D O Paterson, A M Dhareswar, A Bhandari, and K Tsunokawa (1987). The Highway Design and Maintenance Standards Model. Volume 1 - Description of the HDM-III Model. World Bank Publications. Washington, D.C.

Westergaard, H M (1926). Analysis of Stresses in Concrete Pavements Due to Variations of Temperature. Proceedings, Sixth Annual Meeting, Highway Research Board, Washington, D.C.

Westergaard, H M (1948). New Formulas for Stresses in Concrete Pavements of Airfields, Transactions, American Society of Civil Engineers, Volume 113.